UNIVERSITÀ DEGLI STUDI DI NAPOLI
FEDERICO II

PhD THESIS IN CHEMICAL SCIENCES

XXXVI COURSE

Natural compounds as potential new bioherbicides

Supervisor:

Prof. Alessio Cimmino

Co-Supervisor:

Dr. Mónica Fernández-Aparicio

Examiner:

Prof. Alessandra Napolitano

Author:

Gabriele Soriano

Coordinator: **Prof. Angelina Lombardi**

ABSTRACT

Among all pests, holoparasitic weeds represent a tremendous threat to agriculture, having a huge economic impact all over the world. Despite many attempts to contain them, through the use of various traditional management approach, such as fumigation, solarization, intercropping and development of resistant varieties, parasitic weeds persistently adapt and spread, posing growing challenges in effectively minimizing their impact on crops. The holoparasitic weed species broomrapes (*Orobanche*, *Phelipanche*) and the dodder *Cuscuta campestris* are particularly problematic, because they compete with a large number of important cultivated crops, such as tomato, eggplant, potato and sunflower, by penetrating their roots for nutrient and water absorption. They are also known as obligate parasite, in fact they cannot complete their life-cycle without exploiting a suitable host. If an obligate parasite cannot identify and therefore exploit a host, it will fail to complete its life-cycle. In the last years an alternative approach, for the management of these noxious plants, consists in targeting the early stage of parasitic plants seeds development, with the final goal of a progressive reduction of parasitic plant seedbank in the cultivated soil. In this regard, nature comes to the rescue, as source of specialized metabolites that can be used as inhibitors or stimulators, in absence of the host plant, of parasitic plants seed germination and development.

The aim of this PhD project has been the investigation of several weed plants, donor of allelopathic activity, in order to identify natural compounds to be used as bioherbicides. Many different specialized metabolites were isolated, such as glycosylated fatty acids, iridoid glycosides, γ-lactone compounds, sesquiterpene lactones, flavonoids and isoflavonoids. In particular, ephedroidin (**72**) from *Retama raetam*, melampyroside (**76**) from *Bellardia trixago* and arvenic acids from *Convolvulus arvensis*, were identified as species and concentration dependent inhibitors of *Orobanche crenata*, *Orobanche cumana*, *Orobanche minor*, *Phelipanche ramosa* and *Cuscuta campestris* seedling growth.

Furthermore, the acetylenic furanone (4*Z*)-lachnophyllum lactone (**84**) isolated from the plant *Conyza bonariensis* exhibited high percentage of inhibition activity, up to 0.3 mM, against all the plant studied. Specifically, an IC_{50} value of 24.8 μg/mL was observed against *Cuscuta campestris* seedling growth. Thus, considering its activity and the low amount isolated from natural sources, that pose limitation for its deeper and wider investigation, it was selected and total synthesized on gram scale. The developed methodology towards (4*Z*)-lachnophyllum lactone (**84**) synthesis is reported for the first time. Starting from a retrosynthetic analysis, the key step was identified in a Pd-Cu bimetallic cascade cross-coupling cyclization. The five-step methodology allow to obtain the (4*Z*)-lachnophyllum lactone (**84**) on gram scale, besides being easy modulable, whereby changing the intermediate of the synthetic pathway many different analogues can be obtained. Furthermore, two natural analogues were synthesized, namely the (4*E*)-lachnophyllum lactone (**96**) and the (4*Z*,8*Z*)-matricaria lactone (**97**), that showed, in most cases, the same inhibitory trend with slight differences, highlighting the importance of the stereochemistry and unsaturation of the side chain. The design and implementation of this scalable and modulable total synthesis of acetylenic furanones on gram scale, allow the production of large amount of these natural products, overcoming the limit imposed by isolation from natural sources and simplifying the exploration and refinement of bio-formulations. In this regard, first attempts for the development of a novel and easy-to-use tool for the agrochemical industry were already performed. Indeed, preliminary results showed that (4*Z*)-lachnophyllum lactone can be included into cyclodextrins or readily water solubilized by the use of the natural surfactants rhamnolipids, encouraging and paving the way for its final application in field. Additionally, the last step of the developed synthetic strategy towards (4*Z*)-lachnophyllum lactone (**84**), was exploited to obtain several analogues, aiming to gain further understanding into the structural features that impact and define its mode of action. A panel of synthetic analogues deprived of the side chain triple bond were prepared. Specifically, the reactions allow to obtain the δ-lactone, *E* and *Z*-γ-lactone to investigate how side chain unsaturation, length and dimension of the lactone framework can affect the activity. In conclusion, the results obtained contribute to enlarge the pool of natural products to be used as bio-inspired herbicides and provide a practical, ecofriendly and ready-to-use

herbicide, the (4*Z*)-lachnophyllum lactone (**84**), with potential application in the agrochemical industry.

INDEX

1. Introduction

1.1 Holoparasitic weeds: a worldwide problem

Among all pests, parasitic weeds represent a tremendous threat to agriculture, having a huge economic impact all over the world.[1,2] Despite efforts for containment and developing resistant cultivars, these parasitic weeds adapt and continue to spread, causing increasing challenges in managing their impact on crops. Among them, the holoparasitic weed species, broomrapes (*Orobanche*, *Phelipanche*)[3] and the dodder *Cuscuta campestris* are particularly problematic, because they compete with a large number of crops by penetrating their roots for nutrient and water absorption. An holoparasite, also known as obligate parasite, is a parasitic organism that cannot complete its life-cycle without exploiting a suitable host (**Figure 1**). If an obligate parasite cannot identify and therefore exploit a host, it will fail to complete its life-cycle. This is opposed to a facultative parasite, which can act as in a similar way but does not rely on its host to continue its life-cycle.

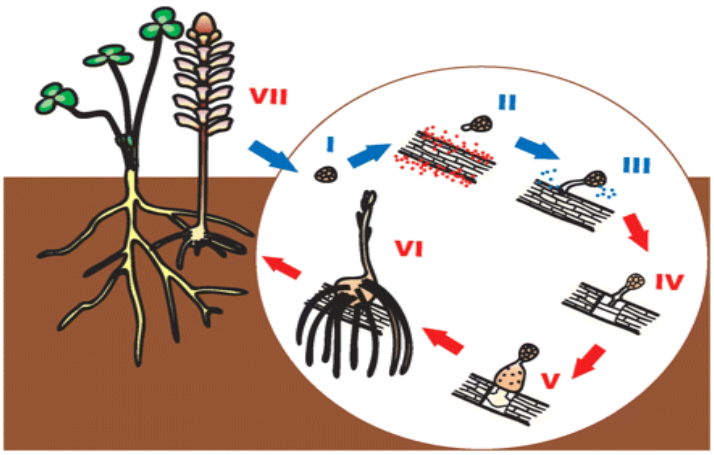

Figure 1. *Life cycle of a root holoparasitic plant, Orobanche minor (adapted from Yoneyama et al. Plant Cell Physiol.* ***2010****, 51 (7), 1095–1103.).*[4]

The parasitic weed branched broomrape, was firstly identified on tomatoes in California in 1928 and has been a target for eradication efforts during the past four decades. Branched broomrapes are classified as "A" pests in California, triggering state-enforced actions such as eradication, quarantine, and crop destruction upon detection in commercial

tomato fields. The detection of branched broomrape leads to quarantine and crop destruction without harvest, severely impacting the tomato industry globally. These weedy plants, are globally recognized as one of the most destructive parasitic plants. As mentioned before, their parasitic action is carried out through the penetration of host roots (**Figure 1**), absorbing not only water but also minerals, and carbohydrates, causing severe damage to the host plant. This damage includes a reduction in aerial biomass and leaf chlorophyll content, resulting in yield losses of up to 80%. The germination of branched broomrape seeds is triggered by host root exudation of chemical signals, making eradication challenging due to the longevity of seeds in the cultivated fields. These weeds have a broad range of hosts including potato, sunflower, tomato, carrot, cabbage, celery, pepper, canola, and lettuce. Their ability to extend its host range to affect new species further complicates control and eradication plans. In addition, branched broomrapes produce tiny seeds which can remain dormient for decades and are easily transported by humans, agricultural equipment, animals, water and wind. Farm machinery, especially harvesters, plays a significant role in the dispersal of broomrape seeds in highly mechanized cropping systems (**Figure 2**).[5]

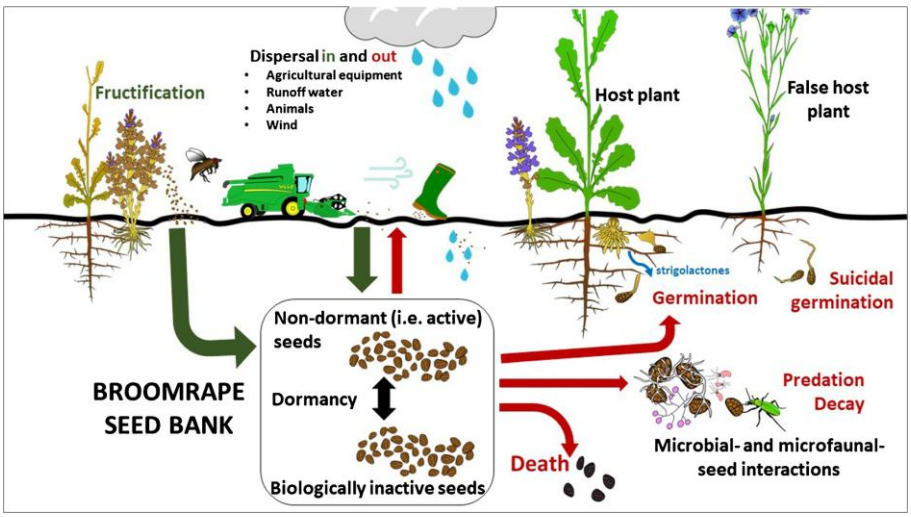

Figure 2. *Balance of broomrape soil seed bank inputs and outputs affecting the broomrape population dynamics in a plot (adapted from Cartry et al. Agron. Sustain. Dev.* ***2021****, 41 (2), 17).*[5]

Effective containment strategies involve both cleaning and sanitization of farming implements, including the removal of plant and soil residues, the use of synthetic chemicals, particularly quaternary ammonium compounds, is explored to eliminate broomrape seeds in

cultivated fields.[6] In the last decades many studies have focused on the severity of *Orobanche* problems in Europe and North Africa based on various reviews. Seven major *Orobanche* species in Europe, including *Orobanche crenata*, *Orobanche cumana*, *Phelipanche ramosa*, *Orobanche aegyptiaca* and *Orobanche foetida* becoming a significant problem in the past 10-20 years. Besides them other parasitic plants, commonly known as field dodders (e.g., *Cuscuta campestris*), negatively affect crop yields worldwide.[7,8]

Figure 3. *Cultivated clover field in Spain, infested by the holoparasite broomrape Orobanche minor.*

The seriousness of parasitic plant issues is very high, but there's a lack of specific quantification of crop losses in recent review, hindering comparisons with earlier assessments. Other recent reviews provided a limited updated calculation of losses but reaffirm the significant issues created by *Orobanche* spp.[8] Specifically, *O. crenata* has a significant economic impact on crops, particularly faba beans, in various countries. In 1991, infestations were estimated to cover 50-70% of cultivated areas in Morocco, Portugal, Spain, Italy and Syria, while the issue is indeed global in reality.[9] The economic losses were substantial, with estimates ranging from 12% to even higher percentages in different countries. The affected crops include peas, lentils, chickpeas, and carrots. Despite efforts to

control *O. crenata*, the problem has persisted, with limited success in available control methods. There are reports of the parasite spreading to new areas, such as Algeria, Spain's central region, Ethiopia, and Sudan. The primary method of reducing the problem is through abandonment of affected crops, leading to a decrease in the infested area. Farmers in various countries have given up growing faba beans and other affected crops due to the challenges posed by *O. crenata*. Overall, despite decades of research, the issue remains a significant concern with severe crop losses in the affected regions. *O. foetida* has an historical presence in western North Africa and southern Europe. However, it has recently become a notable weed problem in crops such as faba beans, chickpeas, and vetch in Tunisia.[10] In Morocco, the species has traditionally affected wild hosts, but there is concerning evidence that it is adapting to attack vetch, a cultivated crop. This observation raises concerns for other countries around the western Mediterranean, where *O. foetida* currently only impacts wild hosts. Known as a unique species, *O. cumana* is significant in many nations, such as Russia, Ukraine, Moldavia, Romania, Turkey, Bulgaria, Spain, Israel, and Hungary.[11] It is found in Spain as well as along the coast of North Africa, but it is more common in eastern Europe and the eastern Mediterranean. For almost a century, researchers have been studying the *O. cumana* issue in sunflowers. Breeding resistant cultivars is one way to combat it, and it can temporarily ease the situation locally. But as more virulent biotypes have emerged, breeding and selection have become necessary, frequently combining DNA from wild *Helianthus* species. The problem was initially noted in Spain in 1958, and by 1998, it had affected about 40,000 hectares. It then spread quickly until 1993. Another time, the presence of the parasitic plants, led to the abandonment of local sunflower cultivation, but things improved when more tolerant sunflower types for oil production were developed. Yield losses were caused by various degrees of infection in Greece, China, and Turkey.[12] Before resistant cultivars were introduced, sunflower agriculture was drastically decreased in the former Yugoslavia in the 1950s. It's unknown how the losses are doing right now in the other impacted nations. The main strategy for controlling *O. cumana* in sunflowers is to use resistant genotypes, however herbicides, particularly imazapic, in Israel have also been used.[12] Imidazolinone-resistant sunflower lines, along with related herbicides, contribute to controlling *O. cumana*, notably in Israel where substantial reductions in the problem have been observed. The main crops that are significantly impacted by *P. ramosa* are those in the *Solanaceae* family, which

includes tobacco, tomatoes, and potatoes. A smaller degree of effect is also seen with other crops. Its effect on hemp and rapeseed has increased noticeably in France, resulting in a "dramatic spread" of the issue. Greece, Nepal, Cuba, and Chile are just a few of the nations outside of its native Mediterranean region where *P. ramosa* has been documented in the past. In 1986, a tomato infestation affected 15,000 hectares in Greece,[13] resulting in an average output loss of 25%. In 1994 infestations of 20,000 hectares of tobacco were reported in Cuba, resulting in yield losses varying from 10% to 50%. Tomato crop loss of up to 80% has been reported in Chile. Around 6,000 hectares in Western Australia[14] are affected by new infestations that have been observed to damage rapeseed and other hosts. *P. ramosa* has recently been reported in the United States too, particularly in Virginia; however, at this time, it is not economically significant. While solarization[15] has proven effective in certain areas, there aren't many broadly effective control strategies overall. Crop rotation is not possible since *P. ramosa* has a wide host range. The only practical course of action in cases of heavy infestation, like large-scale tomato plantations in Sudan and Ethiopia, has been to give up the crops and related canning operations.[16] Comparing with the other species under discussion, the problems associated to *O. minor*, are comparatively mild. Although the impact is not severe, it predominantly affects clovers and lucerne (alfalfa) crops. The plant is widely found across the majority of Europe, the Middle East, and along North Africa's western coast. The USA, South America, Japan, Australia, New Zealand, and southern Africa are among the places it has been introduced. It is unclear if this is a naturally occurring or artificially introduced species in eastern Africa's highland rainforests. It is especially prevalent in Ethiopia, where it only slightly damages crop like faba beans and noog/niger seed.[17] *O. minor* becomes a more significant problem in clover and alfalfa crops grown for seed, where it can spread seeds and form high populations, potentially contaminating the crop seed and preventing its sale. Harvesting or grazing forage crops helps prevent this issue.[18] The significance of *O. minor* has declined with reduced cultivation of Trifolium seed[19] crops in some regions, such as the Netherlands and the UK. Despite the decline in importance, new infestations continue to appear. In Oregon, USA, *O. minor* was first identified in a single field in 1998, and by 2001, it was known in a further 15 sites. In pot experiments, significant reductions in clover biomass and inflorescence mass were observed, indicating its potential impact on affected crops. So considering that they are continuously

spreading worldwide, their impact pose a risk to food security.[8,20] In southern Italy regions, the root holoparasite *P. ramosa*, is causing significant damage to processing tomato crops. As already mentioned before, the extensive infestation is attributed to the plant's high seed production, with each plant capable of producing up to 500,000 small seeds (approximately 0.2-0.3 mm). These seeds can remain viable in the soil for extended periods, up to 20 years in the absence of a host. The parasitized tomato plants exhibit stunted growth initially, followed by a reduction in yield quantity and quality due to the action exerted by parasitic plants.[21]

Common vetch (*Vicia sativa L.*) and bitter vetch (*Vicia ervilia L.*) represent important crop, especially in the Mediterranean Basin. These plants are valued for their high nutritional content and adaptability to different climates and soils and are commonly cultivated for grains or as forage crops, often intercropped with cereals for better yield. Despite their numerous benefits, the cultivation of these vetch species faces challenges, primarily from parasitic weeds, specifically dodders (*Cuscuta* spp.). Unlike broomrapes, dodders are stem parasites that negatively impact dicotyledonous crops worldwide. The difficulty in controlling dodders stems lies in their persistent seedbanks, broad host range, and intimate connections with host plants. The decline in vetch cultivation is attributed to the susceptibility of these plants to parasitic weed infections,[22] compounded by the lack of investment in breeding programs to develop resistant cultivars.[23] Current control strategies for dodders involve herbicides applied to herbicide-resistant crops or the development of infection-resistant crops. However, more research and investment to address these challenges and promote sustainable cultivation of common vetch and bitter vetch in low-input cropping systems are needed. Resistance to the stem parasitic weed *Cuscuta* has been reported in chickpea, characterized by the failure of prehaustorium penetration into the host stem. Vetch species show resistance to root parasitic plants, such as *P. aegyptiaca* and *O. crenata.*[24,25] The difficulties posed by root parasites, highlighting the fact that they inflict serious harm prior to appearing and may result in field losses before being discovered. Many strategies, including biological, chemical, physical, and cultural ones, have been investigated. Soil fumigation and solarization control approach are considered too expensive for widespread application.[26] The herbicide resistance of root pests and their lack of selectivity make it difficult to use herbicides and limit their overall application.[27] Therefore,

there is an urgent need to adopt innovative techniques to effectively eradicate and control root pests in order to eliminate or at least reduce their impact in agriculture.

1.2 Conventional control methods of parasitic plants

Herbicides. Conventional broomrapes control methods adopted some available synthetic herbicides due to their wide spectrum of parasitic weed control, although few of them are able to work selectively.[26] Among them, sulfonylurea herbicides are effective in controlling *Orobanche* when applied directly to the soil in tomato and potato fields.[28] Other herbicides such as glyphosate, imidazolinones, and sulfonylureas, which inhibit key enzymes, have been used for *Orobanche* control. Some of these herbicides show a degree of selectivity, benefiting the host plants affected by *Orobanche*.[29] However, the chemical approach poses some difficulties, such as: lack of application technology, chemical damage to the host, continuous parasite seed germination throughout the season, marginal crop selectivity, environmental pollution, low persistence, and availability.[30] Damages by chemical persistence[31] and availability are other major constraints that limit the successful application of herbicides for parasitic weed control. In addition, in developing countries, the income of subsistence farmers is usually too low to afford them. Furthermore, chemical control options for *Orobanche*, involving two main approaches: applying herbicides either directly to the foliage, or to the soil, many control methods have been exploit during the years. [32]

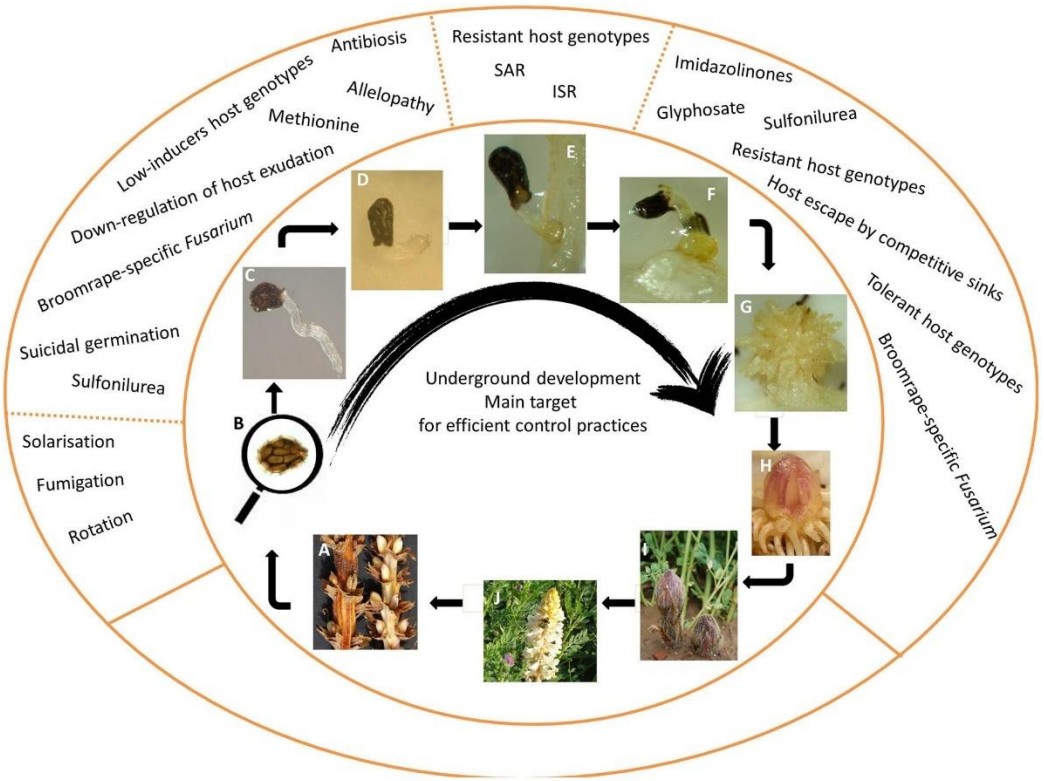

Figure 4. *Main broomrapes treatments and underground development (adapted from Fernández-Aparicio et al. Front. Plant Sci.* ***2016****, 7-29).*[32]

Crop rotation, trap and catch crops. This method consist in rotating susceptible cereal crops with nonhost crops, known as "trap crops." The latter induces germination in parasitic plants seeds but doesn't lead to parasitism on their own. This rotation strategy has been found effective in reducing soil seed levels and increasing yields in subsequent cereal crops.[33] The use of catch cropping, where parasite-susceptible crops are grown, is mentioned but is not commonly employed by small farmers due to limited awareness and the need for adaptation to specific cropping systems.[34,35] Additionally, trap and catch crops are most effective when the parasite soil infestation level is very low. The concept of crop rotations is also extended to reducing *C. campestris* infestation by continuously growing cereals or other grass crops, which act as false hosts and deplete the dodder soil seed bank.[36]

Intercropping. Cereals cultivations with legumes and other crops is a widely adopted practice across many regions in Africa and has been known to decrease *Striga* infestation, as

documented in Kroschel's study in 2001.[37] Specifically, in Kenya, intercropping maize with cowpea and sweet potato has proven to be effective in significantly lowering the occurrence of *Striga* emergence.[38]

Seed bank removal. The primary challenge in the prolonged control of fields infested with *Orobanche*, is the persistence of the seedbank, which can remain viable for many decades, as indicated by Joel et al. in 2006.[39] The two primary methods for eliminating the seedbank are fumigation and solarization.

Fumigation. Many recent studies indicate that fumigating the soil with methyl bromide has proven to be an effective method for controlling *Orobanche* spp. seedbank. However, the international community is phasing out the use of methyl bromide to safeguard the global environment.[40] Although alternative fumigants have been explored as substitutes for methyl bromide, they are found to be less effective and more costly, thus it's important to recognize that all fumigants are expensive, require labor-intensive application, and pose significant environmental hazards, including risks to mammals.[41]

Solarization. Utilizing summer sunlight to attain elevated temperatures (55°C) by employing clear polyethylene mulch to cover the soil for an extended period, as outlined in the work of Katan and deVay in 1991,[42] represents an alternative method for eradicating the seedbank of parasitic weeds. Soil solarization has proven successful in the Middle East for various crops such as tomato, eggplant, faba beans, lentil, and carrot, as demonstrated in the study by Abu-Irmaileh in 1991.[43]

Hand-pulling. This technique is efficient in eliminating parasites, especially in fields with relatively low infestations. However, when dealing with *Striga* spp.,[44] its effectiveness is reduced as much of the harm to the host occurs while the parasite is still underground. In Kenya, certain farmers have successfully managed *Striga*-related issues in their fields using this method. Removing mature *Striga* plants from an infested field only reduces the seed quantity and does not immediately enhance host yields. Instead, regarding the treatment of *Orobanche*, hand-pulling is more effective as the parasite causes less damage underground before emergence.[45] While removing infested branches is beneficial, the optimal control measure for mistletoe involves replacing severely infested trees with less susceptible species.

Hand removal of dodder remains a viable approach for small infestations but becomes expensive if the infestation is extensive.[46]

Host plant resistance. The primary long-term strategy for mitigating damage caused by parasitic weeds is the development of resistant plant varieties. However, conventional breeding has had limited success in producing stable resistance, as indicated by Rubiales in 2003.[47] Despite this, significant advancements have been made in screening methodologies to identify better sources of resistance to parasitic weed-hosts. Notable successes include the release of three *Striga*-resistant sorghum cultivars in Ethiopia between 1999 and 2002. In the case of *Orobanche* spp., resistant sunflower varieties have been developed, but the effectiveness of this resistance has been challenged by new virulent strains in various countries.[48] Two faba bean cultivars with good resistance to *O. crenata* have been released in Egypt. Promising sources of resistance have been identified in wild *Pisum* spp., which have hybridized with cultivated peas. Some tree species, such as pear, Chinese pistachio, crapemyrtle, ginkgo, sycamore, and certain conifers, exhibit resistance to broadleaf mistletoe. Additionally, certain crops show resistance or tolerance to *Cuscuta* spp., with reports of tomato plants resistant or tolerant to *Cuscuta reflexa*. However, sensitivity to highly virulent strains like *Cuscuta pentagona* varies considerably among commercial tomato species.[26,49]

Traditional cultural or herbicidal weed control methods are not highly effective in managing parasitic weeds, and the most efficient control approaches are the development of resistant cultivars, chemical control and fumigation, which however, poses environmental risks, as highlighted by Jacobsohn in 1994, since long ago.[50] Furthermore, the majority of crops impacted by the just described approaches are restricted because there are either not enough approved herbicidal treatments with sufficient selectivity against the parasite and sufficient security for the crop and environment,[51] or there aren't enough commercially accessible resistant cultivars.[52,53] Various control methods have been attempted for parasites, but cost-effective and protective solutions are lacking. Environmental factors influence outcomes, emphasizing the need for an integrated approach to keep parasite populations in check. Recent studies focus on agronomic techniques like organic products and bio-stimulants, but limited information exists on their effectiveness in *Phelipanche* control. Inorganic fertilizers,

are also applied to the soil. Biological agents like *Fusarium* spp. and arbuscular mycorrhiza, as well as biotechnological techniques involving a resistant tomato cultivar, were also used.[21]

1.3 Alternative ecofriendly approach

In order to protect crop plants against parasitic plant infection, a successful approach used in the last decades, aims to target and control broomrapes seeds germination. In fact, one of the major strengths and treatment resistance of these parasitic plants lies in the fact that they are able to produce a very large number of tiny seedlings which, most importantly, remain dormant until the detection of host roots through root-derived germination stimulants (e.g. strigolactones), and only after the detection of these chemical signals their life-cycle started (**Figure 4**).[54,55] At this time, a short radicle emerges from the broomrape seeds, growing in the direction of the host root and developing a multicellular haustorium. The term haustorium is used to described a rootlike structure that grows into or around another structure, in the current case the root of cultivated crop, to withdraw water and nutrients and thus complete their life cycle.[56,57]

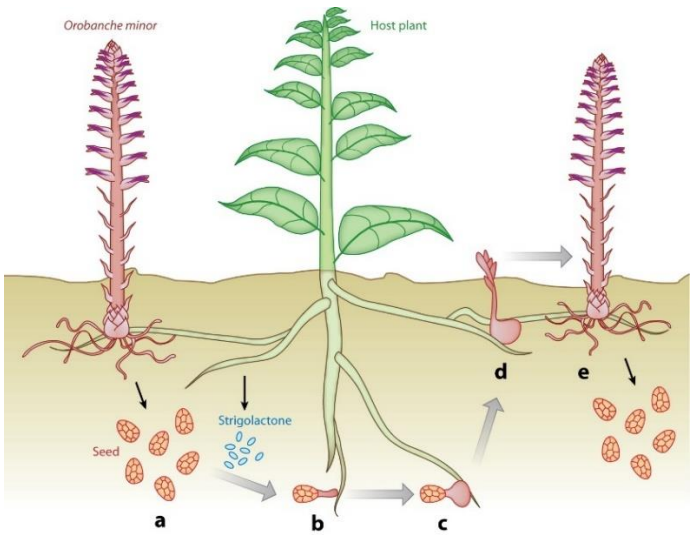

Figure 5. *Orobanche minor life cycle (adapted from Xie et al. Annu. Rev. Phytopathol.* ***2010****, 48 (1), 93–117).*[58]

Considering the just described broomrapes seeds development, it can be readily understood that germination is a key-phase stage and can be used as the main target to rid crop fields of

their presence. In fact, they only sprout when a chemical signal was exuded from the host root, going then immediately attaching to the cultivated plant and thus compromising crop yield at root level. Therefore, by the time they emerge from the soil, it's already too late, because the parasitism mechanism of nutrient withdrawal, through haustorial connections, resulting in severe reductions of crop yields, has long since begun.[59,60] When compared to non-parasitic weeds, the post-attachment herbicidal strategy is defined by four broomrape traits. First off, as broomrape weeds are achlorophyllous, broomrapes will be affected by herbicides that target the photosynthetic process, such as triazines or substituted urease (classified as belonging to the C group in the Herbicide Resistance Action Committee (HRAC) classification). Second, contact herbicides such as 2,4-Dichlorophenoxyacetic acid (2,4-D), applied after broomrape emergence, had little effect on minimizing crop yield loss, because broomrape weed causes harm underground immediately after attachment.[32] Third, this technique is only effective with systemic herbicides applied to herbicide-resistant crop kinds that do not convert the herbicide into inactive forms. Broomrapes underground attachments only take herbicides systemically from the host, not from the soil. Four, despite reports of broomrape's ineffective machinery for assimilation of nitrogen and amino acid fluxes from the host phloem to the parasite, herbicides that inhibit the parasite's amino acid biosynthesis by suppressing the enzymes enolpyruvylshikimate phosphate synthase (EPSPS) and acetolactate synthase (ALS) encoded in the broomrape genus can kill broomrape.[32] Thus, it's urgent to find new environmentally friendly herbicides and alternative methods to control broomrape, that nowadays are essentially based on the use of systemic herbicides, such as glyphosate, an inhibitor of aromatic synthesis, or imidazolinones and sulfonylureas, which are branched-chain amino acid synthesis inhibitors.[51] However, the high potential for weeds to acquire resistance, the decline in approved herbicides, the risks associated to environmental pollution, human and animal health, and even more the lack of new herbicide mode of action, pose a challenge to the sustainability of herbicide control approaches.[61,62]

Recent alternative eco-friendly control approach. Allelopathic plant species can exert orobanchicidal effects helping in achieve effective and enduring control of parasitic weeds, targeting the pre-haustorial stages development. Three distinct methods were used: inducing germination without a host, resulting in suicidal germination;

preventing germination in the presence of a host, leading to inhibition of parasitism; and disrupting subsequent radicle growth and haustorium development. The signalling mechanism, that induce germination, can be used in plant protection, by promoting suicidal germination of the weed in the absence of host crops, achieved by the application of germination stimulants to the soil.[63] A line of the Lithica poem reads: "*All the pests that out of earth arise, the earth itself the antidote supplies*" (Ibn et al., 1781). This citation can be of inspiration to found natural bioactive products against parasitic plants seed germination, using a chemical approach, that does not rely on traditional synthetic herbicides, but specialized metabolites from plants. Indeed, the isolation of allelochemicals from plants root exudates, with the potential to inhibit or to stimulate broomrape development, opens the door to the design of new herbicides based on natural and benign sources.[64] Indeed, a significant number of traditional herbicides have either been banned from the market or are slated for removal due to environmental and toxicological concerns. This makes new efficient, and ecologically friendly alternatives urgent and necessary. Natural product-based pesticides have a number of benefits, including minimal environmental risks, high target selectivity, unique mechanisms of action, and decreased hazards to nontarget creatures and humans.[65] Specialized metabolites from plants, that either stimulate suicidal broomrape germination in the absence of host plants[66] or inhibit broomrape radicle growth towards host roots[67] can target the mode of action used by broomrapes to infect crops, namely host-induced germination and radicle growth towards host roots for haustorium attachment. The parasitic weeds' life cycle is perfectly matched to that of their host plants.[68] These weeds' seeds can only sprout when they come into contact with a certain chemical signal, or germination stimulant. Because plants only generate a very low quantity (15 pg plant^{-1} day^{-1}) of these compounds, it is extremely difficult to isolate and identify germination stimulants from root exudates,[69] although in recent decades enormous strides have been made in the field of chemical technology, on which the isolation of compounds, involved in plant-to-plant communication, is closely dependent. In this regard, results to be of paramount importance the synthesis of these natural products in order to make feasible industrial applications.

1.4 Allelopathic plants, a source of potential new herbicides: history and current trends

The term "allelopathy," is defined by the International Allelopathy Society (IAS) as the study of secondary/specialized metabolites produced by various organisms that influence the growth and development of agricultural and biological systems.[70] Initially considered a branch of ecological sciences, allelopathic studies now span disciplines such as ecology, biochemistry, chemistry, plant physiology, agriculture, forestry, and genomics.[71] The increasing importance of allelopathy is evident through extensive reviews documenting its various aspects.[72] Nowadays, the bioassay-directed strategies used by chemists to identify allelopathic compounds and deal with the difficulties associated with environmental hazards, are of crucial importance.[72] The bioassay-guided fractionation is one of the widely used techniques in plant drug discovery, involving the extraction and biological screening simultaneously, in order to identify the bioactive compounds. Various allelochemicals with diverse structures have been identified, and their impacts on plant life are actively studied. Initially, a classification into more than 10 categories, based on biosynthetic origin was established,[73] encompassing common allelochemicals like simple phenolic acids, quinones, mono- and sesquiterpenes, and flavonoids.[74,75] The 20th century witnessed a resurgence of interest in allelopathy, driven by advancements in techniques for extraction, bioassay, and chemical isolation.[73,76] At the end of the last century, significant progress was made in liquid-column and high-pressure liquid-column chromatography, as well as nuclear magnetic resonance spectroscopy and mass spectrometry for structural elucidation of allelochemicals, thus encouraging the search of natural bioactive compounds.

Although, allelopathy refers to the phenomenon where plants or microbes influence other organisms[77,78] through the production and the use of chemicals known as allelochemicals, it can have both positive and negative effects.[79] Different studies explored various aspects of allelopathy,[80,81] including the interaction of microbes in the decomposition of plant residues and the impact of allelochemicals on soil bacteria.[82,83] Specialized metabolites from allelopathic plant extend across multiple kingdoms, impacting various organisms therefore, despite the original definition of allelopathy addressed plant-plant interactions, there’s a need to reconsider its broader ecological functions.[79]

One cannot fail to notice that the efficacy of microbial secondary metabolites, highlighted by their potential as natural herbicides or templates for eco-friendly agrochemicals is also noteworthy. The expanding database of natural phytotoxins, coupled with advancements in technology and increased attention to this field, anticipates exciting developments in the use of microbial secondary metabolites as eco-friendly herbicides, contributing to environmental and human well-being in the coming years.[84] With the rise of herbicide, insecticide, and fungicide resistance in various species, there is a growing interest in developing diverse and integrated weed management systems.[85]

Based on the above, biologically active substances known as allelochemicals are secreted by donor plants and have the ability to affect target plants. Considering the large number of allelopathic microbial and plant species,[86] only a small number of microbial or plant metabolites have been tested for their herbicidal action, despite the fact that many natural compounds have the potential to be new agrochemicals.[62,87] These compounds, that operate on seed germination and radicle development,[67,88] having anti-parasitic weed action and can be found by the assessment of microbial or plant toxins.[89] Plant-based allelochemical bioherbicides are becoming increasingly popular due to their environmentally friendly attributes, aiming to suppress target weed populations while avoiding harm to the environment.[89] The advantages include water solubility, eco-friendly chemical structures with low amounts of heavy atoms, absence of unnatural rings, a high number of oxygen-, nitrogen-, and sp3-hybridized carbon molecules, high degradability in soil and water, and the potential for new molecular targets in weeds, along with public acceptance.[90] Despite these advantages, certain situations pose drawbacks. The structural complexity of allelochemicals, leading to more stereocenters than synthetic molecules, renders them unstable and rapidly degradable, reducing their environmental half-life. Additionally, the chemical characteristics of allelochemicals contribute to increase synthesis costs. The discovery and establishment of allelochemicals as bioherbicides are acknowledged as more complex compared to synthetic herbicides (**Figure 6**).[90]

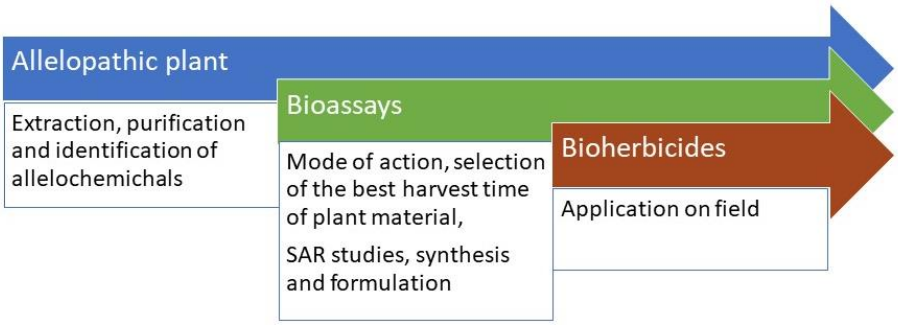

Figure 6. *General bioherbicides development and production flow, involving compounds extraction from natural sources, their bioassays, synthesis and structure activity relationship (SAR), prior to their formulation and application in the field.*

In order to take advantages from nature, as source of allelochemicals, a large number of weed species donor of allelopathic activity, were selected in the present work, with the aim to assess and use their specialized metabolites against germination and radicle growth of *Orobanche crenata* Forsk., *Orobanche cumana* Wallr., *Orobanche minor* Sm., and *Phelipanche ramosa* (L.) Pomel, which are four of the most noxious broomrape weeds affecting crops in many parts of the world. This powerful strategy is grafted onto a perspective that aims to find new potential bioherbicides.

1.5 Stimulation of parasitic plant seed germination

Holoparasitic plants management approach, belonging to the use of specialized metabolites, stimulating seed germination and radical elongation. Stimulation approach is commonly known as "suicidal-germination" and consist in the treatment of the cultivated soil with specific bioactive compounds, in the absence of the host plants.[4] Once the parasitic plant recognizes the presence of stimulating compounds, it readily germinates, but without the opportunity to take nutrients and water from the host plant due to its absence, and thus failing in completing its life cycle and seed production. Therefore, this methodology leads to the death of plants stimulated to germinate, resulting in a reduction of the seedbank in the cultivated soils.[66]

The first bioactive stimulating compound to be isolated, from the roots exudate of *Gossypium hirsutum L.*, was Strigol.[91] Several years later, another compound with a similar structure was isolated from the roots of *Sorghum bicolor* (L.) Moench, the sorgolactone.

However, from an *Orobanche* host, the *Trifolium pratense L.*, also commonly known as red clover, was isolated another strigolactone, namely the orobanchol.[92] From many root exudates of *Striga* host extracts, can be isolated mixtures of these natural products with stimulating activity towards parasitic plants seed germination, albeit in different ratios. It's for this reason, that the collective name of this class of compounds was proposed as "strigolactones" (SLs).[93] Then, two newly interesting stimulating compounds produced by Tobacco plants were isolated, the 2'-epiorobanchol and solonacol.[94] Many more strigolactones were isolated from plant sources, even if the challenges of isolating natural stimulants, specifically strigolactones, from root exudates due to their minute concentrations are very hard.[95] Despite advancements in chromatographic and spectroscopic techniques, the isolation process still requires a significant number of plants, albeit fewer than in the past. The complex chromatographic profile of root exudates necessitates extensive bioassays to identify the desired compounds. The isolated amounts are often too small for precise stereochemistry determination, making total synthesis crucial for structural confirmation, further application and study in field.[96]

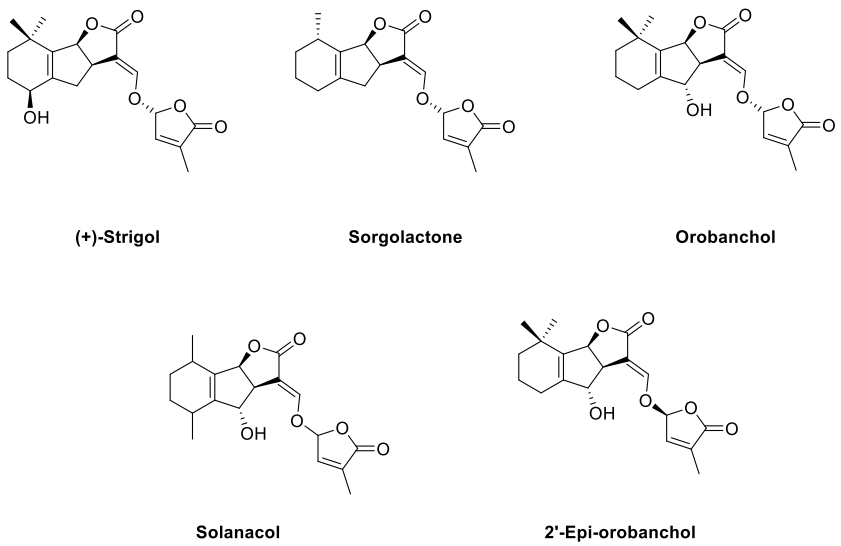

Figure 7. *Strigolactones compound structures.*

All these structurally similar stimulants are featured by a butanolide ring (D-ring) that is coupled to a three-ring, ABC unit, through an enol ether bond. Recent studies focused on understanding which part of SLs molecules is responsible for the biological activity, to better understand the interaction with the protein receptor in the seed of weed. Firstly, the replacement of the A natural ring with an aromatic one provided a highly active analogue, namely the GR 24, which is often used as reference in the stimulation bioassays. Other analogues were prepared substituting the A, B, C rings or lacking of the D ring. Interestingly, SAR data obtained by testing these analogues, led to the conclusion that the bioactiphore of SLs resides in the CD moiety.[96] Furthermore, the initial stages of the molecular interaction between the stimulant and the receptor protein in the parasite seed are not fully understood, but it is proposed that the bioactive part of the molecule is in the CD segment. A tentative molecular mechanism suggests that a nucleophilic functional group at the receptor site reacts with the enone moiety in the CD part of the stimulant in a Michael fashion. This reaction results in the elimination of the D-ring unit, leading to the covalent binding of the ABC portion to the receptor, a chemical change believed to trigger germination. Experimental evidence supports this proposal, showing that modifying the enol ether part of the stimulant leads to a loss of activity.[97] This molecular mechanism guides the design of synthetic strigolactone analogues, which must adhere to the addition-elimination reaction. Although this proposed mechanism is a simplified version, it may involve the enone function in the D reaction, potentially through bidentate binding (**Figure 8**). The details of the receptor pocket are not yet well-defined.

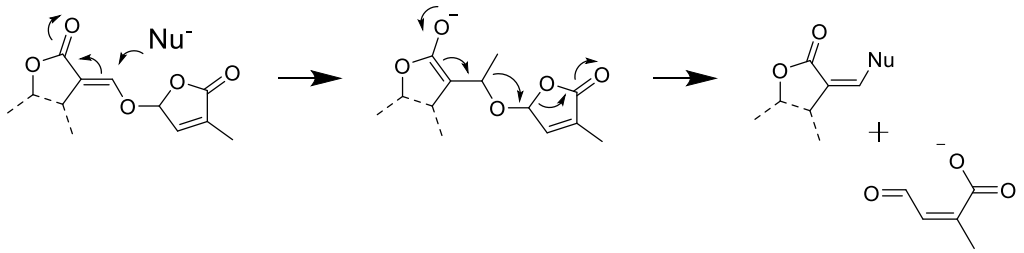

Figure 8. *Molecular mechanism of strigolactones interaction with the receptor protein. The process involves receptor site nucleophilic functional group addition, in a Michael fashion, to the enone moiety of the stimulant CD part, followed by the D-ring unit elimination. This, leads to the covalent binding of the ABC portion, a chemical change that is claimed to be responsible for initiating or triggering germination.*[96]

Besides strigolactones, other compounds belonging to different classes of natural products were isolated as seed germination stimulants. Peagol and peagoldione, strigolactones-like compounds, were extracted from the root exudates of pea crops, severely damaged by *O. crenata* infection, and characterized through spectroscopic methods. These metabolites demonstrate germinative effects on seeds of root parasitic plants, particularly *Orobanche foetida* and *Phelipanche aegyptiaca*. Peagol displays higher efficacy on *Orobanche foetida* and *Phelipanche aegyptiaca* seeds, while peagoldione specifically affects *Phelipanche aegyptiaca*. Interestingly, their impact is limited on *Orobanche crenata* and *Orobanche minor*. Notably, peagol (**Figure 9**) stimulates germination in *Orobanche foetida* seeds, a species that typically does not respond to the synthetic strigolactone analogue GR24, commonly used as a germination standard for *Orobanche*, as said before.[89]

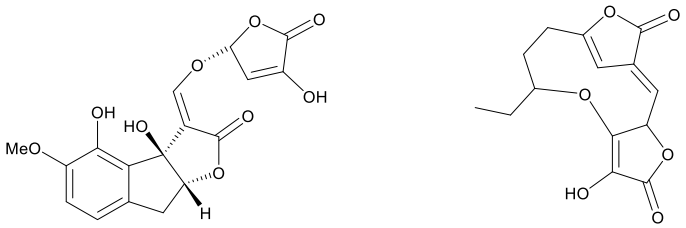

Peagol **Peagoldione**

Figure 9. *Natural compounds with stimulant activity on Orobanche seeds, with strigolactone-like structure.*

Moreover, three new polyphenols designated as peapolyphenols A-C (**Figure 10**), were identified in pea root exudates alongside a previously known polyphenol and a chalcone: (1-(2,4-dihydroxyphenyl)-3-hydroxy-3-(4-hydroxyphenyl)-1-propanone and 1-(2,4-dihydroxyphenyl)-3-(4-methoxyphenyl)propenone). These compounds exhibited potent stimulation of *Orobanche* and *Phelipanche* species seed germination. Notably, only peapolyphenol A, 1,3,3-substituted propanone, and 1,3-disubstituted propenone displayed specific stimulatory effects on *O. foetida*, unlike from other *Orobanche* or *Phelipanche* species tested. This specificity is noteworthy because *O. foetida* does not respond to the commonly used synthetic strigolactone analogue GR24 in germination assays.[98]

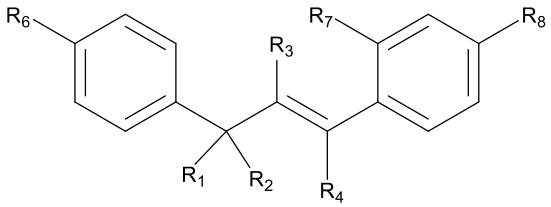

1. R_1+R_2=O R_3=R_6=R_7=OH R_4=R_5=H, R_8=OMe

2. R_1=R_3=R_4=R_5=R_6=R_8=OH R_2=R_7=H

Figure 10. *Structures of peapolyphenols* ***A-C (1-2)****.*

The widespread use of synthetic chemicals, often characterized by low specificity and poor biodegradability, has led to the exploration of alternative approaches for continuous discovering of natural products as models to develop biopesticides with novel chemical structures and modes of action. Thus, in addition to well-known substances like dihydrosorgoleone,[99] sesquiterpene lactones, strigolactones that stimulate parasitic seed germination, various metabolites from different natural compound classes have been identified in the root exudates of pea and common vetch. Furthermore, as legumes are frequently parasitized by broomrape weeds mainly *O.crenata, O. foetida, O. minor and P. aegyptiaca* and therefore their root exudates are an important source of broomrape germination stimulants. The root exudates of several legume crops were studied to discern the form of germination stimulants present. The roots of common vetch (*Vicia sativa*) are a source of a germination-inducing triterpenene, which was isolated from their root exudates and identified as soyasapogenol B (**Figure 11**).

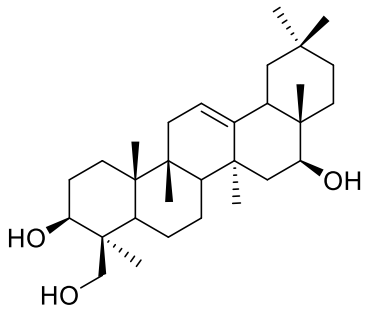

Figure 11. *Structures of soyasapogenol B.*

Similarly, fungal terpenoids and their semi-synthetic derivatives have exhibited seed germination stimulation, while inhibitory effects have been observed in new sesquiterpenoids isolated from *Inula viscosa*. These findings prompted the investigation of the impact of plant allelochemicals and diverse phytotoxins, obtained from fungal pathogens like *Diplodia*, *Didymella*, *Phoma*, *Pyrenophora*, and *Seiridium genera*, on the seed germination and radicle growth of four significant broomrape species. In the study was reported the assessment of metabolites potential from plants and fungi, above mentioned, to either enhance suicidal seed germination or impede germination induced by a germination-inducing factor in *O. crenata*, *O. cumana*, *O. minor*, and *P. ramosa*. 21 phytotoxins from various classes of natural compounds, isolated from pathogenic fungi and an allelopathic plant, were tested.[67] The study revealed that certain compounds, including sphaeropsidin A, cyclohexene epoxides and cytochalasans,[67] negatively affected radicle growth, suggesting potential for herbicides to disrupt the parasitic life cycle before host attachment and resource withdrawal. Some compounds also inhibited broomrape seed germination, strengthening their candidacy for managing broomrape seedbanks in agricultural soils. Specific compounds induced germination in certain broomrape species, highlighting species-specific activity. Notably, inuloxin A and α-costic acid showed a strong effect on *O. cumana*, suggesting a potential strategy for suicidal germination. While some compounds may be too weak for practical field applications, their identification is crucial for understanding the evolutionary strategy of parasitic plants. The study emphasizes the need for further research on these compounds to develop new approaches for parasitic weed control, such as nature-inspired herbicides or engineering resistant crops expressing allelochemicals or phytotoxins

against parasitic weed germination and development. [38] This approach is considered to be as a starting point for the development of new classes of bioherbicides.

Furthermore, recent studies highlighted the activity of compounds from SLs family, in inducing arbuscular mycorrhizal fungi hyphal branching. Arbuscular mycorrhizal (AM) fungi engage in mutualistic symbiotic relationships with over 80% of land plants. These fungi require a host root to complete their life cycle, with limited hyphal growth in the absence of a host. Despite the significance of these interactions, the molecular mechanisms governing signalling and recognition between AM fungi and host plants are not well understood. During the initial stage of host recognition, AM fungal hyphae exhibit extensive branching near host roots before forming the appressorium, which is crucial for penetrating the plant root. Host roots release signalling molecules triggering hyphal branching, but these factors remain unidentified. A branching factor, identified as the strigolactone 5-deoxy-strigol, from the root exudates of *Lotus japonicus* showed the above-mentioned activity. Strigolactones are sesquiterpene lactones known for stimulating seed germination in parasitic weeds. Natural and synthetic strigolactones induced significant hyphal branching in germinating spores of the AM fungus *Gigaspora margarita* at very low concentrations.[100] Thus, some plants are likely to release mixtures of strigolactones into the rhizosphere, exposing both root parasite seeds and arbuscular mycorrhizal (AM) fungi to these compounds when close to any living plant root. However, the germination of root parasite seeds and the branching of AM fungi are often diminished near non-host roots. This indicates that, apart from strigolactones, other signaling chemicals, either enhancing or inhibiting strigolactone action, play a role in the processes of seed germination in root parasitic weeds and hyphal branching in AM fungi. Further investigation is necessary to understand why plants produce various strigolactones and how each contributes to host recognition by both root parasites and AM fungi. Recognizing that strigolactones function as host recognition signals for both symbiosis and parasitism is crucial when developing cost-effective management strategies for root parasitic weeds.[95]

1.6 Inhibition of parasitic plant seed germination

As already mentioned at the end of the above paragraph, the use of inhibitor compounds in the treatment of the cultivated soil infested by seeds of parasitic plants, targets radicle

elongation and, in many cases, induce necrosis of the freshly induced seeds to germinate. The inhibition approach achieves the same result of the stimulation one, i.e. the death of the newly hatched seedling, preventing the completion of parasitic plants life cycle, which results in a reduction of seed production and eradication of seedbank in cultivated soils.

In a work published by Fernández-Aparicio et al. in 2013, was reported the inhibition activity of some allelochemicals isolated from cereals plant, against *O. creanata* seed germination and radicle growth. Cereals belong to the family *Poaceae* (syn. *Gramineae*), which are crucial globally crop for both human and animal consumption, encompassing wheat, barley, oats, rice, maize, sorghum, and rye. Beyond their economic significance, cereals are recognized for their allelopathic effects, which can be exploited for weed management. The allelopathic effects are attributed to various metabolites released by cereals. The research delves into the challenge posed by broomrapes (*Orobanche* and *Phelipanche* spp.), parasitic plants prevalent in Mediterranean regions. Certain broomrape species have adapted to agricultural ecosystems, acting as weeds that feed on the roots of important crops. While diverse control methods have been explored, including physical, cultural, chemical, and biological measures, many are ineffective or lack selectivity for susceptible crops. Presently, farmers primarily rely on resistant cultivars and chemical control with systemic herbicides, but these approaches have drawbacks, necessitating the exploration of novel options. The study identifies the early stages of parasitic weed life, particularly from seed germination to parasitic radicle contact with the host, as crucial targets for control due to the parasitic seedlings' complete dependence on the host for nutrients and water. Broomrape germination is triggered by recognizing of host root exuded metabolites, and interventions aiming at inhibiting parasitic germination or radicle growth could effectively control infections. Some allelochemicals released by cereals, such as hydroxamic acids, caffeic acid, p-coumaric acid, ferulic acid, benzoic acid, gramine, L-tryptophan, and scopoletin, might have applications in controlling broomrapes.[88] Hydroxamic acids, present in both cultivated and wild *Gramineae*, decompose to 2-benzoxazolinone, interfering with the germination and early growth of various crops. Caffeic acid inhibits seed germination and root elongation by disrupting plant water relations, with aquaporins as potential targets. Ferulic and p-coumaric acid inhibit plant growth by targeting acetolactate synthase. Benzoic acid inhibits auxin activity crucial for plant growth. Coumalic acid, an acid pyrone, is implicated in allelopathic

studies. Gramine, an alkaloid in barley, demonstrates inhibitory activity. L-Tryptophan, released into the rhizosphere, inhibits weed root growth. Scopoletin, exuded by cereal roots, is considered responsible for allelopathic effects on weeds. The *O. crenata seeds*, when treated with the negative control showed no signs of germination. In the positive control (GR24), high rates of *O. crenata* seed germination (72.9%) were attained. When used at a concentration greater than 1 μg/mL, 2-benzoxazolinone caused moderate but significant *O. crenata* seed inhibition (about 33%). At all administered concentrations, 6-benzyloxy-2-benzoxazolinone showed no discernible effects. Conversely, germination was significantly suppressed when 6-chloroacetyl-2-benzoxazolinone was used; this suppression was mild but substantial at 1 μg/mL and total at quantities greater than 4 μg/mL. Except for scopoletin, which produced negligible inhibition (19%) at concentrations ≥13 μg/mL, all other allelochemicals examined showed little to no inhibitory action at any dose. Contrary to what was observed for *O. crenata* seed germination, most of the compounds inhibited *O. crenata* radicle growth. The allelochemicals released by cereals, demonstrate orobanchicidal effects, suggesting a practical strategy for broomrape management through the use of cereals as green manure crops or intercrops. However, optimizing this strategy requires understanding the fate of allelochemicals in soil. Specific compounds involved in broomrape suppression vary, and their concentration is influenced by factors such as plant age, organ, cultivar, water stress, temperature, and fertilization. Hydroxamic acids, one type of allelochemical, degrade in soil, reducing the risk of toxic compound accumulation. Timing the incorporation of cereals into the soil is crucial for effective broomrape control during *O. crenata* germination. Breeding programs focused on selecting cereal genotypes with high root exudation levels of germination or radicle growth inhibitors could enhance allelopathic potential. However, allelopathic potential is a complex trait influenced by environmental factors, making it challenging to breed. Classical or marker-assisted breeding, along with understanding the genes responsible for allelochemical biosynthesis, may help enhance allelopathic potential in cereal crops. Selecting cultivars with varying allelochemical content and understanding the genes involved can contribute to the development of high-yielding, allelopathic cultivars through genetic manipulation. The findings aim to contribute to the development of effective and environmentally sustainable strategies for broomrape control in agriculture.[88] Another work published by Andolfi et al. in 2013, researchers isolated four phytotoxic sesquiterpene

lactones, inuloxins A–D, from the aerial parts of the Mediterranean plant Inula viscosa. The phytotoxic activity of these compounds and a-costic acid was evaluated against two parasitic plant species, crenate broomrape (*Orobanche crenata*) and field dodder (*Cuscuta campestris*). Inuloxins A, (**Figure 12**) C, and D exhibited significant activity, causing up to 100% inhibition of seed germination in both parasites. Inuloxin B was less active on *Cuscuta* and inactive against *Orobanche*. A-costic acid (**Figure 12**) had a suppressive effect on dodder seed germination but stimulated broomrape seed germination. These preliminary results suggest potential structure–activity relationships, indicating the phytotoxic potential of the isolated compounds against parasitic plants.[101]

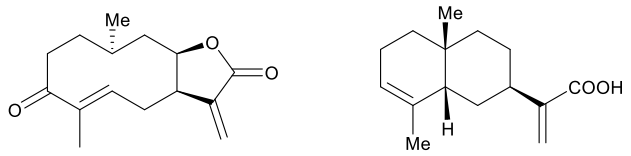

Figure 12. *Inuloxin **A** and α-costic acid structures.*

While *Orobanche* and *Striga* haustoria share a common evolutionary origin, distinctions arise in their host-preattached haustorial stage. In a recent study,[102] haustorium-inducing assays using natural cyclohexene oxides were conducted in *O. cumana*, *O. crenata*, and *S. hermonthica* to identify molecular specificity for haustorium induction across parasitic weed genera. Sphaeropsidone was found to halt radicle elongation and induce attachment organ development in *Striga*, while in *Orobanche*, radicle elongation ceased, and papillae formed at the radicle tip in response to sphaeropsidone. These results suggest a similar mechanism for sphaeropsidone-induced haustorium activity in both Striga and *Orobanche*. A SAR study on hemisynthetic derivatives of sphaeropsidone (**Figure 13**) indicated that the α,β-unsaturated ketone group, the hydroxy group at C-5 (even if esterified), and the epoxy ring play crucial roles in haustorium formation. However, the stereochemistry at C-5, didn't have an essential role in the bioactivity. The SAR study suggested that the ability to initiate haustorium development in *S. hermonthica* might be linked to the conversion of sphaeropsidones and derivatives into 3-methoxyquinone, structurally similar to the haustorium-inducing factor 2,6 dimethoxybenzoquinone found in sorghum root exudates.

Despite structural differences, sphaeropsidones could serve as precursors to the closed 3-methoxyquinone through oxidation. [102]

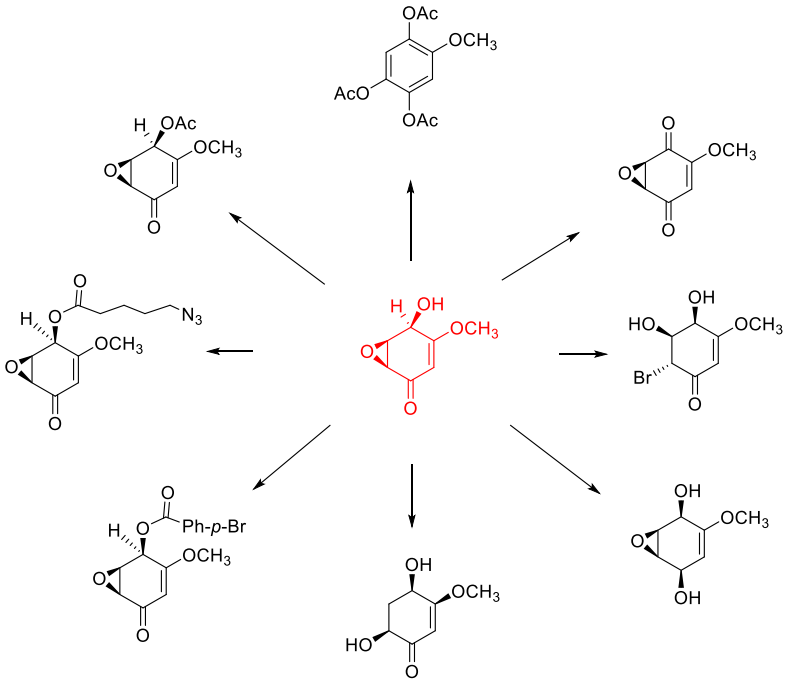

Figure 13. *Sphaeropsidone (red) and its synthetic derivatives.*[103]

In a recent work published by Rial et al. in 2021, focused on the current topic, it is reported that some natural compounds isolated from different resistant varieties of sunflowers root exudates such as the coumarin scopoletin have been identified as inhibitors of haustorial elongation in broomrape. Furthermore, these compounds induce necrosis in germinated seeds, representing a pre-attachment mechanism. Scopoletin, (**Figure 14**) exhibited comparable effects to heliolactone across both resistant and susceptible sunflower varieties. Among the resistant varieties, excluding BR4, scopoletin levels were consistently higher compared to the susceptible ones, often reaching double the values. The scopoletin concentrations in susceptible varieties ranged from 3.60 to 4.32 µg L^{-1}, while in resistant varieties (excluding BR4), they varied from 6.90 to 10.32 µg L^{-1}.[104]

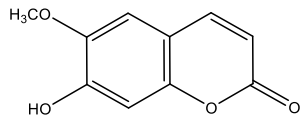

Figure 14. *Scopoletin structure.*

Some allelopathic crops also exudate molecules with the capacity to interfere with the development of broomrape seedlings. Rye plants exudates 4-cyanato-2-methoxyphenol, a 2-cyanato-benzo[1,3]dioxole and a substituted benzo[1,3]dioxolecarbonitrile named ryecyanatines A and B and ryecarbonitrilines B (**Figure 15**) respectively, promote a rapid cessation of *O. cumana*, *O. crenata* and *O. minor* radicle growth hampering the contact of the parasite to the host.[64]

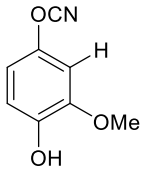

Ryecyanatine A

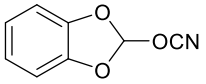

Ryecyanatine B

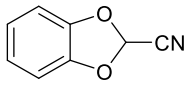

Ryecarbonitriline B

Figure 15. *Ryecyanatine structures.*

Hence, the development of parasitic plants control methodologies based on natural substances could provide a potential alternative, characterized by greater sustainability than traditional methods, in terms of reduced environmental impact and risks associated to animal and human health, resulting in highly effective pest management.

2 Objectives

The aim of the thesis work, was the isolation, chemical characterization and study of biological properties of specialized metabolites, from several weed allelopathic plants, to be selected as suitable candidates for hemi- and total synthesis, along with an exploration of structure-activity relationships (SARs), in order to exploit their potential in field as novel bioherbicides. Indeed, many natural products have potential as novel agrochemicals, but only a few microbial or plant metabolites have been screened for their herbicidal activity. Thus, the allelopathic activity of root extracts from twenty dicotyledonous weed species that usually flourish in broomrape infested fields, was assessed.

The research is summarized below:

- Extraction and bioactivity-guided purification of specialized metabolites from twenty weed plants, mainly *Convolvulus arvensis*, *Reatama raetam*, *Bellardia trixago*, *Centaurea Cineraria* and *Conyza bonariensis*.
- Identification and chemical characterization of bioactive compounds by spectroscopic techniques.
- Bioassays against four root holoparasitic plants: *Orobanche crenata*, *Orobanche cumana*, *Orobanche minor*, *Phelipanche ramosa* and one stem parasitic plant: *Cuscuta campestris*.
- Hemi-synthesis, ecotoxicological and SAR studies of bioactive specialized metabolites
- Total synthesis of (4*Z*)-lachnophyllum lactone
- Early, initial-stage, formulation study

The experiments were mainly carried out at the laboratories of Federico II (Department of Chemical Sciences), at University of Tourin (StrigoLab, Department of Chemistry), at University of Cádiz (Allelopathy Group, INBIO, School of Science) and at CSIC of Cordova (Instituto de Agricultura Sostenible).

3 Materials and methods

3.1 General experimental procedures

Isolation of specialized metabolites. A Bruker 400 Anova Advance (Karlsruhe, Germany) spectrometer was used to record the proton nuclear magnetic resonance (^{1}H NMR) at 400 MHz on. $CDCl_3$ was used as solvent and internal standard. A digital polarimeter JASCO P-1010 (Tokyo, Japan) was used to measure the optical rotations. Liquid Chromatography/Mass Spectrometry-Time of Flight (LC/MS TOF) system AGILENT 6230B (Agilent Technologies, Milan, Italy), High-performance liquid chromatography (HPLC) 1260 Infinity were used to perform Electrospray ionisation mass spectra (ESIMS). Column chromatography (CC) was performed using silica gel (Kieselgel 60, 0.063–0.200 mm, Merck, Darmstadt, Germany). Analytical and preparative silica gel plates (Kieselgel 60, F_{254}, 0.25 and 0.5 mm, respectively, Merck, Darmstadt, Germany), thin-layer chromatography (TLC), were performed. Spots Visualization was carried out by exposure to UV light (254 nm) and/or iodine vapours and/or by spraying first with 10% H_2SO_4 in MeOH and then with 5% phosphomolybdic acid in EtOH, followed by heating at 110 °C for 10 min. Sigma-Aldrich Co. (St. Louis, MO, USA) supplied all the reagents and the solvents**.**

Synthesis. ^{1}H NMR (600 MHz), $^{13}C\{^1H\}$ (150 MHz) NMR spectra were recorded on a Jeol ECZ600R spectrometer used to record the spectra of synthetic products. NMR spectra were recorded at room temperature using residual solvent peak as an internal reference. Chemical shifts (δ) are given in parts per million (ppm) and coupling constants (*J*) in Hertz (Hz). Multiplicities are reported as follows: s (singlet), d (doublet), t (triplet), q (quartet), quint (quintet), sext (sextet), m (multiplet), br (broad). High resolution mass flow-injection analyses were run on a high resolving power hybrid mass spectrometer (HRMS) Orbitrap Fusion (Thermo Scientific, Rodano, Italy), equipped with an ESI ion source. Samples were analysed in methanol solution using a syringe pump at a flow rate of 25 μL/min. Tuning parameters adopted for the ESI source: source voltage 4.0 kV. The heated capillary temperature was maintained at 270 °C. The mass accuracy of the recorded ions (vs. the calculated ones) was ± 2.5 mmu (milli-mass units). Analyses were run using both full MS (150-2000 *m/z* range) and MS/MS acquisition, at 50000 resolutions (200 *m/z*). Low-

resolution GC-MS spectra were recorded at an ionizing voltage of 70 eV on a HP 5989B mass selective detector connected to an HP 5890 GC with a methyl silicone capillary column (EI). Flasks and all equipment used for the generation and reaction of moisture-sensitive compounds were dried by electric heat gun under argon. Reagents and solvents (HPLC grade) were purchased from Sigma-Aldrich. Unless specified, all commercially available reagents were used as received without further purifications. Reactions were monitored by thin-layer chromatography (TLC) carried out on 0.25 mm silica gel coated aluminum plates (60 Merck F_{254}) with UV light (254 nm) as visualizing agent. R_f values refer to TLC carried out on silica gel plates. Chromatographic separations were carried out under pressure on silica gel (40-63 μm, 230-400 mesh) using flash-column techniques. The exact concentration of *n*-BuLi in hexane solution (Sigma-Aldrich) was determined by titration with *N*-benzylbenzamide in anhydrous THF prior to use.[105] Full characterization data, including copies of ^{1}H, $^{13}C\{^{1}H\}$ NMR spectra, have been reported for both the newly synthesized compounds and the known isolated and purified compounds.

3.2 In vitro bioassays against growth of *Cuscuta* seedling

Seeds of *C. campestris* were collected in the summer of 2022 from mature plants parasitizing pea plants at the Institute for Sustainable Agriculture (IAS-CSIC), Alameda del Obispo Research Center (Córdoba, southern Spain, coordinates 37.856 N, 4.806 W, datum WGS84). Dry seeds were separated from capsules by sifting with a 0.6 mm mesh sieve followed by winnowing with a fan. Seeds were stored dry in the dark at room temperature until use for this work.

The germination of *C. campestris* seeds is hindered by a robust seed coat that safeguards seed bank viability in agricultural fields over an extended period.[60] *Cuscuta* germination in the laboratory, was induced by scarification with sulfuric acid for 45 min to eliminate the hard coat.[106] Scarification was followed by thorough rinsing and air drying under a flow cabinet. Then, five scarified *Cuscuta* seeds were placed on 5 cm-diameter sterilized filter paper discs inside 5.5 cm-diameter Petri dishes using tweezers. Dimethyl sulfoxide or methanol solutions of each compound were diluted up to 1 mM in sterilized distilled water. The final methanol concentration, in all treatments, was 2%. For each treatment, triplicate aliquots of 1 mL were applied to filter paper discs containing *Cuscuta* seeds. Triplicate aliquots of a treatment with only sterile distilled water and 2% methanol served as the control. Petri dishes with treated *Cuscuta* seeds were sealed with parafilm, wrapped in aluminum foil, and kept in the dark in a growth chamber with an average temperature of 23 °C and relative humidity of 65% for five days.

In the second in vitro bioassay all the compounds were dissolved in dimethyl sulfoxide and diluted up to 1, 0.5, 0.25, and 0.1 mM in sterilized distilled water. Triplicate aliquots of 1 mL were applied to filter paper discs containing five scarified *Cuscuta* seeds, following the same scarification process as described earlier. Triplicate aliquots of a treatment containing only sterile distilled water and 2% dimethyl sulfoxide were used as a control. Petri dishes with treated *Cuscuta* seeds were incubated in the same conditions as previously described.

3.3 In vitro bioassays against growth of broomrape seedling

All compounds were tested in two independent bioassays, broomrape suicidal germination and radicle growth, conducted according to previous reported protocols.[40] Seeds of four broomrape species *P. ramose*, *O. crenata*, *O. minor* and *O. cumana* underwent surface sterilization by immersion in 0.5% (w/v) NaOCl and 0.02% (v/v) Tween 20 for 5 min, were rinsed thoroughly with sterile distilled water, and dried in a laminar airflow cabinet. Initially, broomrape seeds underwent a conditioning period using warm stratification. Approximately 100 seeds of each broomrape species were placed separately on 9 mm-diameter glass fibre filter paper discs (GFFP) (Whatman International Ltd., Maidstone, UK), moistened with 50 µL of sterile distilled water, and placed in incubators at 23 ◦C for 10 days inside Parafilm-sealed Petri dishes, to allow seed conditioning. Then, GFFP discs containing conditioned broomrape seeds were transferred onto a sterile sheet of filter paper and transferred to new 9 cm sterile Petri dishes. For the assay of suicidal germination, induction stock solutions of each metabolite respectively dissolved in methanol were individually diluted in sterile distilled water up to an equivalent concentration of 100 µM. For the assay of radicle growth inhibition, stock solutions of each metabolite respectively dissolved in methanol were individually diluted to 100 µM using an aqueous solution of GR24. For each assay, triplicate aliquots of each sample were applied to GFFP discs containing conditioned broomrape seeds. Treated seeds were incubated in the dark at 23 ◦C for 7 days, and the percent of germination and radicle growth was determined for each GFFP disc, as described previously,[67] using a stereoscopic microscope (Leica S9i, Leica Microsystems GmbH, Wetzlar, Germany). For germination induction assays, the germination was determined by counting the number of germinated seeds on 100 seeds for each GFFP disk. For the characteristic of radicle growth, the value used was the average of 10 randomly selected radicles per GFFP disc.[107] The germination induction percentage of each metabolite was then calculated relative to the average germination of control seeds (seeds treated with water), and the percentage of radicle growth inhibition of each treatment was then calculated relative to the average radicle growth of control treatment (radicles treated with GR24).[108]

3.4 Statistical Analysis

All bioassays were performed using a completely randomized design. Percentage data were approximated to normal frequency distribution by means of angular transformation and subjected to analysis of variance (ANOVA) using SPSS software forWindows (SPSS Inc., Chicago, IL, USA). The significance of mean differences among treatments was evaluated by the Tukey test. The null hypothesis was rejected at the level of 0.05.

3.5 Calculation of CLogP

Calculations were performed using ChemOffice v20.1 (PerkinElmer, Wal-tham, MA, USA) and the appropriate tool in ChemDraw Professional, while the number of rotable bonds, H-bond acceptors and H-bond donors were calculated using the SwissADME software.[109,110]

3.6 Bioactive compounds phytotoxic screening against *C. campestris*

18 compounds (**Figure 16**) were used to perform a first screening. All the chemicals, unless otherwise specified, were purchased from Sigma-Aldrich (St. Louis, MO, USA): L-lysine (**1**, cat. no. L5501), gramine (**2**, cat. no. G10806), L-tryptophan (**3**, cat. no. PHR1176), L-phenilalanine (**4**, cat. no. P1150000), 2-benzoxazolinone (**5**, cat. no. 157058), hydrocinnamic acid (**6**, cat. no. 135232), *p*-coumaric acid (**7**, cat. no. C9008), caffeic acid (**8**, cat. no. C0625), ferulic acid (**9** cat. no. 12870-8), scopoletin (**10**, cat. no. S2500), umbelliferone (**11**, cat. no. 54826), vanillic acid (**12,** 8.41025.0050), benzoic acid (**13**, cat. no. 242381), coumalic acid (**14**, cat. no. C85409), sesamol (**15**, cat. no. 11428673) from Thermo Fisher Scientific (Waltham, MA, USA), 1,4-benzoquinone (**16**, cat. no. B10358), naringenin (**17,** cat. no. L09834) from Thermo Fisher Scientific and lastly pisatin (**18**) obtained by purification from natural source in our laboratory, as described in literature.[98]

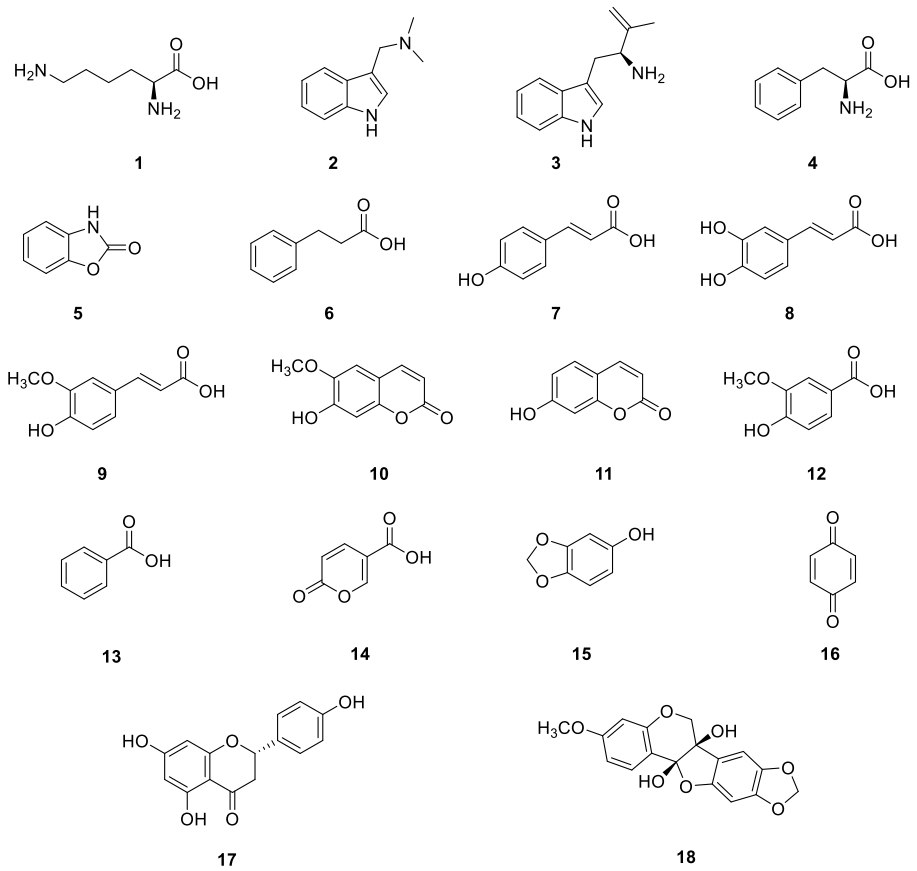

Figure 16 *Chemical structures of the compounds studied in the first screening: L-lysine (**1**), gramine (**2**), L-tryptophan (**3**), L-phenilalanine (**4**), 2-benzoxazolinone (**5**), hydrocinnamic acid (**6**), p-coumaric acid (**7**), caffeic acid (**8**), ferulic acid (**9**), scopoletin (**10**), umbelliferone (**11**), vanillic acid (**12**), benzoic acid (**13**), coumalic acid (14), sesamol (**15**), 1,4-benzoquinone (**16**), naringenin (**17**) and pisatin (**18**).*

SAR study on four 2-benzoxazolinone (**5**) and five hydrocinnamic acid (**6**) structural derivatives were conducted. All the compounds (**Figure 17**) were purchased from Sigma-Aldrich: 3-(4-fluorophenyl)propionic acid (**19**, cat. no. 560502), 3-(4-chlorophenyl)propionic acid (**20**, cat. no. 656151), 3-(4-bromophenyl)propionic acid (**21**, cat. no. 595438), 3-(4-hydroxyphenyl)propionic acid (**22**, cat. no. H52406), 3-(2-hydroxyphenyl)propionic acid (**23**, cat. no. 393533), 6-hydroxy-2(3*H*)-benzoxazolinone (**24**, cat. no. 705500), 6-benzyloxy-2-benzoxazolinone (**25**, cat. no. 653462), 6-chloroacetyl-2-benzoxazolinone (**26**, cat. no. 535400), 5-bromo-2-benzoxazolinone (**27**, cat. no. 653454).

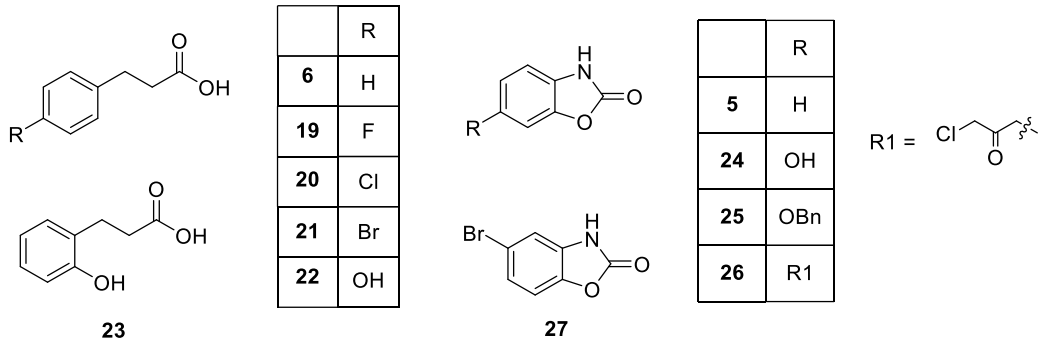

Figure 17 *Chemical structures of derivatives of hydrocinnamic acid (**6**): 3-(4-fluorophenyl)propionic acid (**19**), 3-(4-chlorophenyl)propionic acid (**20**), 3-(4-bromophenyl)propionic acid (**21**), 3-(4- hydroxyphenyl)propionic acid (**22**), 3-(2-hydroxyphenyl)propionic acid (**23**), and derivatives of 2-benzoxazolinone (**5**): 6-hydroxy-2(3H)-benzoxazolinone (**24**), 6-benzyloxy-2-benzoxazolinone (**25**), 6-chloroacetyl-2-benzoxazolinone (**26**), 5-bromo-2-benzoxazolinone (**27**).*

3.7 Identification of structural features of hydrocinnamic acid related to its allelopathic activity against the parasitic weed *C. campestris*

Chemicals. Hydrocinnamic acid and its 21 analogues (**Figure 18**) were procured from Sigma-Aldrich (St. Louis, MO, USA): hydrocinnamic acid (**6**, cat. no. 135232), 3-(2-hydroxyphenyl)propionic acid (**23**, cat. no. 393533), 3-(2-carboxyphenyl)propionic acid (**27**, cat. no. 406465), 3-(3- hydroxyphenyl)propanoic acid (**28**, cat. no. PH011597), 3-(3-methoxyphenyl)propionic acid (**29**, cat. no. 349763), 3-(3-chlorophenyl)propionic acid (**30**, cat. no. 631302), 3-(4- hydroxyphenyl)propionic acid (**22**, cat. no. H52406), 3-(4-methoxyphenyl)propanoic acid (**31**, cat. no. M23527), 3-(*p*-tolyl)propionic acid (**32**, cat. no. 118265), 4-(trifluoromethyl) hydrocinnamic acid (**33**, cat. no. 457035), 3-(4-cyanophenyl)propionic acid (**34**, cat. no. 746010), 3-(4-aminophenyl)propionic acid (**35**, cat. no. 560251), 3-(4-fluorophenyl)propionic acid (**19**, cat. no. 560502), 3-(4-chlorophenyl)propionic acid (**20**, cat. no. 656151), 3-(4-bromophenyl)propionic acid (**21**, cat. no. 595438), 3-(4-carboxyphenyl)propionic acid (**36**, cat. no. 531553), 3,4-dihydroxyhydrocinnamic acid (**37**, cat. no. 102601), 3-(3-hydroxy-4-methoxyphenyl)propionic acid (**38**, cat. no. CDS006461), 3-(3-chloro-4-methoxyphenyl) propionic acid (**39**, cat. no. 638773), hydrocinnamoyl chloride (**40**, cat. no. 249440), ethyl 3-phenylpropionate (**41**, cat. no. 284416), 3-phenyl-1-propanol (**42**, cat. no. 140856).

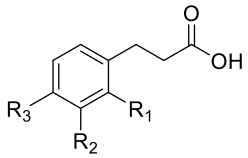

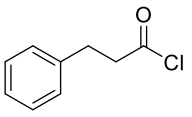

40

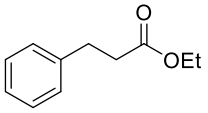

41

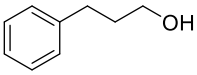

42

	R_1	R_2	R_3		R_1	R_2	R_3
6	H	H	H	**34**	H	H	CN
23	H	H	H	**35**	H	H	NH_2
27	OH	H	H	**19**	H	H	F
28	COOH	OH	H	**20**	H	H	Cl
29	H	OCH_3	H	**21**	H	H	Br
30	H	Cl	H	**36**	H	H	COOH
22	H	H	OH	**37**	H	OH	OH
31	H	H	OCH_3	**38**	H	OH	OCH_3
32	H	H	CH_3	**39**	H	Cl	OCH_3
33	H	H	CF_3				

Figure 18 *Chemical structures of hydrocinnamic acid and derivatives used in the study.*

3.8 Structure-activity relationship (SAR) study of trans-Cinnamic acid and derivatives on the parasitic weed *C. campestris*

Chemicals. *trans*-Cinnamic acid and its analogs (**Figure 19**) were purchased from Sigma-Aldrich (St. Louis, MO, USA): *trans*-cinnamic acid (**43**, cat. n. C80857), hydrocinnamic acid (**6**, cat. n. 135232), 3-phenylpropionaldehyde (**44**, cat. n. 8045420100), *trans*-cinnamaldehyde (**45**, cat. n. 8025050250), *trans*-cinnamyl alcohol (**46**, cat. n. 108197), *trans*-*o*-coumaric acid (**47**, cat. n. H22809), *trans*-*m*-coumaric acid (**48**, cat. n. H23007), *trans*-*p*-coumaric acid (**49**, cat. n. C9008), *trans*-caffeic acid (**50**, cat. n. C0625), *trans*-ferulic acid (**51**, cat. n. 128708), *trans*-sinapic acid (**52**, cat. n. D7927), *trans*-4-methoxycinnamic acid (**53**, cat. n. M13807), *trans*-2-methylcinnamic acid (**54**, cat. n. 433101), *trans*-4-methylcinnamic acid (**55**, cat. n. M35800), *trans*-2-(trifluoromethyl)cinnamic acid (**56**, cat. n. 233080), trans-4-(trifluoromethyl)cinnamic acid (**57**, cat. n. 233099), *trans*-3-fluorocinnamic acid (**58**, cat. n. 290483), *trans*-3-chlorocinnamic acid (**59**, cat. n. 8413240010), *trans*-4-fluorocinnamic acid (**60**, cat. n. 222720), *trans*-4-chlorocinnamic acid (**61**, cat. n. C31600), trans-4-bromocinnamic acid (**62**, cat. n. 260975), *trans*-3,4-(methylenedioxy)cinnamic acid (**63**, cat. n. 146242), methyl *trans*-cinnamate (**64**, cat. n. 173282), benzylcinnamate (**65**, cat. n. 234214), and phenylpropiolic acid (**66**, cat. n. P31205).

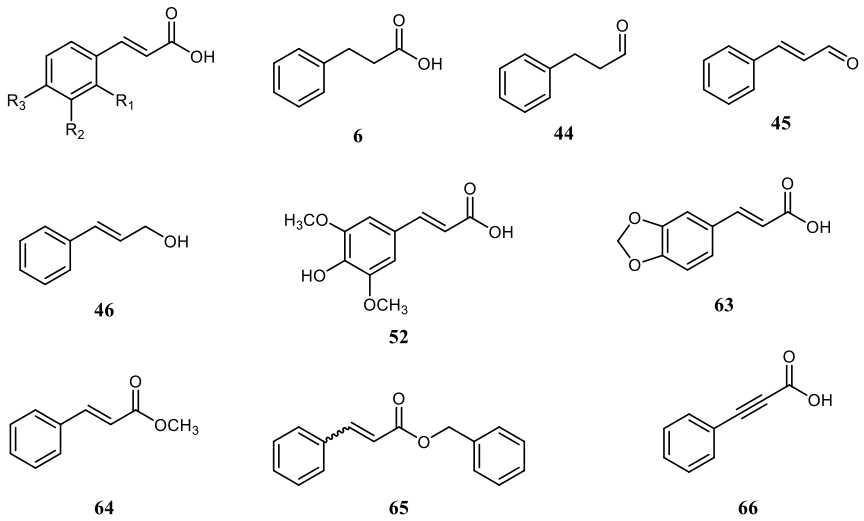

	R_1	R_2	R_3		R_1	R_2	R_3
43	H	H	H	**55**	H	H	CH_3
47	OH	H	H	**56**	CF_3	H	H
48	H	OH	H	**57**	H	H	CF_3
49	H	H	OH	**58**	H	F	H
50	H	OH	OH	**59**	H	Cl	H
51	H	OCH_3	OH	**60**	H	H	F
53	H	H	OCH_3	**61**	H	H	Cl
54	CH_3	H	H	**62**	H	H	Br

Figure 19. *Chemical structures of trans-cinnamic acid derivatives used in the study.*

3.9 Plant material and growth conditions of weed species

All the weed species seeds reported in **Table 1**, unless otherwise specified in this section, were gathered during the 2016–2017 season from a buckwheat field at the Institute for Sustainable Agriculture (IASCSIC), Alameda del Obispo Research Center (Cordoba, southern Spain, coordinates 37.856 N, 4.806 W, datum WGS84). These weed species are commonly found in agricultural fields in southern Spain, where *O. crenata* and *O. cumana* also flourish. In the spring of 2020, the collected weed seeds underwent surface sterilization through immersion in 0.5% (w/v) NaOCl and 0.02% (v/v) Tween 20, for 5 minutes. They were then thoroughly rinsed with sterile distilled water and dried in a laminar airflow cabinet. The seeds were planted in pots, each containing a mixture of 1:1 sand and peat (1 L each). These pots were kept in a greenhouse for 40 days, with a day/night temperature regime of 23/20 °C and a light/dark cycle of 16/8 hours.

Between December 2017 and February 2018, the aerial parts of *Retama raetam* plant were harvested during the plant's flowering stage. The investigation took place in the Souf region, situated in the northeastern part of the Algerian Sahara, spanning from 33° to 34° north latitude and 6° to 8° longitude, with an elevation of 40 meters above sea level.[111] The plant material underwent a thorough cleansing with distilled water to eliminate dust particles and was subsequently air-dried at room temperature for several days. Finally, it was processed into a powder using a blender.

Two populations of *Bellardia trixago*, distinguished by flower color (white and yellow), were harvested during the flowering stage in spring 2021 in Cordoba, southern Spain (coordinates 37.856 N, 4.806 W, datum WGS84). Following harvest, *Bellardia trixago* plants were promptly transported to the laboratory. The plants were divided into three components: flowers, above-ground green organs (stems and leaves), and roots. Each component was rapidly frozen with liquid nitrogen, preserved at -80 °C, lyophilized, and the resulting dry material stored in darkness at 4 °C until further use. *Orobanche* seeds were obtained from mature *O. cumana* infected sunflower plants in southern Spain. The dry parasitic seeds were separated from capsules using winnowing with a 0.6 mm mesh sieve and stored in darkness at room temperature until utilized for this study.

In February 2022, specimens of *Centaurea cineraria* L. subsp. *cineraria* were gathered in the municipality of Massa Lubrense, located in the Metropolitan City of Naples,

Italy. The collection occurred during a period when the plants were not flowering or fruiting, focusing on the terminal portions of leafy twigs from approximately 30 individuals. To minimize the risk of sampling clonal individuals, these individuals were spaced 5-10 meters apart. Subsequently, the collected plant material underwent a cleansing process with distilled water to eliminate dust particles, followed by air-drying for a few days at room temperature. The dried material was then ground into a powder using a blender. For the study, seeds of broomrape (*Orobanche* and *Phelipanche*) from four species of root parasitic weeds were utilized. *O. crenata* seeds were collected in 2019 from mature *Orobanche* plants infecting peas in Spain, while *O. cumana* seeds were collected in 2017 from mature *Orobanche* plants infecting sunflowers in Spain. Additionally, seeds of *O. minor* were collected in 2015 from *Orobanche* plants infecting red clover in France, and seeds of *P. ramosa* were collected in 2015 from *Phelipanche* plants infecting tobacco in France. Broomrape seeds were gathered using a 0.6 mm mesh-size sieve (Filtra) from the dry inflorescences of *O. crenata* infecting faba bean plants in Spain, *O. cumana* infecting sunflower plants in Turkey, *O. minor* infecting red clover in France, and *P. ramosa* infecting oilseed rape in France. These collected seeds were kept dry in the dark at 4°C until needed.

Plant family	Plant species	EPPO code	Weight in mg of CH_2Cl_2 Organic extract. (extraction %)
Amaranthaceae	*Amaranthus albus*	AMAAL	14.4 (0.2)
Amaranthaceae	*Amaranthus retroflexus*	AMARE	19.9 (0.3)
Asteraceae	*Conyza bonariensis*	ERIBO	23.6 (0.4) **a***
Asteraceae	*Silybum marianum*	SLYMA	16.6 (0.2)
Asteraceae	*Centaurea cineraria*	CENCI	492.1 (1.0)
Boraginaceae	*Heliotropium europaeum*	HEOEU	21.2 (0.3)
Brassicaceae	*Capsella bursa-pastoris*	CAPBP	22.1 (0.8)
Brassicaceae	*Diplotaxis erucoides*	DIPER	29.6 (0.5)
Brassicaceae	*Diplotaxis virgata*	DIPVG	41.9 (0.7)
Convolvulaceae	*Convolvulus arvensis*	CONAR	77.4 (1.3)
Fabaceae	*Retama raetam*	RTARE	6700.0 (2.5)
Malvaceae	*Malva sylvestris*	MALSI	36.2 (0.7)
Orobanchaceae	*Bellardia trixago*	BEQTR	**b***
Papaveraceae	*Fumaria officinalis*	FUMOF	39.0 (1.9)
Polygonaceae	*Polygonum aviculare*	POLAV	29.7 (0.5)
Portulacaceae	*Portulaca oleracea*	POROL	25.5 (0.4))
Solanaceae	*Datura stramonium*	DATST	18.6 (0.3)
Solanaceae	*Solanum nigrum*	SOLNI	30.1 (0.5)
Urticaceae	*Urtica dioica*	URTDI	19.3 (0.3)
Zygophyllales	*Tribulus terrestris*	TRBTE	27.5 (0.5)

Table 1 *Plants selected by observation on field, for their allelophatic activity.* ***a**** *= aerial parts of Conyza bonariensis were studied too.* ***b**** *= Different organs of Bellardia trixago plant were extracted, however the green organs of the white-flowered population were the most studied due to the most interesting chromatographic profile and highest yield of ethyl acetate extraction (1.45 g, 0.77 %).*

Since, broomrapes primarily infect the roots of host crops and typically develop underground, extracts from the roots of weeds were utilized. The goal was to identify potential allelopathic signals present in plant rhizospheres. To collect the roots and the aerial parts, weed plants in the vegetative stage were taken out of the pots. The roots were carefully washed in distilled water, quickly dried with filter paper, and immediately frozen. The frozen roots were then stored at -80°C until lyophilization.

3.10 Extraction of weed plants dried roots and aerial parts

Approximately 6.0 g of dried root tissue of each weed plant was milled in a *Waring* blender, and the resulting powder was extracted at room temperature, overnight with a H_2O/MeOH (200 mL, 1:1, v:v) mixture, under stirring in the dark. The resulting suspension was then centrifuged for 1 h at 7000 r.p.m., at 4 °C. The supernatants were, in most cases, extracted with solvents of increasing polarity (*n*-hexane, CH_2Cl_2 and EtOAc). The organic extracts were combined, dried (adding Na_2SO_4), filtered and evaporated under reduced pressure.[112,113]

Initially, 3.0 g of *B. trixago* flowers, green organs and roots of each population were separately extracted, using the procedure just described, in order to perform a preliminary activity screening against broomrapes parasitic plants. The weight of each extract is reported in **Table 2**.

***Bartsia trixago* organ**	***n*-Hexane extract wt.**	**CH_2Cl_2 extract wt.**	**EtOAc extract wt.**
White flowers	2.8 mg	12.1 mg	27.3 mg
White roots	1.3 mg	3.4 mg	13.4 mg
White green organs	1.0 mg	10.5 mg	44.6 mg
Yellow flowers	1.2 mg	10.1 mg	21.0 mg
Yellow roots	1.4 mg	3.8 mg	13.8 mg
Yellow green organs	2.7 mg	19.3 mg	11.5 mg

Table 2 *Organic extract weights obtained from different Bartsia trixago organs.*

The aerial parts of *C. cineraria* plant were extracted using the same procedure, while the total *R. raetam* plant material was not subjected to an initial screening due to the already known allelopathic activity of these native Algerian Saharan ecosystem plant.[111]

4 Experimental

4.1 *Convolvulus arvensis*

Plant material. *C. arvensis* seeds were surface sterilized using a solution of 0.5% (w/v) sodium hypochlorite and 0.02% (v/v) Tween 20 for 5 minutes. Thereafter, the seeds were thoroughly rinsed with distilled water and dried in a laminar airflow cabinet. Subsequentially, mechanical scarification was applied to the *C. arvensis* seeds, and they were then planted in a greenhouse in 1 L pots filled with a mixture of sand and peat (1:1, v:v). After a growth period of 40 days, under conditions of 23/20 °C and a 16/8 h day/night cycle, *Convolvulus* plant stems were cut at a height of 2–3 cm above the soil surface. The roots were carefully washed, dried with filter paper, promptly frozen, and stored at -80 °C until lyophilization. The lyophilized roots of *C. arvensis* (235.0 g) were extracted using the procedure described in section **3.10**.

Activity-guided fractionation of Convolvulus arvensis extract. The CH_2Cl_2 residue (3.754 g) was purified by column chromatography (CC), eluted with a $CHCl_3$/*i*-PrOH mixture, increasing the *i*-PrOH percentage from 5 to 30, followed by the use of EtOH to elute the most polar compounds, to finally afford 10 groups of homogeneous fractions. The activity of the obtained fractions was tested in radicle growth bioassays as described above. The ninth fraction, namely F9 (198.95 mg), showed the strongest toxicity towards broomrape radicles. Hence, it was further purified by reversed-phase CC, at medium pressure, eluted by CH_3CN/H_2O (7:3 v/v), yielding three fractions, namely F9.1–F9.3 and tested. The most phytotoxic one, F9.2 was selected for further analysis as described in the following paragraphs (**Figure 20**).

Acid hydrolysis, aglicones extraction and monosaccharides TLC analysis of glycosides fractions. Hydrolyzation with 2M TFA (1 mL) of F9.2 (2.0 mg), at 120 °C for 2 h, was performed. Then the reaction was stopped adding Milli Q water and dried under reduced pressure. The obtained residue was dissolved in MeOH and analyzed by TLC on silica gel, eluted with *i*-PrOH/H_2O (8:2, v/v), in comparison with standard of fucose,

galactose, mannose, xylose, glucose and rhamnose. Afterwards, extraction with EtOAc allowed to separate the aglycone from the hydrolyzed solution, and the extract obtained was named F9.2-aglycone (1.1 mg). TLC an1 ^{1}H NMR analysis, were carried out on the F9.2-aglycone, after reaction with an ethereal solution of diazomethane (**Figure 20**).

Derivatization of monosaccharides and the HPLC analysis of the aldose enantiomers derivative. D-Derivatives: L-cysteine methyl ester (12.0 mg) was reacted with D-glucose (10.0 mg), in pyridine (300 μL), at 60 °C for 1 h. Then, phenyl isothiocyanate (100 μL) was added to the mixture and further reacted at 60 °C for 1 h. The residue obtained after solvent evaporation, was purified by TLC eluted with $CHCl_3$:MeOH:H_2O (40:10:1, v/v/v), to afford a white amorphous solid (8.0 mg). The same procedure was applied to D-galactose, D-mannose, D-rhamnose, D-fucose, D-arabinose and D-xylose. Furthermore, L-aldose (10 mg) was reacted using the same method described for the D-enantiomers. ^{1}H NMR and ESI MS analysis were caried out on the obtained derivatives. The spectroscopic data were in accordance with those previously reported in literature.[114] The hydrolyzed mixtures, derived by the just described purification step of the hydrolyzed F9.2, were dissolved in pyridine (150 μL) and converted into the corresponding methyl 2-(polyhydroxyalkyl)-3-(o-tolylthiocarbomoyl)-thiazolidine-4R-carboxylates through a reaction with L-cysteine methyl ester hydrochloride (6.0 mg) and phenyl isothiocyanate (50 μL). Analytical HPLC analysis was conducted using a Chromaster system (VWR, Hitachi, Darmstadt, Germany) equipped with an RP18 Purospher® STAR column (Merck, Darmstadt, Germany) with particles size of 5 μm and dimensions of 250 X 4.6 mm², with an isocratic elution, using 25% CH_3CN in a 0.1% HCOOH water solution at a flow rate of 0.8 mL/min. The analysis wavelength was set at 250 nm, for peaks detection of D-glucose, L-rhamnose, and D-fucose.[115–117]

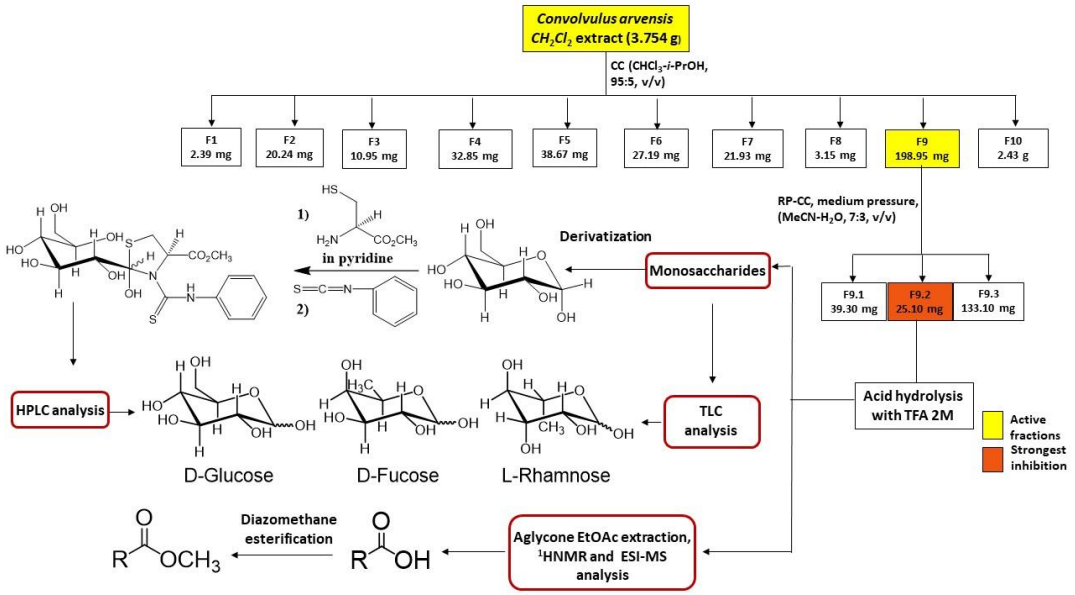

Figure 20. *Activity-guided purification scheme of arvensic acids mixtures and monosaccharides analysis.*

4.2 *Retama raetam*

Flavonoids and isoflavonoids extraction and purification. Plant material (273.7 g) was extracted using the procedure reported in the section **3.10**. The CH_2Cl_2 residue (6.7 g) was purified by CC eluted with CH_2Cl_2/i-PrOH (9/1, v/v), yielding thirteen homogeneous fractions (F1–F13). The most active fractions (F2–F5, **Figure 21**) were further purified. In particular, the F2 residue (70.2 mg) was purified by CC eluted with CH_2Cl_2/MeOH (97/3, v/v), yielding seven groups of homogeneous fractions (F2.1–F2.7). The F2.3 residue (21.2 mg), was further purified by TLC eluted with CH_2Cl_2/MeOH (97/3, v/v), yielding alpinumisoflavone (**67**, 12.9 mg). The combined F3-F4 (235.6 mg), were purified by CC eluted with CHCl3/*i*-PrOH (95/5, v/v), affording seven further fractions (F3-4.1-F3-4.7). The F3-4.4 was subjected to two TLC purification steps, eluted with $CHCl_3$/MeOH (95/5, v/v) and EtOAc/n-hexane (4/6, v/v), respectively, yielding hydroxyalpinumisoflavone (**68**, 3.2 mg), laburnetin (**69**, 1.3 mg), and licoflavone C (**70**, 3.1 mg). From the purification of F5 residues (98.2 mg), by CC eluted with CH_2Cl_2/MeOH (95/5, v/v), other four fractions were obtained (F5.1-F5.4). The F5.2 was further purified by a three times eluted TLC, with acetone/*n*-hexane (4/6, v/v), in order to afford four metabolites, identified as retamasin B (**71**, 3.3 mg), ephedroidin (**72**, 10.1 mg), and further amounts of laburnetin (**69**, 1.0 mg) and licoflavone C (**70**, 1.1 mg).

Alpinumisoflavone (**67**): ^{1}H and ^{13}C NMR data are in agreement with those previously reported.[118,119] ESI MS (+) *m/z*: 695 $[2M + Na]^+$, 337 $[M + H]^+$.

Hydroxyalpinumisoflavone (**68**): 1H NMR data are in agreement with those previously reported.[108] ESI MS (+) *m/z*: 727 $[2M + Na]^+$, 333 $[M + H]^+$.

Laburnetin (**69**): ^{1}H and ^{13}C NMR data are in agreement with those previously reported.[120] ESI-MS (+), *m/z*: 355 $[M + H]^+$.

Licoflavone C (**70**): ^{1}H and ^{13}C NMR data are in agreement with those previously reported.[121] ESI-MS (+), *m/z*: 339 $[M + H]^+$.

Retamasin B (**71**): ^{1}H and ^{13}C NMR data are in agreement with those previously reported.[122] ESI-MS (+), *m/z*: 727 $[2M + Na]^+$, 353 $[M + H]^+$.

Ephedroidin (**72**): [α]D25 0 (c 0.4, MeOH), ^{1}H and ^{13}C NMR data are in agreement with those previously reported.[120] ESI-MS (+), *m/z*: 355 $[M + H]^+$.

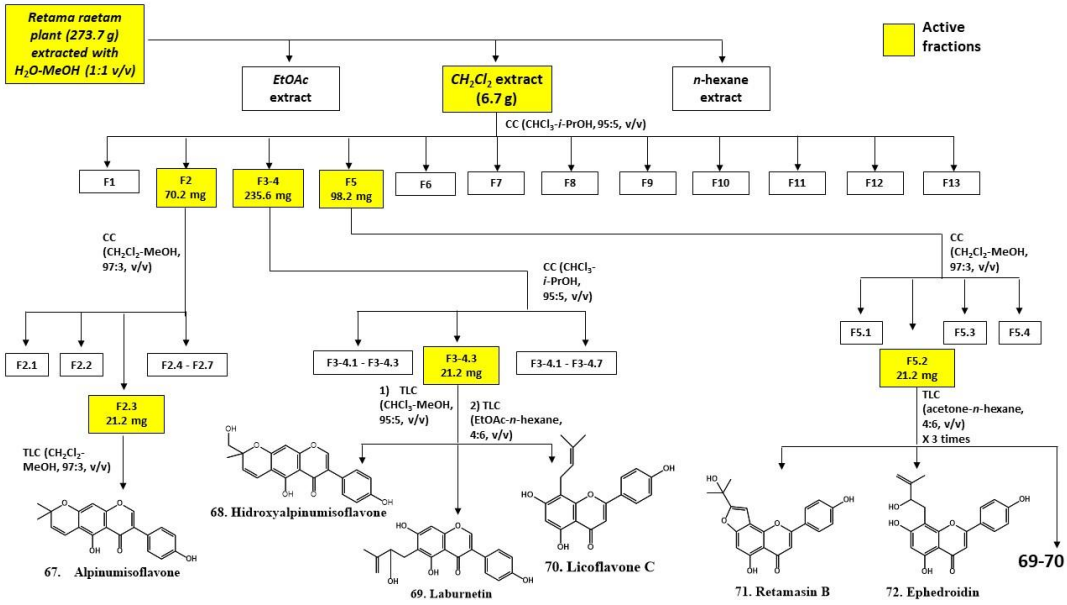

Figure 21. *Retama raetam* specialized metabolites purification scheme.

X-ray Crystal Structure Analysis of Alpinumisoflavone. Compound **67** was dissolved in a low amount of MeOH:H_2O (9.0:1.0) mixture solvent and slowly evaporated to afford a suitable single crystal for X-ray analysis. The data of X X-ray diffraction were collected on a Bruker-Nonius KappaCCD diffractometer (Bruker-Nonius, Delft, The Netherlands) (graphite mono-chromated MoKα radiation, λ = 0.71073 Å). The structure was solved by direct methods (SIR97 program)[123] and anisotropically refined by the full-matrix least-squares method on F2 against all independent measured reflections (SHELXL-2018/3 program).[124] H atoms of hydroxy groups were located in different Fourier maps and freely refined. All the other hydrogen atoms were introduced in calculated positions and refined according to the riding model. Platon TwinRotMap check suggests 2-axis (0 0 1) [1 0 4] twinning with basf 0.10, and refinement was performed using the HKLF5 data file. The figure of the ORTEP view was generated using the ORTEP-3 program.[125] Crystallographic Data of 1: C20H16O5; Mr= 336.33; monoclinic, space group P21/c; a = 13.774(4) Å, b = 5.940(3)Å, c = 19.936(5) Å, β = 99.673(15)◦; V = 1607.9(10) Å3; T = 173 K; Z = 4; Dc = 1.389 g cm−3; μ = 0.100 mm−1, F (000) = 704. Independent reflections: 9456. The final R1

values were 0.0569, wR2 = 0.1129 (I > 2σ(I)). Goodness of fit on F2 = 1.081. Largest diff. peak and hole = 0.203 and −0.252 e/Å3.

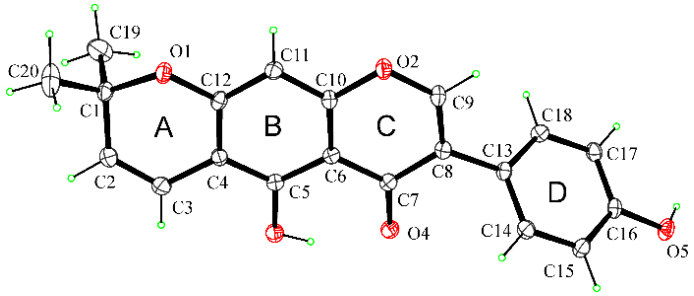

Figure 22. ORTEP view of alpinumisoflavone (**67**) with thermal ellipsoids drawn at the 30% probability level.

Stemphylium vesicarium Antifungal Assay. *R. raetam* aerial parts extract was tested against the phytopathogen *Stemphylium vesicarium*, following a method reported by Yusoff et al.,[126] with few modifications. Dissolution of the crude extract and the fractions obtained by it, in MeOH, mixed with 5 mL of cooled PDA to obtain a final concentration of 2 mg/mL and 250 µg/mL, respectively, were prepared. Then, the mix was carefully located into Petri dishes and left to dry. Fungal plugs (6 × 6 mm diameter) derived from the growing edge of *S. vesicarium* mycelium were positioned at the centre of the plates and cultivated for 7 days at 28 ± 2 °C. Plates with only fungal plugs served as the control, while the fungicidal pentachloronitrobenzene (PCNB) (Sigma-Aldrich, Saint-Louis, MO, USA), dissolved in toluene, was used as positive control. Toluene and MeOH were used as negative controls. The in vitro antifungal bioassays of the purified metabolites were conducted according to the previously described method,[127] with few modifications. The metabolites and PCNB, dissolved in 8% acetone and toluene respectively, were placed at the four opposite sides of each Petri dish, 1 cm away from the fungal plug at the centre of the plate, at a final concentration of 50 µg/mL. Acetone and toluene were used as negative controls. The plates were incubated for 6/7 days at 28 ± 2 °C. The percentage of inhibition of the fungal growth was calculated using the following formula: % = [(Rc − Ri)/Rc] × 100 (1), where Rc is the radial growth of the test fungi in the control plates (mm), and Ri is the radial growth of the fungi in the presence of different compounds tested (mm). The results demonstrate the

antifungal activity of different compounds, analyzed by ANOVA using Tukey's test. The experiments were performed in triplicate.

4.3 Bellardia trixago

Extraction and Purification of Different Iridoid Glycosides White green organs (189.0 g) were extracted using the procedure reported in the section **2.5**. The EtOAc residue (1.45 g) was purified by CC eluted with CH_2Cl_2/MeOH (8.5/1.5, v/v) yielding nine homogeneous fractions (F1-9), as reported in **Figure 23**. The residue of F3 (54.6 mg) was purified by TLC eluted with EtOAc/MeOH/H_2O (9/0.75/0.25, v/v/v), yielding six groups of homogeneous fractions (F3.1-F3.6). F3.1 was identified as benzoic acid (**73**, 10.8 mg) and F3.5 as melampyroside (**76**, 8.4 mg). The residue of fraction F4 (584.7 mg) yielded pure melampyroside (**76**). The residue (77.9 mg) of F5 was purified by TLC eluted by CH_2Cl_2/EtOAc/MeOH (2/2/1, v/v/v), yielding two homogeneous fractions. The first fraction of the latter purification yielded a further amount of melampyroside (**76**, 20.4 mg, for a total of 613.5 mg). The residue of F6 (498.4 mg) was purified by CC eluted with CH_2Cl_2/EtOAc/MeOH (2/2/1, v/v/v), yielding seven fractions (F6.1-F6.7). The residue of F6.4 (36.5 mg) was further purified by reverse-phase TLC eluted with MeCN/H2O (4/6, v/v), yielding gardoside methyl ester (**77**, 2.0 mg), bartsioside (**74**, 13.9 mg), and mussaenoside (**78**, 6.1 mg). The residue (64.7 mg) of F7 was purified by TLC eluted with EtOAc/MeOH/H2O (8.5/1/0.5, v/v/v) giving further amount of mussaenoside (6, 2.3 mg, for a total of 8.4 mg) and aucubin (**75**, 12.4 mg).

Benzoic acid (73): ^{1}H NMR spectrum was in agreement with data previously reported.[128] ESI MS (-) *m/z*: 121 $[M - H]^-$.

Bartsioside (74): [α]D22-71.9 (c 0.64, MeOH) [lit. [88]: [α]D25-86.4 (c 0.5 MeOH)].[129] ^{1}H NMR spectrum (Figure S2) was in agreement with data previously reported.[130] ESI-MS (+), *m/z*: 330 $[M + H]^+$.

Aucubin (75): [α]D22-89.8 (c 1.0, MeOH) [lit. [90]: [α]D26-92.8 (c 0.27, MeOH)].[90] ^{1}H NMR spectrum (Figure S3) was in agreement with data previously reported.[131–133] ESI-MS (+), *m/z*: 347 $[M + H]^+$.

Melampyroside (76): [α]D22-69.6 (c 0.79, MeOH) [lit. [90]: [α]D26-52.9 (c 0.31, MeOH)].[90] ^{1}H and ^{13}C NMR spectra (Figures S4 and S5) were in agreement with data

previously reported,[134] while its NOESY spectrum is reported in Figure S6. ESI MS (+) *m/z*: 451 $[M + H]^+$.

Gardoside methyl ester (77): [α]D22-49.8 (c 0.20, MeOH) [lit. [94]: [α]D20-46 (c 0.3, MeOH)].[135] ^{1}H NMR spectrum (Figure S7) was in agreement with data previously reported.[134,136] ESI-MS (+), *m/z*: 389 $[M + H]^+$.

Mussaenoside (78): [α]D22-81.3 (c 0.30, MeOH) [lit. [90]: [α]D26-77.9 (c 0.32, MeOH)].[90] ^{1}H NMR spectrum (Figure S8) was in agreement with data previously reported.[133,137] ESI-MS (+), *m/z*: 391 $[M + H]^+$.

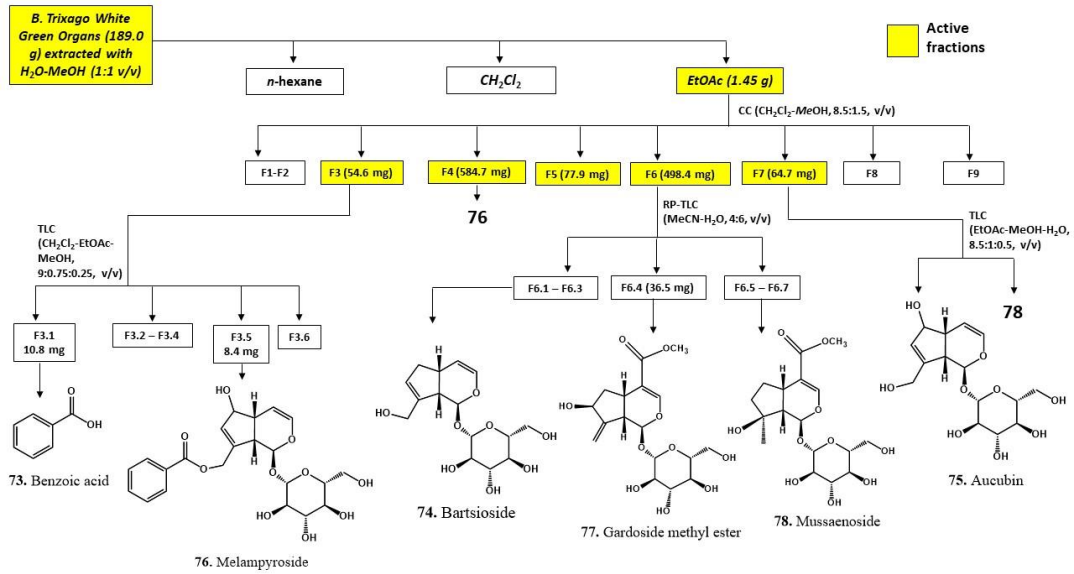

Figure 23. Purification scheme of *B. trixago*, white green organs, EtOAc extract.

Ecotoxicity Analysis of Melampyroside. The ecotoxicological tests were carried out on green freshwater algae *Raphidocelis subcapitata*, macrophyte *Lepidium sativum*, water flea *Daphnia magna*, nematode *Caenorhabditis elegans* and bacterium *Aliivibrio fischeri* to expand the range of endpoints due to differences in species sensitivity and exposure. Testing on *R. subcapitata* was performed using as end- point the algal growth inhibition after 72 h of exposure and was based on ISO 8692:2012. The algal density was determined by spectrophotometric analysis (DR5000, Hach Lange GbH, Weinheim, Germany). Ecotoxicity tests were carried out in triplicate, at 25 ± 1 ◦C with constant illumination of 6700 lux.

Testing on *L. sativum* was performed according to ISO 11269-1:2012[138] considering germination and root elongation as endpoint after 72 h. Seeds (n = 10) were exposed in triplicate in Petri dishes and incubated at 25 ± 1 ◦C in darkness. *Daphnia magna* test was conducted according to UNI EN ISO 6341:2013[139] and the endpoint evaluated was the immobilization after 24 h. Daphnids (less than 24 h old) were exposed to the samples at 20 ± 2 ◦C, in darkness without feeding. Test on *C. elegans* was carried out, with a few modifications, according to the ASTM E2172-01 Standard Method (2014) using the 24 h mortality endpoint. The test was performed using age-synchronous adult nematodes exposed at 20 ◦C to compound 4, without feeding. Test on *A. fischeri* was based on ISO 11348-3:2007[139] and the inhibition of the bioluminescence of the bacterium after 30 min of exposure was measured as endpoint. The test was performed using Microtox® Model 500 (M500) analyzer with osmotic adjustment solution (OAS) at 15 ± 1 ◦C.

4.4 ***Centaurea cineraria***

Extraction and purification of different sesquiterpene lactones Plant aerial parts (50.0 g), of dried and minced *C. cineraria* L. subsp. *Cineraria*, were extracted for 24 h, using the the same procedure of the section **2.5**. The residues were combined to obtain 85.2 mg (*n*-hexane), 492.1 mg (CH_2Cl_2) and 317.1 mg (EtOAc) of organic extracts. The CH_2Cl_2 one was purified by CC eluted with $CHCl_3$/*i*-PrOH (9/1, *v/v*) yielding eight homogeneous fractions (F1-8, **Figure 24**). F3 (34.7 mg) was further purified though two successive TLC steps, on direct and reverse phase, eluted with $CHCl_3$/*i*-PrOH (95/5, *v/v*) and CH_3CN/H_2O (4/6, *v/v*), yielding salonitenolide (**81**, 18.1 mg) in a pure form. RPTLC purification of F4 (8.6 mg), eluted with EtOH/H_2O (6/4, *v/v*), yield a pure compound identified as isocnicin (**79**, 6.6 mg). The residue of F5 (27.4 mg) was further purified using CH_2Cl_2/MeOH (9/1, *v/v*) as eluent, yielding the pure 11β,13-dihydrosalonitenolide (**82**). F6 (277.8 mg) corresponded with a pure compound identified as cnicin (**80**).

Isocnicin (**79**): ^{1}H NMR spectrum was in agreement with data previously reported.[140] ESIMS (+) *m/z*: 401 $[M + Na]^+$ consistent with the molecular formula $C_{20}H_{26}O_7$.

Cnicin (**80**): ^{1}H NMR spectrum was in agreement with data previously reported.[141] ESIMS (+) *m/z*: 379 $[M + H]^+$, consistent with the molecular formula $C_{20}H_{26}O_7$. $[\alpha]_D$ +160.4 (*c* 0.10, MeOH), $[\alpha]_D$ +169.6 lit.[141]

Salonitenolide (**81**): ^{1}H NMR spectrum was in agreement with data previously reported.[141] ESIMS (+) *m/z*: 287 $[M + Na]^+$ consistent with the molecular formula $C_{15}H_{20}O_4$. $[\alpha]_D$ +195.9 (*c* 0.38, MeOH), $[\alpha]_D$ +199.4 lit.[141]

11β,13-Dihydrosalonitenolide (**82**): ^{1}H NMR spectrum was in agreement with data previously reported.[140] ESIMS (+) *m/z*: 267 $[M + H]^+$, consistent with the molecular formula $C_{15}H_{22}O_4$. $[\alpha]_D$ +101.2 (*c* 5.0, $CHCl_3$), $[\alpha]_D$ +98 lit. [140]

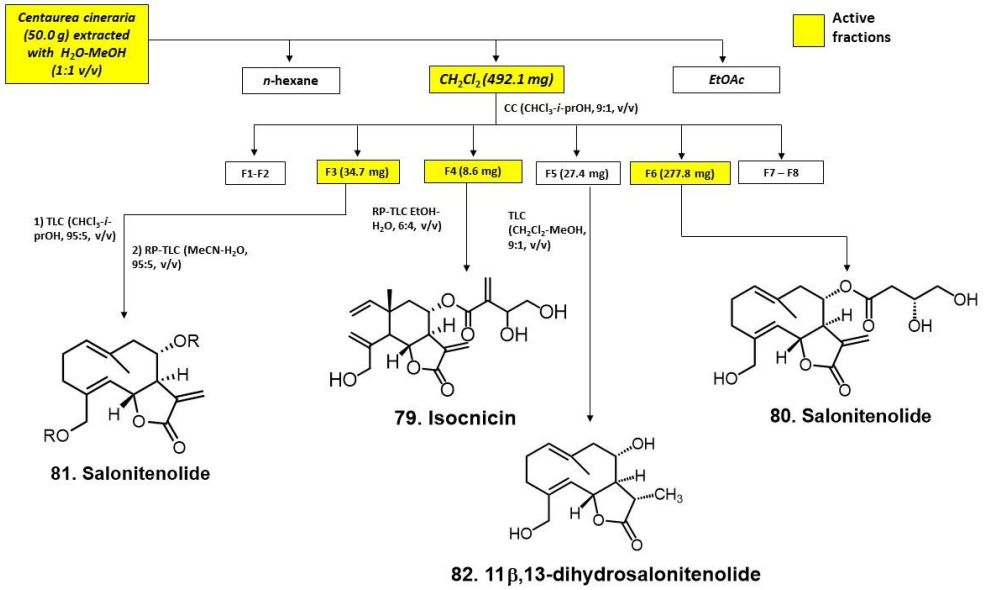

Figure 24. Purification scheme of *C. Cineraria* CH_2Cl_2 extract.

*Synthesis of 8,15-O,O'-diacetylsalonitenolide (**83**)* 3.0 mg of Salonitenolide (**81**, 0.011 mmol) were dissolved in pyridine (20 μL), and reacted with acetic anhydride (20 μL), overnight at room temperature. The reaction was stopped adding MeOH and evaporated under a N_2 stream, after the formation of the azeotrope by benzene addition. The residue obtained (3.2 mg) was purified by analytical TLC, eluted with $CHCl_3$/*i*-propanol (97/3, *v/v*), affording 8,15-*O*,*O*-diacetylsalonitenolide (**83**) in 73% yield (2.8 mg, 0.008 mmol).

Salonitenolide (**81**) diacetylation, to afford compound **83,** was confirmed by NMR and ESIMS spectroscopic data (Figures S5, S6, S9 and S10) analysis. Mainly, two new singlet signals at δ 2.11 and 2.10 ppm, in the ^{1}H NMR spectrum of compound **83** denoted the acetylation of two hydroxyl groups, which was also confirmed by the *m/z* value of 371 obtained in the ESIMS analysis of compound **83**, corresponding to a sodium adduct $[M + Na]^+$ of a compound with a molecular weight of 348.

4.5 (4*Z*)-Lachnophyllum lactone from *Conyza bonariensis*

(4Z)-Lachnophyllum Lactone extraction and identification. The extraction of *C. bonariensis*-lyophilized tissues (27.0 g) was performed using the same procedure reported in the section **2.5**. The CH_2Cl_2 residue (60 mg), showing specific inhibitory activity against *C. campestris*, was purified by TLC eluted with EtOAc/*n*-hexane (6/4, v/v), yielding five homogeneous fractions which were tested for allelopathic activity against *Cuscuta* seedling growth. The fraction with the strongest phytoxicity against *Cuscuta* was further studied as described below.

Plant material. *C. bonariensis* plants were harvested during the phenological stage, when the inflorescence emerged, in the 2022 spring in Cordoba, southern Spain (coordinates 37.856 N, 4.806 W, datum WGS84). After, *C. bonariensis* shoots were promptly transported to the laboratory and frozen using liquid nitrogen, preserved at -80 °C, later lyophilized, and the resultant dry material stored at 4 °C in the dark.

Conyza bonariensis shoots specialized metabolites isolation and identification. A total of 240.0 g of *C. bonariensis* shoots were extracted, following the same procedure reported in the section **2.5**. The extraction was carried twice, and each organic extract was combined, yielding 169.1 mg (n-hexane), 276.1 mg ($CHCl_3$) and 295.9 mg (EtOAc). A schematic purification representation is reported in **Figure 25**. Purification of the *n*-hexane extract, by CC on Si-gel, eluted with $CHCl_3$/*i*-PrOH (9/1, v/v), yielded seven homogeneous fractions (F1-F7). Purification of F2 (41.7 mg), by TLC eluted with *n*-hexane/EtOAc (9/1, v/v), yielded five groups of homogeneous fractions (F1.1-F1.5). The residue of F1.4 (47.1 mg) was purified by TLC eluted with n-hexane/EtOAc (95/5, v/v), yielding a pure compound identified as (4*Z*)- lachnophyllum methyl ester (**85**, 10.1 mg). The purification of F3 (93.0 mg), by TLC, eluted with *n*-hexane/EtOAc (4/1, v/v), yielded four groups of homogeneous fractions (F3.1-F3.4). A further amount of compound **85** (15.9 mg) was obtained by F3.1. F3.2 purification was identified as the pure (4*Z*)-lachnophyllum lactone (**84**, 32.6 mg), the residue of F3.3 was identified as (4*E*,8*Z*)-matricaria lactone (**87**, 3.8 mg), while F3.4 was identified as (4Z,8Z)-matricaria lactone (**86**, 9.3 mg). Purification of CH_2Cl_2 residue, by CC on Si-gel, eluted with $CHCl_3$/*i*-PrOH (95/5, v/v), yielding nine homogeneous fractions (F1-F9). The residue of F1 (32.2 mg) was further purified by TLC eluted *n*-hexane/EtOAc (4/1, v/v), yielding a further amount of (4*Z*)-lachnophyllum lactone (**84**, 13.3 mg, for a total amount of 45.9 mg). Purification of F4 (42.6 mg), by TLC, eluted with $CHCl_3$/*i*-PrOH (9/1, v/v), yielding two pure compounds identified as methyl 4-hydroxy-3-methoxybenzoate (methyl vanillate, **88**, 4.8 mg) and as methyl 4-hydroxybenzoate (**89**, 6.4 mg). TLC Purification of F5 (34.6 mg), eluted with $CHCl_3$/*i*-PrOH (98/2, v/v), yielding a pure compound identified as hispidulin (**90**, 6.2 mg). The EtOAc organic extract was purified by CC on Si-gel, eluted with $CHCl_3$/*i*-propanol (95/5, v/v), yielding six homogeneous fractions (F1-F6). TLC purification of F1 (37.6 mg), eluted with $CHCl_3$/*i*-PrOH (98/2, v/v), yielding a further amount of methyl 4-hydroxy-3-methoxybenzoate (**88**, 5.0 mg) and of methyl 4-

hydroxybenzoate (**89**, 7.4 mg). The residue of F2 (12.6 mg) was purified by TLC eluted with $CHCl_3$/*i*-PrOH (98/2, v/v), yielding further amount of hispidulin (**90**, 3.4 mg).

(4*Z*)-Lachnophyllum methyl ester (**85**): ^{1}H NMR spectrum was in agreement with data previously reported.[142] ESI MS (+) *m/z*: 177 $[M+H]^+$.

(4*Z*)-Lachnophyllum lactone (**84**): ^{1}H NMR spectrum was in agreement with data previously reported.[143] ESI MS (+) *m/z*: 163 $[M+H]^+$.

(4*Z*,8*Z*)-Matricaria lactone (**86**): ^{1}H NMR spectrum was in agreement with data previously reported.[144] ESI MS (+) *m/z*: 161 $[M+H]^+$.

(4*E*,8*Z*)-Matricaria lactone (**87**): ^{1}H NMR spectrum were in agreement with data previously reported.[145] ESI MS (+) *m/z*: 161 $[M+H]^+$.

Methyl 4-hydroxy-3-methoxybenzoate (**88**): ^{1}H NMR spectrum was in agreement with data previously reported.[146] ESI MS (+) *m/z*: 183 $[M+H]^+$.

Methyl 4-hydroxybenzoate (**89**): ^{1}H NMR spectrum was in agreement with data previously reported.[147] ESI MS (+) *m/z*: 153 $[M+H]^+$.

Hispidulin (**90**): 1H NMR and ^{13}C NMR spectra were in agreement with data previously reported.[148,149] ESI MS (+) *m/z*: 301 $[M+H]^+$.

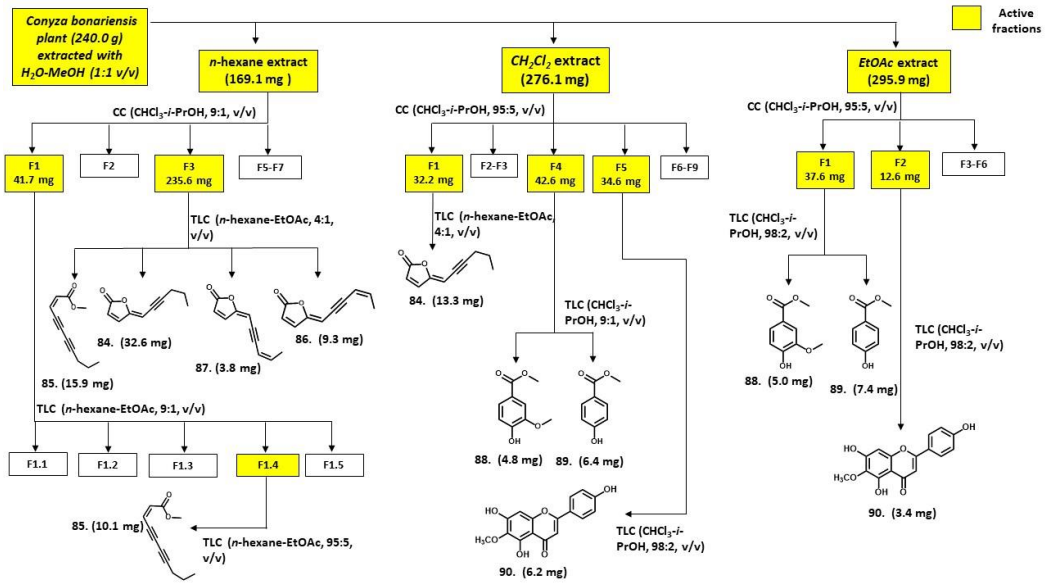

Figure 25. Purification scheme of *C. Bonariensis* extracts.

4.6 Total synthesis of (4*Z*)-lachnophyllum lactone

Retrosynthetic analysis. The ideation of a potential retrosynthetic pathway, was the first step in the design of a synthetic procedure towards (4*Z*)-lachnophyllum lactone (**84**) (**Scheme 1**). The crucial phase was identified in a Pd-Cu bimetallic cascade cross coupling-cyclization[105,150] process between 1,3-eptadiyne (**Scheme 1**, green) and 3-*Z*-iodoacrylic acid (**Scheme 1**, blue). Commercially accessible precursors, such as propiolic acid and 1-pentyne, can be readily utilized to prepare these coupling partners (**Scheme 1**)

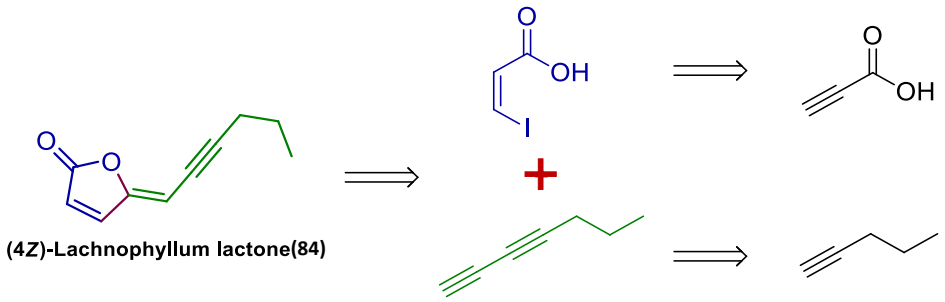

Scheme 1. (4*Z*)-Lachnophyllum lactone (**84**) retrosynthetic analysis *(adapted from Soriano et al. J. Agric. Food Chem, **2024**, 72, 4737-4746).*[151]

General synthetic procedure. The synthesis of (4*Z*)-lachnophyllum lactone (**84**, **Scheme 2**) started with iodation of pent-1-yne, to obtain 1-iodopent-1-yne (**91**), which was directly used in a cross-coupling reaction with TMS-acetylene to afford the hepta-1,3-diyn-1-yltrimethylsilane (**92**). The latter was then deprotected, to get the 1,3-heptadiyne (**93**) and used in a cross-coupling reaction with 3-*Z*-iodoacrylic acid (**95**), readly obtained by iodation of propiolic acid (**94**), to finally afford compound **84**. 1-Iodopent-1-yne (**91**). Pent-1-yne (2, 6.0 mL, 60.8 mmol, 1.0 eq.) was dissolved in dry THF (40 mL). Then the solution was cooled at -78 °C and n-butyllithium (2.5 M in hexane, 60.8 mmol, 1.0 eq.) was added dropwise. To prevent exothermic runaway during the electrophilic quench, iodine (15.25 g, 60.8 mmol, 1.0 eq.) was portioned into the solution after the mixture had been agitated for ten minutes at -78 °C. After bringing the mixture to room temperature, it was stirred continuously for sixteen hours. After that, the deep orange solution was extracted using ethyl alcohol (3 x 20 mL) and diluted with sat. NH_4Cl. The combined organic layers were washed with sat. $Na_2S_2O_3$ (1 x 10 mL), brine (1 x 10 mL) and then dried over anhydrous Na_2SO_4, filtered and concentrated in vacuo to afford 1-iodopent-1-yne (**91**, 8.72 g, 75% yield, Rf = 0.3 in pentane)

as a yellow oil, which was directly used in the following synthetic step without further purification. ^{1}H NMR (600 MHz, CDCl3): δ 2.33 (t, J = 7.0 Hz, 2H), 1.53 (m, 2H), 0.97 (t, J = 7.4 Hz, 3H). EI-MS *m/z* (%): 194 (M+, 100), 165 (31), 65 (28), 41 (71), 39 (39).[116,117]

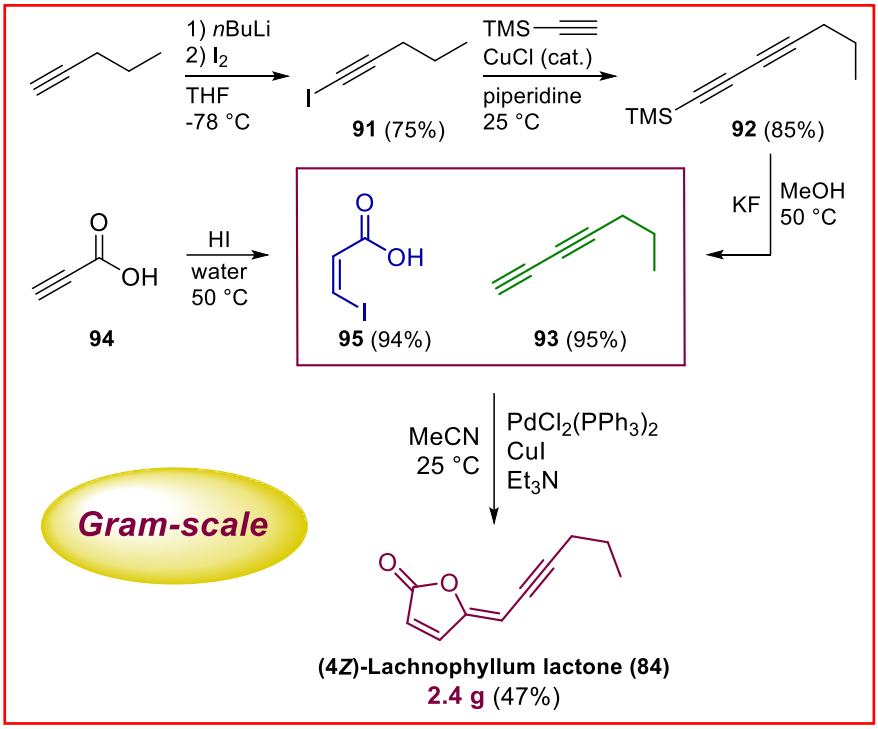

Scheme 2. Gram-scale synthetis of (4*Z*)-lachnophyllum lactone (**84**) *(adapted from Soriano et al. J. Agric. Food Chem, **2024**, 72, 4737-4746).*[151]

*Hepta-1,3-diyn-1-yltrimethylsilane (**92**).* Piperidine (22 mL) was added to a flame-dried flask and degassed with argon for 30 minutes. Then, 1-iodopent-1-yne (**91**, 8.60 g, 44.3 mmol, 1.0 eq.) and ethynyltrimethylsilane (13.06 g, 133.0 mmol, 3.0 eq.) were added and the reaction mixture was cooled at 0 °C. Subsequently, CuCl (439 mg, 4.43 mmol, 0.1 eq.) was added and the reaction mixture was stirred for 3 hours at room temperature under argon atmosphere. Extraction with Et_2O (3 x 20 mL) was performed after mixture quenching with sat. NH_4Cl. The obtained organic layers were combined and washed with 1M HCl (1 x 10 mL), brine (1 x 10 mL) then dried over anhydrous Na_2SO_4, filtered and concentrated under reduced pressure. The residue was purified by flash column chromatography (petroleum ether), to obtain a colorless oil (**92**, 6.14 g, 85% yield, Rf = 0.6 petroleum ether). ^{1}H NMR (600 MHz, CDCl3): δ 2.24 (t, J = 7.0 Hz, 2H), 1.55 (m, 2H), 0.98 (t, J = 7.4 Hz, 3H), 0.17

(s, 9H). ^{13}C NMR (150 MHz, CDCl3): δ 88.6, 83.1, 80.2, 65.7, 21.8, 21.3, 13.6, -0.2 (3C). EI-MS *m/z* (%): 164 (M+, 12), 150 (16), 149 (100), 120 (6).[152,153]

*1,3-Heptadiyne (**93**).* To An argon degassed MeOH (60 mL) solution of compound **92** (6.0 g, 36.6 mmol, 1.0 eq.) was added KF (21.25 g, 366.0 mmol, 10.0 eq.). The reaction mixture was stirred for 1 hour at 50 °C. After cooling to room temperature, the mixture was diluted with water (120 mL), extracted three times with pentane (15 mL) and the combined organic layers concentrated under reduced pressure after drying over anhydrous Na_2SO_4. Flash column chromatography purification (pentane), gave the pure **93** as a colorless oil (3.37 g, 95% yield, Rf = 0.6 pentane). ^{1}H NMR (600 MHz, CDCl3): δ 2.24 (t, J = 7.0 Hz, 2H), 1.96 (s, 1H), 1.57 (m, 2H), 0.99 (t, J = 7.4 Hz, 3H). ^{13}C NMR (150 MHz, CDCl3): δ 79.3, 65.9, 60.4, 21.7, 21.5, 13.6. EI-MS *m/z* (%): 92 (M+, 70), 91 (100), 65 (21), 63 (49), 62 (25), 51 (16).[152,153]

*3-Z-iodoacrylic acid (**95**).* HI (57 % w. in water, 10.5 mL) was added to a solution of propiolic acid (**94**, 2.5 mL, 40.0 mmol) in water (10 mL) and stirred at 50 °C for 18 hours. Then, the mixture was allowed to cool at room temperature and the aqueous phase was extracted with Et_2O (3 x 10 mL). The combined organic extracts were washed with sat. aqueous $Na_2S_2O_3$ (1 x 5 mL), dried over anhydrous Na_2SO_4 and the solvent removed in vacuo to afford crude **95**. The reaction crude was then rinsed with pentane to afford pure 3-Z-iodoacrylic acid (**95**, 7.4 g, 94% yield Rf = 0.6 MeCN/H2O 6/4 v/v) as a white solid. ^{1}H NMR (600 MHz, DMSO-d6): δ 12.82 (br s, 1H), 7.60 (d, J = 8.9 Hz, 1H), 6.96 (d, J = 8.9 Hz, 1H). 13C NMR (150 MHz, DMSO-d6): δ 165.8, 131.0, 96.4.[105,154,155]

*(4Z)-Lachnophyllum lactone (**84**).* A solution of 1,3-heptadiyne (**93**, 2.91 g, 31.6 mmol, 1.0 eq.), 3-*Z*-iodoacrylic acid (**95**, 6.95 g, 35.1 mmol, 1.1 eq.) and triethylamine (6.6 mL, 47.4 mmol, 1.5 eq.) in dry acetonitrile (200 mL), was degassed for 30 min with argon. Then, $PdCl_2(PPh_3)_2$ (1.123 g, 1.6 mmol, 0.05 eq.) and CuI (300 mg, 1.6 mmol, 0.05 eq.) were sequentially added. The reaction mixture was stirred overnight for 16 hours at room temperature under argon atmosphere, then it was quenched with 50 mL of sat. NH_4Cl. The mixture was extracted with EtOAc (3 x 20 mL). The combined organic extracts were dried over anhydrous Na_2SO_4 and the solvent removed under reduced pressure. Purification of the residue was carried out by flash column chromatography (petroleum ether/EtOAc 9/1 v/v),

to obtain pure a slightly yellow oil (**84**, 2.40 g, 47% yield, Rf = 0.3 petroleum ether/EtOAc 9/1 v/v). ^{1}H NMR (600 MHz, $CDCl_3$): δ 7.36 (d, J = 5.4 Hz, 1H), 6.22 (d, J = 5.4 Hz, 1H), 5.31 (t, J = 2.2 Hz, 1H), 2.42 (dt, J = 7.1, 2.2 Hz, 2H), 1.61 (sext, J = 7.1 Hz, 2H), 1.02 (t, J = 7.1 Hz, 3H). ^{13}C NMR (150 MHz, CDCl3): δ 169.1, 156.2, 142.8, 120.3, 104.7, 95.2, 74.9, 22.2, 22.0, 13.7. EI-MS *m/z* (%): 162 (M+, 94), 147 (20), 133 (36), 120 (18), 119 (22), 105 (31), 91 (29), 82 (100), 79 (23), 77 (57), 54 (43), 51 (42). ESI-HRMS $[M+H]^+$: *m/z* 163.0757, $C_{10}H_{11}O_2^+$ requires 163.0754.[144,154,156]

Synthesis of analogues. Derivatization of compound **84** was carried out in one step to obtain two of its natural analogues namely, (4*E*)-lachnophyllum lactone (**96**), (4*Z*,8*Z*)-matricaria lactone (**97**) (**Scheme 3**) following the procedures below reported.

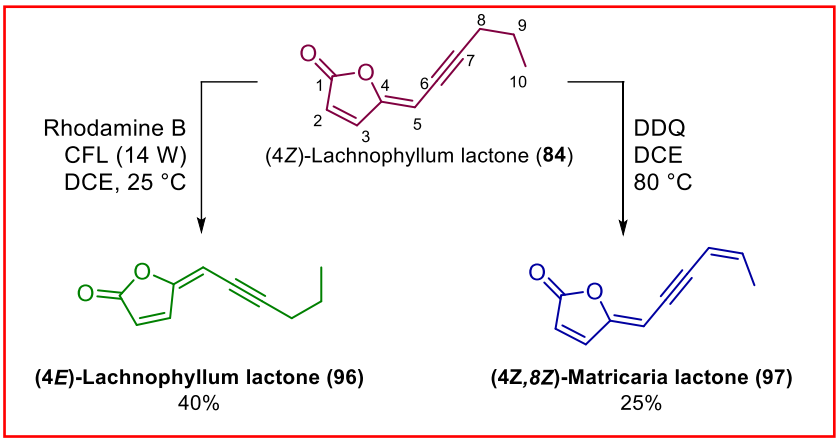

Scheme 3. (4*Z*)-Lachnophyllum lactone (**84**) synthetic derivatives (**96** *via* photoisomerization and **97** *via* radical oxidation) *(adapted from Soriano et al. J. Agric. Food Chem,* ***2024****, 72, 4737-4746).*[151]

*(4E)-Lachnophyllum lactone (**96**).* Dry dichloroethane (60 mL) was used to prepare a solution of (4*Z*)-lachnophyllum lactone (**84**, 100 mg, 0.62 mmol, 1.0 eq.), stirred and exposed to a compact fluorescent lamp (14 W) for 36 hours in a closed chamber (**Scheme 3**), after addition of rhodamine B (17 mg, 0.035 mmol, 0.05 eq.). The reaction mixture was then passed through a short pad of silica and the solvent was removed under reduced pressure. Flash column chromatography purification (petroleum ether/EtOAc 9/1 v/v), gave pure **96** as a slightly yellow oil (40 mg, 40% yield, Rf = 0.5 petroleum ether/EtOAc 9/1 v/v). ^{1}H NMR (600 MHz, CDCl3): δ 7.72 (d, J = 5.5 Hz, 1H), 6.26 (dd, J = 5.5, 1.5 Hz, 1H), 5.73 (dd, J = 2.6, 1.5 Hz, 1H), 2.39 (dt, J = 7.2, 2.6 Hz, 2H), 1.61 (sext, J = 7.2 Hz, 2H), 1.02 (t,

J = 7.2 Hz, 3H). ^{13}C NMR (150 MHz, CDCl3): δ 169.3, 157.7, 140.5, 121.1, 100.8, 96.2, 74.5, 22.1, 22.0, 13.7. EI-MS *m/z* (%): 162 (M+, 84), 147 (19), 133 (36), 105 (32), 91 (29), 82 (100), 77 (59), 54 (45), 51 (44). ESI-HRMS $[M+H]^+$: m/z 163.0757, $C_{10}H_{11}O_2^+$ requires 163.0754.[156,157] Unreacted starting material **84** was recovered (50 mg, 50% yield , Rf = 0.3 petroleum ether/EtOAc 9/1 v/v) during the flash chromatographic purification procedure.

*(4Z,8Z)-Matricaria lactone (**97**).* A dry dichloroethane (10 mL) solution of (4*Z*)-lachnophyllum lactone (1, 100 mg, 0.62 mmol, 1.0 eq.) and triethylamine (130 µL, 0.93 mmol, 1.5 eq.) was prepared and then, degassed 30 minutes with argon. After, 2,3-dichloro-5,6-dicyano-1,4-benzoquinone (422 mg, 1.86 mmol, 3.0 eq) was added and the mixture was stirred at 80 °C for 4 hours under argon atmosphere (**Scheme 3**). The reaction mixture was then passed through a short pad of silica (treated previously with 30 mL of DCM + 0.5% Et_3N for silica neutralization) and the solvent was then removed under reduced pressure. Flash column chromatography purification (petroleum ether/EtOAc 9/1 v/v + 0.5% Et3N for initial silica neutralization), gave pure **97** (25 mg, 25% yield, Rf = 0.6 petroleum ether/EtOAc 9/1 v/v) as a slightly yellow oil. Pure product **97** was stored and handled in the dark, to avoid photodegradation. ^{1}H NMR (600 MHz, $CDCl_3$): δ 7.40 (d, J = 5.4 Hz, 1H), 6.25 (d, J = 5.4 Hz, 1H), 6.16 (dq, J = 10.8, 7.0 Hz, 1H), 5.72 (ddq, J = 10.8, 2.7, 1.7 Hz, 1H), 5.48 (d, J = 2.7 Hz, 1H), 1.97 (dd, J = 7.0, 1.7 Hz, 3H). ^{13}C NMR (150 MHz, CDCl3): δ 168.9, 156.0, 142.6, 142.0, 120.5, 110.0, 99.5, 94.8, 88.1, 16.6. EI-MS m/z (%): 160 (M+, 100), 131 (29), 103 (33), 82 (21), 78 (38), 77 (19), 54 (20). ESI-HRMS $[M+H]^+$: *m/z* 161.0600, $C_{10}H_9O_2^+$ requires 161.0597.[158]

Biological Assays. The phytotoxic and antimicrobial activities of (4*Z*)-lachnophyllum lactone (**84**) and its analogues (4*E*)-lachnophyllum lactone (**96**) and (4Z,8Z)-matricaria lactone (**97**) were evaluated against four types of pests affecting Mediterranean agriculture, i.e. the stem parasitic weed *C. campestris*, the root parasitic weeds *O. minor* and *P. ramosa*, the autotrophic weed *C. bonariensis* and the fungal pathogen *Verticillium dahliae*.

Germination and Growth Inhibition Bioassays on Cuscuta campestris. The phytotoxicity screening against stem parasitic weeds was conducted as previously reported.6 Seeds of *C. campestris* were collected in 2022 from pea plants, parasitized by it, at Córdoba, southern Spain. For the induction of C. campestris germination, their seeds must be scarified, with

sulfuric acid for 45 min, followed by thorough rinses with sterile distilled water. Then, twenty scarified seeds were placed, using tweezers, onto 5 cm diameter filter paper discs inside 5.5 cm diameter Petri dishes. Compounds **84**, **96**, and **97** were dissolved in dimethyl sulfoxide and then diluted to 1, 0.6, 0.3 and 0.1 mM in sterile water. The final concentration of dimethyl sulfoxide in all treatments was 1%. Triplicate aliquots of 1 mL of each treatment were applied to filter paper discs containing the scarified C. campestris seeds. Triplicate aliquots of treatment, containing only 1% of dimethyl sulfoxide, were used as a control. Petri dishes containing the treated seeds were sealed with parafilm and incubated in the dark at 23 °C for 5 days. Then, the seedling length was measured in each of the five randomly chosen C. campestris seedlings for each of the three replicate filter paper discs per treatment. Seedling growth for each treatment was calculated in relation to the seedling growth of the corresponding control.

Germination and growth Inhibition of Conyza bonariensis. *C. bonariensis* seeds were gathered in 2020 from mature *C. bonariensis* plants in pea fields at Córdoba, southern Spain. Compounds **84**, **96**, and **97** were dissolved in dimethyl sulfoxide and then diluted to concentrations of 1, 0.6, and 0.3 mM in 0.9% water agar at 50º C. The final concentration of dimethyl sulfoxide in all treatments was 1%. Triplicate aliquots of 5 mL for each treatment were poured into 5.5 cm diameter Petri dishes. Triplicate aliquots of a treatment containing only 1% dimethyl sulfoxide were utilized as a control. Tweezers were used to place twenty *C. bonariensis* seeds onto the surface of the agar medium, and the Petri dishes were then incubated under 16-hour lighting at 23 °C. After 7 days, the length of the radicle was measured for each of the five randomly selected *C. bonariensis* seedlings on each of the three replicate Petri dishes per treatment. The inhibition of root growth induced by each treatment was calculated relative to the root growth induced by the control.

V. dahliae antifungal bioassays. The assessment of antimicrobial activity against *V. dahliae* using the defoliating pathotype (isolate V-135 I) from vegetative compatibility group VCG1A, which was isolated from olive trees in Córdoba, southern Spain. Compounds **84**, **96**, and **97** were dissolved in dimethyl sulfoxide and then diluted to concentrations of 1, 0.6, and 0.3 mM in potato dextrose agar (PDA) medium at 50ºC. The final concentration of dimethyl sulfoxide was 1%. Triplicate aliquots of 5 mL for each treatment were poured into

5.5 cm diameter Petri dishes. Triplicate aliquots of a treatment containing only 1% dimethyl sulfoxide served as a control. 1Mycelial plugs (6 mm in diameter) were extracted from the edges of 10-day-old colonies of *V. dahliae* isolate V-135 I growing on PDA medium. These plugs were then transferred to the Petri dishes with the same medium supplemented with each of the compounds **84**, **96**, and **97** treatments. The Petri dishes were sealed with Parafilm and kept at 23°C in the dark for 15 days. For each treatment, the mycelial growth of the colony in each Petri dish was measured every 3 days in two perpendicular directions and compared with the control. The data on mycelial growth from day 3 to day 15 after inoculation for each treatment concentration were converted to the Area Under the Growth Progress Curve (AUGPC) according to the methodology of Shaner and Finney (1977).[159]

4.7 (4Z)-Lachnophyllum lactone analogues synthesis

(4Z)-Lachnophyllum lactone analogues general synthetic procedure. A solution of each of the terminal alkynes (**98-104**, 1.0 mm, 1.0 eq.) reported in the **Figure 26**, 3-*Z*-iodoacrylic acid (**95**, 1.1 eq.) and triethylamine (1.5 eq.) in dry acetonitrile (25 mL), was degassed for 30 min with nitrogen. Then, $Pd(OAc)_2$ (0.05 eq.), PPh_3(0.05), and CuI (0.05 eq.) were sequentially added (**Figure 26**). After, the reaction mixture was stirred overnight for 18 hours at room temperature, under nitrogen atmosphere and finally, quenched with 20 mL of sat. NH_4Cl. The obtained mixture was extracted with EtOAc (3 x 20 mL). The combined organic extracts were dried over anhydrous Na_2SO_4 and the solvent removed under reduced pressure. Purification of the residue was carried out by column chromatography eluted with petroleum ether/EtOAc 9/1 v/v, then increasing the EtOAc percentage from 10%, up to 30 %, to obtain pure slightly yellow oils (**105-121**).

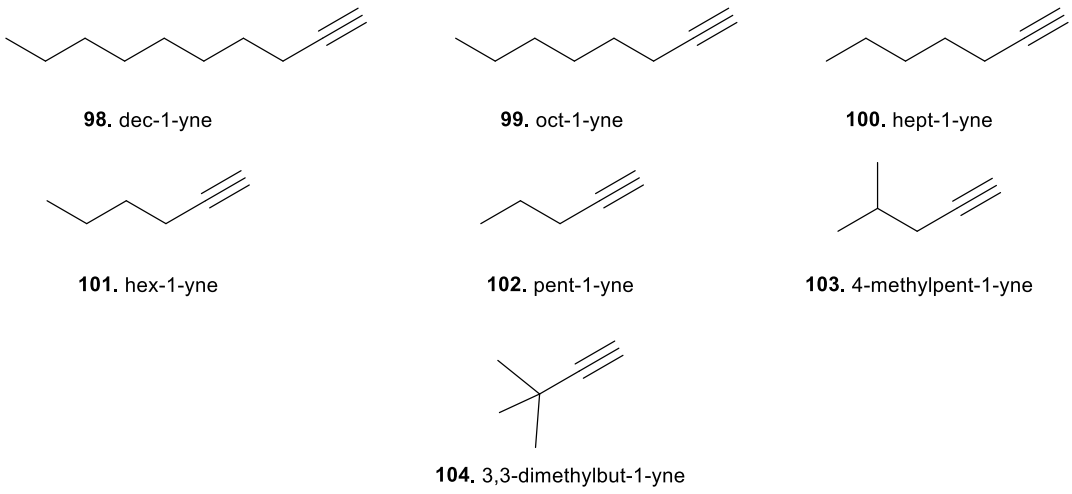

Figure 26. Different terminal alkynes used to prepare (4*Z*)-lachnophyllum lactone analogues.

5 Results and discussion

5.1 Mode of action insights from SAR studies of different allelopathic compounds

Considering their potential allelopathic activity,[160] **27** commercially available and natural synthesized products, were selected to perform a first in vitro screening, through their application (1 mM), on scarified *C. campestris* seeds. Five days after treatment, inhibition of *C. campestris* growth was significantly affected to varying degrees. Considering the different and wide range of tested compounds activity, a first classification was done, aiming to select the most active ones. The compounds 2-benzoxazolinone (**5**), hydrocinnamic acid (**6**) and pisatin (**18**) showed the highest inhibition activity, compared to the control (89.2 ± 0.9%, 88.5 ± 1.2% and 81.6 ± 9% of inhibition, respectively, **Figure 27A–C**). However, *p*-coumaric acid (**7**), a *trans*-cinnamic acid analogue whose SAR features are describe after, showed low but significance level of inhibition.

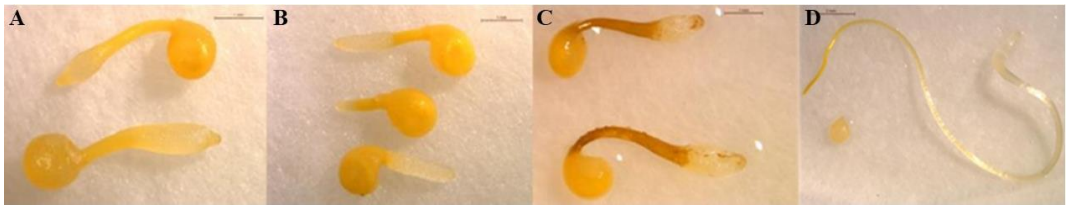

Figure 27. *Growth inhibition observed in 1 mM treatments of C. campestris with (**A**) 2-benzoxazolinone (**5**), (**B**) hydrocinnamic acid (**6**) and (**C**) pisatin (**18**) in comparison with (**D**) control (adapted from Moreno-Robles et al. Agriculture, **2022**, 12, 1746-1760).*[7]

<u>*2-benzoxazolinone (**5**) SAR studies*</u> The growth inhibition of 2-benzoxazolinone, was studied in a second in vitro bioassay, varying its concentration from 0.1 to 1 mM. A comparison with four derivatives, (**24-27**) was carried out, too. Five days after treatment, inhibition of *Cuscuta* growth was differently affected by the type of 2-benzoxazolinone derivative and its concentration (ANOVA, $p < 0.001$). Specifically, all the derivatives tested showed lower activity in comparison with compound **5**, which stood out showing inhibition values higher than 80% both at 1 and 0.5 mM. At a concentration of 1 mM and 0.5 mM only its brominated derivative (**27**, **Figure 28)** showed significant activity (79.3 ± 6.9% and 45.23 ± 5.3%, respectively).

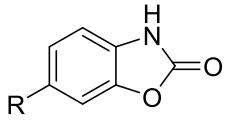

5. 2-benzoaxozolinone

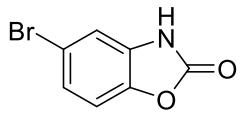

27. 5-bromo-2-benzoaxozolinone

Figure 28. *Chemical representation of compound* ***5*** *and* ***27****.*

*Hydrocinnamic acid (**6**) SAR studies*

The *Cuscuta* growth inhibition by hydrocinnamic acid (**6**) was studied in vitro in comparison with 21 structural analogues (**19-23**, **27-42**, Figure **13**) in a range of concentrations 0.25-1 mM, in order to calculate their IC_{50} (**Table 3**). Five days after treatment, *Cuscuta* growth was significantly affected by the concentration applied (ANOVA, $p < 0.001$). ClogP was calculated too (**Table 3**).

Compound	CLog*p*	IC50 (µM)	R^2
6	1.903	518	0.9961
23	1.186	572	0.9978
27	0.746	>1000	-
28	1.236	>1000	-
29	1.822	334	0.9950
30	2.616	<250	-
22	1.236	>1000	-
31	1.822	879	0.9990
32	2.402	415	1.000
33	2.786	<250	-
34	1.336	~1000	-
35	0.676	>1000	-
19	2.046	<250	-
20	2.616	<250	-
21	2.766	<250	-
36	1.646	>1000	-
37	0.639	>1000	-
38	1.085	>1000	-
39	2.445	488	0.9987
40	2.228	484	0.9979
41	2.808	511	0.9981
42	1.712	~1000	-

Table 3. *IC_{50} and CLogp values of compounds* ***6, 19-23, 27-42.***

In general, by comparison with hydrocinnamic acid (**6**), whose IC_{50} value was 518 µM, the bioactivity was influenced by the position and the type of functional groups it

contained. Hydroxyl groups had a negative effect on the bioactivity to varying degrees, depending on where the alcohol was substituted. The ortho derivative (IC_{50} = 572 µM) resulted to be far more active than the *meta* or *para* ones (IC_{50} > 1000 µM). The higher activity of the hydroxylated derivative at the *ortho* position was also found in a previous study on *Cuscuta*,[7] which may be due to its ability to cyclize and form coumarins.[161] On the other hand, halogenated derivatives (**19**-**21**, **30**) showed high CLog*p* value and IC_{50} < 250 µM (**Table 3**). This close relationship between high CLog*p* and inhibition values, could be related to a preferentially distribution of these compounds in the hydrophobic environments, such as the lipid bilayer of the membrane. In this regard, recent studies reported that cinnamic acid and its derivatives produce changes in the permeability of the cell membrane[162] and reduce H+ ATPase activity.[163] The ethyl ester form (**41**) of hydrocinnamic acid (**6**), have similar IC_{50} values (518 and 511 µM, respectively), even though the CLog*p* was very different (2.808 and 1.903, respectively). Thus, neither the lipophilicity or the acidity of the compounds appeared to be affecting the bioactivity. This finding might be a key factor, since the control of the solubility and acidity of the bioactive compound by esterification may ease the future formulation of some related natural bioactive compounds to be used as biopesticides. The overall structure–activity relationship is summarized below (**Figure 29**).

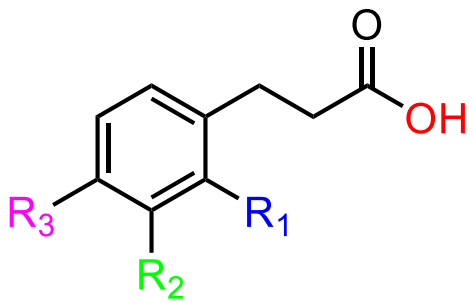

Figure 29. *Hydrocinammic acid (**6**) derivatives framework.*

a. The absence of the carbonyl group decreases the activity
b. Halogens at R_2 or R_3 positions notably increase the activity
c. Methyl or trifluoromethyl group at R_3 increase the activity
d. Methoxy group at R_2 increase the activity, at R_3 decreases the activity
e. Cyano and amino groups at R_3 notably decrease the activity

f. Hydroxyl groups at R_1, R_2 or R_3, decrease the activity
g. Carboxy group at R_1 or R_3 notably decrease the activity
h. Halogens substitution of OH preserve the activity

*Trans-cinnamic acid (**43**) SAR studies*

The inhibitory activity of *trans*-cinnamic acid (**43**) against the seedling growth of *C. campestris* was studied in vitro. *trans*-Cinnamic acid inhibited growth by 38.9 ± 4.3 % in comparison with *C. campestris* seedlings treated with the negative control when tested at 1 mM. In order to discover structural features responsible of the activity, 24 structural analogues (**6**, **44**-**66**, **Figure 19**) were tested on *C. campestris* growth in comparison with the parent compound, *trans*-cinnamic acid (**43**). This study allowed to confirm the already found high phytotoxicity exhibited by hydrocinnamic acid (**6**) and described the strongest bioactivity of 3-phenylpropionaldehyde (**44**), *trans*-cinnamaldehyde (**45**), *trans*-4-(trifluoromethyl)cinnamic acid (**57**), *trans*-3-chlorocinnamic acid (**59**), and *trans*-cinnamate (**64**), all with IC_{50} values less than 500 µM (**Table 4**). All of them caused at least 80% inhibition at the highest concentration tested (1 mM), which decreased to around 45–60 % when the concentration was halved (0.5 mM). The IC_{50} and CLog*P* values are reported in the **Table 4**.

Compound	CLog*P*	IC50 (µM)	Compound	CLog*P*	IC50 (µM)
43	2.239	>1000	**55**	2.738	>1000
6	1.903	777	**56**	3.122	-
44	1.873	497	**57**	3.122	399
45	2.049	408	**58**	2.382	~1000
46	1.608	>1000	**59**	2.952	461
47	1.572	>1000	**60**	2.382	~1000
48	1.572	-	**61**	2.952	955
49	1.572	-	**62**	3.102	876
50	0.975	-	**63**	2.204	>1000
51	1.421	-	**64**	2.465	331
52	1.204	-	**65**	4.233	-
53	2.158	>1000	**66**	1.785	-
54	2.738	-			

Table 4. *IC_{50} and CLogp values of compounds* ***6, 43-66****.*

The SAR study revealed structural features with significance for the inhibitory activity of

C. campestris growth. Firstly, regarding the degree of the side chain unsaturation, in comparison with *trans*-cinnamic acid (**43**), a decreased growth-inhibitory activity was observed in phenylpropiolic acid (**66**), with a triple bond, and a more pronounced, higher activity was observed in hydrocinnamic acid (**6**), characterized by a simple bond. These results indicate that the nature of the C_2-C_3 bond, is a key factor influencing the growth-inhibitory activity. Hydroxyl groups in the aromatic ring had a negative effect, as can be observed by activity profile comparison of compound **43** with the hydroxylated derivatives **47**-**50**. These results are in agreement with those reported in the previous study of hydroxyl substitution in the hydrocinnamic acid structure against *C. campestris* growth.[164] However, among the hydroxylated derivatives the ortho- one (**47**), is the most most phytotoxic, probablybe due to its ability to cyclize and form coumarins. Infact, cyclization into scopoletin and umbelliferone occurs from cinnamic acid but requires an ortho alcohol,[165] which could be the explanation for the increased activity found for the ortho hydroxylated derivative. The results showed that the most active compound was the methyl ester derivative of *trans*-cinnamic acid (**64**), with an IC_{50} of 331 µM. Nonetheless, other compounds exhibited close levels of inhibition (**3**, **4**, **16**, and **18**). The overall structure–activity relationship is summarized below (**Figure 30**).

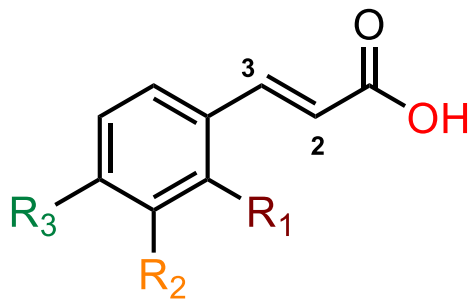

Figure 30. *trans-cinammic acid (**43**) derivatives framework.*

a. Side chain degree of unsaturation affects the activity
b. Hydroxyl groups at R_1, R_2 or R_3, decrease the activity
c. Substitution of OH with OCH_3 notably increase the activity

5.2 Allelopathic plant extracts investigation against parasitic plant seed germination

Since root parasitic weeds have evolved a unique multicellular structure termed haustorium, that attaches and penetrate the host, to withdraws water and nutrients,[61,166] the identification of compounds from natural sources with herbicidal activity against pre-attached broomrape stages is important to provide alternative strategies for parasitic weed management. Nature is a generous source of pesticides[88] but only a small fraction of microbial and plant metabolites has been screened for herbicidal activity.[167] From the investigation of microbial and plant toxins, many compounds with allelopathic activity against parasitic weeds affecting seed germination and radicle development have been discovered. In this context a first investigation of plants (**Table 1**), which from field observations were found to be donors of allelopathic activity, was performed. Organic extracts and aqueous phase, were studied for their potential inhibitory activity of broomrape radicle growth (**Figures 31**).[167] Two concentrations were tested, 100 and 10 μg of root extract /ml GR24. When the concentration of 10 μg of root extract /ml of GR24 is used, none of the weed root extracts showed growth inhibitory activity on treated broomrape radicles in comparison with control radicles (broomrape radicles treated with GR24). While, significant inhibition of broomrape radicle growth was observed, at concentration of 100 μg of root extract /ml GR24. Specifically, roots of *C. arvensis* consistently inhibited the radicle growth of all broomrape species studied. The organic extract, of the just mentioned plant, showed an average growth inhibition of 56.9 % ± 4.7 in *O. crenata*, 45.3 % ± 3.2 in *O. cumana*, 57.7 % ± 1.1 in *O. minor* and 82.5 % ± 1.2 in *P. ramosa* radicles. Furthermore, *C. arvensis* root organic extract induced an intense yellowing of *O. crenata* radicles with swollen root tips (**Figure 31**). *O. crenata* radicles were not inhibited by root extracts of any other weed species. On the contrary, *P. ramosa* radicles were sensitive to radicle growth inhibition of all weed extracts except for *D. stramonium, H. europaeum, M. sylvestris, S. nigrum* and *U. dioica.* Similarly, radicle growth of *O. minor* was significantly inhibited by all weed extracts except for *A. retroflexus, D. stramonium, M. sylvestris, P. oleracea* and *S. nigrum.* Besides *C. arvensis, C. bonariensis* showed good level of inhibition too, however, a low but still significant inhibitory activity was found in *A. retroflexus, D. stramonium, P.oleracea* and *T. terrestris.*

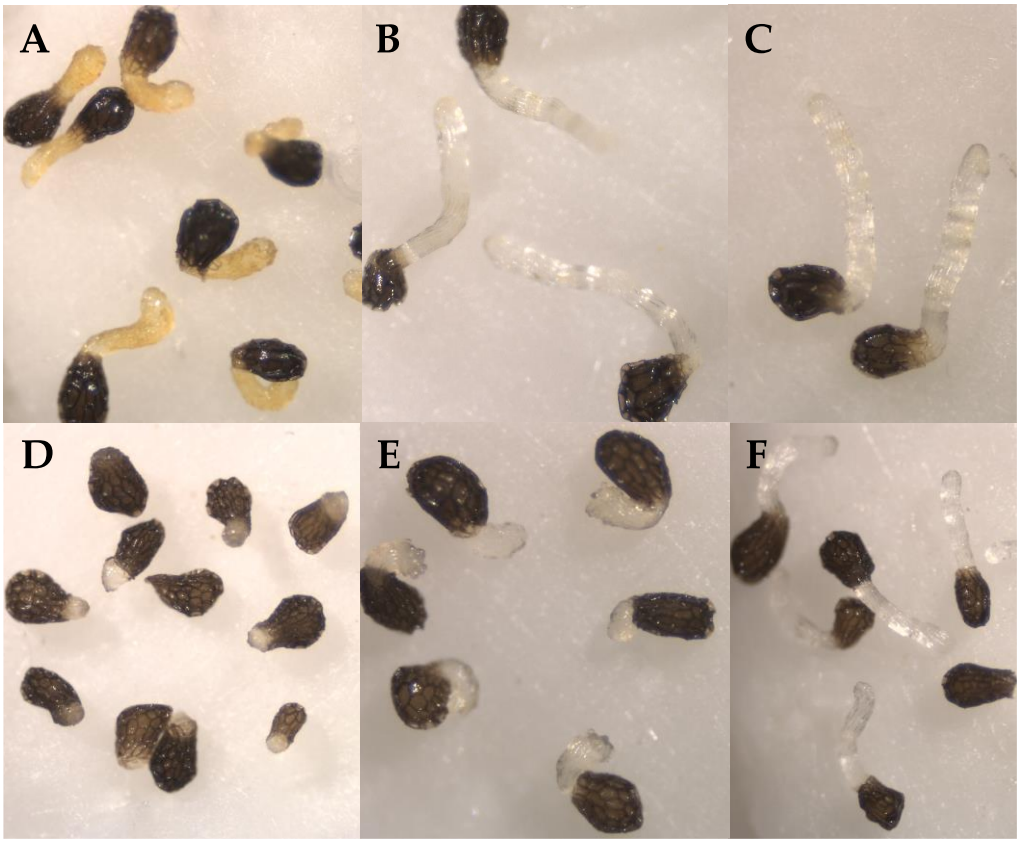

Figure 31. *CH_2Cl_2 organic root extract effect of (**A** and **D**) C. arvensis and (**B** and **E**) P. oleracea both compared with control (**C** and **F**), on radicle growth of (**A**-**C**) O. crenata and (**D**-**F**) P. ramose (adapted from Fernandez-Aparicio et al. Phytopatol. Mediterr. **2021**, 60 (3), 455-466).*[168]

The organic extracts were analyzed by HPLC recorded in the conditions reported in Materials and Methods section. The HPLC chromatograms obtained showed different profiles for each plant. The optimized HPLC analysis of *C. arvensis* and *C. bonariensis*, two of the most promising plant organic extracts, are reported in **Figure 32**. In particular, the extracts analyzed were those of *C. bonariensis* showing high germination-inducing activity in *P. ramosa* and *O. minor* but was not active in *O. cumana* nor *O. crenata*; *H. europaeum* and *S. nigrum* that showed high activity in seed germination of *O. cumana* and *P. ramosa* but not in *O. minor* nor *O. crenata; A. albus* and *A. retroflexus* that showed high levels of germination in *O. cumana* seeds, but showed low or null activity in seeds of *O. crenata, O. minor* and *P. ramosa; Convolvulus arvensis* did not induce any germination in

any of the broomrape species tested. Among the active organic extracts, those obtained from *C. arvensis, C. bonariensis* were selected for future studies focused on the isolation and characterization of the bioactive metabolites with herbicidal activity targeting the early stages of broomrape seed germination considering the promising TLC profiles confirmed by HPLC analysis. The roots of these selected plants could be used for the first time in the biocontrol of *Orobanche* and *Phelipanche* species. Phytochemical analysis on these weed species components have been already reported for some of the plant used in this study. From *C. arvenis* carbohydrates, coumarins, saponins flavonoids, lipids, steroids, terpenoids, alakoids, tannins and lactones were isolated,[169] while glycosides and monoterpenes were isolated from *C. bonariensis*.[170]

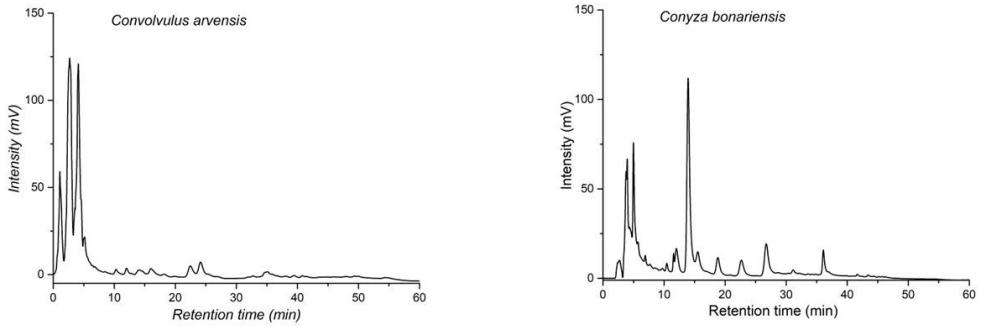

Figure 32. *HPLC chromatogram of C. arvensis and C. bonariensis.*[168]

5.3 Convolvulus arvensis

Following the previous allelopathic screening,[168] *C. arvensis* was selected as a reservoir of allelopathic compounds, to be tested against the radicle growth of four troublesome broomrape species. The determination of bioactive metabolites was carried out through an activity-guided purification process of lyophilized roots from *C. arvensis* CH_2Cl_2 extract (**Figure 20**), followed by spectroscopic analysis of the fractions obtained. By CC fractionation of *C. arvensis* CH_2Cl_2 extract, 10 fractions were obtained. The latters were then bioassayed, against broomrape parasitic plants to identify the most phytotoxic ones. However, only F9 inhibited radicles growth of all the broomrape species tested, causing abnormal radicles development, with a length reduction compared to the control. The average radicle growth inhibition induced by *C. arvensis* F9 was 50.8 ± 0.3% for *O. crenata*, 73.2 ± 0.8% for *O. cumana*, 65.4 ± 0.4% for *O. minor* and 71.4 ± 1.4% for *P. ramosa* radicles. In all the broomrape species, no significant phytotoxicity was observed when their radicles were treated with the rest of the fractions (F1 to F8 and fraction F10) (data not shown). Thus, F9 was selected for further purification, using RP-CC at medium pressure eluted by MeCN/H_2O (7:3 v/v), yielding three fractions, tested against broomrape radicle growth. From the bioassays results, was evident that only F9.2 caused phytotoxicity with an average inhibition, compared to their corresponding control radicles, of 73.5 ± 0.8% in *O. crenata*, 86.8 0.3% in *O. cumana*, 81.7 ± 1.9% in *O. minor* and 77.0 ± 0.5% in *P. ramosa* radicles. Otherwise, fractions F9.1 and F9.3 did not induce significant phytotoxicity in radicles of any of the broomrape species (**Figure 33,34**).

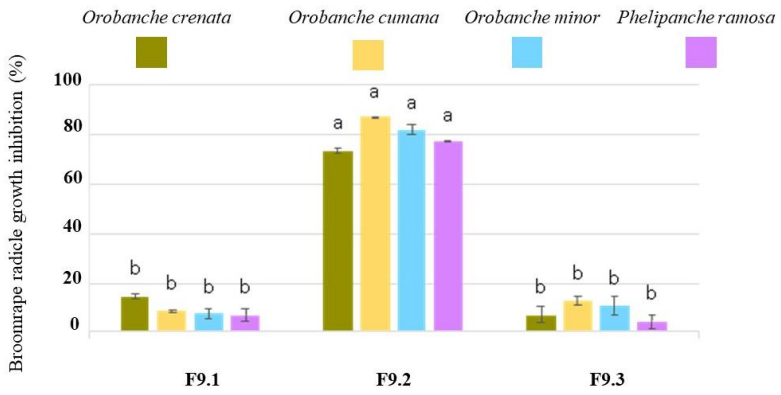

Figure 33. *F9s Convolvulus arvensis activity on broomrapes species (adapted from Soriano et al. Agriculture,* ***2022****, 12, 585-594).*[171]

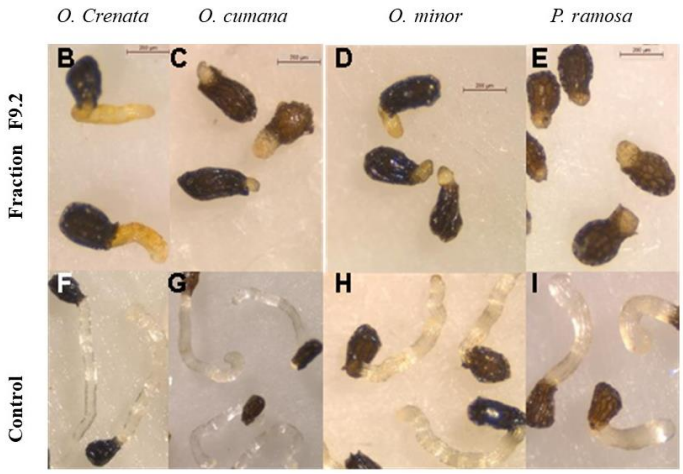

Figure 34. *Convolvulus arvensis F9.2 effect on radicles of (**B**) Orobanche crenata, (**C**) Orobanche cumana, (**D**) Orobanche minor and (**E**) Phelipanche ramosa in comparison with the effect of the control treatment in (**F**) Orobanche crenata, (**G**) Orobanche cumana, (**H**) Orobanche minor and (**I**) Phelipanche ramose (adapted from Soriano et al. Agriculture, **2022**, 12, 585-594).*[171]

In order to confirm F9.2 strong inhibitory activity against the broomrape species tested, a subsequent dose–response screening was conducted, at 100, 50 and 10 µg /mL (**Figure 35**).

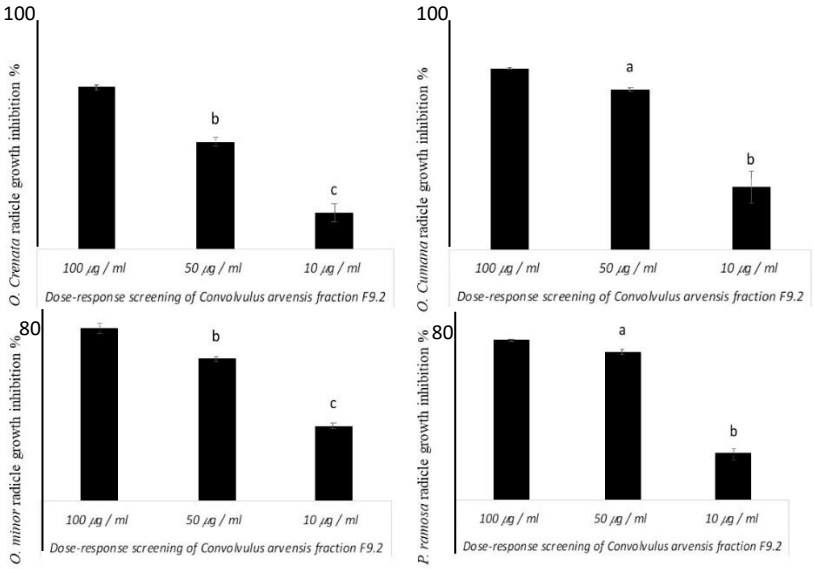

Figure 35. *Dose–response curve of the phytotoxic activity of Convolvulus arvensis fraction F9.2 on radicle growth expressed as a % with respect to the growth of radicles treated with control treatment. For each broomrape species, bars with different letters are significantly different according to the Tukey test (p = 0.05). Error bars represent standard error (adapted from Soriano et al. Agriculture, **2022**, 12, 585-594).*[171]

From ^{1}H NMR spectrum the signals of anomeric protons at δ 6.3–4.6 ppm, complex signals in the range of δ 4.3–3.2 ppm typical of hydroxylated ring protons and singlets at δ 1.2 ppm for 6-deoxy sugar residues, were detected. Furthermore, aliphatic signals, diagnostic of fatty acids in the range of δ 2.8–1.8 ppm were observed. Finally, peaks in the range 1074–1380 u.m.a., of the ESI-MS spectra were observed. The analysis and comparison of ^{1}H NMR (**Figure 36**) and ESI MS data with those reported in the literature, [115–117] allowed to identify F9.2, as a mixture of arvensic acids.

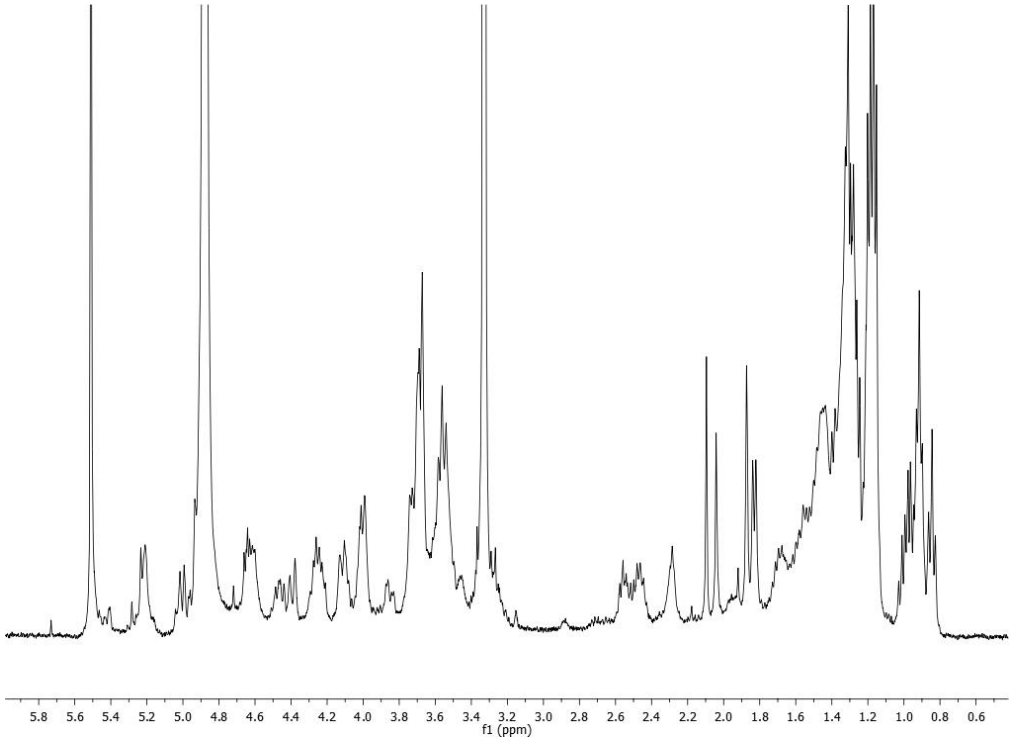

Figure 36. *1H NMR spectrum of fraction F9.2 recorded at 400 MHz in CD_3OD (adapted from Soriano et al. Agriculture,* ***2022****, 12, 585-594).*[171]

They consist of a polysaccharide scaffold containing fucose, rhamnose and glucose residues bonded to hydroxyl or dihydroxyl fatty acids (**Figure 37**). The arvensic acids differ one from another by the nature and the number of monosaccharides. Thus, to examine the monosaccharide composition, F9.2 was hydrolyzed following the procedure outlined in the Materials and Methods section. Subsequently, EtOAc extraction was performed on the hydrolyzed solution to separate aglycones from the sugar components.

The aglycones underwent a reaction with diazomethane, and the presence of fatty acids was confirmed using TLC, revealing more apolar compounds compared to the initial ones. Additionally, its ^{1}H NMR spectrum displayed methoxy signals, affirming the formation of methyl esters. Furthermore, in order to identify the monosaccharide residues of the polysaccharide scaffold, the dried hydrolyzed residue was dissolved in MeOH and analyzed by TLC on silica gel, eluted with *i*-PrOH-H_2O (8:2, v/v), in comparison with standard samples of galactose, glucose, mannose, xylose, rhamnose and fucose allowing to confirm the presence of rhamnose, fucose and glucose. Additionally, using the procedure reported in the Material and Methods section, the hydrolyzed mixture was derivatized, and analyzed by HPLC. The comparison of L-rhamnose, D-fucose and D-glucose standards retention times, with those obtained by the analysis of derivatized hydrolized mixture allowed to confirm their presence. Further efforts to purify F9.2 and determine the structure of pure arvensic acids, failed due to the mixture homogeneity and low amount available. In fact, these resin glycosides commonly found in the *Convolvulaceae* family, exhibit slight structural variations that pose challenges in their separation. Recent investigations identified different arvensic acid structures. Fan et al. isolated arvensic acids A–D,[116] characterized by an heptasaccharide bonded to 12-hydroxypentadecanoic or 12-hydroxyhexadecanoic acids. The same authors, revealed arvensic acids E-J, featuring hexa- and heptasaccharide core and less common aglycones, such as 11-hydroxyhexadecanoic and 11-hydroxyheptadecanoic acids.[115] Lu et al. identified two new arvensic acids, K and L,[117] with a pentasaccharide chain and the same aglycone as arvensic acids E–J. Although these arvensic acids were assessed for cytotoxic activity and showed no effect on studied cancer cell lines, they have drawn attention for their diverse pharmacological bioactivities, including aortic vasorelaxant properties,[172] anticonvulsant and neuroprotective effects,[173] and α-glucosidase inhibitory activity.[174] Remarkably, this work is the first to explore the allelopathic role of arvensic acids against weed development. Although, further investigation to better understood which of them is the responsible of the activity are needed, their synthesis on gram scale to obtain the amounts for industrial applications might be difficult, due to the complexity of the structure.

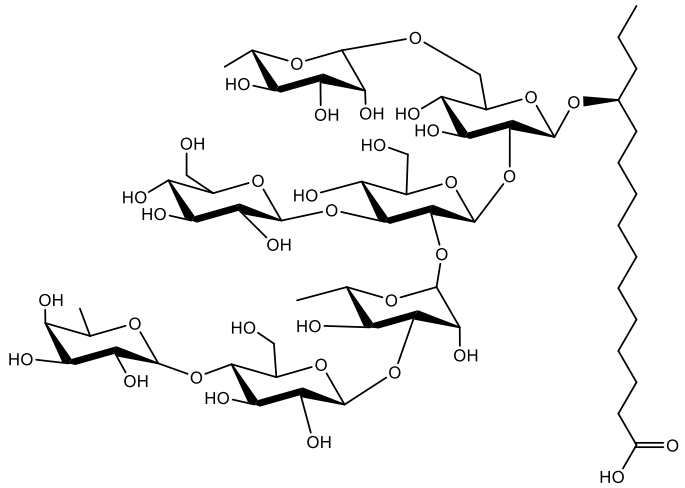

Figure 37. *Arvensic acid structure framework (adapted from Soriano et al. Agriculture,* ***2022****, 12, 585-594).*[171]

5.4 Retama raetam

Another plant recognized for its allelopathic potential is *R. raetam*,[111] and as such, it was detailed studied. The process of bioactivity-guided purification involved conducting anti-fungal bioassays against the phytopathogenic fungus *S. vesicarium*. Fractionation of the crude CH_2Cl_2 extract by CC, allowed to obtained 13 fractions (F1–13) with diverse chemical profiles. Interestingly, the activity exhibited by the fractions F2–F5 (~60%) resulted stronger than the one displayed by the total crude extract (~43%) and comparable to the commercial fungicide pentachloronitrobenzene (PCNB), used as a positive control (**Figure 38**). This experimental evidence highlights the crucial role of the pure bioactive specialized metabolites identification, even when the entire extract exhibits effectiveness.

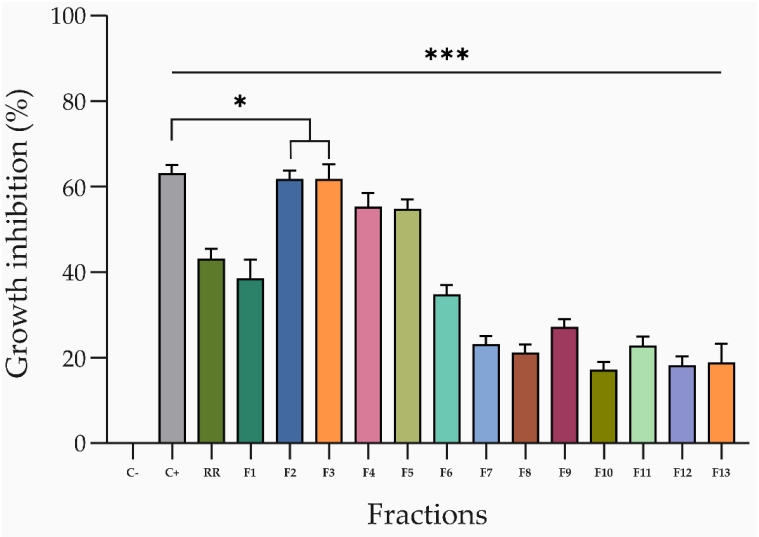

Figure 38. *R. raetam CH_2Cl_2 crude extract (RR) and fractions inhibitory effect, on the mycelium of S. vesicarium, at a concentration of 2 mg/mL (crude extract) and 250 µg/mL (fractions), respectively. The negative control was absolute methanol (C−), and the positive control was 200 µg/mL of PCNB. The fungal growth inhibition is represented as the percentage reduction of the fungal mycelia diameter in the treated plate compared to that in the control plate. All experiments were performed in triplicate with three independent trials. Data are presented as means ± standard deviation (n = 3) compared to the control. *** p < 0.0001 and * p < 0.05 (adapted from Soriano et al. Toxins,* ***2022****, 14, 311-322).*[113]

The further purification, by combination of CC and TLCs techniques (**Figure 21**), allowed to afford six pure metabolites (**Figure 39**), as described in the Materials and Methods Section. A first investigation of their ^{1}H NMR and ESI MS spectra (**Figures 42-55**) showed that they are isoflavonoids and flavonoids with different substitutions. Then the

comparison of spectroscopical data with those reported in literature allow to their identification as alpinumisoflavone (**67**),[118,119] hydroxyalpinumisoflavone (**68**),[108] laburnetin (**69**),[120] licoflavone C (**70**),[121] retamasin B (**71**),[122] and ephedroidin (**72**) (**Figure 39**).[108]

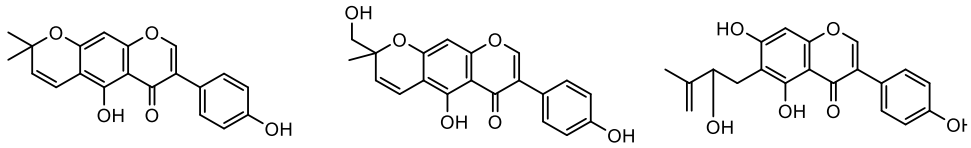

67. Alpinumisoflavone

68. Hidroxyalpinumisoflavone

69. Laburnetin

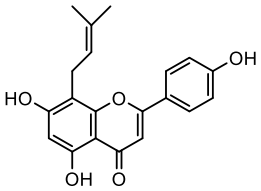

70. Licoflavone C

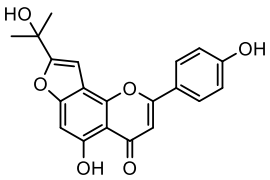

71. Retamasin B

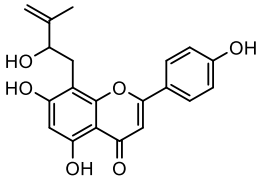

72. Ephedroidin

Figure 39. *Retama raetam* specialized metabolites structure.

An X-ray diffractometric analysis confirmed the structure of alpinumisoflavone (**67**), and its ORTEP view is reported in **Figure 17**. The X-ray crystal structure is reported to undoubtedly identify the compound **67** as alpinumisoflavone.[175]

Three nearly coplanar fused rings and an out-of-plane twisted phenyl ring constitute the compound framework. Due to the low amount available, among the chiral compounds (**68**, **69** and **72**), only the absolute configuration of ephedroidin, at the C-2" was determined by the application of a modified Mosher method.[176] Treatment of compound **72** with S-MTPA chloride produce its ester derivative, which showed two sets of signals with an enantiomeric ratio of 50:50, indication that **72** is an enantiomeric mixture of 2"(S)- **72** and 2"(R)- **72**. Treatment with R-MTPA chloride produce the same result. This was confirmed by an obtained optical rotation value of zero [α]D25 0 (c 0.4, MeOH), too.

Bioassays The compounds isolated (**67-72**) were spot-inoculated on PDA plates to

assess their activity against the fungal phytopathogen *S. vesicarium*. Only laburnetin (**69**) showed significant effectiveness when spot-inoculated at a concentration of 50 µg/mL, impeding the growth of *S. vesicarium* by approximately 55%. This confirms the antagonistic impact observed in the most potent fractions, which restrained the growth of *S. vesicarium* mycelium by roughly 60%. Notably, the commercial fungicide PCNB, applied at a concentration of 0.5 mg/mL, exhibited an antagonistic effect comparable to that of laburnetin at a concentration 10 times lower (50 µg/mL) (**Figure 40**). This highlighted the potential of natural compounds as a viable substitute of traditional pesticides. Conversely, the other compounds displayed fungal inhibition rates of around 20%. Considering the results obtained, it is plausible to attribute the primary role in the antagonistic effect observed in the *R. raetam* extract against the fungus *S. vesicarium* to laburnetin.

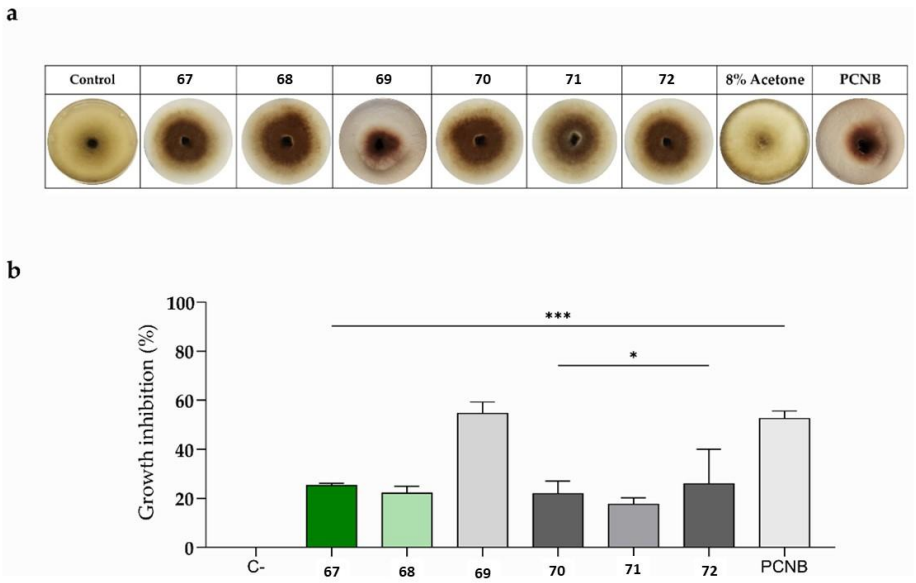

Figure 40. *Effects of alpinumisoflavone (**67**), hydroxyalpinumisoflavone (**68**), laburnetin (**69**), licoflavone C (**70**), retamasin B (**71**), and ephedroidin (**72**) against S. vesicarium. The plot shows the fungal growth inhibition exerted by the tested compounds at a concentration of 50 µg/mL. (**a**) Representative photos of the biological assay for in vitro inhibition of mycelial growth of S. vesicarium. 8% Acetone and 0.5 mg/mL PCNB were used as negative and positive controls, respectively. (**b**) Fungal growth inhibition reported as the percentage of the reduction in the diameter of the fungal mycelium in the treated plate compared to that in the control plate. *** $p < 0.0001$ and * $p < 0.05$ (adapted from Soriano et al. Toxins, **2022**, 14, 311-322).*[113]

The isoflavonoid laburnetin (**69**) has already been isolated from the *Genista* genus,[108] as well as from other plants, and its antimicrobial activity was demonstrated.[177] To the best of our knowledge, here, the antifungal activity of this compound against *S. vesicarium* is being reported for the first time, showing that laburnetin could be proposed as a natural antagonist for the control of this phytopathogen that infests several important cultivated species.

R. raetam, a plant species exhibiting allelopathic properties, was harvested from the Saharan ecosystem in the Souf region of southeastern Algeria. The allelochemicals produced by this plant have the potential to serve as alternative agrochemicals, addressing the adverse impacts associated with synthetic herbicides in plant–plant interactions. In this context, the isolated specialized metabolites (**67-72**) were examined in two distinct parasitic weed bioassays to explore the potential effects of *R. raetam* metabolites on either inducing suicidal stimulation or inhibiting the radicle growth of broomrapes.

Firstly, the activity of compounds **67-72** on seeds germination of four parasitic weed species, namely *O. crenata*, *O. cumana*, *O. minor*, and *P. ramosa*, was assessed through in vitro germination bioassays. The synthetic germination stimulant GR24, employed as a positive control, resulted in germination levels of 53.2% ± 1.7%, 64.6% ± 1.8%, 91.7% ± 1.7%, and 94.2% ± 0.4% for *O. crenata*, *O. cumana*, *O. minor*, and *P. ramosa*, respectively. Conversely, null germination occurred when seeds of the broomrape species were treated with either the negative control (distilled water) or compounds **67-72**. The findings from the germination bioassay indicate that none of the isolated metabolites from *R. raetam*'s stem act as inducers of suicidal germination in the studied broomrape species. Implementing inducers of suicidal germination in the field, particularly in the absence of a specific host, serves as a control strategy against obligate root parasitic weeds. This approach exploits the subsequent parasitic growth post-germination, ultimately causing the death of the parasite through nutrient deprivation in the absence of host-derived nutrients.[67]

In a second bioassay, the six isolated compounds (**67-72**) were evaluated at a concentration of 100 µM to assess their potential as inhibitors of radicle growth in *O.*

crenata, *O. cumana*, *O. minor* and *P. ramosa*. Among the tested compounds, minimal to no activity was observed, except for ephedroidin (**72**), which exhibited a pronounced inhibitory effect on the normal development of *O. cumana* radicles when compared to the control radicles of *O. cumana* (**Figure 41**). Ephedroidin induced a robust toxic effect, characterized by darkening in the *O. cumana* radicle, leading to an average length inhibition of 80.8% ± 1.6% compared to the radicle control (**Figure 41**). These toxic effects on broomrape radicles align with previous descriptions of similar effects caused by cytochalasans.[67]

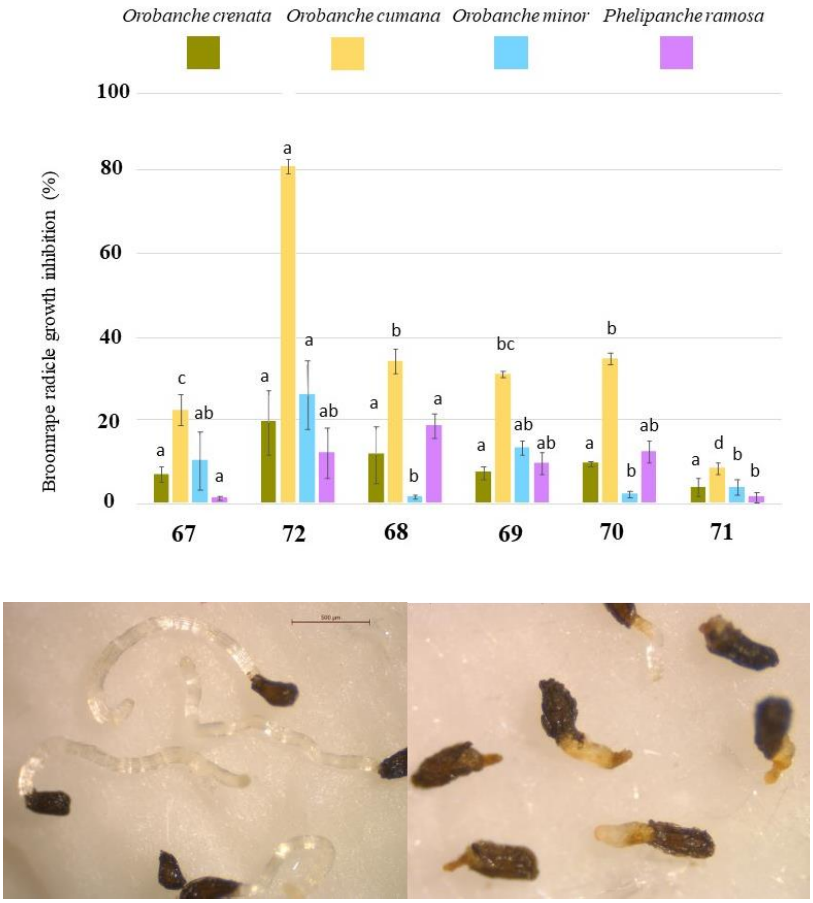

Figure 41. *Inhibition plot of broomrape radicle growth induced by alpinumisoflavone (**67**), ephedroidin (**72**), hydroxyalpinoisolflavone (**68**), laburnetin (**69**), licoflavone C (**70**), and retamasin B (**71**), expressed as a percentage with respect to the control GR24. Photographs illustrating the effects of ephedroidin in radicles of O. cumana: (**left**) control, (**right**) 100 µM ephedroidin. Analysis of variance was applied to angular transformed replicate data. For each broomrape species, bars with different letters are significantly different according to the Tukey test (p = 0.05). Error bars represent standard error. (adapted from Soriano et al. Toxins, **2022**, 14, 311-322).*[113]

Laburnetin (**69**) and ephedroidin (**72**) were previously isolated from *Genista ephedroides* and from *R. raetam*.[108] Recently, ephedroidin was tested in many biological areas, showing among others, inhibition of nitric oxide synthase (iNOS) and nuclear factor kappa B (NF-κB), as well as in decreasing oxidative stress. Besides the bioactivity previously reported, the results of the present work, showed how ephedroidin (**72**) strongly inhibit *O. cumana* seeds development, paving the way for its use as natural herbicide against this dangerous parasitic weed.

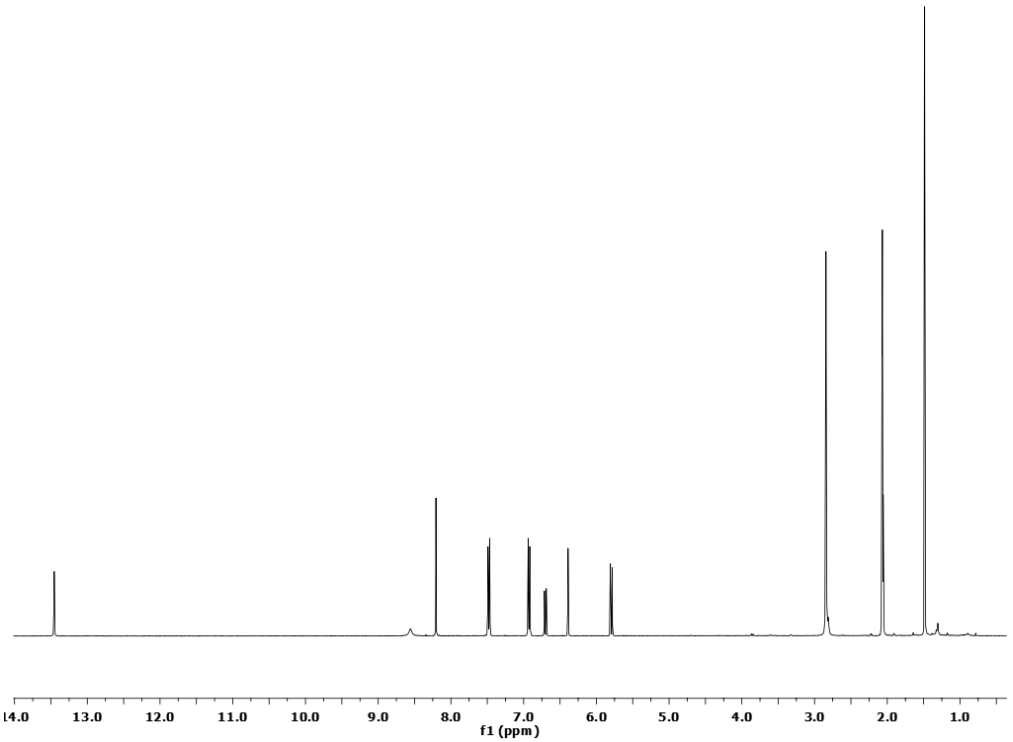

Figure 42. ^{1}H NMR spectrum of alpinumisoflavone, **67** (acetone-d_6, 400 MHz).

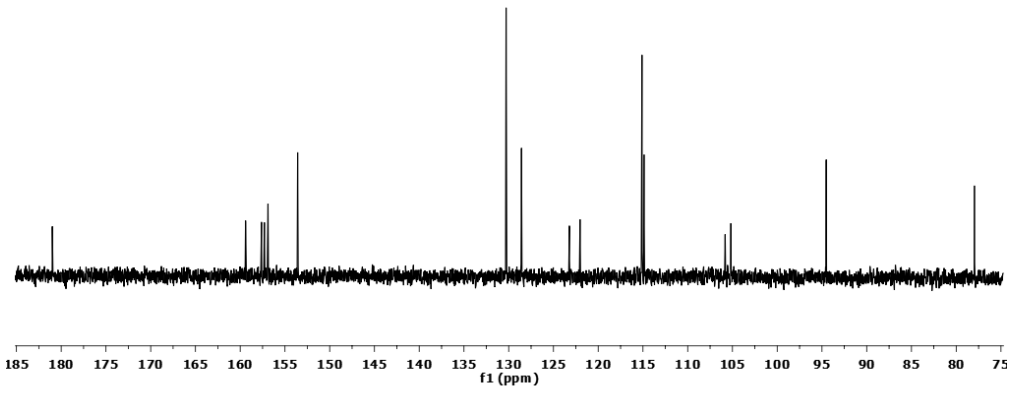

Figure 43. ^{13}C NMR spectrum of alpinumisoflavone, **67** (acetone-d_6, 100 MHz).

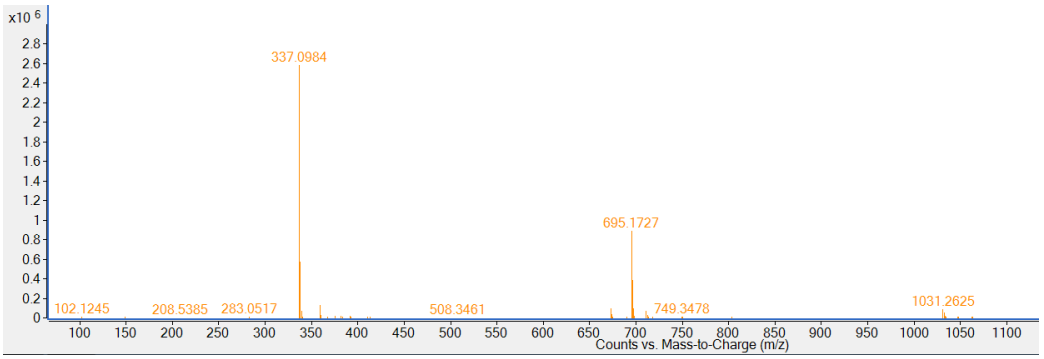

Figure 44. ESI MS spectrum of alpinumisoflavone, **67** recorded in positive modality.

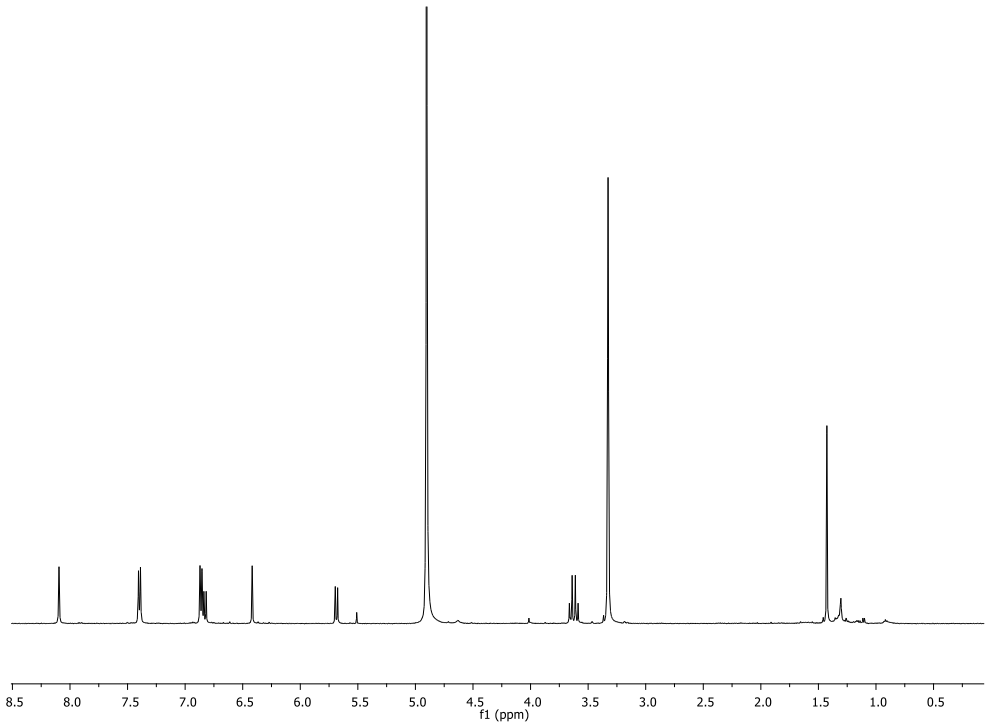

Figure 45. *^{1}H NMR spectrum of hydroxyalpinumisoflavone,* ***68*** *(acetone-d_6, 400 MHz).*

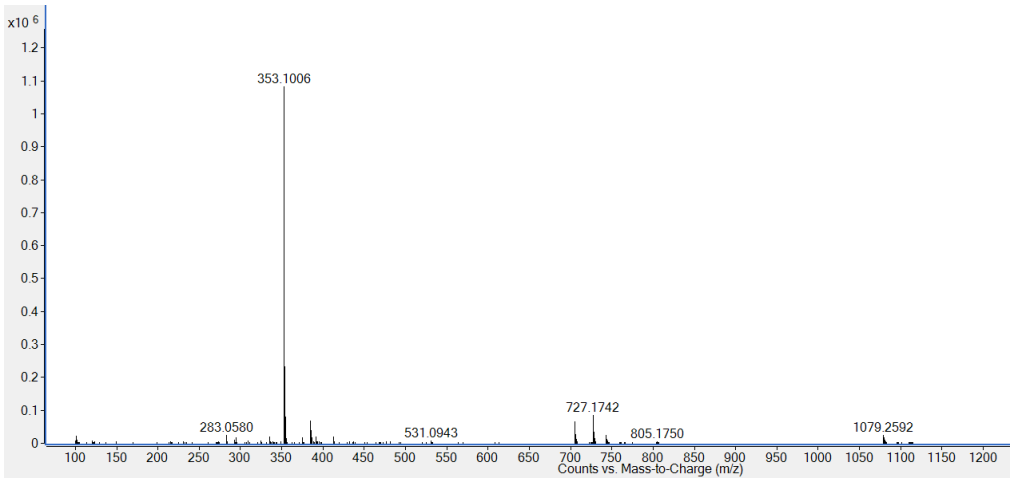

***Figure 46**. ESI MS spectrum of hydroxyalpinumisoflavone, **68** recorded in positive modality.*

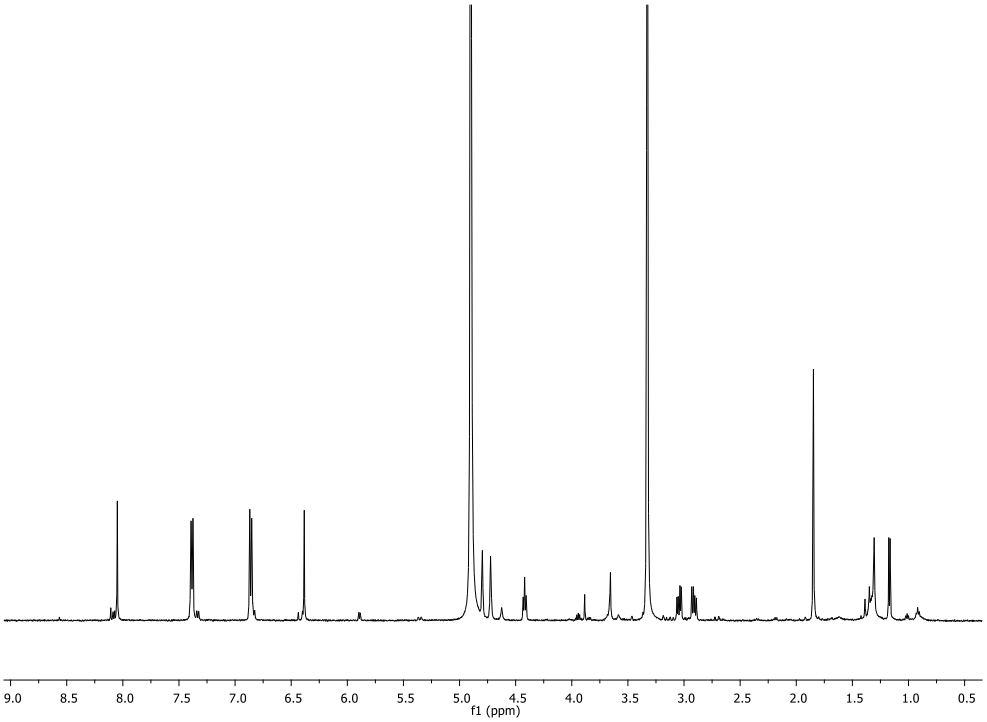

Figure 47. *^{1}H NMR spectrum of laburnetin,* ***69*** *(acetone-d_6, 400 MHz).*

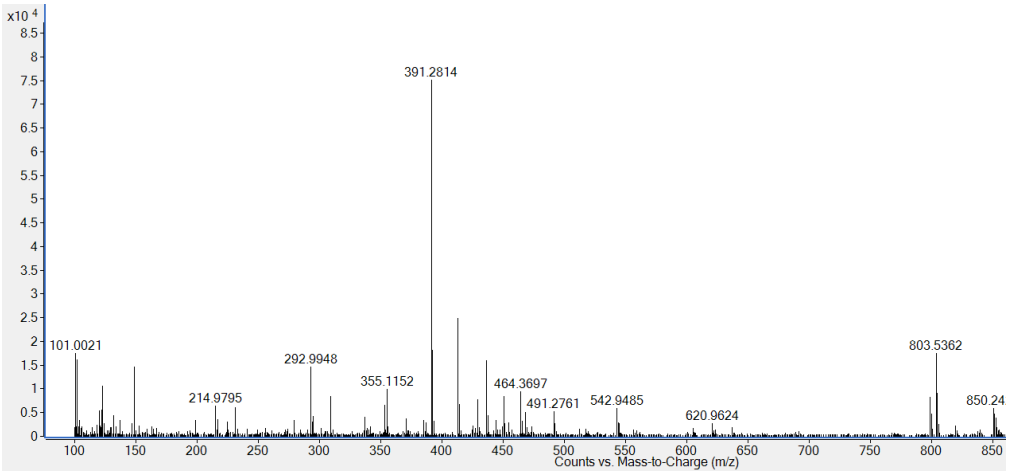

Figure 48*. ESI MS spectrum of laburnetin,* ***69*** *recorded in positive modality.*

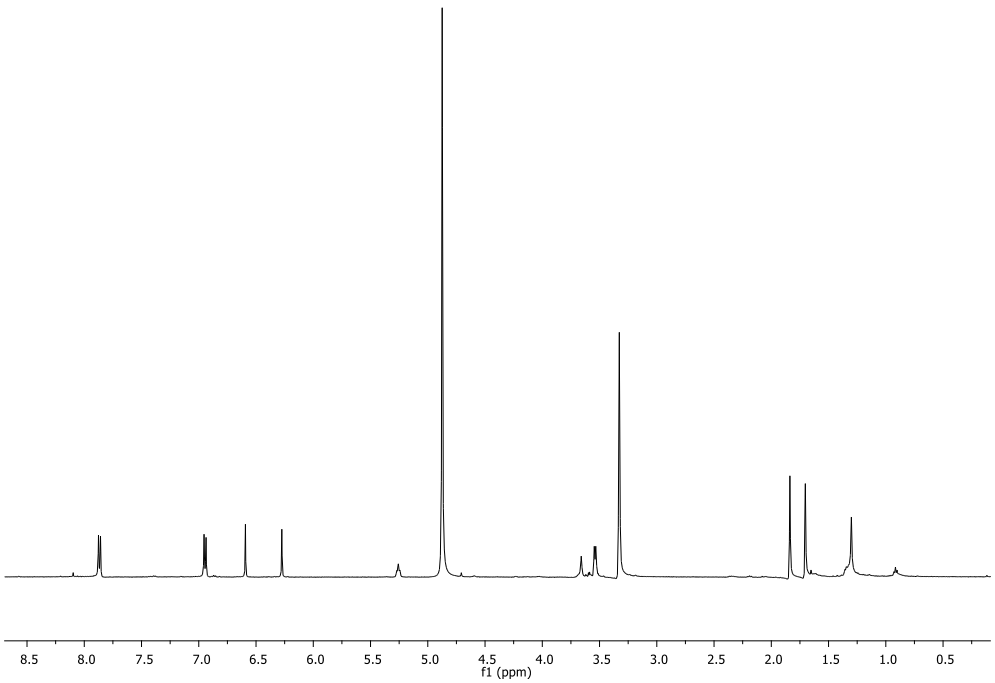

Figure 49. *^{1}H NMR spectrum of licoflavone C,* ***70*** *(acetone-d_6, 400 MHz).*

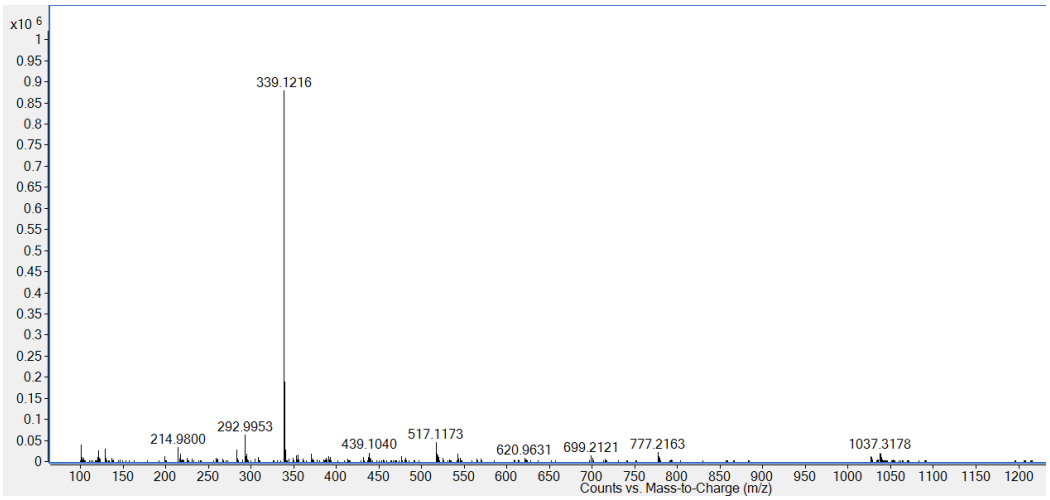

Figure 50. *ESI MS spectrum of licoflavone C,* ***70*** *recorded in positive modality.*

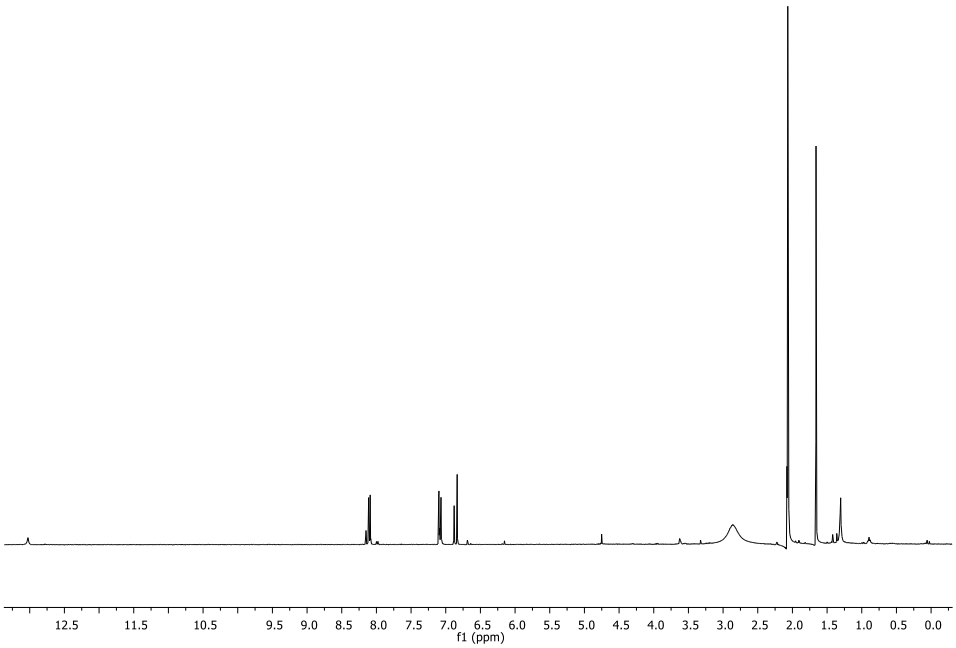

Figure 51. *^{1}H NMR spectrum of retamasin B,* ***71*** *(acetone-d_6, 400 MHz).*

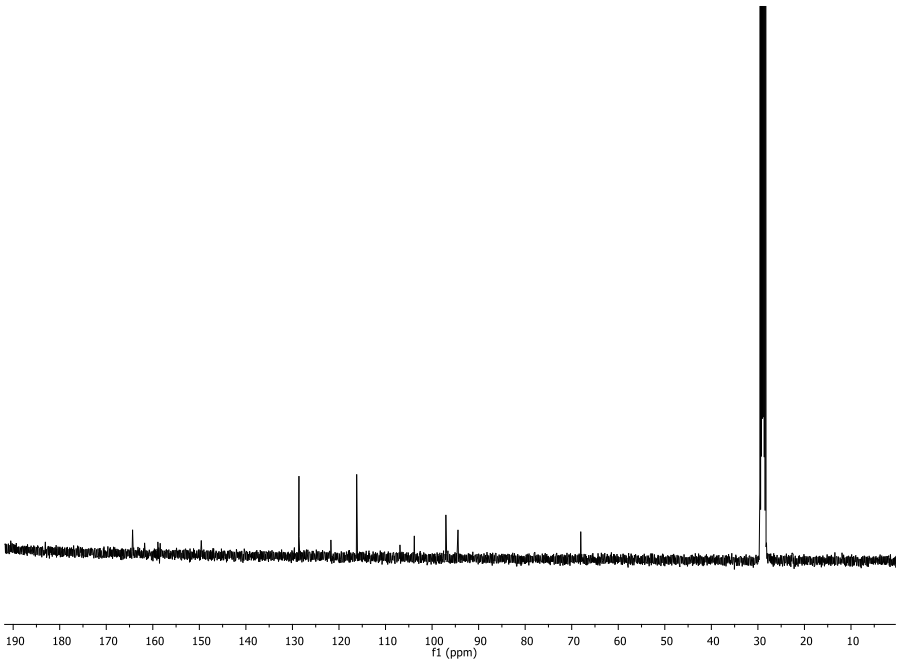

Figure 52. *^{13}C NMR spectrum of of retamasin B,* ***71*** *(acetone-d_6, 100 MHz).*

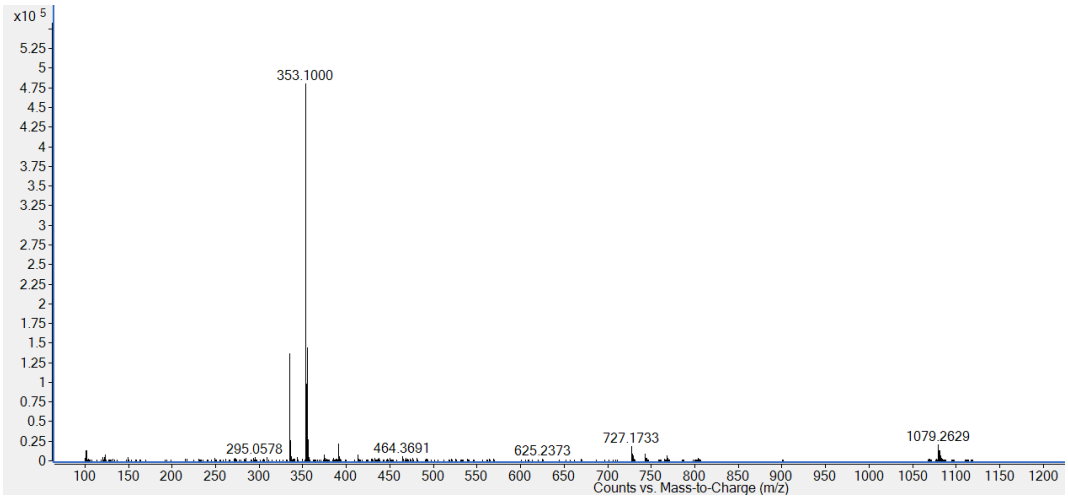

Figure 53. *ESI MS spectrum of retamasin B,* ***71*** *recorded in positive modality.*

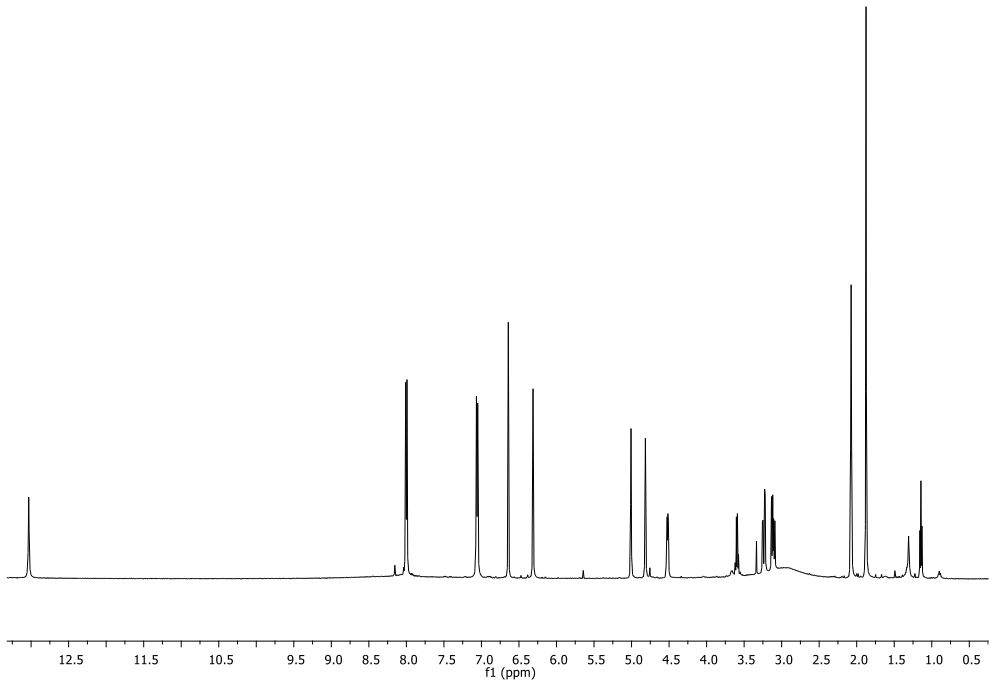

Figure 54. *^{1}H NMR spectrum of ephedroidin,* ***72*** *(acetone-d_6, 400 MHz).*

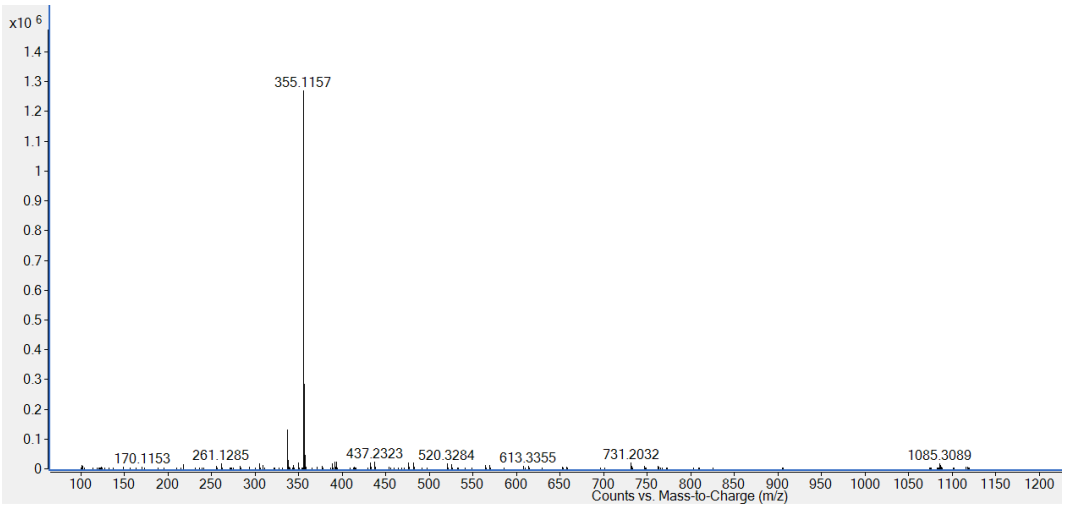

Figure 55. *ESI MS spectrum of ephedroidin,* ***72*** *recorded in positive modality.*

5.5 *Bellardia trixago*

As well as *R. raetam*, also *B. trixago* was not included in the first screening, but considering its allelopathic potential, many efforts have been done for isolation and bioanalysis of its specialized metabolites. Thus, three different organs (flowers, aerial vegetative green organs and roots) of two populations (a white-flowered and yellow-flowered population) were extracted, following the procedure described in the *Materials and Methods section*. The obtained *B. trixago* extracts, were tested against *O. cumana* radicle growth (**Figure 56**) at a concentration of 100 μg/mL. The results obtained showed that EtOAc extract, of both the with and yellow-flowered population, are the only ones to strongly inhibit radicle growth. Previous studies reported both quantitative and qualitative differences in the chemical compositions across various populations of *B. trixago*, as well as among the different plant organs.[178] Formisano et al. identified insecticidal activity in the roots of a specific *B. trixago* population collected in Italy, with comparatively lower activity observed in the aerial parts of plants from the same population.[179]

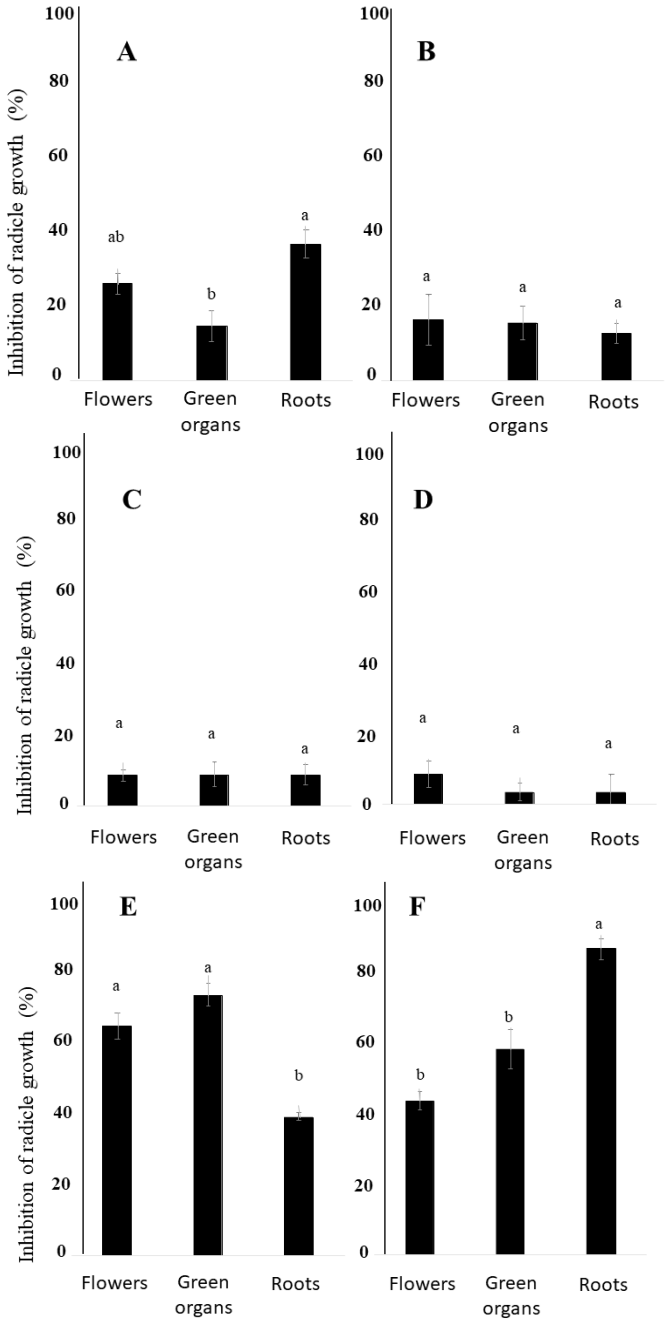

Figure 56. *Allelopathic effects on O. cumana radicle growth induced by extracts prepared from sequential extractions with n-hexane (**A**,**B**), dichloromethane (**C**,**D**), and ethyl acetate (**E**,**F**) of three types of B.trixago organs: flowers, aerial green organs and roots of two Bellardia trixago populations-a white-flowered population (**A**,**C**,**E**) and yellow-flowered population (**B**,**D**,**F**). Bars with different letters are significantly different according to the Tukey test (p = 0.05). Error bars represent the standard error of the mean (adapted from Soriano et al. Toxins, **2022**, 14, 559-571).*[180]

Within the white-flowered population, the most potent inhibitory activity was identified in EtOAc extract of the aerial parts, specifically in the green vegetative organs, followed by the flowers EtOAc extract (68.31 ± 2.9% and 60.1 ± 3.4% inhibition, respectively, compared to the control). In the yellow-flowered population of *B. trixago*, the most significant inhibition of *Orobanche* was found in the EtOAc extract from the roots (average inhibition of 79.5 ± 2.9%), followed by the EtOAc extracts from the aerial parts of plants, including both green organs and flowers (53.5 ± 5.1% and 40.1 ± 2.5% inhibition, respectively, compared to the control).

With the perspective of an allelopathic screening, a preliminary qualitative assessment of the chromatographic profiles of all EtOAc extracts was conducted. This assessment revealed the consistent presence of a main compound and a common pattern of secondary metabolites across different populations and plant organs (data not shown). This, coupled with the greater availability of vegetative green tissues in the laboratory, led to the selection of the EtOAc extract from the green organs of the white-flowered population for the isolation and characterization of inhibitors of *O. cumana* radicle growth. Thus, 189.0 g of lyophilized green organs from the white population were extracted using the procedure outlined in the Materials and Methods section. The resulting sample yielded 1.45 g (0.77%) of EtOAc organic extract, which was fractionated through various steps of purification via CC and preparative TLCs, as detailed in **Figure 23**. This process yielded six pure compounds identified as benzoic acid (**73**, 10.8 mg), bartsioside (**74**, 13.9 mg), aucubin (**75**, 12.4 mg), melampyroside (**76**, 642.3 mg), gardoside methyl ester (**77**, 2.0 mg), and mussaenoside (**78**, 6.1 mg) (**Figure 57**). The structures of these compounds were validated through NMR spectroscopy (Figure **58**-**65**) and MS, along with a comparison to literature data. Optical rotation enabled the unequivocal identification of the stereochemistry of the compounds by referencing values from the natural iridoids, a well-established family of natural products with absolute stereochemistry previously reported through chiroptical methods and X Ray.[181,182] Compounds **73**–**78** were previously isolated from *B. trixago*[131,136] and other iridoid-containing plants.[183,184]

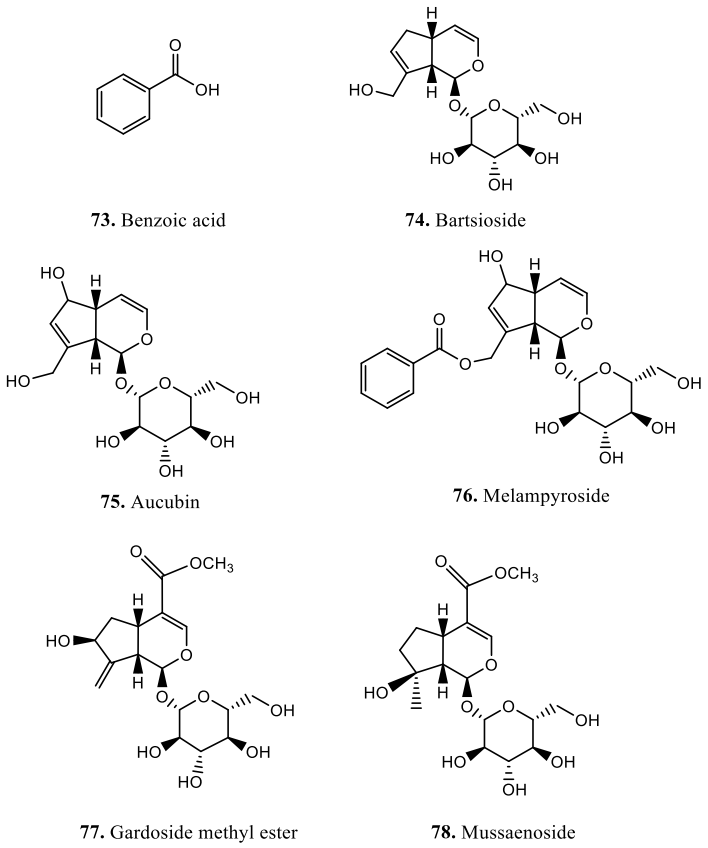

Figure 57. *B. trixago specialized metabolites structures.*

They were assayed against *O. cumana* radicles growth at a concentration of 100 µg/mL (**Figure 58**). Compounds **74** and **78** exhibit good level of inhibition (61.1 ± 1.5% and 65.9 ± 2.9%, respectively) however, the strongest inhibitor resulted to be the melampyroside (72.6 ± 0.9%). This works, is the first documentation of the inhibitory effects on *Orobanche* radicle growth attributed to compounds **74**, **76**, and **78**. Notably, their inhibitory activity surpasses that of compound **73**, a phenolic acid acknowledged for its weedicide properties.[185] Melampyroside was firstly identified in *Melampyrum silvaticum L.*.[186] On the other hand, compounds **74**, **75**, **77**, and **78** were first isolated from *B. trixago*,[187] *Aucuba japonica* Thunb.,[188] *Melampyrum arvense* L.,[189] and *Mussaenda parviflora* Miq.,[190] respectively. Recent literature has highlighted the anti-inflammatory properties of compound **76**, as well as other iridoids not discussed here. This information is linked to a study investigating the potential activity of *Odontites vulgaris* against rheumatoid arthritis. Additionally, in a prior

study that involved various iridoids, compound **76** was identified as cardioactive in Wistar rats.[191]

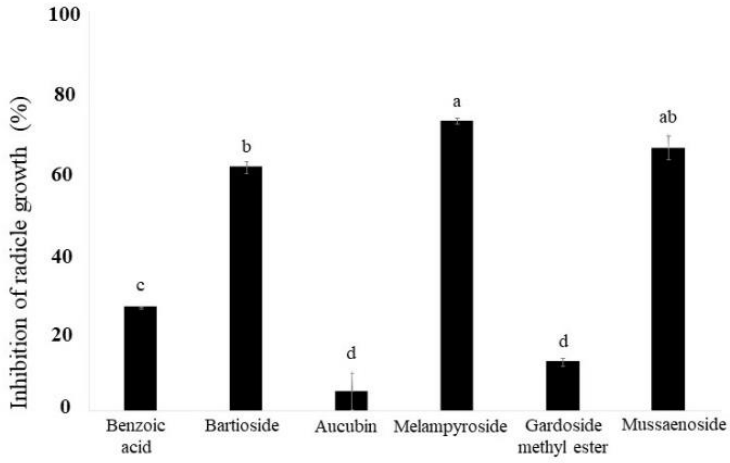

Figure 58. *Inhibition of O. cumana radicle growth induced by benzoic acid (**73**), bartioside (**74**), aucubin (**75**), melampyroside (**76**), gardoside methyl ester (77) and mussaenoside (**78**) at 100 µg/mL. Bars with different letters are significantly different according to the Tukey test (p = 0.05). Error bars represent the standard error of the mean (adapted from Soriano et al. Toxins, **2022**, 14, 559-571).*[180]

Despite their similar chemical structures, prior reports have highlighted variations in the biological activities of compounds **75** and **76**. Extracted from *M. arvense*, benzoic acid, aucubin and melampyroside demonstrated antiprotozoal effects on different species, exhibiting a certain degree of specificity to particular species.[192] Notably, among the highly active compounds **74**, **76**, and **78** against *O. cumana* growth, compound **76** induced some level of phytotoxicity, manifested as darkening in the *O. cumana* radicles (**Figure 59**). In recent studies, compounds **75**, **76**, and **78** were tested as antioxidant, [193,194] although no DPPH scavenging activity was observed, an intriguing discovery emerged from a β-carotene bleaching assay. Specifically, mussaenoside exhibited antioxidant properties, while melampyroside demonstrated pro-oxidant activity by accelerating the oxidation of β-carotene faster than the spontaneous rate, and aucubin showed no antioxidant activity. The pro-oxidative effect of **76** could potentially harm plant tissues, explaining the observed phytotoxicity. However, the connection between the pro-oxidant activity of melampyroside and the absence of antioxidant activity in aucubin, and how these factors may be linked to the observed growth inhibition (or lack thereof), remains unclear.

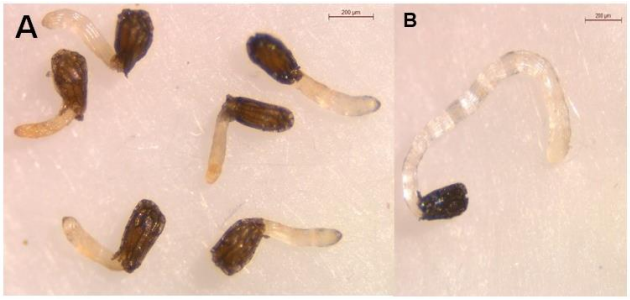

Figure 59. *Growth of Orobanche cumana radicles treated with melampyroside (**4**) at 100 µg/mL (**A**) and control (**B**) (adapted from Soriano et al. Toxins, **2022**, 14, 559-571).*[180]

The CLogP values for the isolated compounds were computed in an attempt to establish a correlation with the observed inhibitory activity of compounds **73**–**78** (see **Table 5**). Negative values were obtained for all compounds, except **73**, suggesting a preference for aqueous media. A good solubility in water is crucial to facilitate compound transport to the active site; however, excessively low lipophilicity may hinder the ability to traverse the cell membrane.[195] Consequently, compounds with higher absolute CLogP values (exceeding |2|), such as **75** and **77**, exhibit lower bioactivity, whereas the most active ones **76** (-1.153), **78** (-1.849), and **74** (-1.941) have lower CLogP values. In the case of melampyroside, its reduced affinity to water, coupled with the presence of the benzoyl group, could positively impact bioactivity through the enzymatic mediated release of this group inside the cell. As previously noted, benzoic acid alone has been reported to possess phytotoxic properties. The notably lower activity of compound **73** compared to **76** might be attributed to two factors: their lipophilicity (CLogP: +1.885) and a potential synergistic effect with compound **76** post-metabolization.

	73	**74**	**75**	**76**	**77**	**78**
CLog*P*	1.885	−1.941	−4.028	−1.153	−2.133	−1.849

Table 5 *Calculated logP for compounds.*

Ecotoxicological tests are deemed a valuable tool for the initial screening of compound toxicity, particularly in plant extracts.[196] The ecotoxicity of compound **76** was assessed in three aquatic and two terrestrial organisms, utilizing varying concentrations starting from 100 µg/mL, the effective concentration applied against *O. cumana*. The impact of compound

76 on *R. subcapitata*, *L. sativum*, *D. magna*, *C. elegans*, and *A. fischeri* is reported in **Figure 60**. The ecotoxicity results revealed significant variations in the sensitivity of the tested organisms, reflecting differences in sensitivity between plant species and other organisms to compound **76**. Melampyroside exhibited the highest toxicity towards daphnia (24 h EC50 = 33.26 μg/mL), nematodes (24 h EC50 = 57.23 μg/mL), and bacteria (EC50 30′ = 76.05 μg/mL). However, its toxicity was less pronounced algae and macrophytes, with a 72 h EC50 ≥ 100 μg/mL. Notably, when assessing the effect on L. sativum across concentrations, the difference was not statistically significant from 5 μg/mL to 100 μg/mL. Moreover, the growth observed with these treatments did not significantly differ from the control group (**Figure 60B**). This differing species-specific sensitivity to melampyroside could potentially be attributed to the non-absorption of this compound by certain plants, suggesting a selectivity of melampyroside in inhibiting the radicle growth of *O. cumana*.[197]

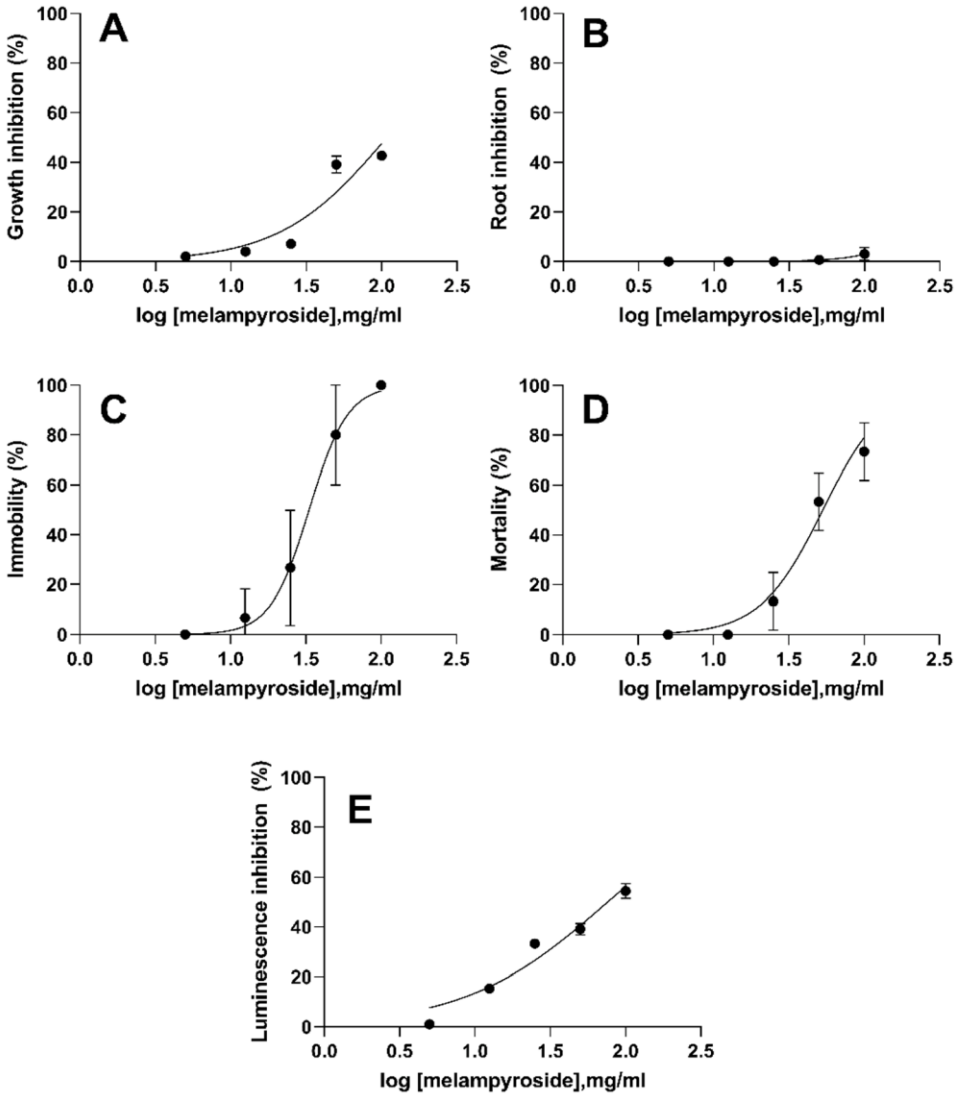

Figure 60. *Concentration–response curves of melampyroside (**76**) for R. subcapitata (**A**), L. sativum (**B**), D. magna (**C**), C. elegans (**D**) and A. fischeri (**E**). Error bars correspond to 95% confidence intervals. Dotted lines represent the fitting to the effect equation (adapted from Soriano et al. Toxins, **2022**, 14, 559-571).*[180]

Considering the EU Directive 93/67/ECC (EC, 1996),[198] where EC50 values below 1.0 μg/mL are deemed highly toxic, those ranging from 1.0 to 10 μg/mL are considered toxic, 10 to 100 μg/mL are classified as slightly toxic, and values above 100 μg/mL are non-toxic, the results obtained indicate that compound **76** exhibited minimal to no toxicity. Unlike certain highly toxic compounds, melampyroside might be regarded as a potential agent against parasitic weeds, presenting an optimal toxicity/selectivity ratio.

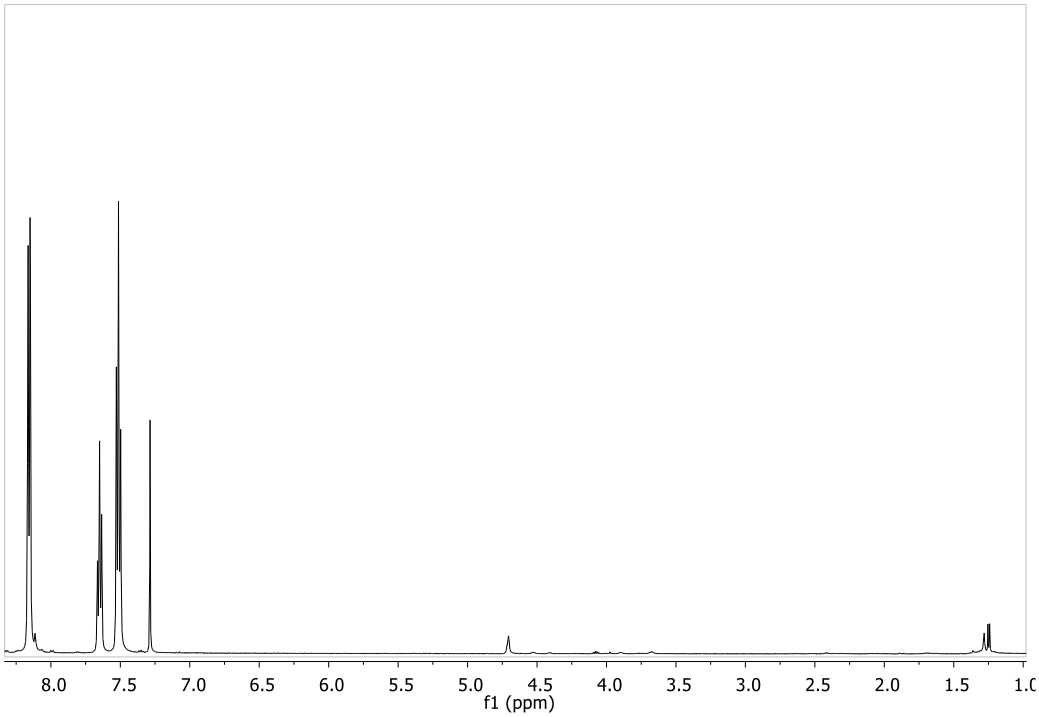

Figure 61. *^{1}H NMR spectrum of benzoic acid,* ***73*** *($CDCl_3$, 400 MHz).*

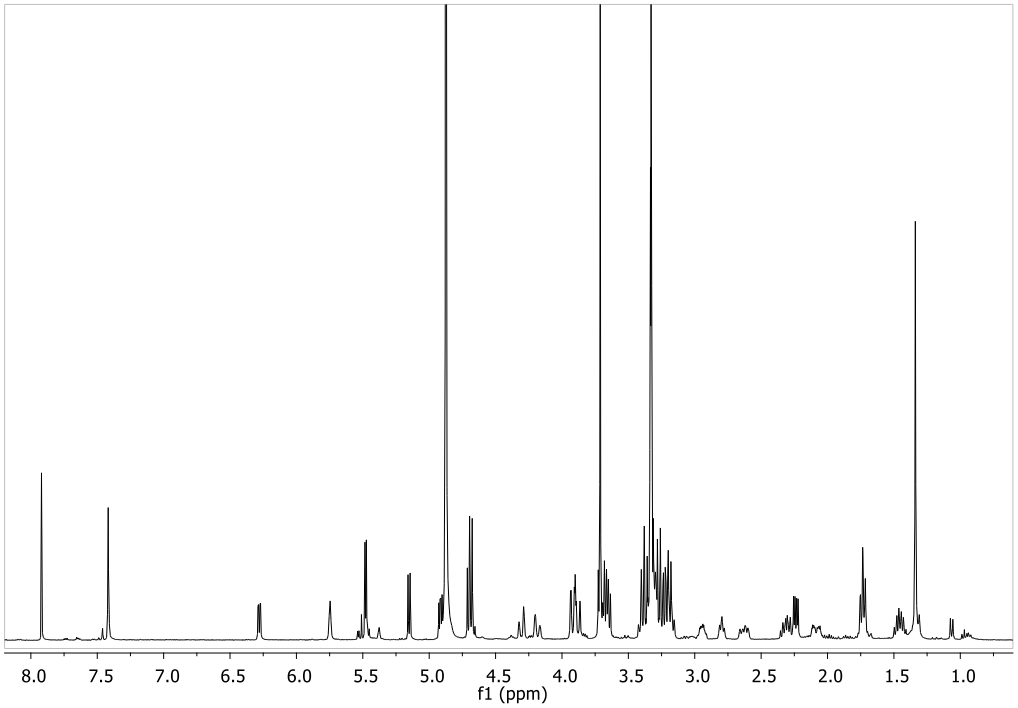

Figure 62. *^{1}H NMR spectrum of bartsioside,* ***74*** *(MeOD, 500 MHz).*

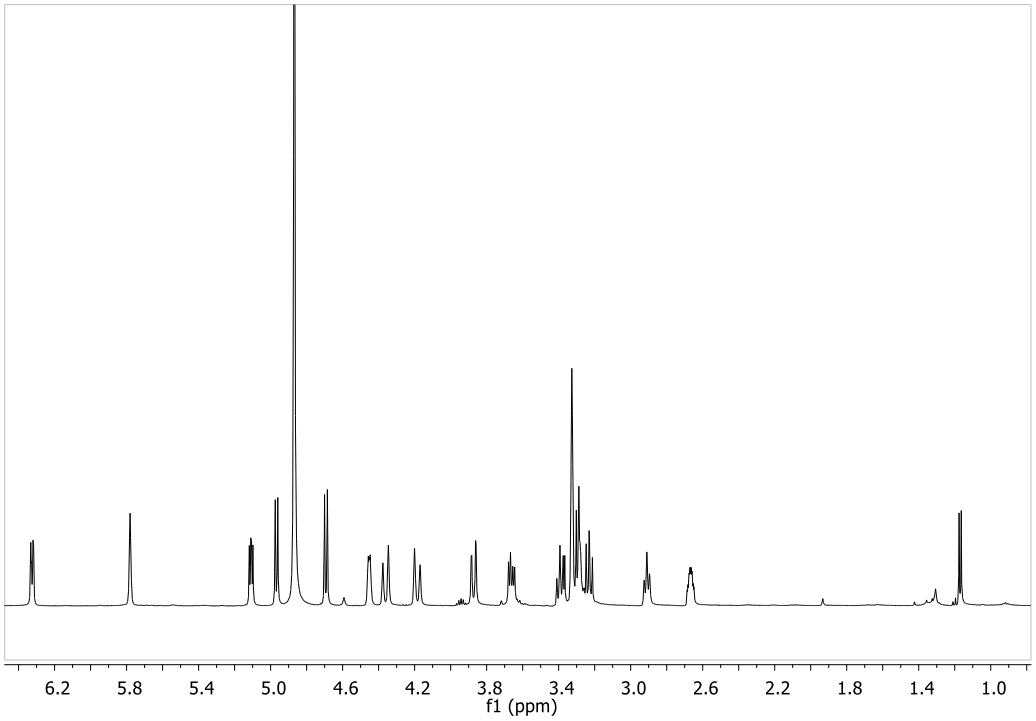

Figure 63. *^{1}H NMR spectrum of aucubin,* ***75*** *(MeOD, 400 MHz).*

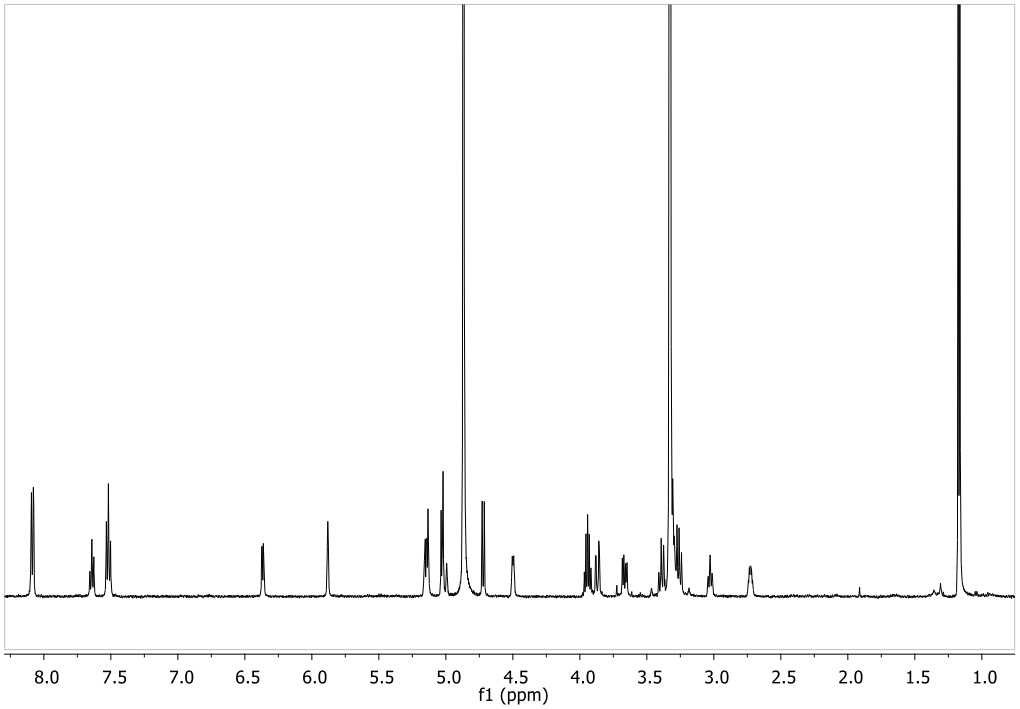

Figure 64. *^{1}H NMR spectrum of melampyroside,* ***76*** *(MeOD, 400 MHz).*

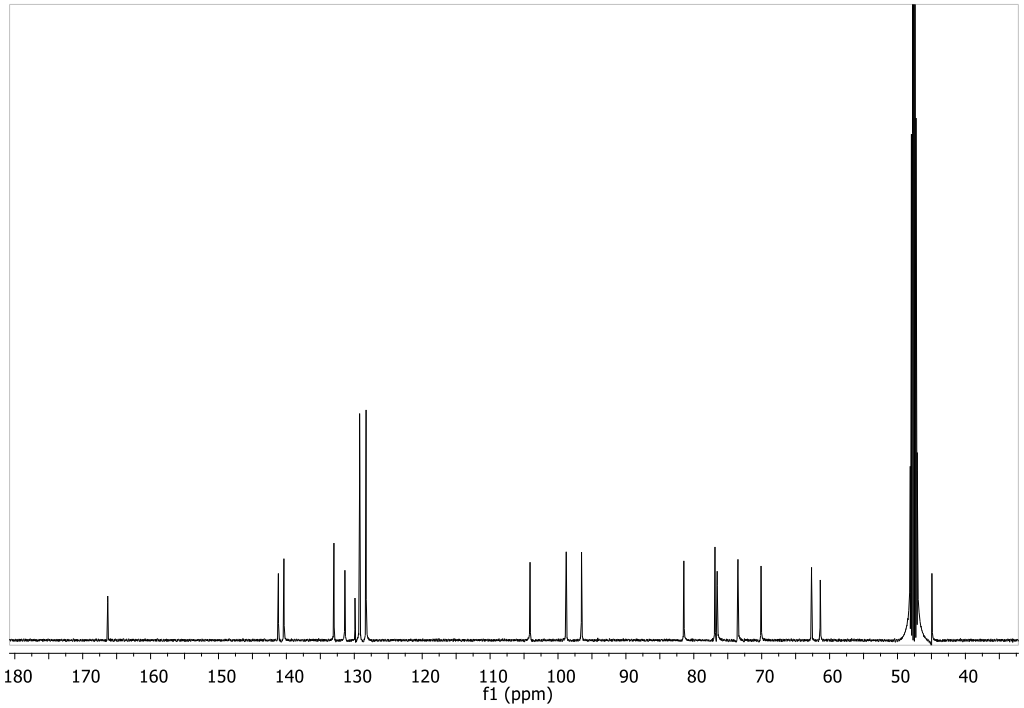

Figure 65. *^{13}C NMR spectrum of melampyroside,* ***76*** *(MeOD, 100 MHz).*

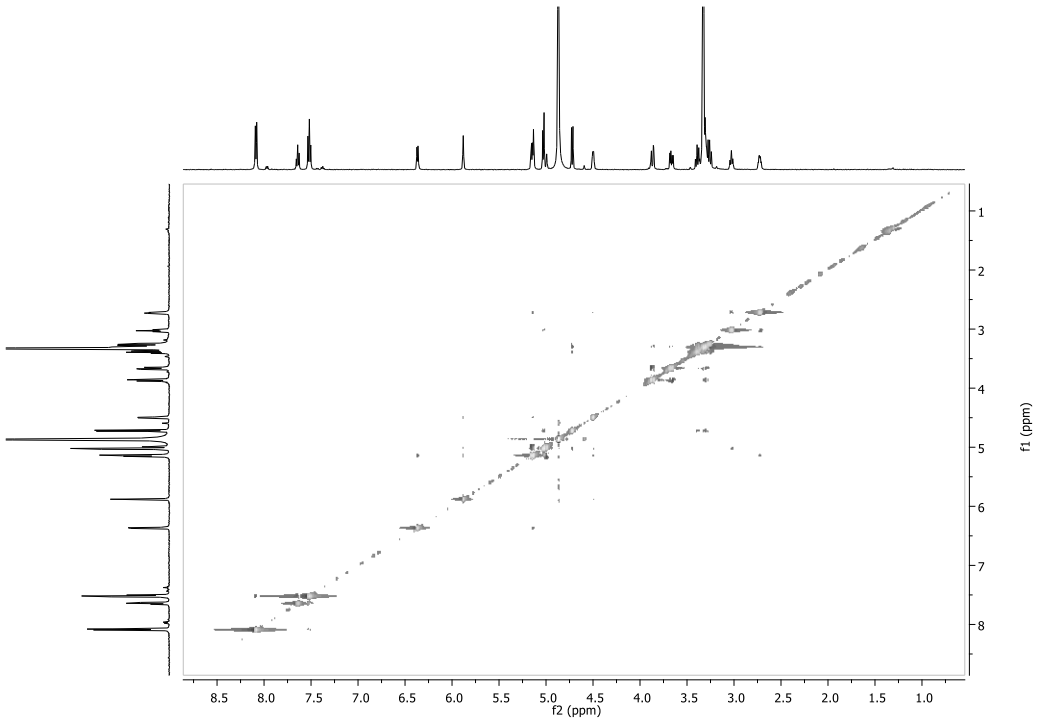

***Figure 66**. NOESY spectrum of melampyroside, **76** (MeOD, 400 MHz).*

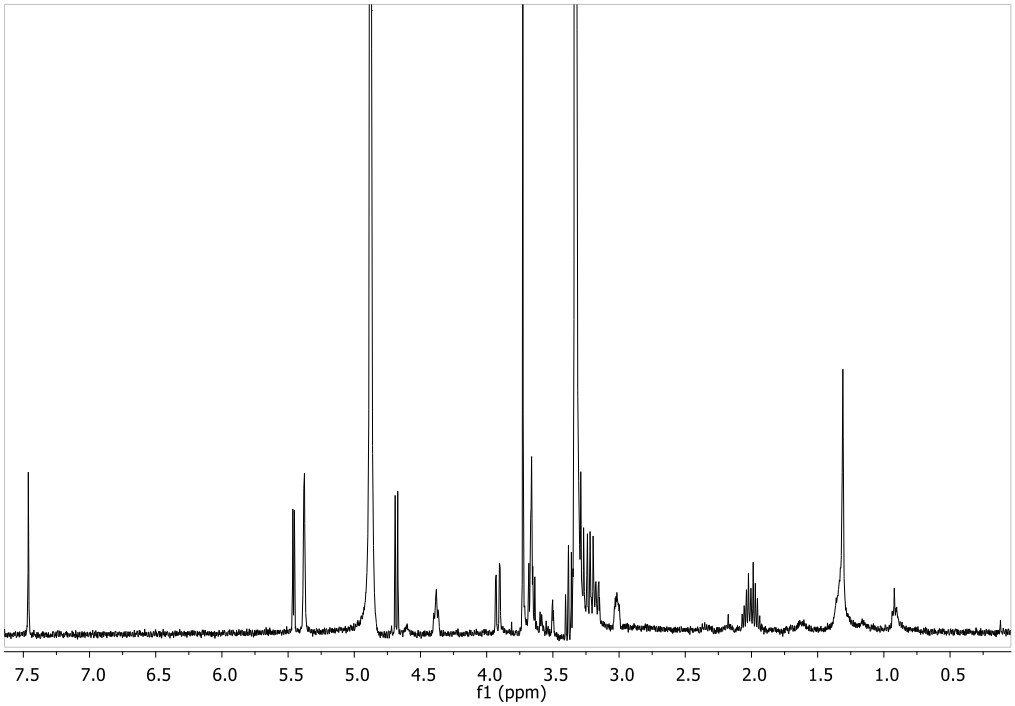

***Figure 67**. [1]H NMR spectrum of gardoside methyl ester, **77** (MeOD, 400 MHz).*

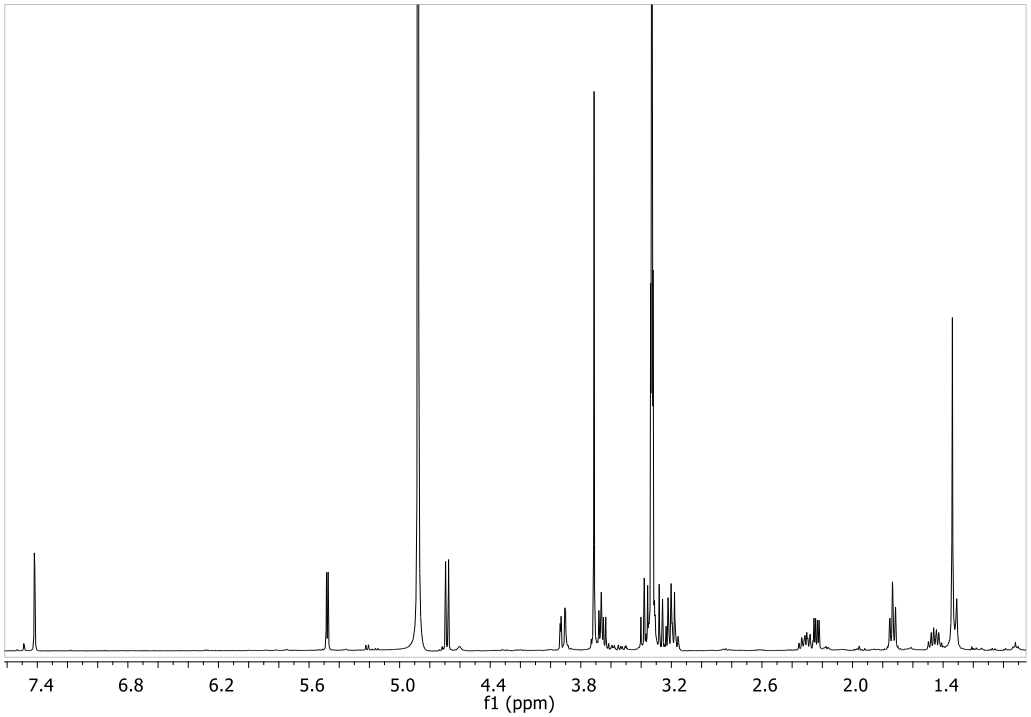

Figure 68. *^{1}H NMR spectrum of mussaenoside,* ***78*** *(MeOD, 500 MHz).*

5.6 *Centaurea Cineraria*

Dried *C. cineraria* L. subsp. *cineraria* aerial parts, were extracted using the procedure reported in the Material and methods section. Thus, 170.2 mg were obtained using *n*-hexane, 984.2 mg using dichloromethane (CH_2Cl_2) and 634.1 mg using ethyl acetate (EtOAc).

Bio-activity guided purification of specialized metabolites. Preliminary TLC analyses revealed the presence of a main metabolite in the CH_2Cl_2 extract, with a lesser amount detected in the EtOAc extract. The extracts obtained were then assessed for their ability to induce suicidal seed germination or inhibit radicle growth through independent bioassays on seeds from four broomrape species (*P. ramosa*, *O. minor*, *O. cumana*, and *O. crenata*). Distilled water was used as the solvent, and concentrations of 100 and 10 µg/mL of dry extract were tested. In the radicle inhibition bioassay, the CH_2Cl_2 extract, applied at 100 µg/mL, demonstrated significant activity across all broomrape species (**Figure 69**).

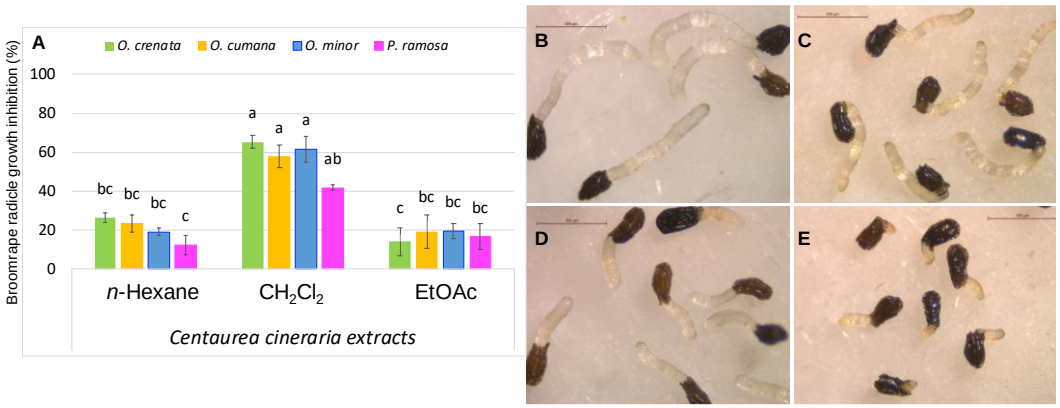

Figure 69. (A) *Extracts effects on radicle growth of broomrape (P. ramosa, O. minor, O. cumana and O. crenata) obtained by extraction with n-hexane, CH_2Cl_2 and ethyl acetate of Centaurea cineraria aerial parts. Different letters show significant difference between compounds by Tukey's multiple comparison test ($p < 0.05$). Error bars represent the standard error of each mean (n=3). (**B-E**) Illustrative pictures of O. cumana (**B** and **D**) and O. minor (**C** and **E**) treated with control (**B** and **C**) and CH_2Cl_2 extract (**D** and **E**) (adapted from Zorrilla et al., Plants, **2023**, 13, 178-192).*[199]

Specifically, the CH_2Cl_2 extract showed high activity levels against *O. crenata*, *O. cumana*, and *O. minor* (65.4 ± 3.6%, 57.9 ± 5.9%, and 61.5 ± 6.7% inhibition, respectively), as compared to negative control samples. In the germination induction bioassay, no activity was observed against any of the four broomrape species under investigation (data not shown). In order to isolate the metabolites demonstrating

phytotoxic effects on radicle growth, the most potent extract (CH_2Cl_2) was purified, leading to the isolation of four pure compounds identified as isocnicin (**79**), cnicin (**80**), salonitenolide (**81**), and 11β,13-dihydrosalonitenolide (**82**) (**Figure 69**). Their optical and spectroscopic data (**Figure 75-84**) are in accordance with previously reported data.[140,141,200] The isolated compounds belong to sesquiterpene lactones described for the *Centaurea* genus.[201] The present study is the first report on the identification and isolation of salonitenolide (**81**) and 11β,13-dihydrosalonitenolide (**82**) from *C. cineraria*.

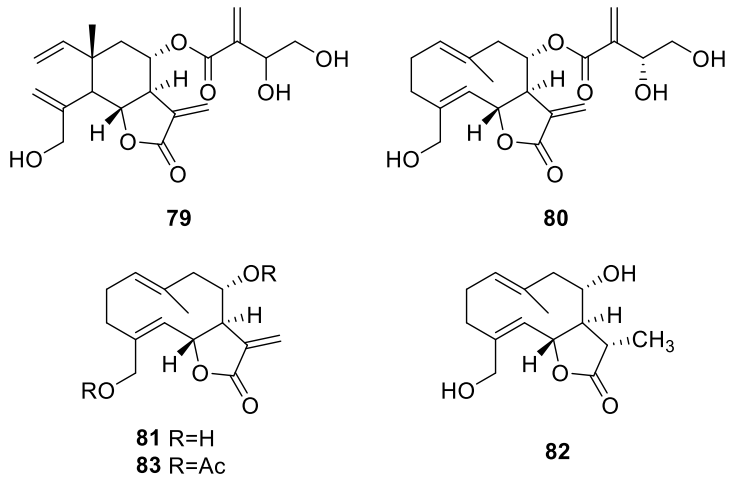

Figure 70. (A) *Structures of isocnicin (**79**), cnicin (**80**), salonitenolide (**81**), 11β,13-dihydrosalonitenolide (**82**), and the synthetic derivative 8,15-O,O'-diacetylsalonitenolide (**83**).*

<u>*Bioassays against broomrapes.*</u> In an initial screening, isocnicin (**79**) and cnicin (**80**) demonstrated activity against *O. crenata*, *O. cumana*, *O. minor*, and *P. ramosa* within the concentration range of 1.0-0.1 mM (**Figure 71**). At 1 mM, isocnicin (**79**) achieved nearly complete inhibition of radicle growth for *O. crenata* (99.0 ± 0.2%), *O. cumana* (99.3 ± 0.5%), and *O. minor* (99.5 ± 0.5%). Substantial inhibition levels were also observed at 0.5 mM (90.6 ± 1.1%, 95.8 ± 0.3%, and 87.4 ± 0.8%, respectively). **Figures 72E-H** illustrate how, in addition to inhibiting radicle growth, isocnicin (**79**) induced darkening of the broomrape radicles when applied at 1 and 0.5 mM. For cnicin (**80**), similar trends were observed against *O. cumana* and *O. minor*, but there was a decrease in activity from 0.5 mM

against O. crenata and P. ramosa (**Figure 71**). The darkening effect on broomrape radicles induced by isocnicin (**79**) was not observed following cnicin treatments (**Figures 72I-L**), nor in the control radicles (**Figures 72A-D**). Consequently, inhibitory activity was identified for both elemanolide and germacranolide structures. As indicated in the literature, the biological activity of sesquiterpene lactones is closely linked to the lactone ring.[202] However, the enhanced activity observed for isocnicin (**79**), particularly against *O. crenata*, should be attributed to a structural advantage of the elemanolide framework scaffold when compared to germacranolides.

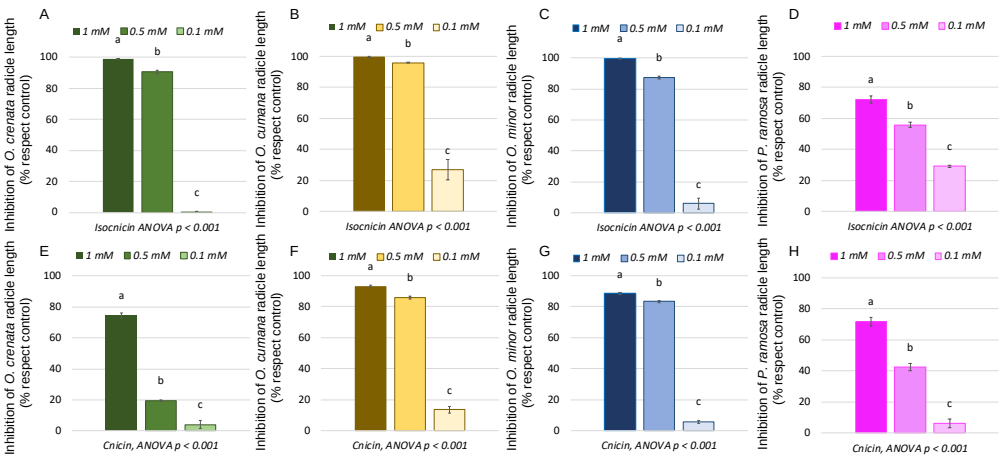

Figure 71. *Growth inhibition induced by isocnicin (**1**, upper row) and cnicin (**2**, lower row) in radicles of O. crenata, O. cumana, O. minor and P. ramosa. Bars with different letters are significantly different according to the Tukey test ($p < 0.05$). Error bars represent the standard error of the mean (adapted from Zorrilla et al., Plants, **2023**, 13, 178-192).*[199]

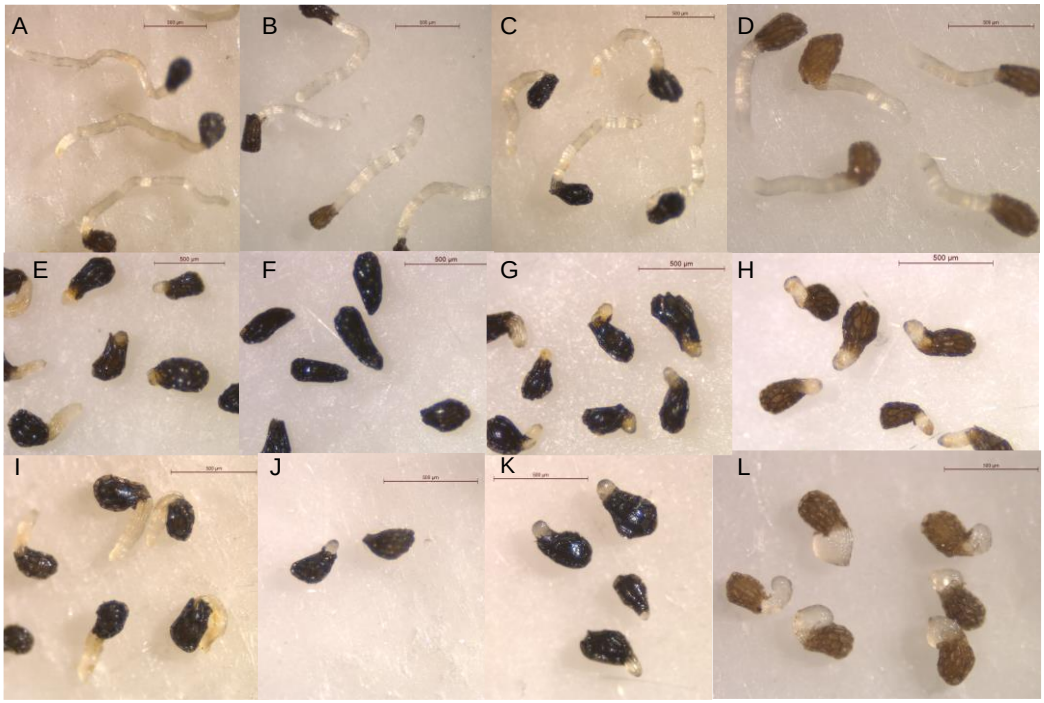

Figure 72. *Growth Control treatments (**A–D**), isocnicin (**1**, **E–H**) and cnicin (**2**, **I–L**) applied at 0.5 mM on radicles of O. crenata (**A,E,I**), O. cumana (**B,F,J**), O. minor (**C,G,K**), and P. ramosa (**D,H,L**) (adapted from Zorrilla et al., Plants, **2023**, 13, 178-192).*[199]

The activities of salonitenolide (**81**) and 11β,13-dihydrosalonitenolide (**82**) were assessed in the same type of bioassay, with the concentration range adjusted to 1.0-0.3 mM, based on the aforementioned results. The activity profiles obtained were notably divergent, with compound **81** demonstrating high inhibition levels in most cases (**Figure 73 A-D**), whereas compound **82** exhibited weak activity, consistently below 15.4 ± 4.6% (**Figure 73E-H**, **Figure 74A-L**). Specifically, salonitenolide (**81**) achieved inhibitions against *O. crenata* at 83.4 ± 0.7%, 82.2 ± 0.7%, and 57.1 ± 2.4%, against *O. cumana* at 89.4 ± 0.4%, 87.3 ± 1.9%, and 64.2 ± 4.3%, against *O. minor* at 84.6 ± 1.4%, 84.5 ± 0.4%, and 76.8 ± 3.5%, and against *P. ramosa* at 58.5 ± 10.1%, 46.2 ± 3.2%, and 12.7 ± 4.6% (at 1 mM, 0.6 mM, and 0.3 mM, respectively). Aiming at providing insights on the bioactivity of salonitenolide (**81**), its acetylated derivative, 8,15-O,O'-diacetylsalonitenolide (**83**), was synthetically obtained and tested. The latter exhibited the strongest activity among all isolated compounds from *C. cineraria*, completely inhibiting the radicle growth of *O. crenata* and *O. minor* at all

concentrations tested. It also inhibited *O. cumana* radicles by 100 ± 0.0%, 100 ± 0.0%, and 92.5 ± 0.6%, and *P. ramosa* radicles by 100 ± 0.0%, 88.3 ± 2.2%, and 66.4 ± 1.3%, at respective concentrations of 1, 0.6, and 0.3 mM (**Figure 73I-L**, **Figure 74M-P**).

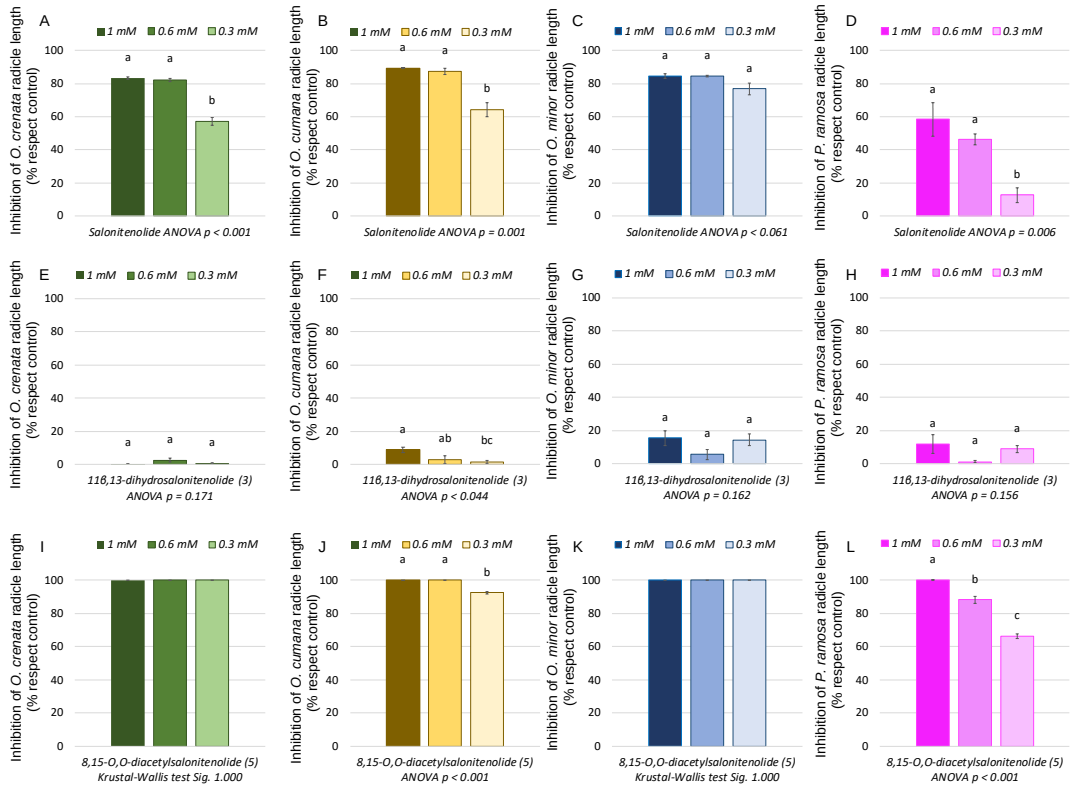

Figure 73. *Growth inhibition induced by salonitenolide (**81**, **A-D**), 11β,13-dihydrosalonitenolide (**82**, **E-H**), and 8,15-O,O-diacetylsalonitenolide (**83**, **I-L**) in radicles of O. crenata, O. cumana, O. minor and P. ramosa. Bars with different letters are significantly different according to the Tukey test (p < 0.05). Error bars represent the standard error of the mean (adapted from Zorrilla et al., Plants, **2023**, 13, 178-192).*[199]

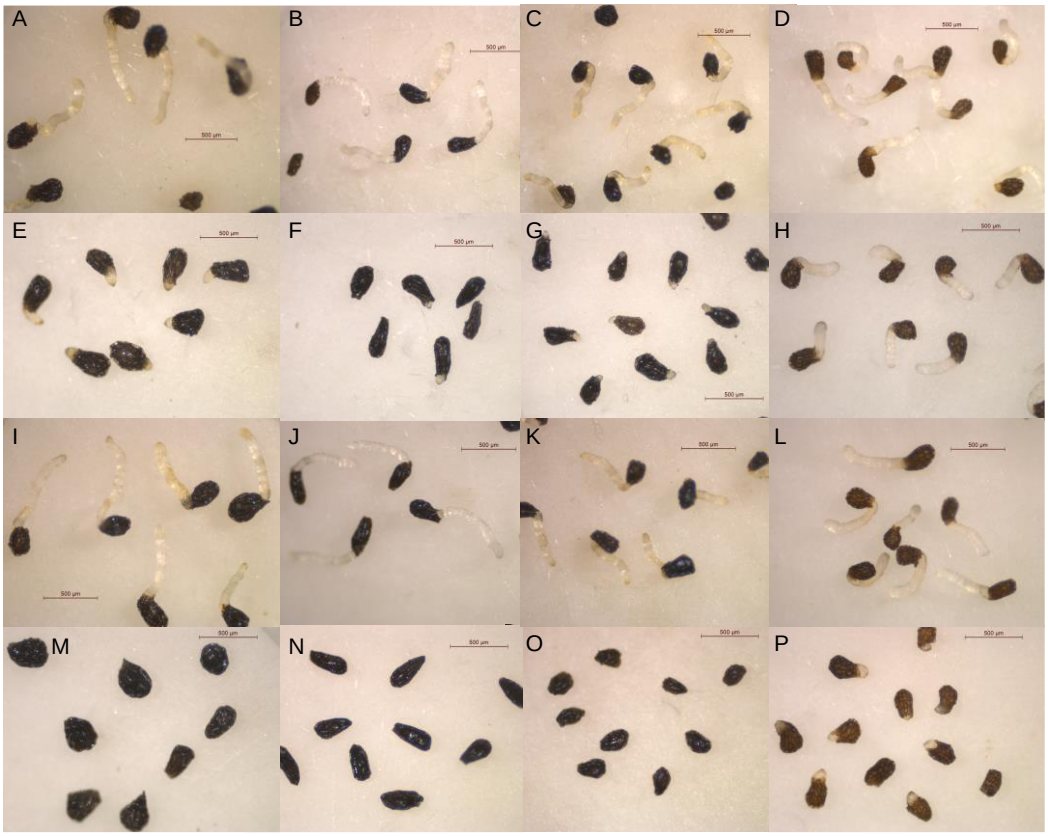

Figure74. *Treatments with control (**A**–**D**), salonitenolide (**81**, **E-H**), 11β,13-dihydrosalonitenolide (**4**, **I-L**), applied at 1 mM and 8,15-O,O-diacetylsalonitenolide (**83**, **M-P**) on radicles of O. crenata (**A,E,I,M**), O. cumana (**B,F,J,N**), O. minor (**C,G,K,O**), and P. ramosa (**D,H,L,P**) (adapted from Zorrilla et al., Plants, **2023**, 13, 178-192).*[199]

From a structural perspective, two distinct types of sesquiterpene lactones were isolated. Isocnicin (**79**) features an elemanolide structure, while compounds **80-82** are germacranolides. Few specific lactones produced by *Centaurea* spp. have been identified as phytochemicals, with cnicin (**80**) being widely studied in different fields, including reports on its phytotoxicity.[167] Consequently, the inhibitory activity of the isolated compounds against broomrape radicle growth was evaluated. The results obtained allowed to discuss some structure-activity relationships (SAR). The key one is the importance of the double bond in the α,β-unsaturated lactone ring of the sesquiterpene lactones in the inhibition of broomrape, given the poor activity of 11β,13-dihydrosalonitenolide (**82**) in comparison with

the results of the other compounds tested. It could be highlighted how a previous study showed that a 11,13-dihydro sesquiterpene lactone could be active on bioassays with broomrapes.[203] At comparing parameters like lipophilicity and the total rotable bonds, H-bond donors and H-bond acceptors, the similar values for compounds **81** and **82** (**Table 6**) may indicate that these are not directly correlated with the loss of activity by compound **82**.

	Isocnicin (**79**)	Cnicin (**80**)	Salonitenolide (**81**)	11β,13-Dihydrosalonitenolide (**82**)	8,15-*O,O'*-diacetylsalonitenolide (**83**)
Clog P	0.37	0.63	0.61	0.64	2.45
Rotable bonds	8	6	1	1	5
H-bond acceptors	7	7	4	4	6
H-bond donors	3	3	2	2	0

Table 6. *ClogP values and number of rotable bonds, donors and acceptors H-bond of compounds **79-83**.*

The second SAR finding concerns the acetylation of hydroxyl groups, representing a noteworthy enhancement in inhibitory activity. This improvement is evident in compound **83** when compared to salonitenolide (**81**), resulting in a substantial increase in inhibition, especially at lower concentrations. This evidence could be explained by a better solubility of the compound within hydrophobic environments like the lipid bilayers of membranes, as justified by the lipophilicity expressed by the partition coefficient values calculated by the Clog*P* algorithm for compounds **79-83** (**Table 6**). Even though compounds **79-83** accomplish the Lipinskii rule for the optimal Clog*P* value for herbicides ($\leq$ 3.5),[204] compound **83** has a notably different value (2.45) in comparison to those of compounds **79-82** (0.37-0.64), which could therefore justify the different level of activity. Moreover, the improved activity of compound **83** could be related with the absence of H-bond donor atoms in its structure, unlike the structures of compounds **79-82** (**Table 6**). Regarding the induction of broomrape germination, despite the lack of activity in *C. cineraria* organic extracts as germination inducers, a bioassay with compounds **79-83** was conducted on seeds of *P. ramosa*, *O. minor*, *O. cumana*, and *O. crenata* to assess their suicidal germination induction activity, using the concentration range described earlier for radicle inhibition. No activity was observed in any of the cases, confirming that the absence of activity in the extracts was not due to potential minor metabolites interfering with the bioactivity. Additionally, the

acetylation of compound **81** was not a modification capable of altering its behaviour for suicidal germination activity. The presented results align with the context of the biology and management of parasitic weeds. The germination of broomrape seeds is typically triggered by specific compounds released by potential host plants in the vicinity. While the family of phytohormones known as strigolactones is extensively studied, various sesquiterpene lactones produced by plants have been identified as potent germination elicitors for certain broomrape species, while remaining inactive for others. This study contributes to the field of parasitic weed research by exploring sesquiterpene lactones, delving into mechanisms, biosynthesis, and the development of bioactive derivatives against parasitic weeds. Furthermore, considering that the active compounds contain an α,β-unsaturated lactone ring, they could serve as starting material for the synthesis of new strigolactone analogues using established strategies. Reports on the synthesis of cnicin derivatives also encourage the exploration of additional derivatives with improved activities in bioassays with parasitic plants.

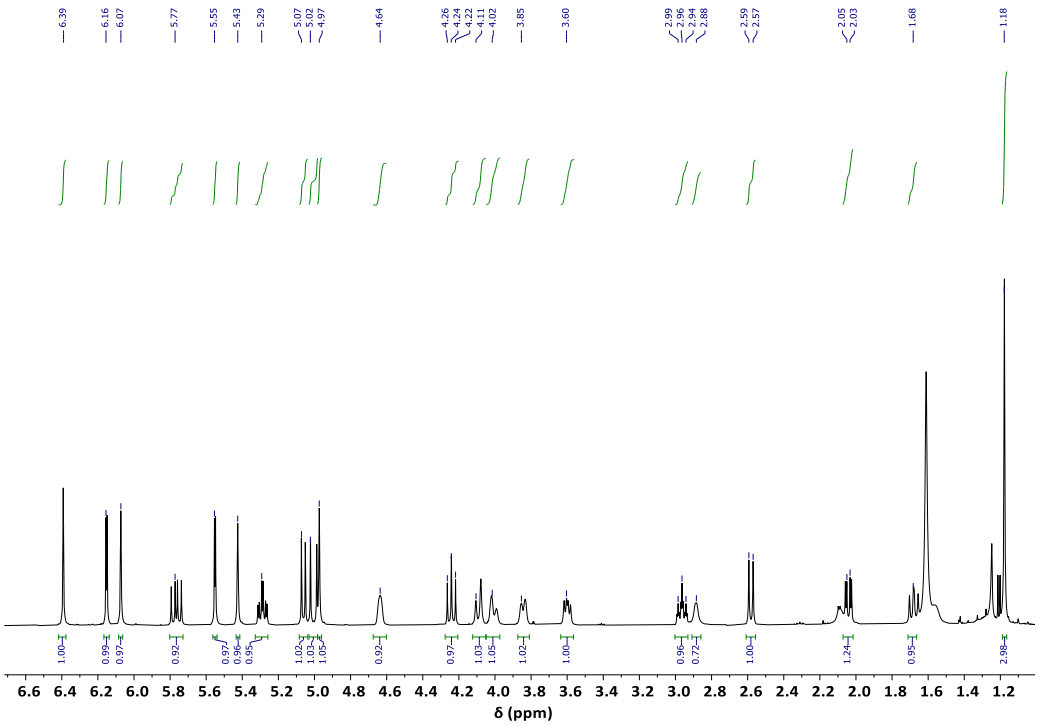

Figure 75. *^{1}H NMR spectrum of isocnicin (**79**) recorded in $CDCl_3$ at 400 MHz.*

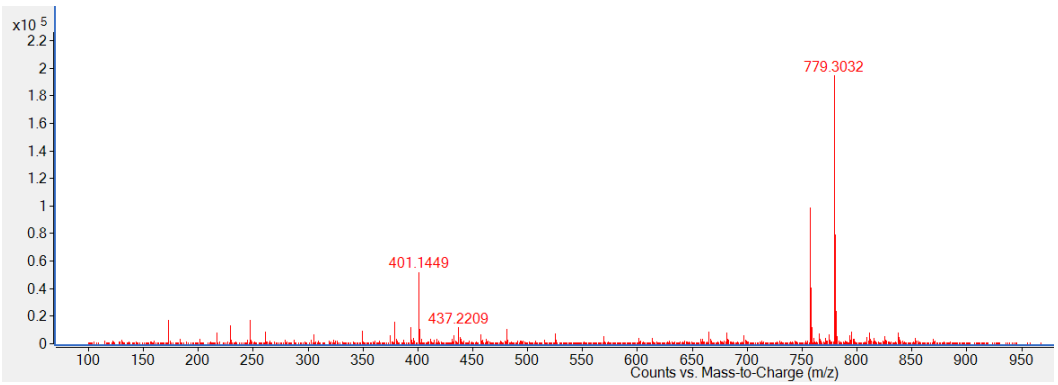

Figure 76. *ESI MS spectrum of isocnicin (**79**) recorded in positive mode.*

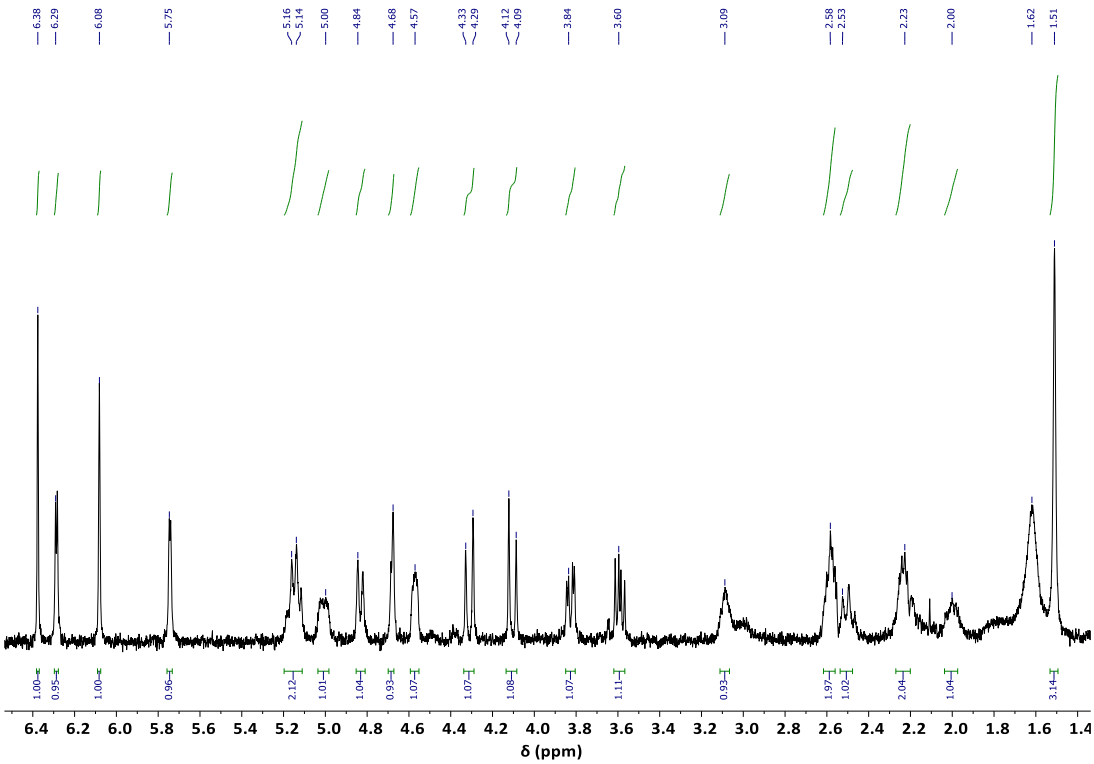

Figure 77. *^{1}H NMR spectrum of cnicin (**80**) recorded in $CDCl_3$ at 400 MHz.*

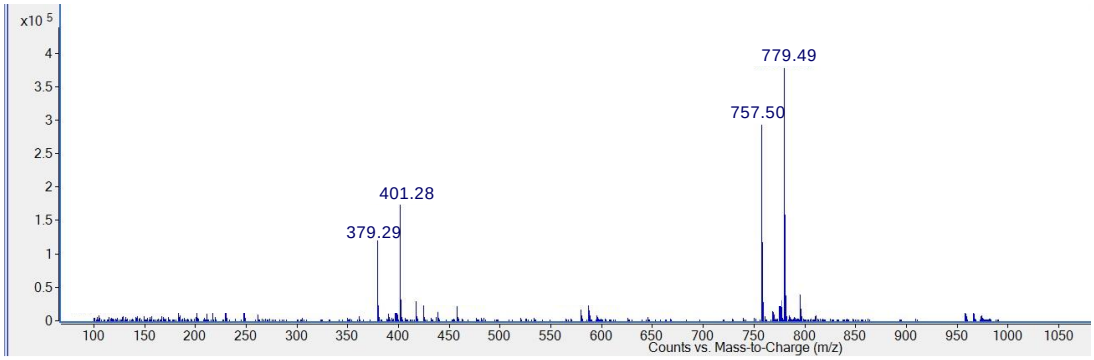

Figure 78. *ESI MS spectrum of cnicin (**80**) recorded in positive mode.*

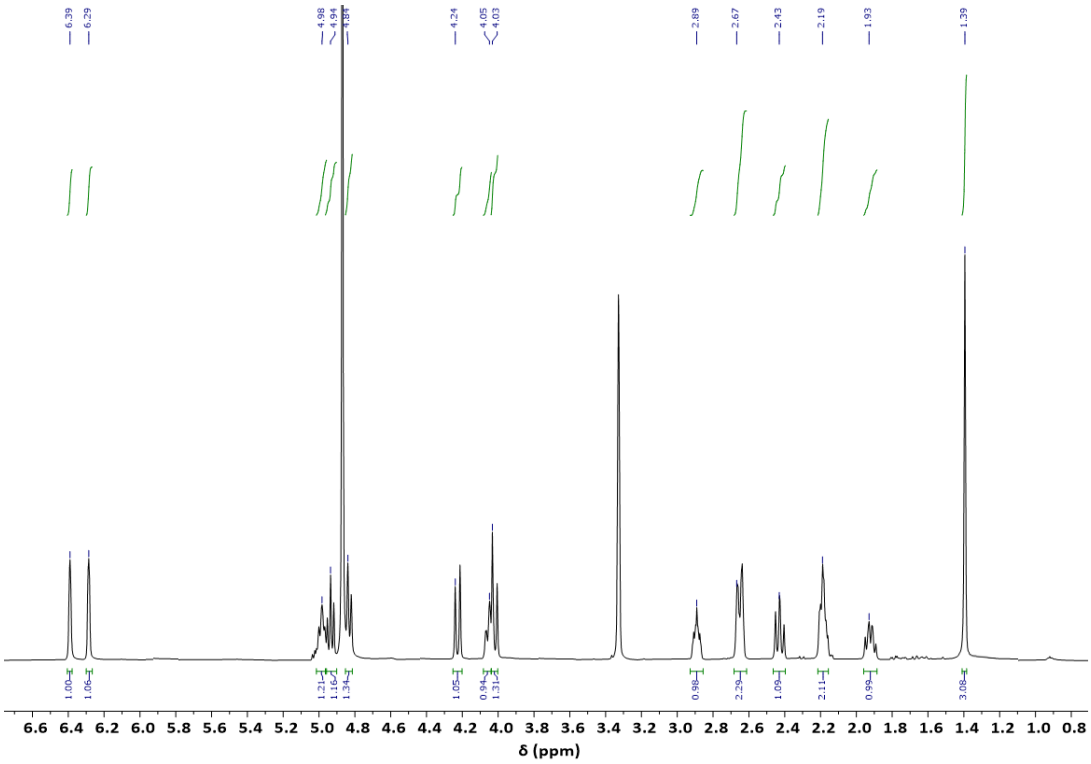

Figure 79. *^{1}H NMR spectrum of salonitenolide (**81**) recorded in MeOD at 400 MHz.*

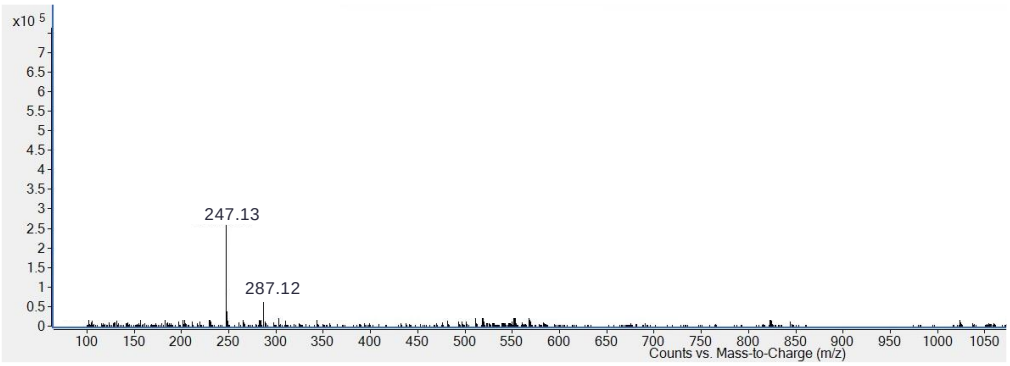

Figure 80. *ESI MS spectrum of salonitenolide (**81**) recorded in positive mode.*

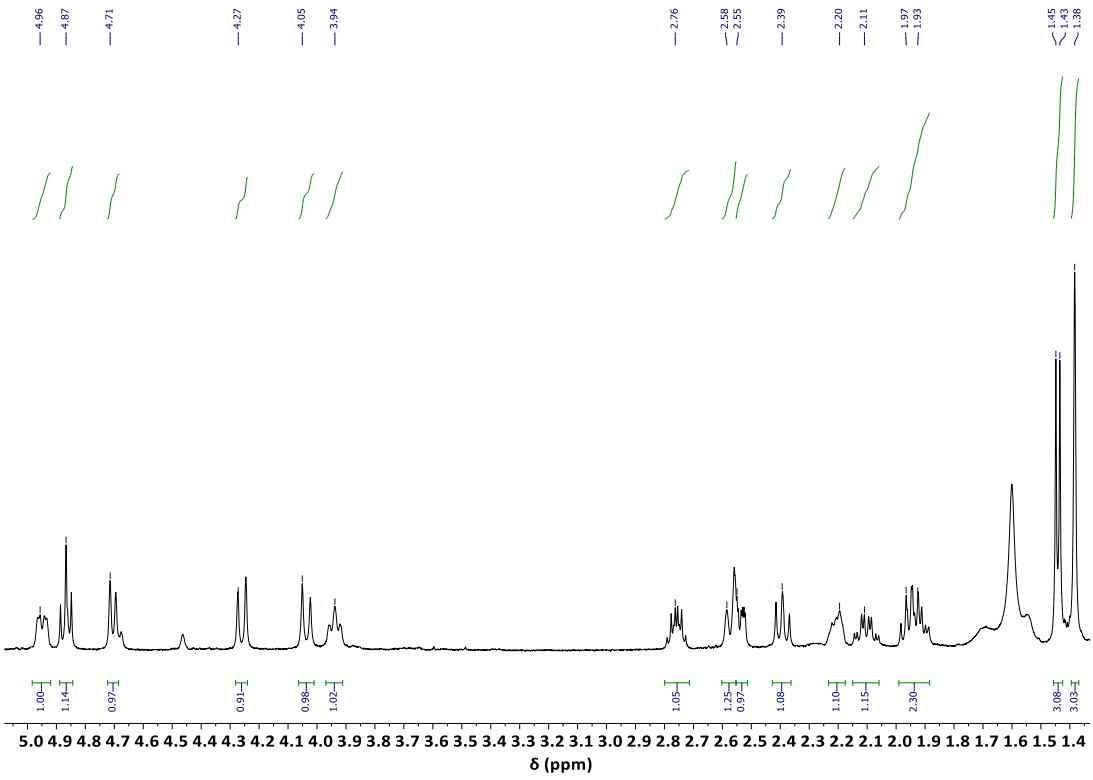

Figure 81. *^{1}H NMR spectrum of 11β,13-dihydrosalonitenolide (**82**) recorded in $CDCl_3$ at 400 MHz.*

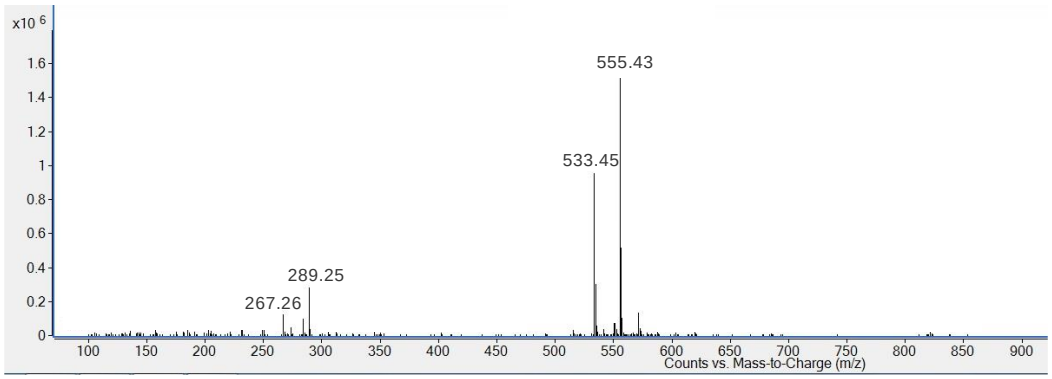

Figure 82. *ESI MS spectrum of 11β,13-dihydrosalonitenolide (**82**) recorded in positive mode.*

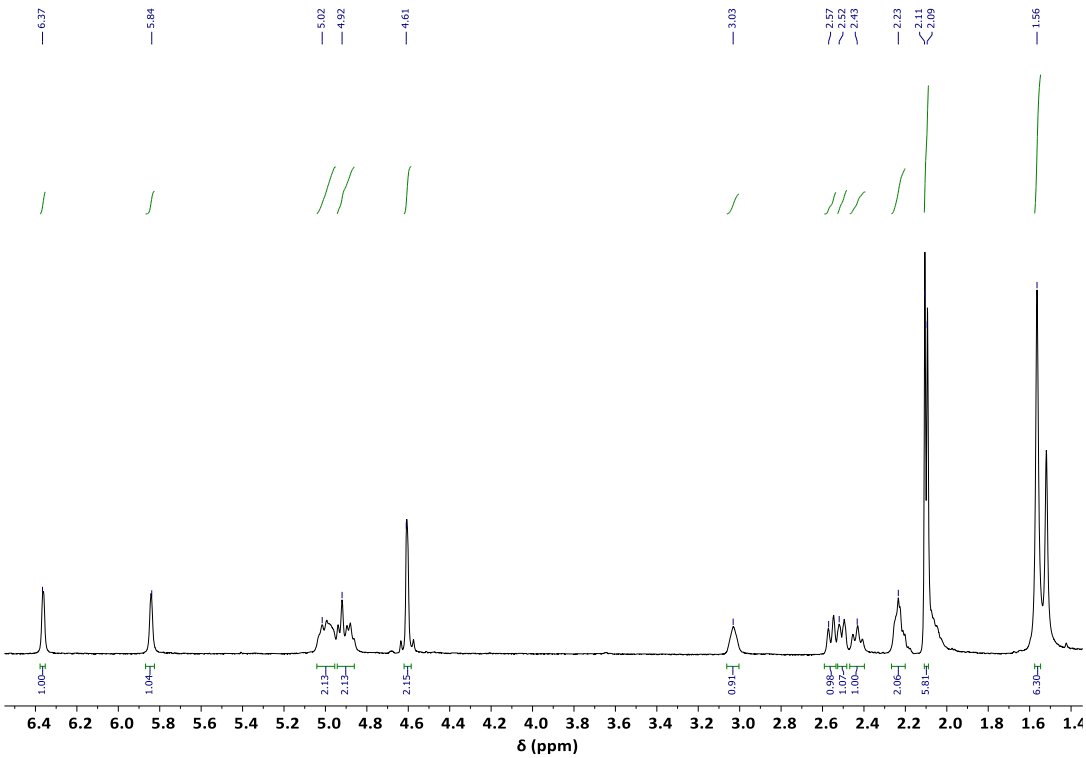

Figure 83. *^{1}H NMR spectrum of 8,15-O,O'-diacetylsalonitenolide (**83**) recorded in $CDCl_3$ at 400 MHz.*

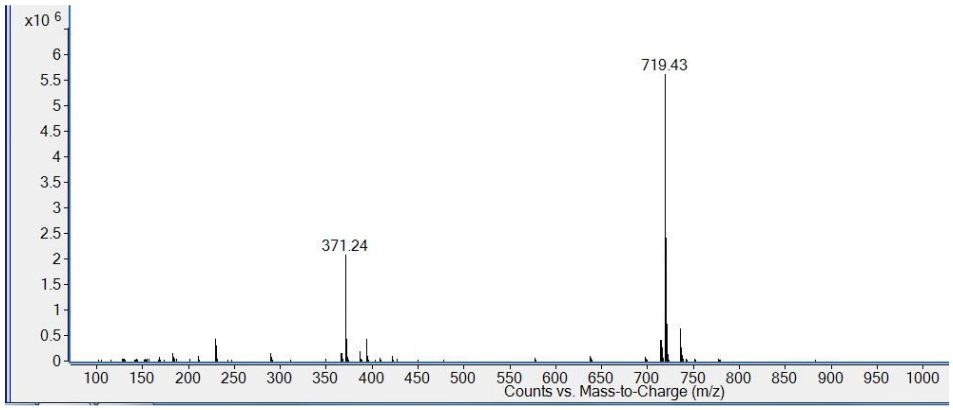

Figure 84. *ESI MS spectrum of 8,15-O,O'-diacetylsalonitenolide (**83**) recorded in positive mode.*

5.7 *Conyza bonariensis*

Inspired by the results obtained in the allelopathic plants assessment study, which found *C. bonariensis* extract with significant inhibitory activity against broomrape radicle growth, it was tested against *C. campestris* as well. This was, the guide for the isolation and identification of compounds with allelopathic activity. The CH_2Cl_2 extract was fractionated by TLC, resulting in five homogeneous fractions (CBA, CBB, CBC, CBD, and CBE).

The phytotoxicity screening revealed that among the five fractions of the *Conyza* extract, the CBB fraction caused the most pronounced phytotoxicity in seedlings of *Cuscuta* (**Figure 85**).

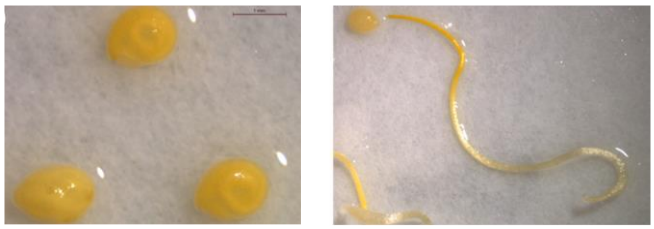

Figure 85. *Images illustrating the phytotoxic effect on C. campestris seeds (left), when treated with the CBB fraction, containing the (4Z)-lachnophyllum lactone, compared with the control (right) (adapted from Fernández-Aparicio et al., Agriculture,* ***2022****, 12, 790-803).*[143]

This phytotoxicity, manifested as abnormal growth in the *Cuscuta* seedlings, with a reduction in length compared to the control seedlings. Upon investigation of the active fraction CBB, the study of the ^{1}H NMR and ESI MS spectra revealed it to be a pure compound identified as (4*Z*)-lachnophyllum lactone (**84**), specifically the (*Z*)-5-(hex-2-yn-1-ylidene)furan-2(5H)-one (see **Figure 86**, Rf = 0.76, 5.10 mg). The structure was confirmed by comparing the ^{1}H NMR data with those reported in literature.[157,205] The configuration of the double bond was deduced from the presence of coupling signal between H-5 with H-3 and H-2 in the NOESY spectrum (**Figure 87).** Additionally, the chemical shifts of H-5 (δ = 5.33) and C-5 (δ = 94.5) closely matched those reported for lachnophyllum lactone and other natural furanones, specifically those with an α Z-disubstituted vinyl group, remarkably distinct from those with an E-vinyl group.[157,206] This structural identification was further corroborated by the ESI MS data, which displayed the sodiated adduct $[2M + Na]^+$ and protonated $[2M + H]^+$ dimers, as well as protonated $[M + H]^+$ ions at *m/z* 347, 325, and 163,

respectively. Notably, the ^{1}H NMR data of the (*Z*) and (*E*) isomers of the acetylenic lactone were documented when both compounds were isolated from *Baccharis paniculata*, revealing a distinct upfield shift of proton H-5 for the *Z*-isomer.[157]

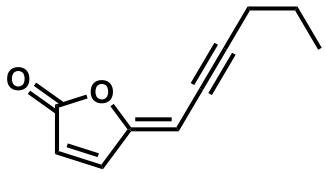

Figure 86. *(4Z)-Lachnophyllum lactone structure.*

A subsequent dose–response screening was conducted to validate the phytotoxicity of (4*Z*)-lachnophyllum lactone (**84**), confirming the inhibitory activity of *Cuscuta* seedling growth at concentrations ranged from 100 to 10 µg/mL. An IC_{50} value of 24.8 µg/mL was observed.

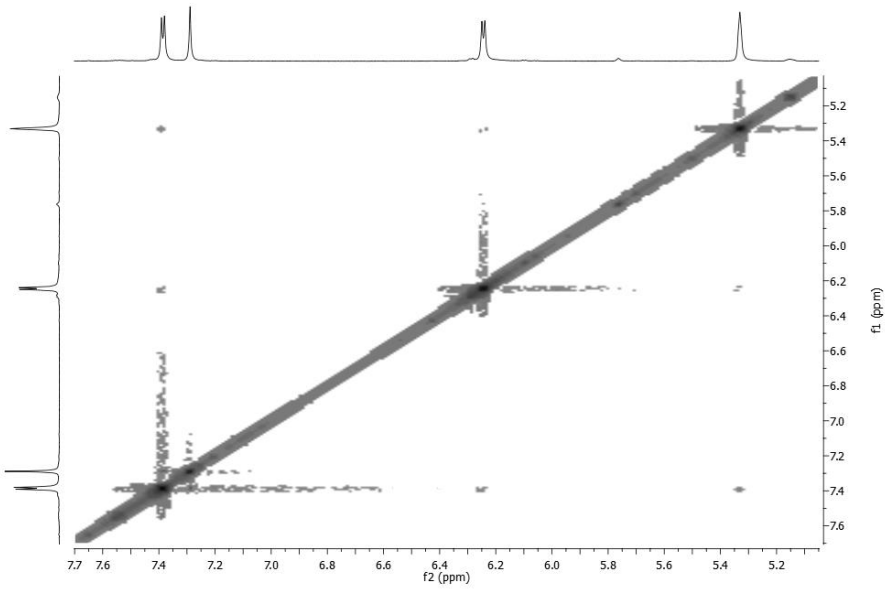

Figure 87. (4*Z*)-lachnophyllum lactone NOESY spectra recorded in $CDCl_3$ at 500 MHz.

5.8 *Conyza* allelochemicals

Organic Extractions of Conyza Bonariensis Shoots and Evaluation of Inhibitory Activity on Broomrapes. *C. bonariensis* lyophilized shoots were extracted by maceration with a hydroalcoholic solution as described in the Material and methods Section. The allelopathic activity, of the extracts obtained, was assessed at a concentration of 100 μg/mL through two independent bioassays: germination induction and radicle growth. For the germination induction assay, *Conyza* extracts were diluted in distilled water and tested on seeds of four broomrape species (*O. crenata*, *O. cumana*, *O. minor*, and *P. ramosa*). The results obtained, showed no germination when seeds of all broomrape species were treated with the negative control (distilled water). On the other hand, the inhibitory radicle growth bioassay, tested on the same broomrapes species and conducted by mixing each extract with the germination stimulant GR24, provided good results. Specifically, all the extracts exhibited the highest growth inhibitory activity on radicles of *O. cumana* (59.4 ± 3.3%, 63.7 ± 2.1%, and 42.0 ± 0.9% inhibition for n-hexane, dichloromethane, and ethyl acetate extracts, respectively) and *O. minor* (54.5 ± 9.3%, 68.7 ± 4.9%, and 65.6 ± 2.7% inhibition for n-hexane, dichloromethane, and ethyl acetate extracts, respectively). *P. ramosa* radicles showed moderate levels of inhibition, while *O. crenata* radicles exhibited low or negligible inhibition.

Isolation of the pure metabolites. Once the activity of the organic extracts was confirmed, they were further purified as described in the material and methods section. Seven pure metabolites (**84**–**90**, **Figure 88**) were isolated and identified as (4*Z*)-lachnophyllum methyl ester (**85**, 26.0 mg), (4*Z*)-lachnophyllum lactone (**84**, 45.9 mg), (4*Z*,8*Z*)-matricaria lactone (**86**, 9.3 mg), (4*E*,8*Z*)-matricaria lactone (**87**, 3.8 mg), methyl 4-hydroxy-3-methoxybenzoate (**88**, 9.8 mg), methyl 4-hydroxybenzoate (**89**, 13.8 mg) and hispidulin (**90**, 9.6 mg).

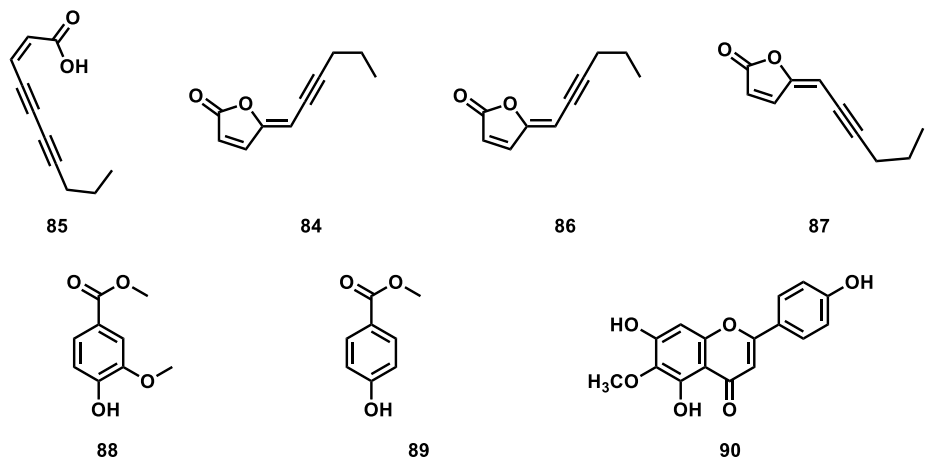

Figure 88. *Conyza bonariensis specialized metabolites.*

Compounds' structure was confirmed by comparison of the NMR and MS data (**Figure 90-104**) with those reported in literature (see Section **2.11**). The molecular ion peak and the ^{1}H NMR spectra of compound **85** indicated the obtaining of (4*Z*)-lachnophyllum methyl ester, already isolated from *C. bonariensis*, corresponding to the opened furanone lactone. However, compounds **84**, **86**, **87** are featured of a 2-furanone ring to a diversly unsaturated chain. The signals attributed to the hydrogen atoms of the chain in the ^{1}H NMR spectra, along with the molecular ion peak values obtained for these three compounds (*m/z*: 161–163), suggested that compounds **84**, **86**, and **87** varied from each other in terms of unsaturation or the configuration of the double bonds. Thus, compound **84** was identified as (4*Z*)-lachnophyllum lactone,[207] whereas the unsaturated analogues **86** and **87** contain a double bond in positions $C_8 = C_9$, whose structure corresponds with that of matricaria lactone. The main difference observed by comparing the ^{1}H NMR data of compounds **86** and **87**, was that H-5 appeared 0.43 ppm higher in the (4*Z*,8*Z*)-matricaria lactone (**86**). In fact, compounds **86** and **87** were geometric isomers at their $C_4 = C_5$ double bonds.[144,145]

The analysis ^{1}H NMR spectra of compounds **88** and **89**, allow their readily identification as benzene-derived aromatic compounds. Furthermore, the presence in both compounds of a hydroxyl and a methyl ester group in para positions, plus an additional *ortho*-methoxy group in compound **88** were confirmed by analysis of their molecular ion peak values. Thus, they were identified as methyl 4-hydroxybenzoate (**89**)[147] and methyl 4-hydroxy-3-methoxybenzoate (**88**).[146] The experimental NMR spectra and molecular ion peak

of compound **90** were consistent with those of a flavonoid containing a methoxy group and three hydroxyl groups as substituents. The compound was identified as hispidulin by a comparison of its data with those already reported for this flavonoid.[148,149] Notably, hispidulin is a flavonoid known for its anti-inflammatory and antioxidant properties.[208] It holds potential for use as an anticancer drug[209] and has demonstrated activity as a quorum sensing inhibitor, with potential in the control of infections caused by *Pseudomonas aeruginosa*.[210] Additionally, it has exhibited activity in phytotoxic assays affecting the root and seedling growth as well as seed germination of crop species like radish, cucumber, and onion.[211]

The allelopathic effects of compounds **84-90** were examined on four broomrape species (*O. crenata*, *O. cumana*, *O. minor*, and *P. ramosa*) at concentrations of 1 and 0.1 mM using two distinct bioassays: germination induction and radicle growth inhibition. The germination bioassay involved diluting each compound in distilled water. As expected, no germination occurred when seeds of all broomrape species were treated with the negative control (distilled water). The positive control, the synthetic strigolactone GR24, exhibited high germination activity (71.1 ± 1.4%, 63.5 ± 1.2%, 80.5 ± 2.0%, and 74.9 ± 1.3% of germination for O. crenata, O. cumana, O. minor, and P. ramosa, respectively). Notably, methyl 4-hydroxybenzoate (**89**) and hispidulin (**90**) displayed significant stimulatory activity. Specifically, compound **89** stimulated germination in *P. ramosa* at 1 mM (58.1 ± 3.0%) and 0.1 mM (26.7 ± 1.9%), while showing no germination induction in the other studied broomrape species. The absence of activity in methyl 4-hydroxy-3-methoxybenzoate (**88**) suggested a direct influence of the *p*-methoxy group on the observed loss of activity compared to compound **89**. Similar losses of activity in flavonoid-induced *Gigaspora rosea* germination have been reported previously by Scervino et al.[212] Compound **89** exhibited significant stimulatory activity on *O. cumana* at 1 mM (31.2 ± 2.7%) and 0.1 mM (5.3 ± 1.4%), while no germination induction was observed in the other studied broomrape species. Suicidal germination of root parasitic weeds induced by the isoflavone uncinanone B from *Desmodium uncinatum* has been reported.[213]

The growth inhibitory activity of compounds **84-90** was assessed on radicles of *O. crenata*, *O. cumana*, *O. minor*, and *P. ramose* (**Figure 89**). As germination of broomrape

seeds is naturally inhibited until the detection of germination stimulants, the radicle growth bioassay was conducted by mixing each test compound with the germination stimulant GR24. The results indicated a significant effect on radicle growth inhibition for the type of compound (ANOVA, $p < 0.001$), broomrape species (ANOVA, $p < 0.001$), compound concentration (ANOVA, $p < 0.001$), and the interaction between compound x broomrape species (ANOVA, $p < 0.001$) or compound x concentration (ANOVA, $p < 0.001$). Both (4*Z*)-lachnophyllum lactone (**84**) and (4*Z*,8*Z*)-matricaria lactone (**86**) emerged as the most active compounds at concentrations of 1 mM and 0.1 mM. Compound **86** exhibited the strongest inhibition activity on radicles in all tested broomrape species, with inhibition values exceeding 80% in most cases. At 1 mM, nearly 100% inhibition was observed for *O. cumana*, *O. minor*, and *P. ramosa*. The activity exhibited by compound **84** is also noteworthy, with inhibition values exceeding 70% in most cases. These results, coupled with recent findings against *C. campestris*,[207] underscore the potential of (4*Z*)-lachnophyllum lactone (**84**) as a promising allelochemical for parasitic weed control.

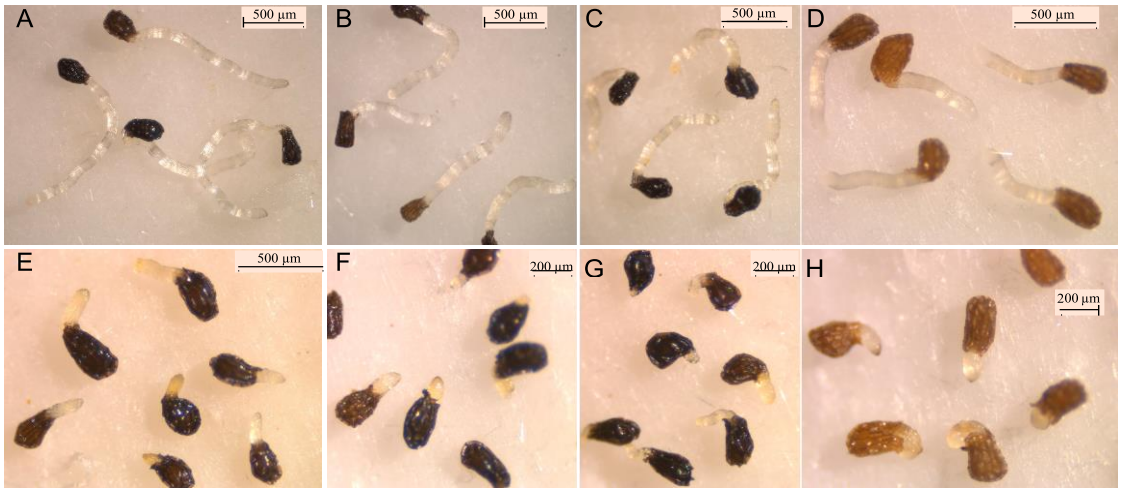

Figure 89. *Treatments with control (**A**–**D**) and compound (4Z,8Z)-matricaria lactone (**86**) applied at 0.1mM (**E**–**H**) on radicles of O. crenata (**A**,**E**); radicles of O. cumana (**B**,**F**); radicles of O. minor (**C**,**G**); and radicles of P. ramosa (**D**,**H**) (adapted from Cala Peralta et al., Molecules, 2022, 27, 7421-7433).*[214]

By comparison of compounds **84** and **86** activity with that of the other tested compounds, a notable enhancement, particularly evident at the lowest concentration (0.1 mM), is evident.

Methyl 4-hydroxybenzoate (**89**) exhibits moderate activity in reducing radicle growth inhibition at 1 mM for O. cumana, O. minor, and P. ramosa (around 60% inhibition). Structurally, the high inhibition exhibited by (4*Z*)-lachnophyllum lactone (**84**) and (4*Z*,8*Z*)-matricaria lactone (**86**) significantly decrease when the lactonic ring is opened (compound **85**). However, comparing the activity of compounds **86** (4*Z*) and **87** (4*E*), the loss of activity in compound **87** is attributed to the geometry of the $C_4 = C_5$ double bond. Lipophilicity values (CLogP) further contribute to understanding different behaviour, in fact the higher lipophilicity of compound 85 is linked to the lower activity. Similar CLogP values for geometric isomers **86** and **87** imply that their distinct activity is likely due to different reactivity rather than solubility. Lastly, aromatic compounds **88** and **89** show that the *p*-methoxy group is associated with reduced inhibitory activity, consistent with the germination induction bioassay findings.

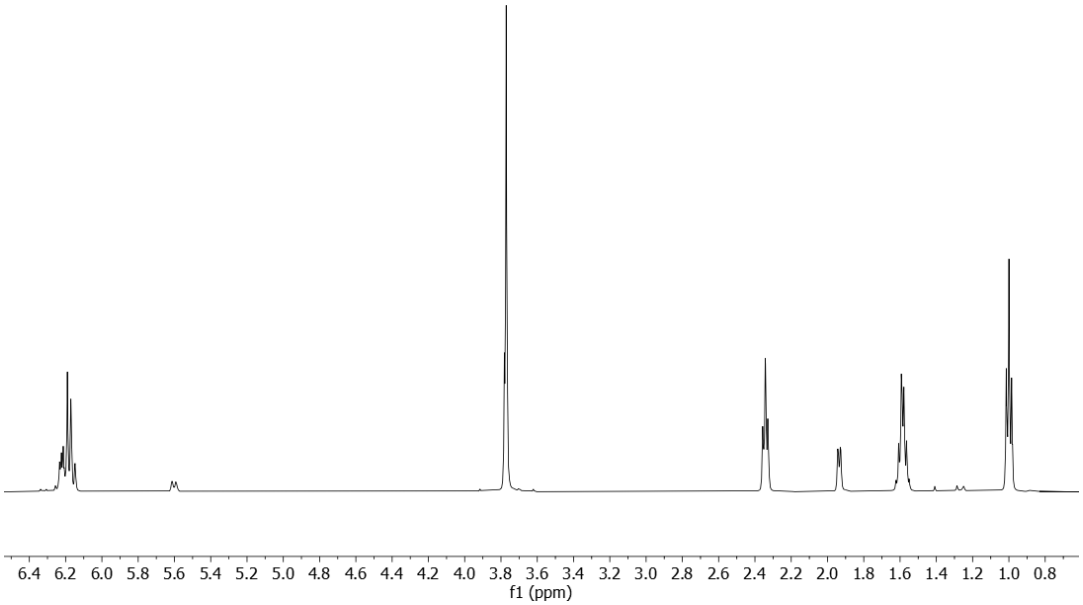

Figure 90. *^{1}H-NMR spectrum of (4Z)-lachnophyllum methyl ester (**85**) recorded in $CDCl_3$ at 500 MHz.*

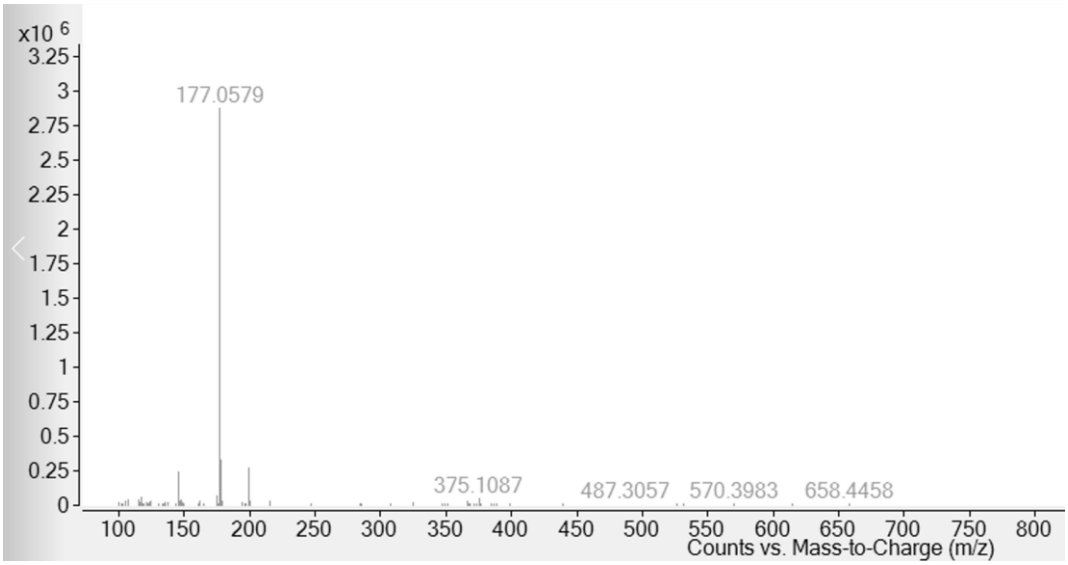

Figure 91. *ESI MS spectrum of (4Z)-lachnophyllum methyl ester (**85**) recorded in positive modality.*

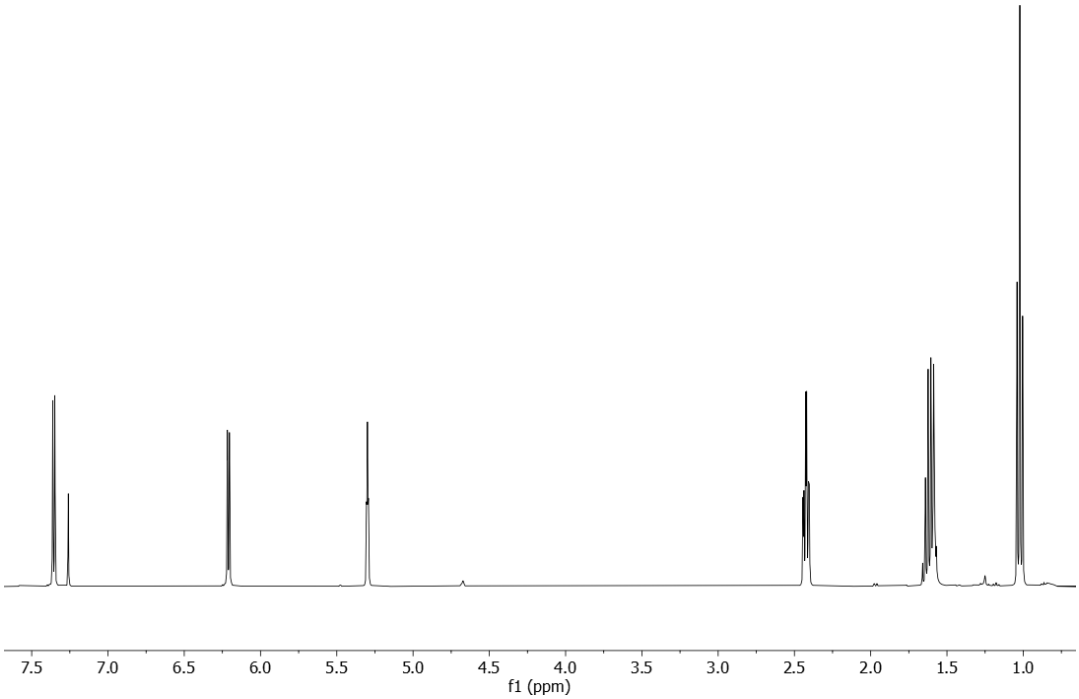

Figure 92. *^{1}H-NMR spectrum of (4Z)-lachnophyllum lactone (**84**) recorded in $CDCl_3$ at 500 MHz.*

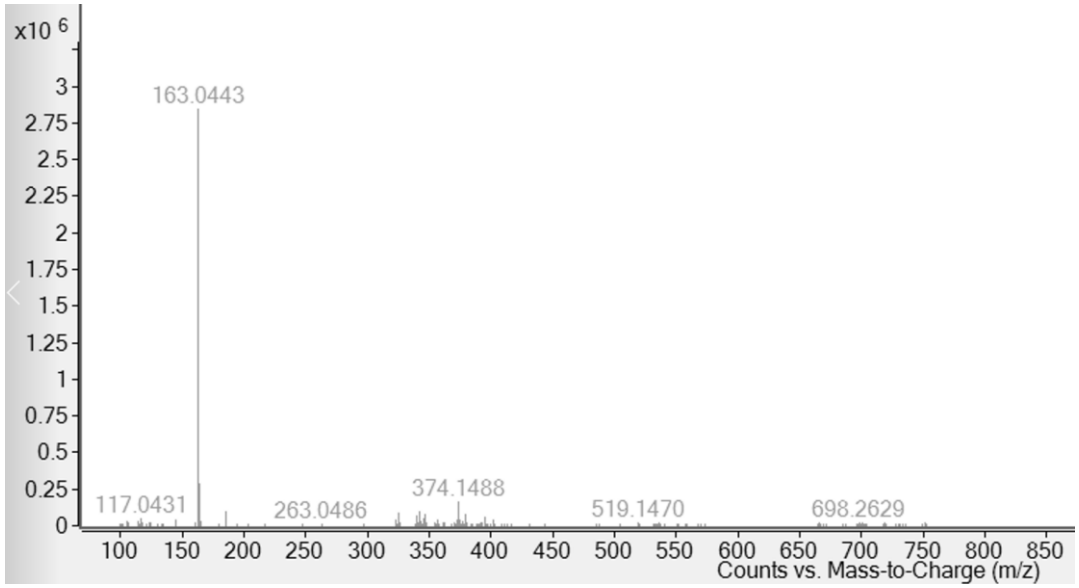

Figure 93. *ESI MS spectrum of (4Z)-lachnophyllum lactone (**84**) recorded in positive modality.*

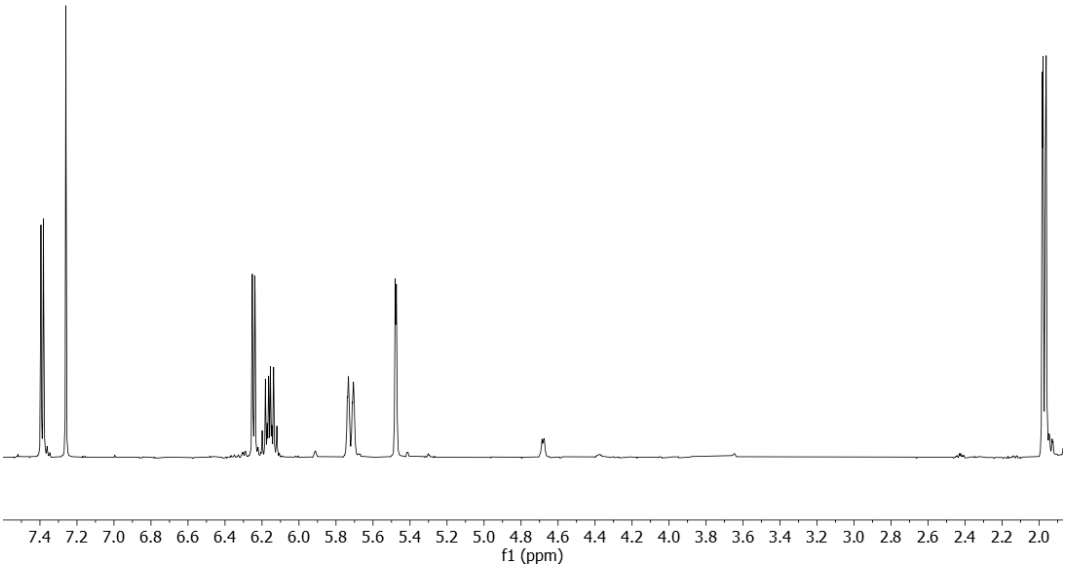

Figure 94. *^{1}H-NMR spectrum of (4Z,8Z)-matricaria lactone (**86**) recorded in $CDCl_3$ at 500 MHz.*

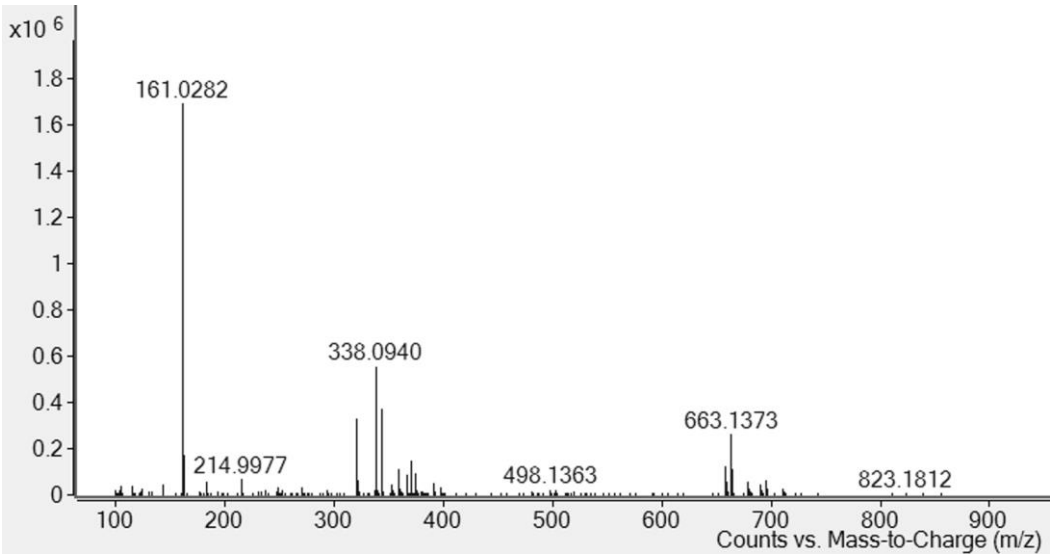

Figure 95. *ESI MS spectrum of (4Z,8Z)-matricaria lactone (**86**) recorded in positive modality.*

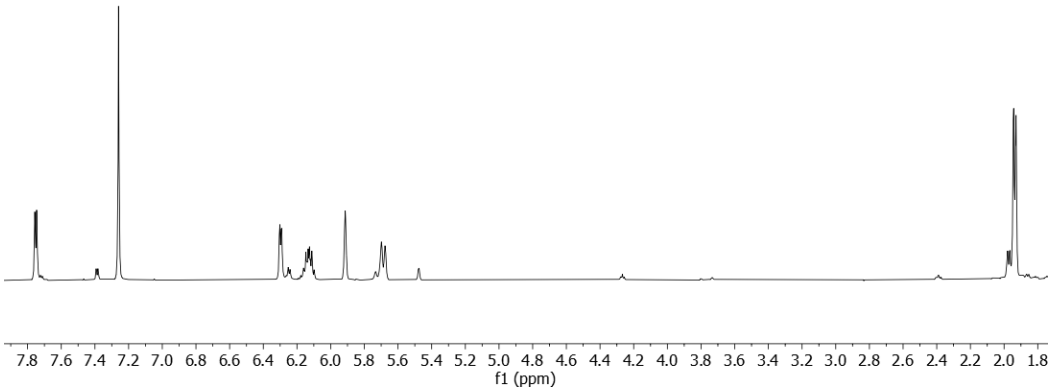

Figure 96. *^{1}H-NMR spectrum of (4E,8Z)-matricaria lactone (**87**) recorded in $CDCl_3$ at 500 MHz.*

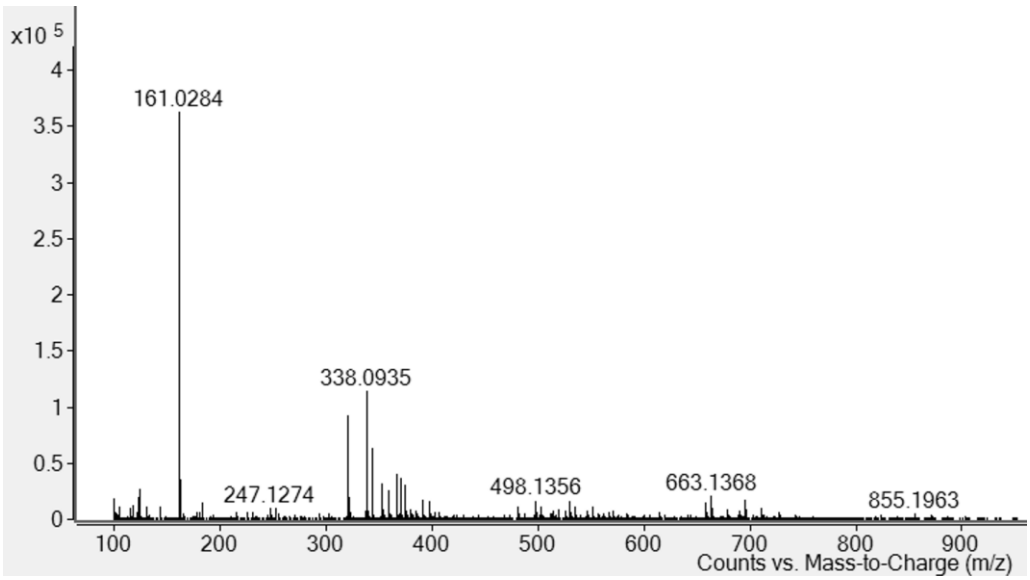

Figure 97. *ESI MS spectrum of (4E, 8Z)-matricaria lactone (**87**) recorded in positive modality.*

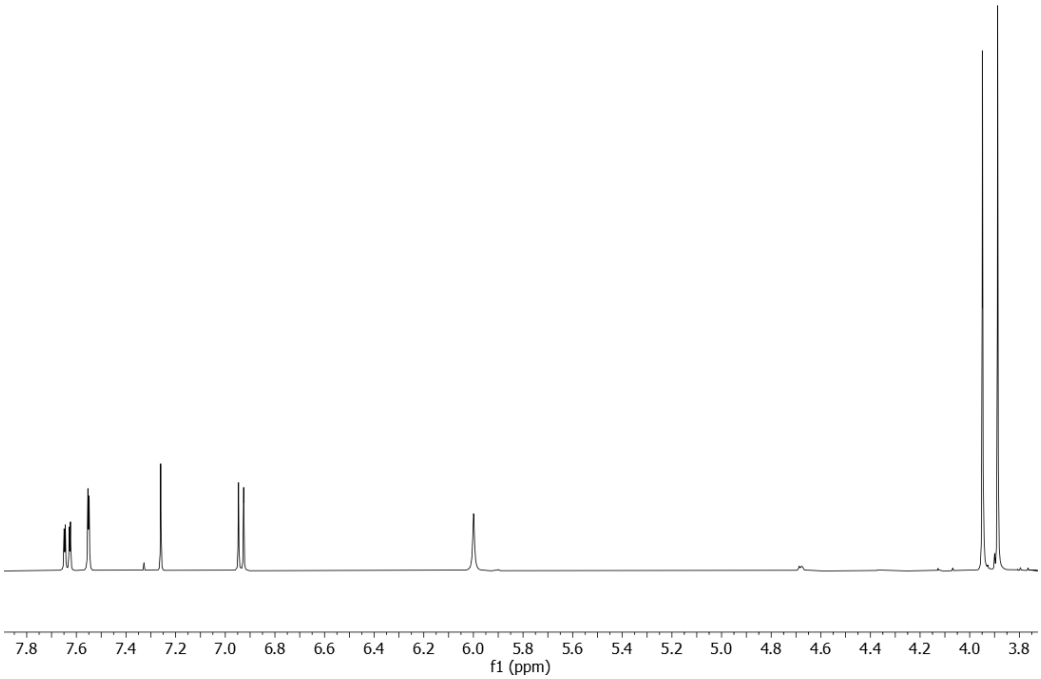

Figure 98. *^{1}H-NMR spectrum of methyl 4-hydroxy-3-methoxybenzoate (**88**) recorded in $CDCl_3$ at 500 MHz.*

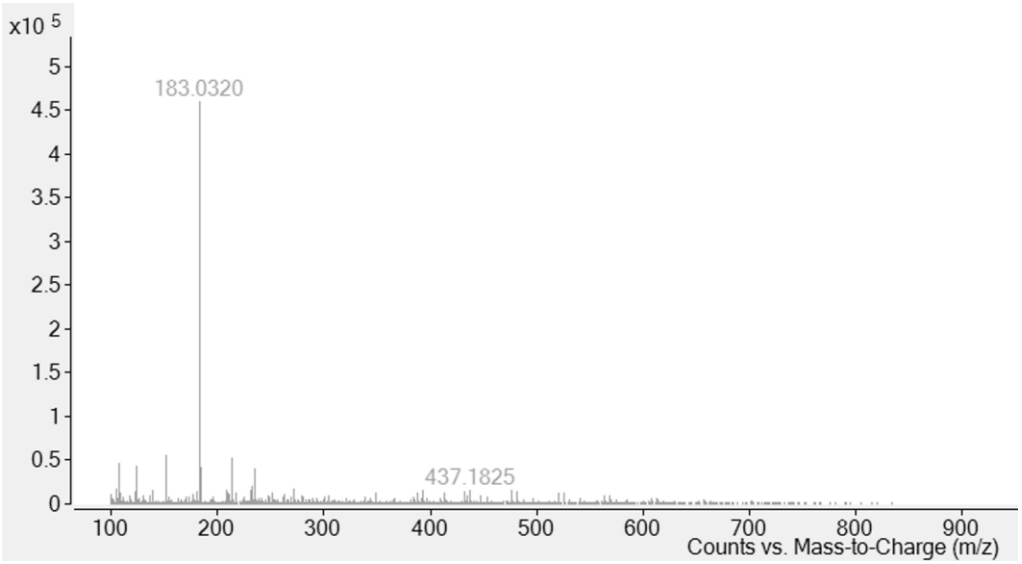

Figure 99. *ESI MS spectrum of methyl 4-hydroxy-3-methoxybenzoate (**88**) recorded in positive modality.*

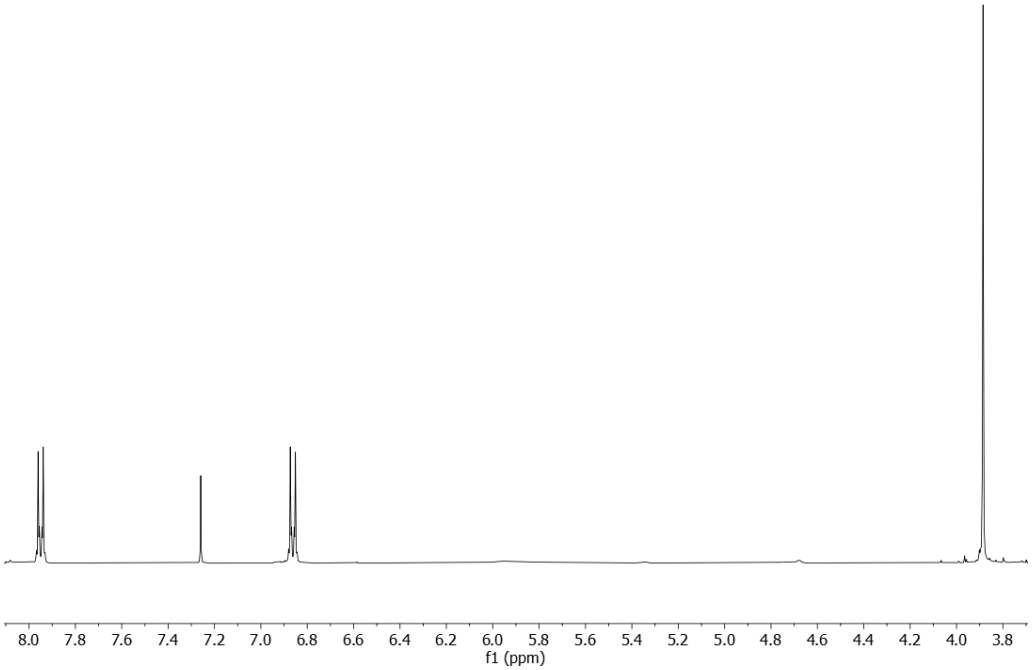

Figure 100. *^{1}H-NMR spectrum of methyl 4-hydroxybenzoate (**89**) recorded in $CDCl_3$ at 500 MHz.*

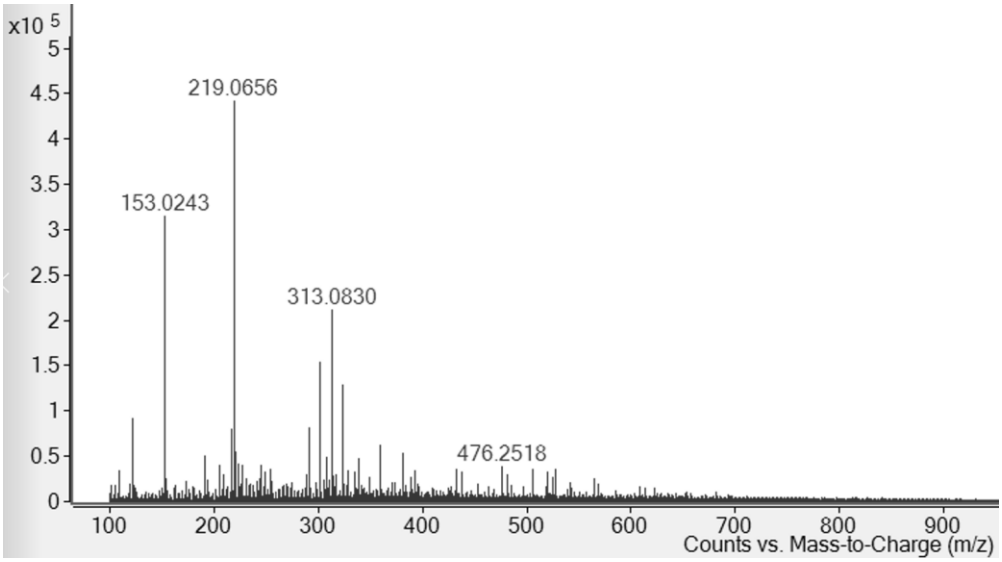

Figure 101. *ESI MS spectrum of methyl 4-hydroxybenzoate (**89**) recorded in positive modality.*

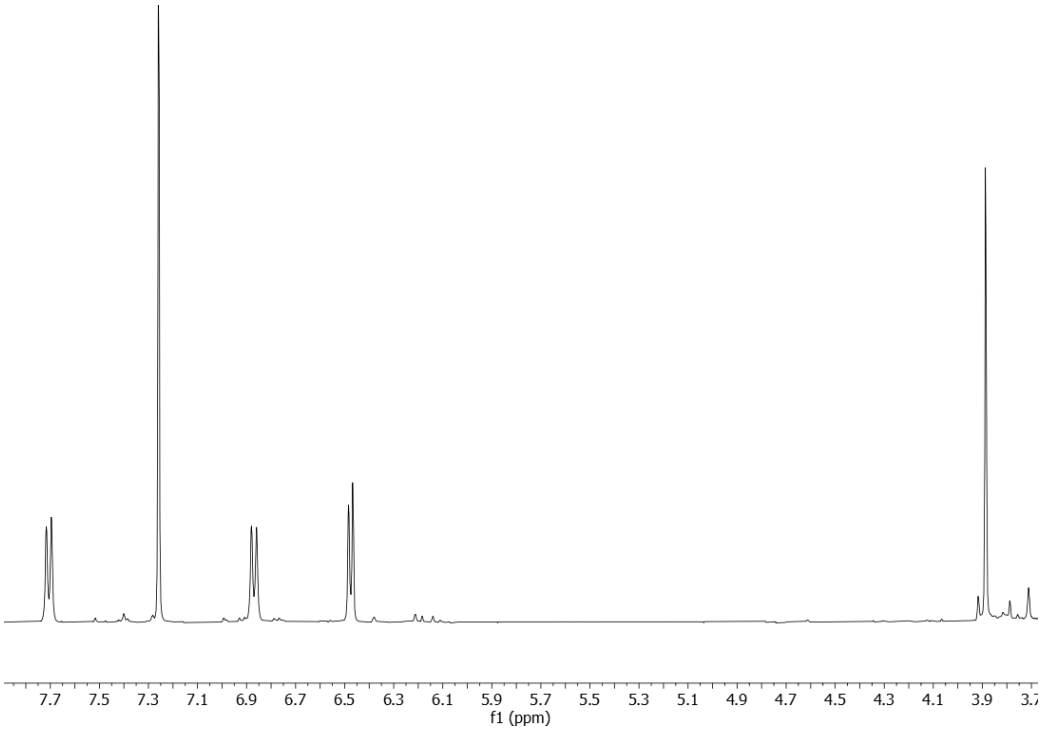

Figure 102. *^{1}H-NMR spectrum of hispidulin (**90**) recorded in $CDCl_3$ at 500 MHz.*

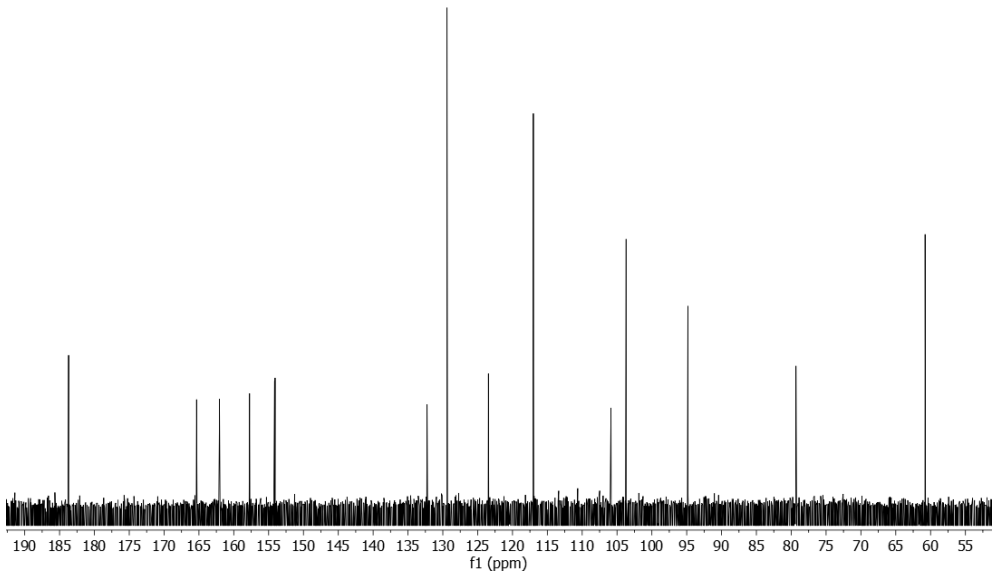

Figure 103. *^{13}C-NMR spectrum of hispidulin (**90**) recorded in $(CD_3)_2CO$ at 125 MHz.*

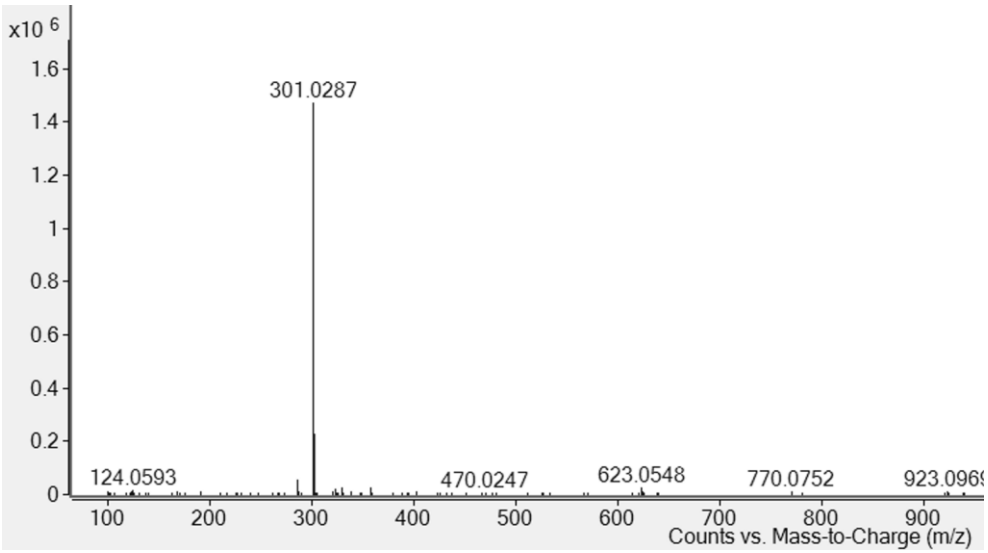

Figure 104. *ESI MS spectrum of hispidulin (**90**) recorded in positive modality.*

5.9 (4*Z*)-Lachnophyllum lactone total synthesis

Considering the high phytotoxic activity exhibited by (4*Z*)-lachnophyllum lactone (**84**), isolated from *C. bonariensis* extract, observed against stem and root parasitic weeds,[207,214] and the relatively small structure framework in respect to many other specialized metabolites isolated from the previous described and investigated allelopathic plants, it was selected to be synthesized on gram scale in order to broadens its field of application especially in the agrochemical industry and overcome the limitations associated to isolation from natural sources.

Thus, a retrosynthetic pathway analysis represented the first step, in the design of a synthetic methodology, towards (4*Z*)-lachnophyllum lactone (**84**) (**Scheme 1**).[214] The crucial step was identified in a Pd-Cu bimetallic cascade cross coupling-cyclization (25,26) between 1,3-eptadiyne (**Scheme 1**, green) and 3-*Z*-iodoacrylic acid (**Scheme 1**, blue). Commercially available precursors, such as propiolic acid and pent-1-yne, allowed to readily synthesized the coupling partners **93** and **95** (**Scheme 1** right, **Scheme 2**). Thus, using a convergent approach, where the cyclization to afford the 2-furanone ring is the essential end-step, we were able to total synthesize the (4*Z*)-lachnophyllum lactone (**84**).

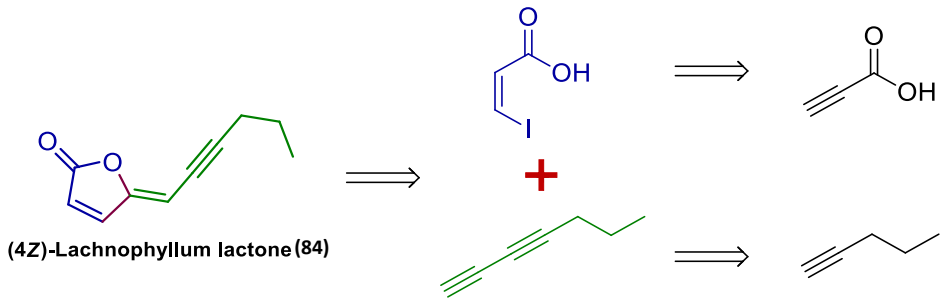

Scheme 1. *(4Z)-Lachnophyllum lactone (**84**) retrosynthetic analysis (adapted from Soriano et al. J. Agric. Food Chem, **2024**, 72, 4737-4746).*[151]

The synthesis of several substituted butenolides, including the (4*Z*)-lachnophyllum lactone (**84**), has already been reported in 1981 by Asaoka and co-workers.[215] Nevertheless, a carefully analysis of the procedure reported allowed us to understand that it can hardly be used and adopted to the industry field due to the employment of toxic reagents and the

characterization techniques, which have been found to be outdated. Moreover, this procedure, is not stereoselective, leading to the formation of an isomeric mixture.

Basing on retrosynthetic analysis, described before (**Scheme 1**), an alternative procedure involving the use of a Pd catalyst bis(triphenylphosphine)palladium(II) dichloride worked as expected.[156] Thus, the first step consisted in the preparation 1-iodopent-1-yne (**91**) in high yield, as described in materials and methos section, starting from pent-1-yne.[216,217] Next, compound **91** was used in a cross-coupling reaction with TMS-acetylene to obtain the hepta-1,3-diyn-1-yltrimethylsilane (**92**),[152] in high yield. It is essential to highlight that, in the two aforementioned steps, as well as in the last reaction, utmost caution was required to prevent the presence of oxygen, which would undoubtedly result in unwanted homocoupling byproducts. This issue was effectively circumvented by purging the reaction mixture with argon before introducing all components of the catalytic system. In the next-to-last synthetic strategy step, we drew inspiration by a procedure reported in 1990 by Ma and Lu,[218] regarding the hydrohalogenation of propiolic acid using lithium halogen reagents. The authors suggested a mechanism in which the intermediate cation is arranged in a bridge between the carbonylic oxygen and the triple bond,[155,218] channelling the *cis*-stereospecificity. In the current work, the proton could act in a similar way, allowing to obtain the 3-*Z*-iodoacrylic acid (**95**), whose configuration is pivotal in the final synthetic step, facilitating the spontaneous 5-exo-dig cyclization. Using the procedure described in the material and methods section, the 3-*Z*-iodoacrylic acid (**95**) was obtained in 95% yield (**Scheme 2**, **95**), confirming our hypothesis. After TMS deprotection from hepta-1,3-diyn-1-yltrimethylsilane (**92**), the resulting 1,3-eptadiyne (**93**)[153] was reacted with the previously obtained 3-*Z*-iodoacrylic acid (**95**) in a Pd-Cu bimetallic cascade lactonization, as previously detailed, yielding the (4*Z*)-lachnophyllum lactone (**84**). It's important to highlight that the described sequence was initially fine-tuned on a small scale (less than 5 mmol). Once favorable results in terms of yield were achieved, the process was scaled up to produce the desired compound on a gram scale. The overall yield of (4*Z*)-lachnophyllum lactone (**84**) starting from 1-pentyne is of 28.5%.[151]

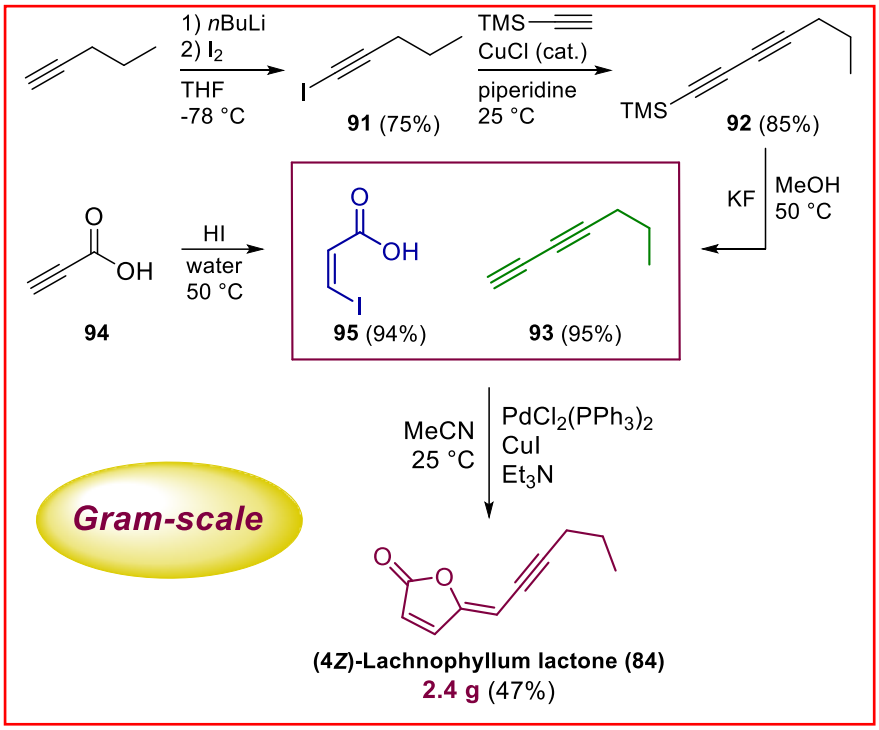

Scheme 2. *Gram-scale synthetis of (4Z)-lachnophyllum lactone (**84**) (adapted from Soriano et al. J. Agric. Food Chem, **2024**, 72, 4737-4746).*[151]

With the final goal of delving deeper into the structure-activity relationship (SAR) of the (4*Z*)-lachnophyllum lactone (**84**), the target compound served as substrate to produce both the *E* stereoisomer (**96**, **Scheme 3**) through a photocatalyzed reaction involving a radical intermediate,[156] and the (4*Z*,8*Z*)-matricaria lactone (**97**, Scheme 3) using 2,3-dichloro-5,6-dicyano-1,4-benzoquinone as oxidizing agent.[158] It's noteworthy that the method developed in the current work is easily adaptable for obtaining various derivatives. By using acetylenic compounds with longer or shorter alkyl chains, or incorporating different functional groups or heteroatoms in the intermediates structure, a range of analogues could be generated, opening up the possibility for exploring SAR. In this context, the potential synthesis of 3-*E*-iodoacrylic acid could be considered, to achieve the production of the synthetic open-ring analogue of (4*Z*)-lachnophyllum lactone. Subsequently, we proceeded to assess the bioactivity of the synthetic (4*Z*)-lachnophyllum lactone (**84**).

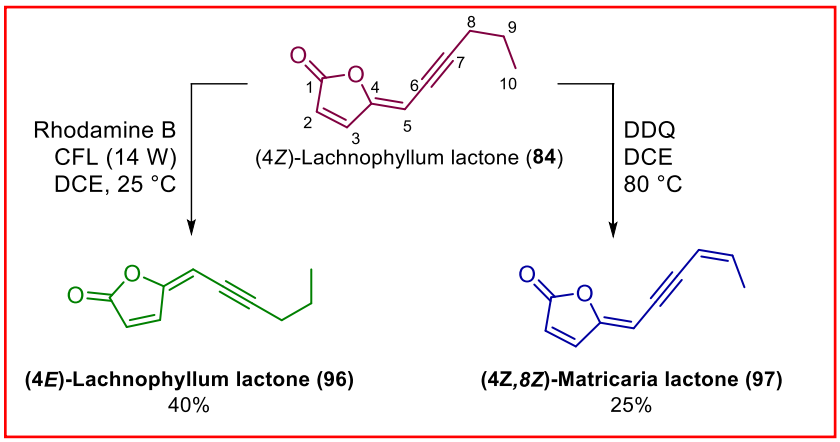

Scheme 3. (4*Z*)-Lachnophyllum lactone (**84**) synthetic derivatives (**96** *via* photoisomerization and **97** *via* radical oxidation) *(adapted from Soriano et al. J. Agric. Food Chem, **2024**, 72, 4737-4746).*[151]

Bioactivity. In the ongoing study, the anti-parasitic-weed activity of the synthetic (4*Z*)-lachnophyllum lactone (**84**) against *C. campestris* as well as *O. minor* and *P. ramosa* was confirmed. When applied at 1mM the (4*Z*)-lachnophyllum lactone (**84**) inhibited the growth of seedlings of *C. campestris* by 97.04 ± 1.58 % and the growth of radicles of *O. minor* and *P. ramosa* by respectively 83.87 ± 0.51% and 80.73 ± 2.58 %.

The results obtained by the comparison of compound **84** activity with those of its two structural derivatives, **96** and **97**, when tested in the growth inhibitory bioassay against *C. campestris*, showed significant differences only when applied at a concentration of 0.1 mM. Specifically, 32.17 ± 4.64 % using **84,** to 43.22 ± 2.69 % using **96** and 63.08 ± 5.03 % using **97** inhibition was observed. Inhibitory activity against *O. minor* was significantly different among the compounds at all concentrations tested. In particular, the growth inhibitory activity was higher for **97** and lower for **96** than that shown by **84**. Also, against *P. ramosa* the growth inhibitory activity of **96** was significantly lower when applied at the concentrations of 0.6 and 0.3 mM compared with **84** and **97** (**Figure 105, 106**).

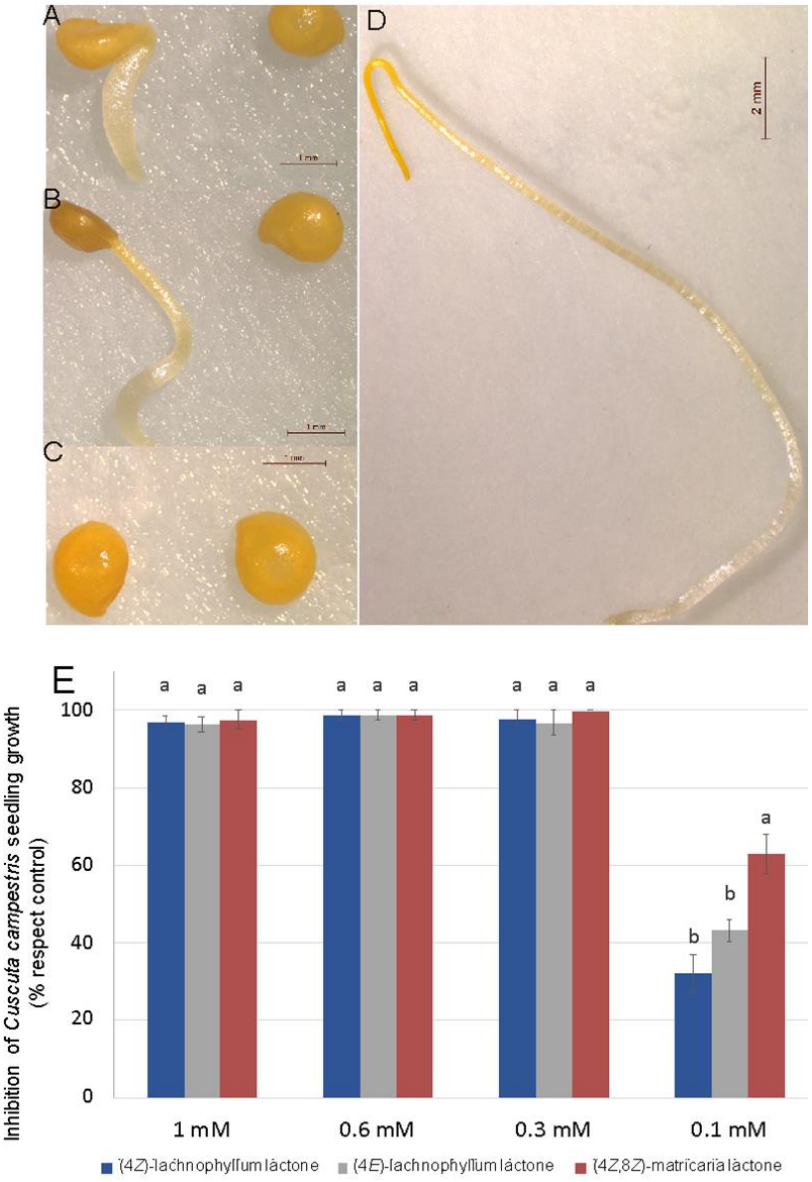

Figure 105. *Effect of compound and concentration on Cuscuta campestris. Illustrative pictures of 5-day-old C. campestris seedlings showing stunted growth induced by 0.3 mM treatments of* ***84*** *(A),* ***96*** *(B) and* ***97****(C) in comparison with healthy growth observed in seedlings treated with control (D). Effect of* ***84***, ***96***, ***97*** *applied at concentration range 1 - 0.1 mM on C. campestris seedling growth on filter paper (E) (adapted from Soriano et al. J. Agric. Food Chem,* ***2024****, 72, 4737-4746).*[151]

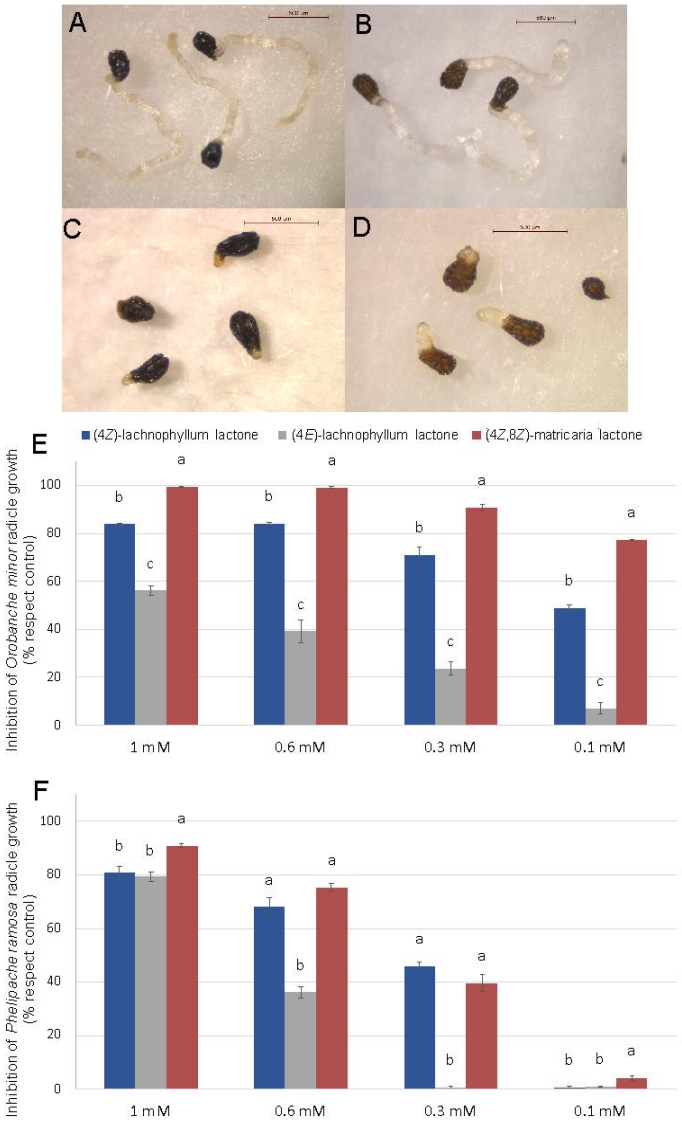

Figure 106. *Effect of compound and concentration on two broomrape species O. minor and P. ramosa. Illustrative pictures of 7-day-old O. minor (A) and P. ramosa (B) seedlings showing healthy growth when treated with control in comparison with the stunted growth induced by compound* ***97*** *treatments on O. minor seedlings at 0.3 mM (C), and on P. ramosa seedlings at 1 mM (D). Effect of (4Z)-lachnophyllum lactone, (4E)-lachnophyllum lactone (4Z, 8Z)-matricaria lactone and (4E, 8Z)-matricaria lactone applied at concentration range of 1 - 0.1 mM on radicle growth of O. minor (E) and P. ramosa (F) seedlings growing in glass fiber filter paper (adapted from Soriano et al. J. Agric. Food Chem,* ***2024****, 72, 4737-4746).*[151]

Furthermore, the phytotoxic activity against the autotrophic weed *C. bonariensis* and antimicrobial activity against the olive pathogen *V. dahliae* were assessed.[219] Specifically, compound **84**, inhibit root length seedlings of *C. bonariensis* by 82.52 ± 0.37 %, 84.13 ± 0.14%, at concentrations of 0.6, 0.3 and 0.1 mM respectively (**Figure 107 A,B,E**).

At concentrations of 0.6 and 0.3 mM, compound **96** induced the lower inhibitory activity (78.77 ± 2.04 %, and 70.15 ± 1.85 %), while compound **97** induced the stronger inhibition (91.92 ± 4.09 %, and 88.46 ± 0.78%, **Figure 107**).

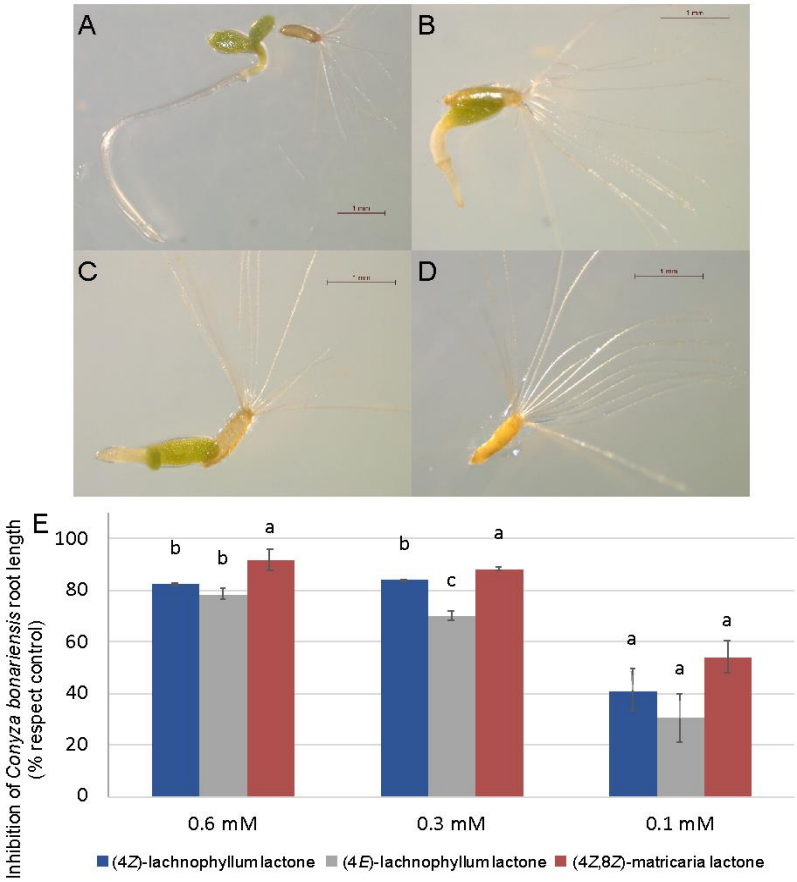

Figure 107. *Effect of compound and concentration measured on 7-day-old Conyza bonariensis growing on agar. Illustrative pictures of healthy C. bonariensis seedlings treated with control (A), in comparison with stunted growth induced on C. bonariensis seedlings by treatments of 0.6 mM of (4Z)-lachnophyllum lactone (B), (4E)-lachnophyllum lactone (C) and (4Z, 8Z)-matricaria lactone (D). Effect of (4Z)-lachnophyllum lactone, (4E)-lachnophyllum lactone, and (4Z, 8Z)-matricaria lactone applied at concentration range 0.6 - 0.1 mM on C. bonariensis seed germination (E) and root growth (F) (adapted from Soriano et al. J. Agric. Food Chem,* ***2024****, 72, 4737-4746).*[151]

The antimicrobial activity against the mycelial growth of *V. dahliae* was assessed at 3-day intervals, following the inoculation of the fungus on Petri dishes supplemented with compounds **84**, **96** and **97** at 1, 0.6 and 0.3 mM (**Figure 108**). At 1 mM all compounds (**Figure 108A-E**) significantly reduced the mycelial growth of the pathogen compared to the control treatments at all exposure times tested (3, 6, 9, 12 and 15 days after inoculation). The area under the growth progress curve (AUGPC) was decreased by a 57.0, 44.9 and 68,1% in the petri dishes treated with **84**, **96** and **97** compared with the AUGPC observed in the control treatment. At 0.5 mM (Figure 4F), mycelial growth was only inhibited by compounds **84** and **97** and this inhibition was observed after 6 days of exposure (AUGPC inhibited by 22.6% and 27.2% respectively). No inhibitory effect was observed in any of the compounds when they were applied at 0.3 mM (**Figure 108**).

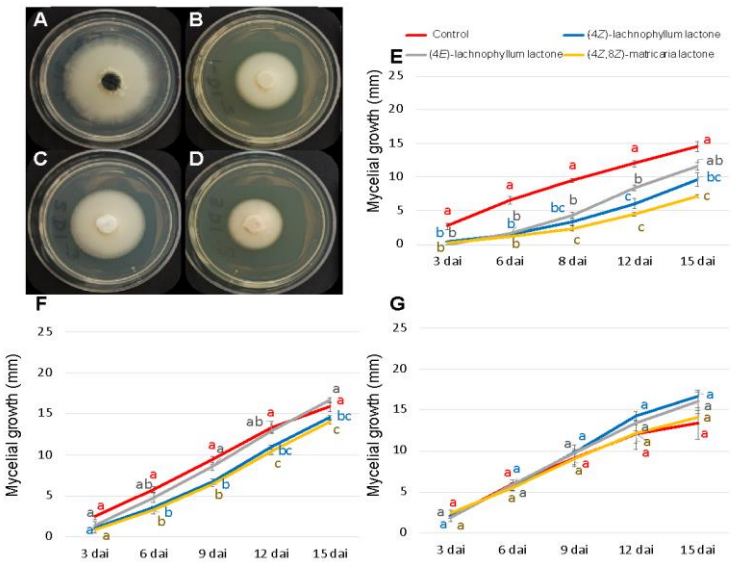

Figure 108. *Effect of compound and concentration on the mycelial growth of V. dahliae. Illustrative pictures of V. dahliae mycelial growth in 5.5 cm diameter Petri dishes observed 15-day after inoculation on PDA supplemented with control (A), and 1 mM treatments of* ***84*** *(B),* ***96*** *(C) and* ***97*** *(D). Effect compounds applied at 1 mM (E), 0.6 mM (F) and 0.3 mM (G) on V. dahliae mycelial growth measured at 3 day-intervals (adapted from Soriano et al. J. Agric. Food Chem,* ***2024****, 72, 4737-4746).*[151]

In conclusion, the outcomes of the present study, highlight and endorse the successfull design and comprehensive implementation of a five-step methodology, to synthesize the (4*Z*)-lachnophyllum lactone (**84**) on gram scale. This compound, initially isolated in limited quantities from natural sources, has now been produced in significant amounts. This amounts facilitates extensive test across various biological domains, enhancing the understanding of its activities and, importantly, positioning it for potential inclusion in biopolymer as an easily deployable tool for the agrochemical industry. Notably, starting from **84,** two simple additional synthetic steps yielded the analogues (4*E*)-lachnophyllum lactone (**96**) and the (4*Z*,8*Z*)-matricaria lactone (**97**). The protocol's flexibility allows for modifications to generate additional analogues, supporting SAR studies aimed at elucidating the structural features responsible for biological activities.

When tested against four weed species (*C. campestris, O. minor, P. ramosa,* and *C. bonariensis*) and the fungal pathogen *V. dahliae* the three compounds (**84**, **96** and **97**) exhibited varying degree of activity. *C. campestris* proved to be the most sensitive species as the three compounds highly inhibited the seedling growth up to 0.3 mM. In particular, at the lowest concentration (0.1 mM) on *C. campestris* compound **97** demonstrated the highest activity followed by compounds **96** and **84** emphasizing the influence of an additional double bond on the side chain of the furanone ring. This trend was consistent when testing the compounds on the other weeds and the fungal pathogen *V. dahliae.* In fact, compound **97** robustly inhibited the radicle growth of *O. minor* (**Figure 106E**) as well as that of *C. bonariensis* (**Figure 107**) at all the concentration tested and that of *P. ramosa* only at the higher concentrations tested (**Figure 106F**). Notably, compound **96** exhibited a reduced activity compared to compounds **84** and **97**. These results underscore the importance of the double bond geometry at C-4, on root parasitic weeds and the autotrophic weed compared to stem parasitic weed. The findings contribute to the pool of natural compounds suitable for application as bio-inspired herbicides and the butenolide core found in natural strigolactones too opens the way for testing (4*Z*)-lachnophyllum lactone and analogues for strigolactone-like bioactivity,[220,221] broadening potential applications. The substantial amount obtained overcomes the limitations associated with isolation from natural sources, facilitating exploration and refinement for bio-formulation, presenting a promising prospect for advancements in the agrochemical industry.

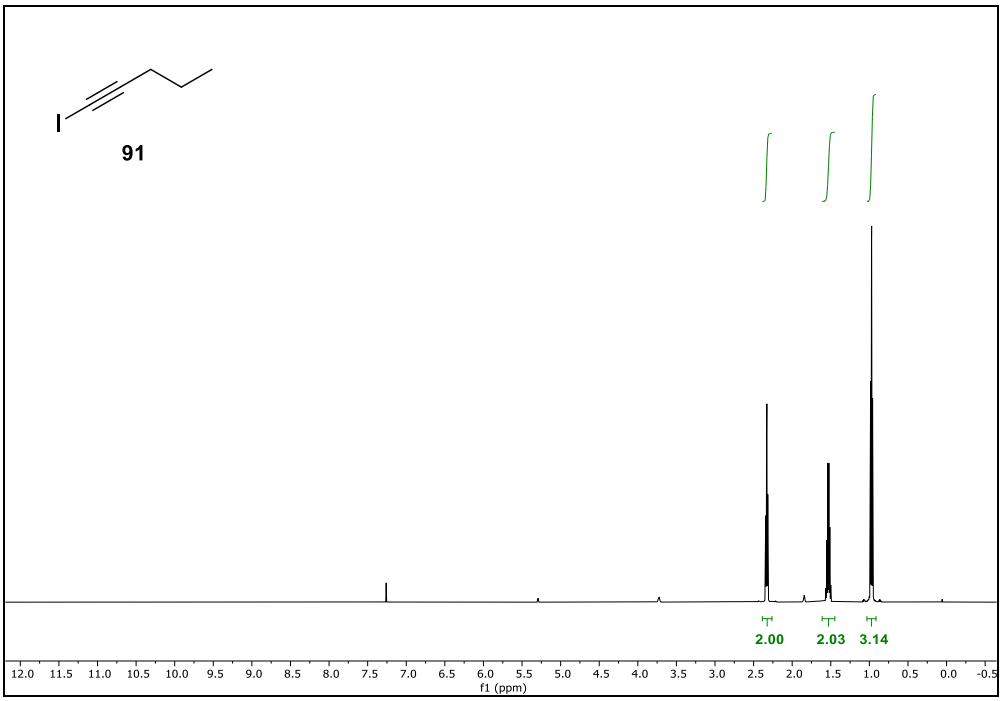

Figure 109. *[1]H NMR spectrum of 1-iodopent-1-yne,* ***91*** *($CDCl_3$, 600 MHz).*

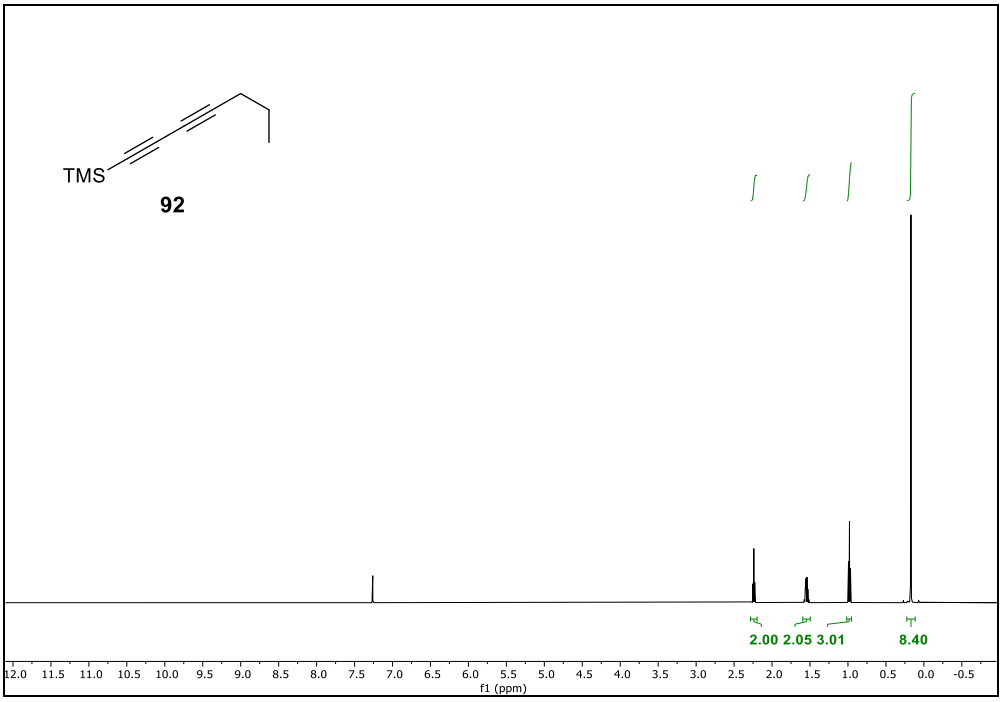

Figure 110. *[1]H NMR spectrum of hepta-1,3-diyn-1-yltrimethylsilane,* ***92*** *($CDCl_3$, 600 MHz).*

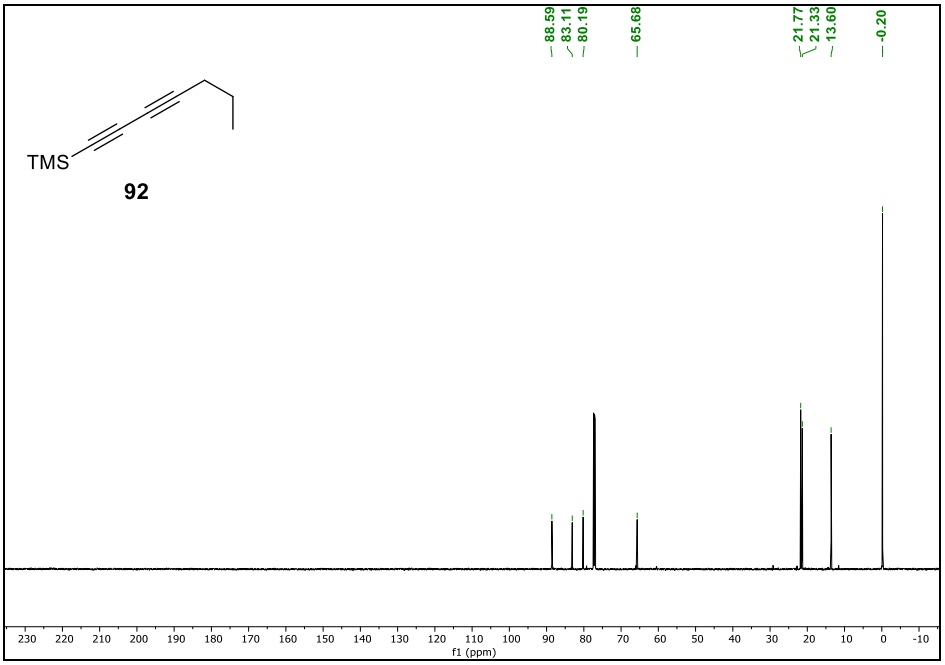

Figure 111. *^{13}C NMR spectrum of hepta-1,3-diyn-1-yltrimethylsilane,* ***92*** *($CDCl_3$, 150 MHz).*

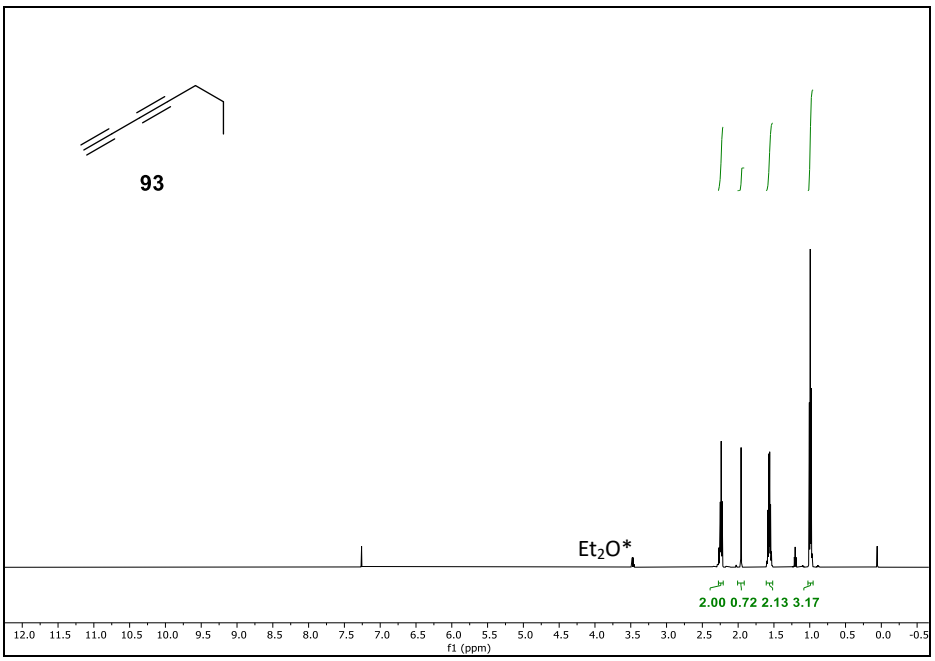

Figure 112. *^{1}H NMR spectrum of 1,3-heptadiyne,* ***93*** *($CDCl_3$, 600 MHz).*

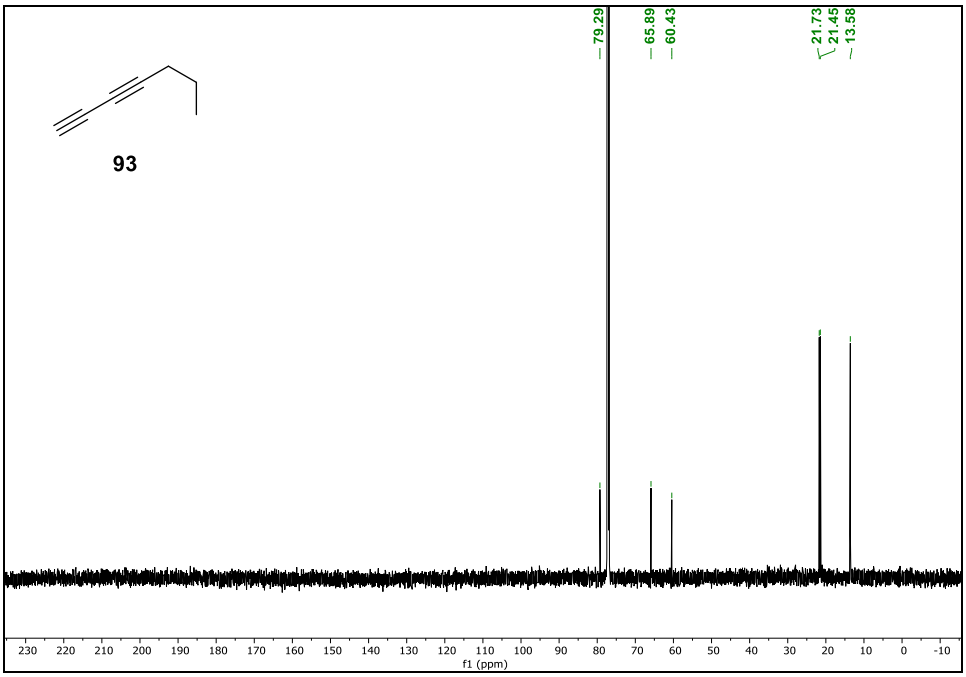

Figure 113. *^{13}C NMR spectrum of hepta-1,3-diyn-1-yltrimethylsilane,* ***93*** *($CDCl_3$, 150 MHz).*

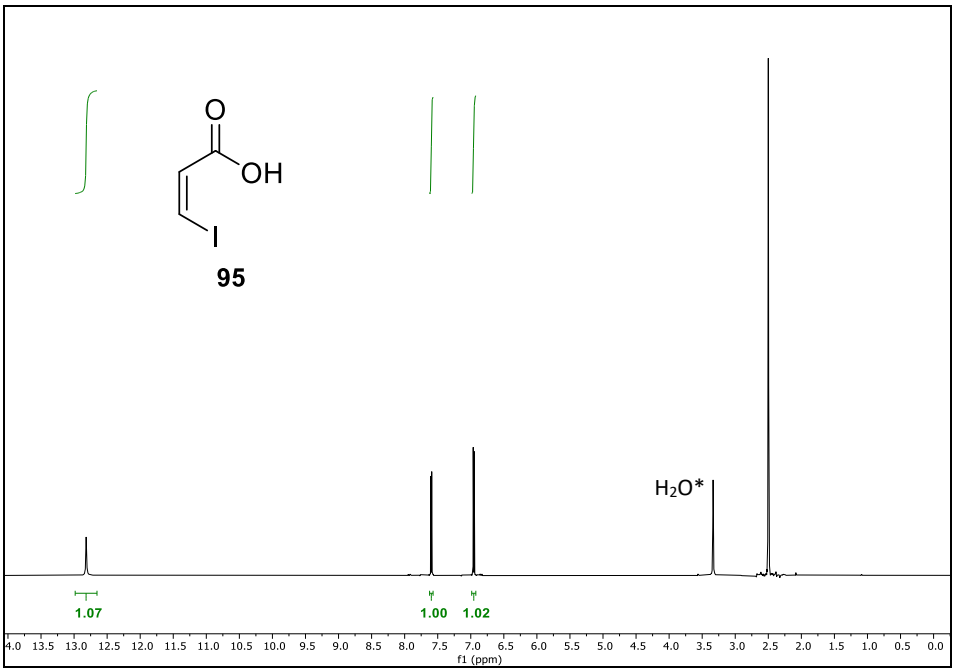

Figure 114. *^{1}H NMR spectrum of 3-Z-Iodoacrylic acid,* ***95*** *(DMSO-d_6, 600 MHz).*

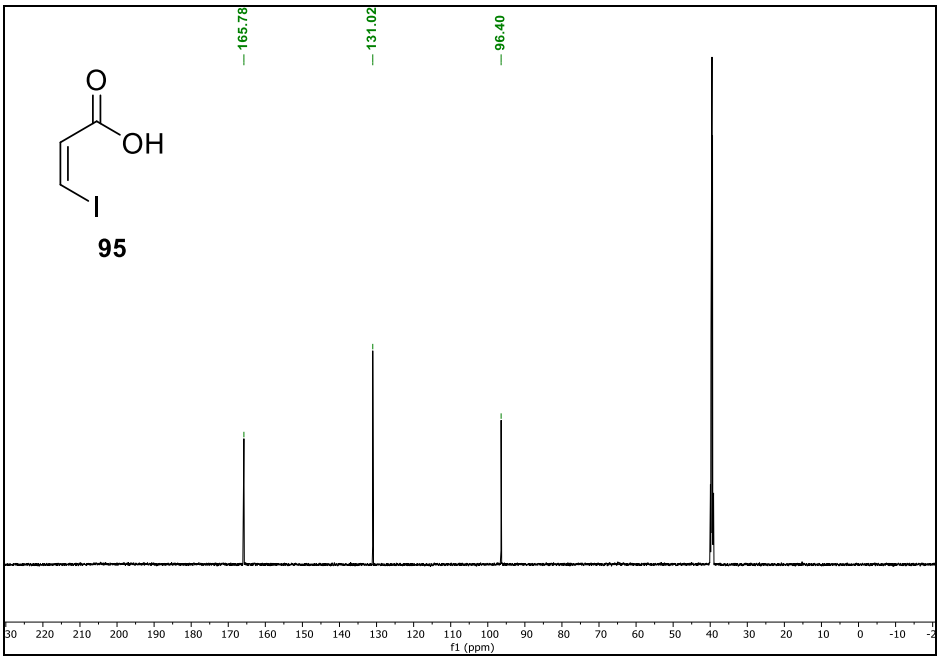

Figure 115. *^{13}C NMR spectrum of 3-Z-iodoacrylic acid,* ***95*** *(DMSO-d_6, 150 MHz).*

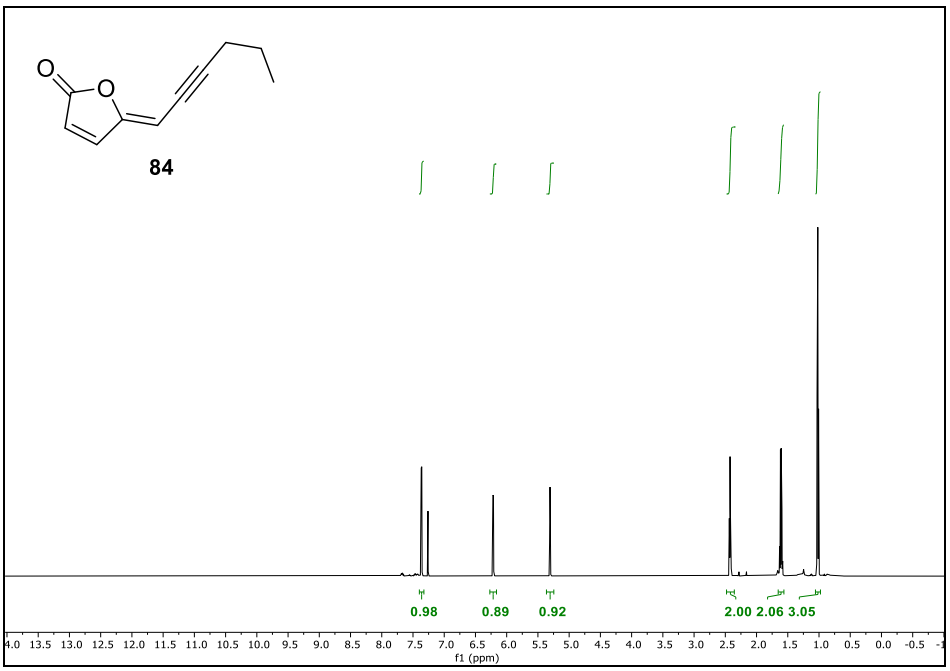

Figure 116. *^{1}H NMR spectrum of (4Z)-lachnophyllum lactone,****84*** *($CDCl_3$, 600 MHz).*

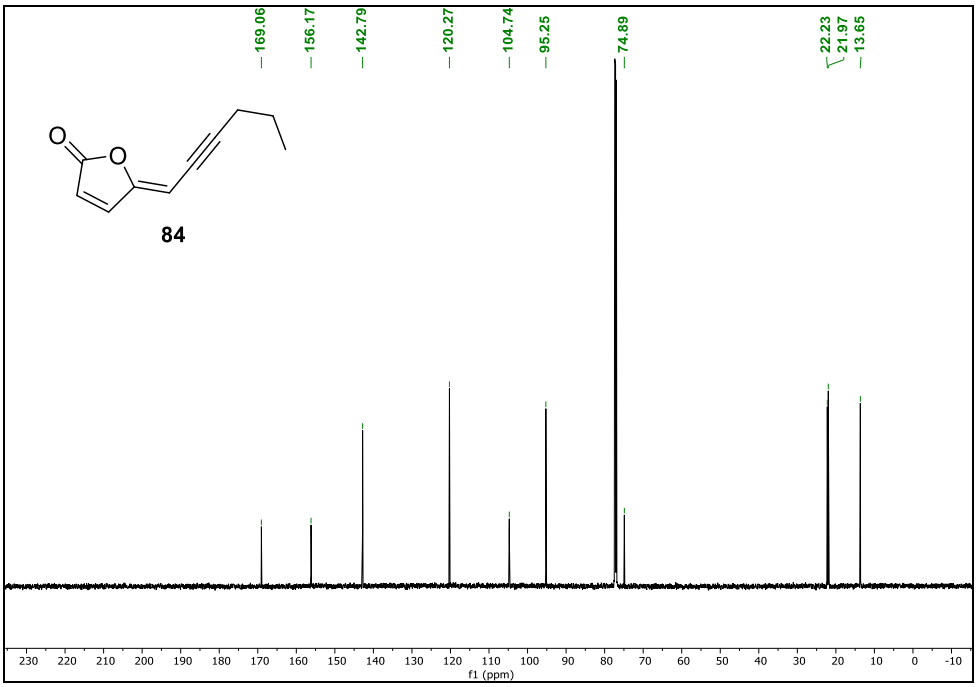

Figure 117. *^{13}C NMR spectrum of (4Z)-lachnophyllum lactone,* ***84*** *($CDCl_3$, 150 MHz).*

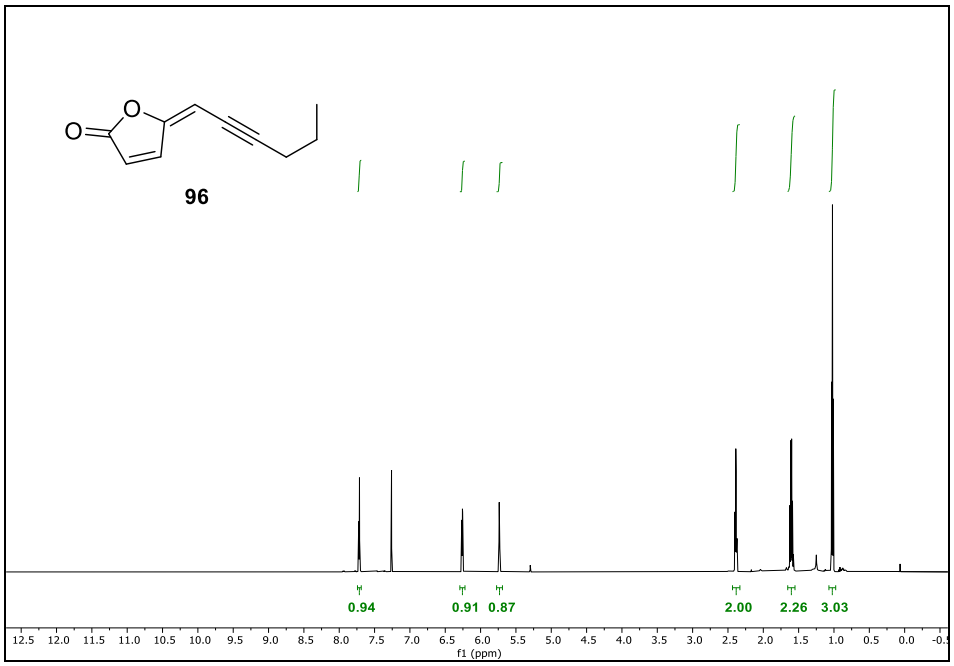

Figure 118. *^{1}H NMR spectrum of (4E)-lachnophyllum lactone,* ***96*** *($CDCl_3$, 600 MHz).*

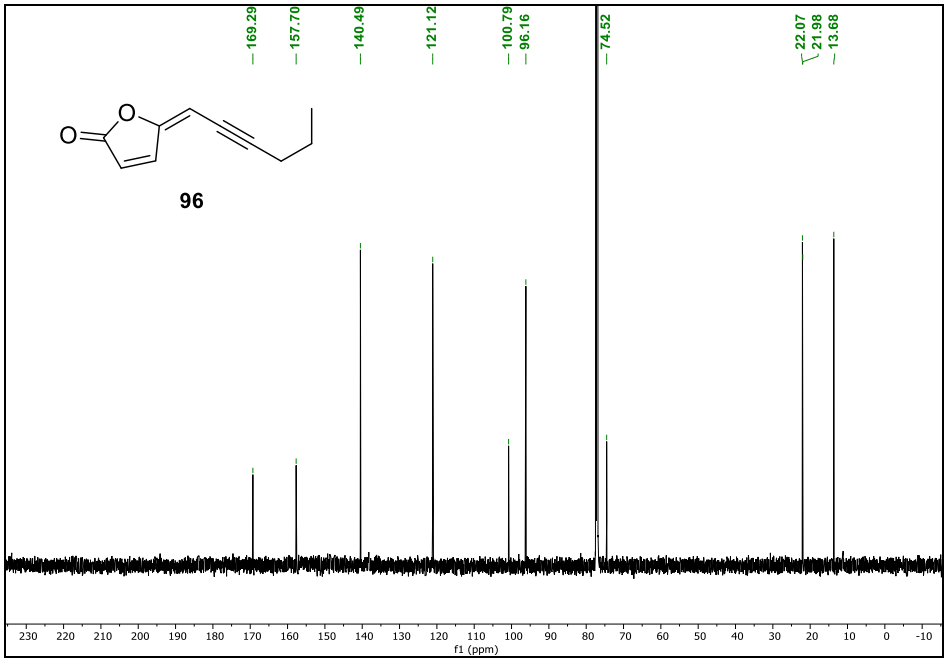

Figure 119. *^{13}C NMR spectrum of (4E)-lachnophyllum lactone,* ***96*** *($CDCl_3$, 150 MHz).*

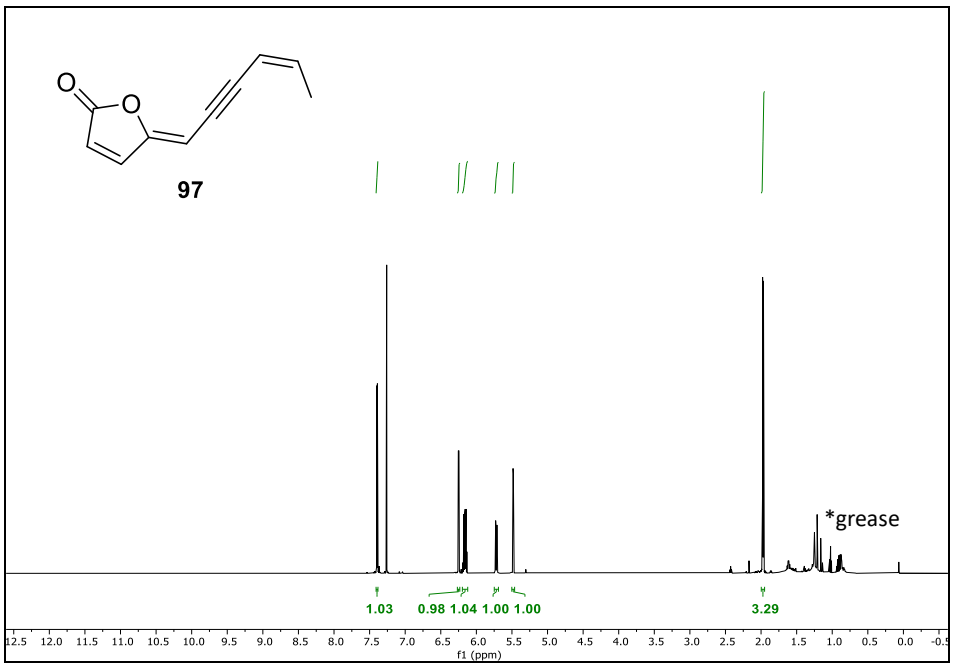

Figure 120. *^{1}H NMR spectrum of (4Z,8Z)-matricaria lactone,* ***97*** *($CDCl_3$, 600 MHz).*

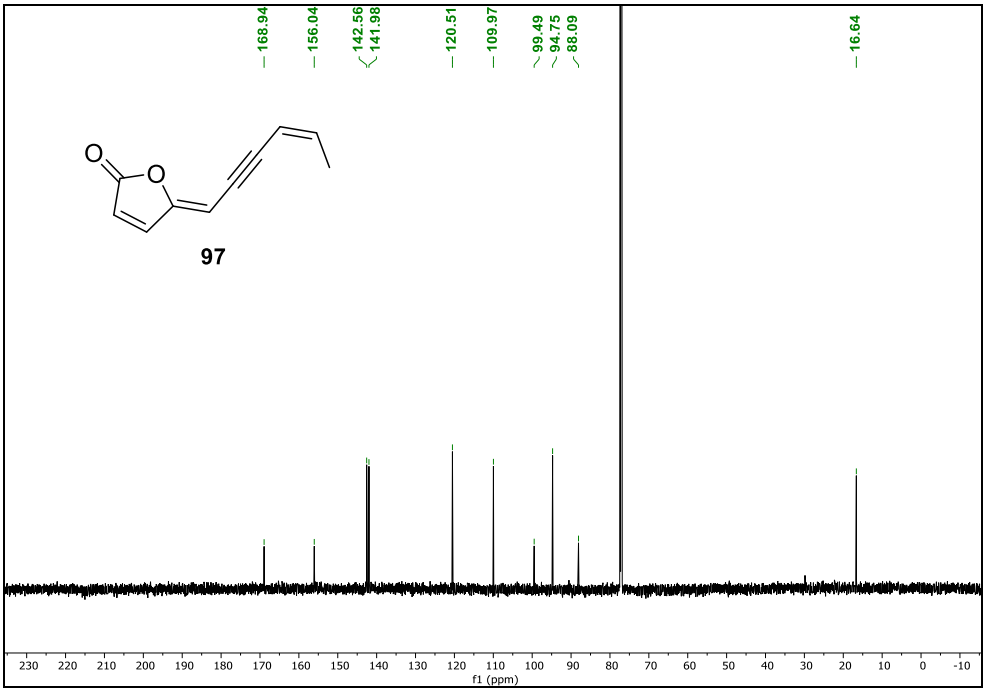

Figure 121. *^{13}C NMR spectrum of (4Z,8Z)-matricaria lactone,* ***97*** *($CDCl_3$, 150 MHz).*

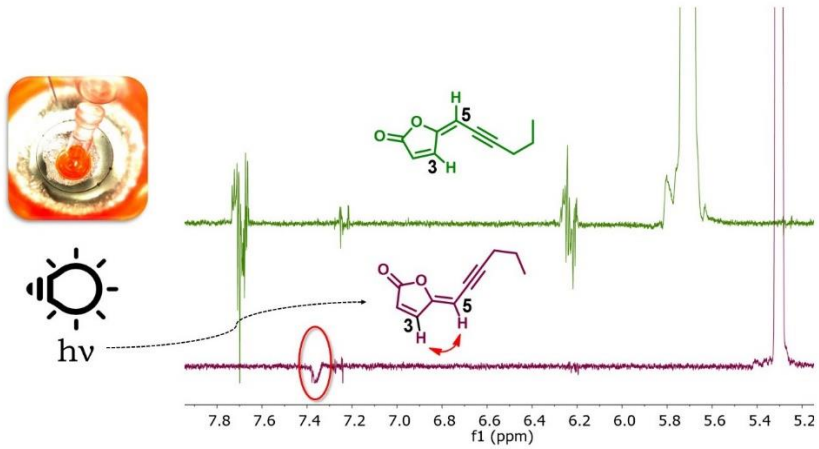

Figure 122. *1D NOESY comparation of the two lachnophyllum lactone stereoisomers (compound* ***84*** *purple line, compound* ***96*** *green line****,*** *$CDCl_3$, 600 MHz).*

Sample	Elemental formula	Molecular weight [g/mol]	Theoretical m/z	Measured m/z	Δmass ppm	Adduct
GS1	$C_{10}H_{10}O_2$	162,1852	163.0754	163.0757	1.84	$[M+H]^+$

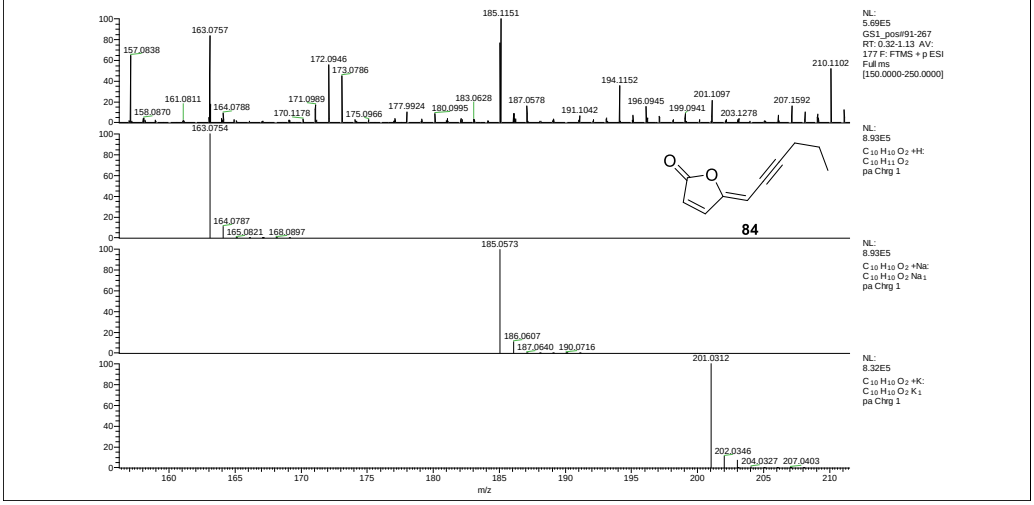

***Figure 123**. ESI-HRMS analyses of (4Z)-lachnophyllum lactone, **84**.*

Sample	Elemental formula	Molecular weight [g/mol]	Theoretical m/z	Measured m/z	Δmass ppm	Adduct
GS2	$C_{10}H_{10}O_2$	162,1852	163.0754	163.0757	1.84	$[M+H]^+$

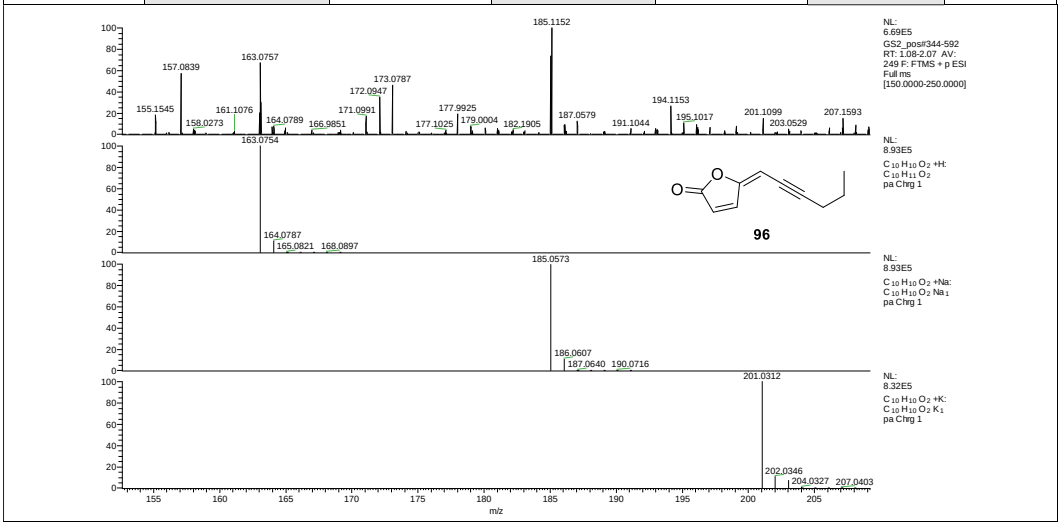

***Figure 124**. ESI-HRMS analyses of (4E)-lachnophyllum lactone, **96**.*

Sample	Elemental formula	Molecular weight [g/mol]	Theoretical m/z	Measured m/z	Δmass ppm	Adduct
GS3	$C_{10}H_8O_2$	160,1693	161.0597	161.0600	1.86	$[M+H]^+$

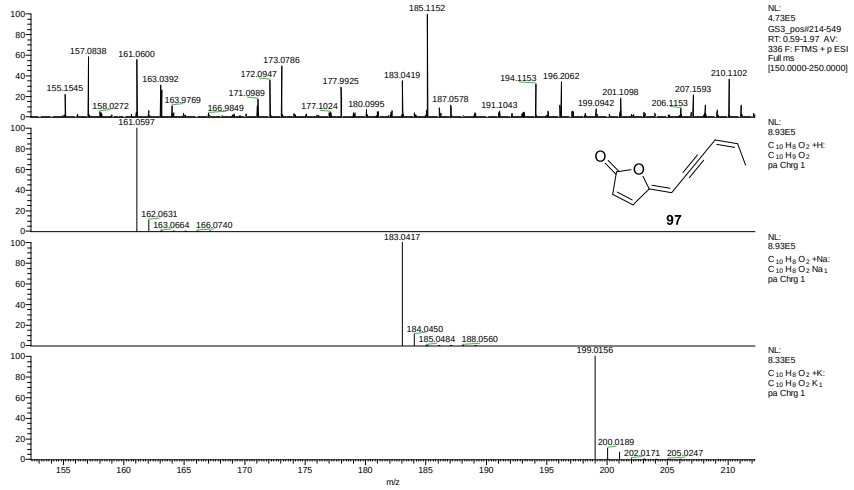

***Figure 125**. ESI-HRMS analyses of (4Z,8Z)-matricaria lactone, **97**.*

5.10 (4*Z*)-Lachnophyllum lactone analogues synthesis

The last step of the developed synthetic strategy towards (4*Z*)-lachnophyllum lactone (**84**), was exploited to obtain several analogues, aiming to gain further understanding into the structural features that impact and define its mode of action. Thus, taking inspiration from some general concepts that could be drawn from hydrocinamic acid SAR study (**Section 5.1**), no hydroxyl derivatizations were performed. Indeed, -OH incorporation has the potential to improve the solubility in water, making the obtained compounds more practical for field use, however, this structural change have a detrimental effect on the activity. A strong correlation between high CLog*p* and inhibition values, might suggest a connection to the selective distribution of these compounds in the hydrophobic environments, such as the lipid bilayer of the membrane. Recent works reported that cinnamic acid and its derivatives can induce alterations in the permeability of the cell membrane[162] and decrease H^+ ATPase activity.[163]

Furthermore, SAR studies on *trans*-cinnamic acid have unveiled structural features affecting the inhibitory activity against *C. campestris* growth. Initially, concerning the degree of side chain unsaturation, a diminished growth-inhibitory activity was observed in phenylpropiolic acid (**66**), characterized by a triple bond, in comparison with *trans*-cinnamic acid (**43**). Conversely, hydrocinnamic acid (**6**), featuring a single bond exhibit a more pronuced and higher activity. These findings underscore the significance of the nature of the C_2-C_3 bond as a pivotal factor influencing growth-inhibitory activity. The just described result jointly with the high availability of commercial terminal alkyne reagents, encouraged toward preparation of analogues deprived of side chain triple bond.

Additionally, the inhibitory activity of compounds isolated from *C. cineraria* against broomrape radicle growth, revealed some structure-activity relationships (SAR). Among these, the crucial one is the importance of the double bond in the α,β-unsaturated lactone ring of the sesquiterpene lactones, and its key role in the broomrape inhibition, determining the poor activity of 11β,13-dihydrosalonitenolide (**82**) in comparison with the results obtained by testing other compounds.[203] Depending on their electronic properties, the α,β-unsaturated carbonyl functionalities exhibit a wide range of reactivities, namely oxidation, Michael addition, radical scavenging or double bond isomerization. The alteration of the α-position within the α,β-unsaturated carbonyl system, a concept not extensively explored, has

the potential to yield new and highly interesting derivatives. In the context of drug development, irreversible binding within the active sites has proven to be one answer to drug resistance in cancer treatment. In general, natural products containing the α,β-unsaturated carbonyl unit showed diverse biological activities that could be translated into innovative pharmaceutical agents.[222,223] Hence, the incorporation of this system in a larger cycle (δ-lactone) to observe the influence on the mode of action, was performed too.

The idea of synthesizing (4*Z*)-lachnophyllum lactone analogues, featuring longer or even shorter alkyl chain, was inspired by some insights obtained by the same work. Specifically, the comparison of hydrocinnamic acid ethyl ester (**41**) and compound **6** revealed similar IC_{50} values despite significant differences in CLog*p*. This observation suggested that neither the lipophilicity or the acidity of the compounds seems to influence their bioactivity when tested against broomrapes.

Finally, from a parallel study, aimed to compared the yield and selectivity of different catalysts, when used in last step of (4*Z*)-lachnophyllum lactone (**84**) preparation, it was evident that bis(triphenylphosphine)palladium(II) diacetate ($Pd(OAc)_2(PPh_3)_2$) catalyst, was characterized by lower yield and less selectivity. The reaction yield, using the just mentioned catalyst, resulted to be, as general trend, 50 % for the *Z*-γ-lactone, 20 % for the *E*-γ-lactone and 20 % for the δ-lactone. Although, further studies are needed, this experimental evidence was exploited, using the aforementioned catalyst, for a faster production of multiple analogues. Specifically, in most reactions, the δ-lactone and two γ-lactone isomers were obtained. The partners of the cyclization reaction are the 3-*Z*-iodoacrylic acid (**95**) and different terminal alkynes (**Scheme 4, Figure 21**), leading to the formation of compounds deprived of the triple bond on the side chain. A total of seventeen analogues of compound **84** were prepared (**Figure 126-183**) and the bioassays are in progress, to evaluate the role of the side chain unsaturation, length and the lactone dimension.

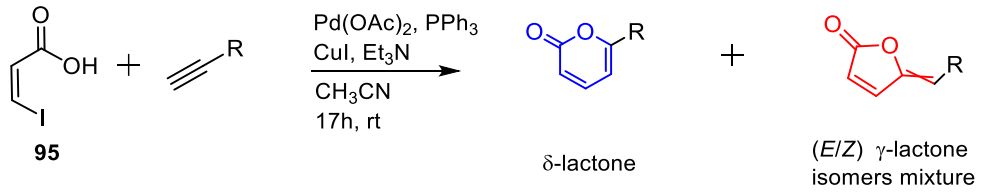

Scheme 4. Analogues synthesis of (4*Z*)-lachnophyllum lactone general synthetic procedure.

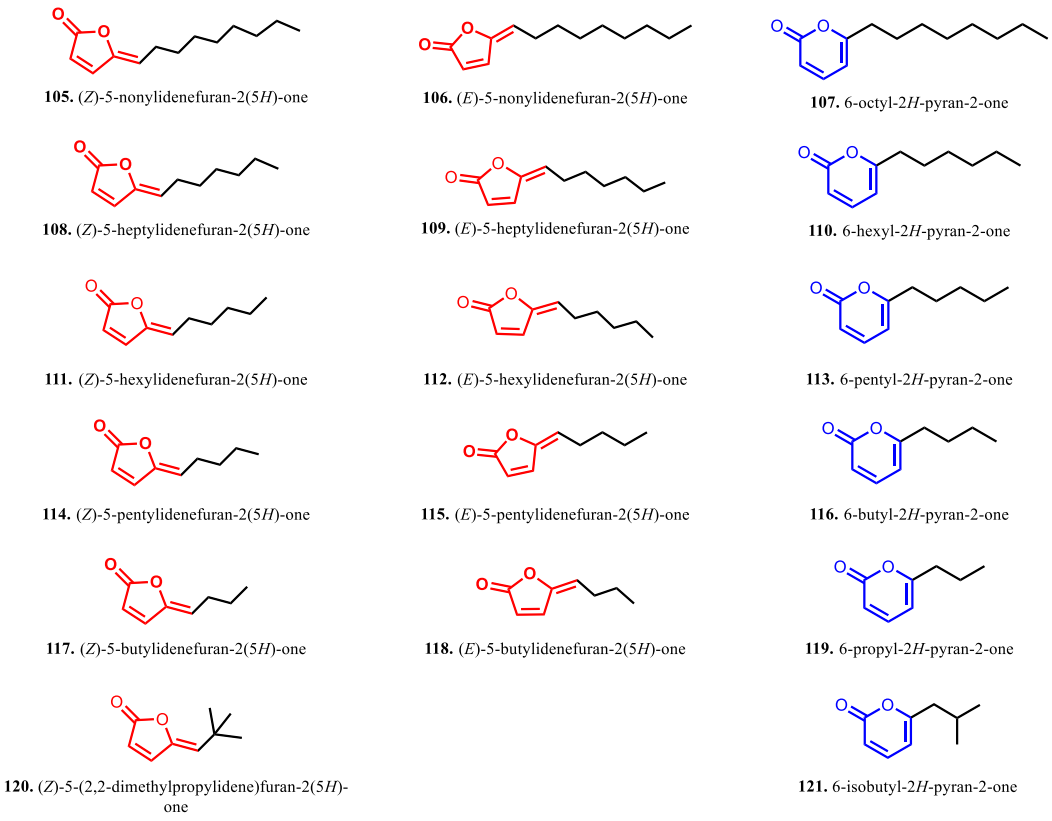

Figure 126. (4*Z*)-Lachnophyllum lactone synthetic analogues.

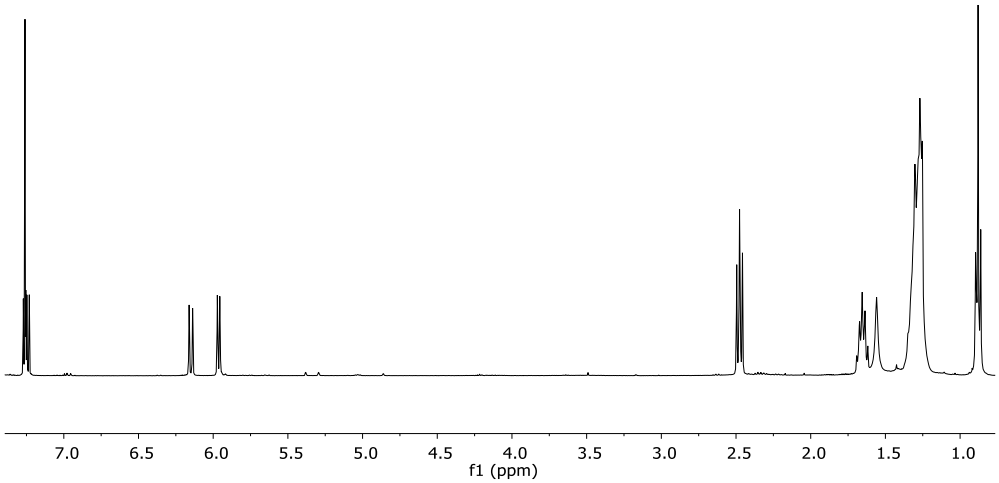

Figure 127. ^{1}H NMR spectra**.** 6-octyl-2H-pyran-2-one (**107**) *($CDCl_3$, 400 MHz).*

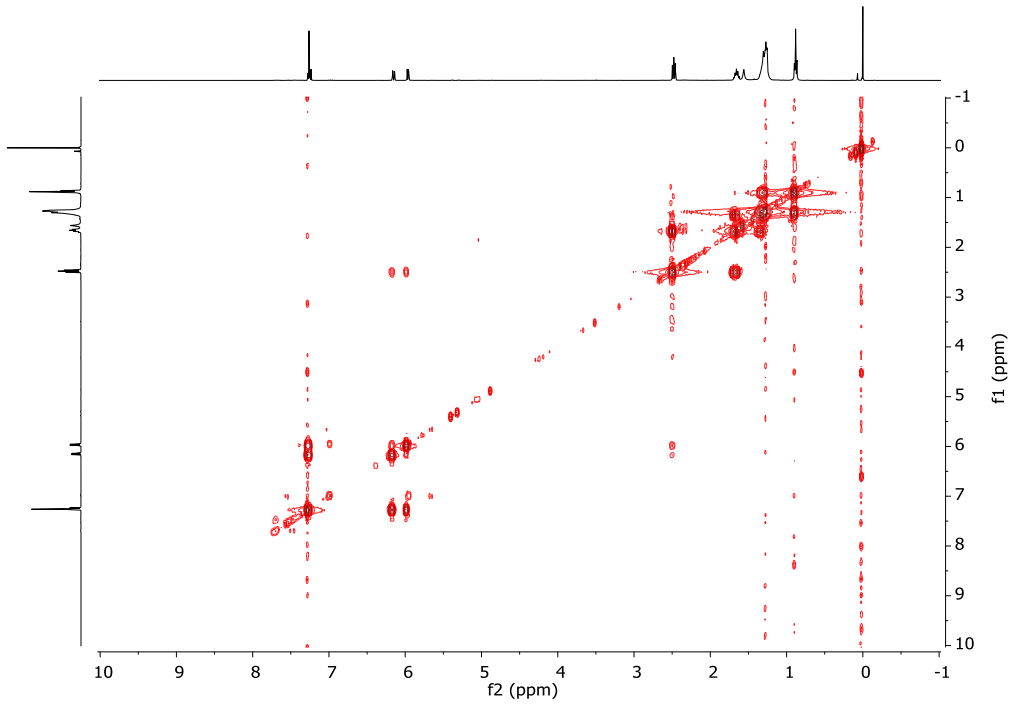

Figure 128. COSY spectra of 6-octyl-2H-pyran-2-one (**107**) (*$CDCl_3$).*

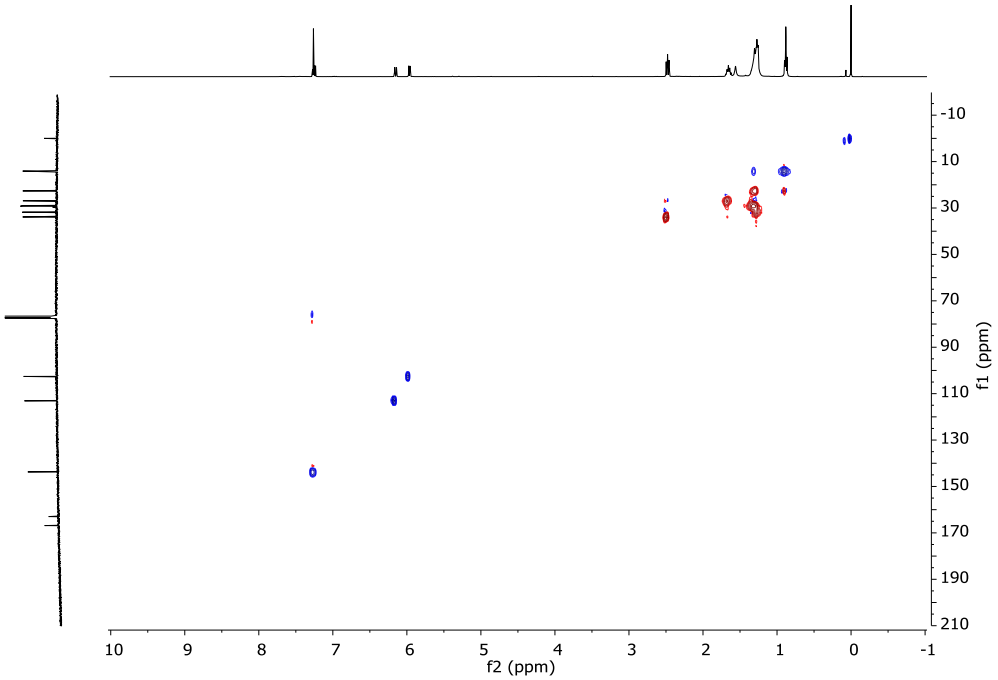

Figure 129. HSQC spectra of 6-octyl-2H-pyran-2-one (**107**) ($CDCl_3$).

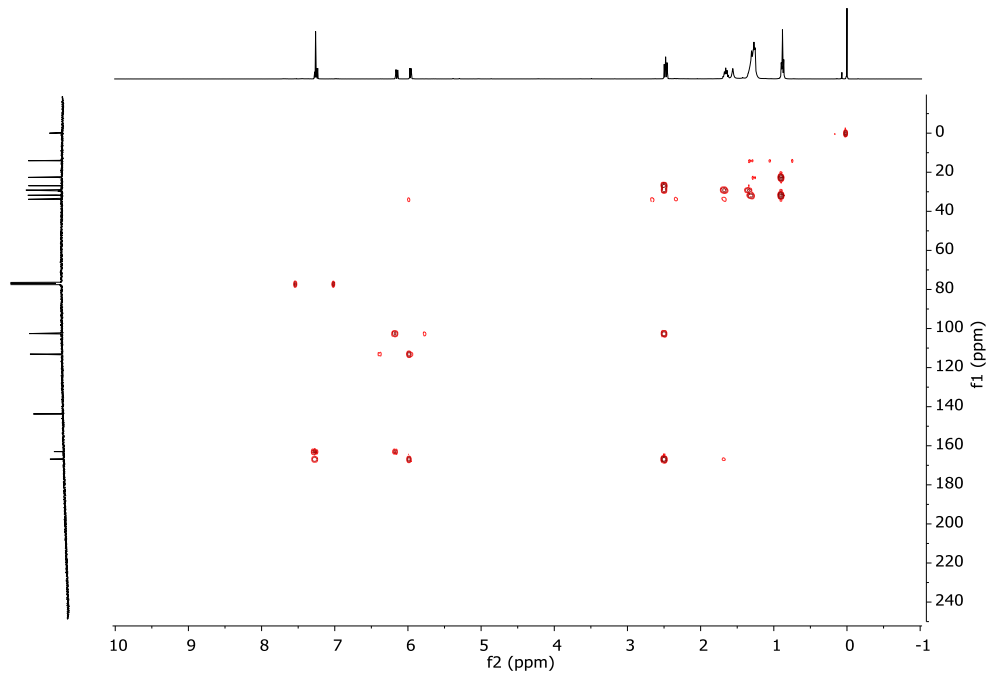

Figure 130. HMBC spectra of 6-octyl-2H-pyran-2-one (**107**) ($CDCl_3$).

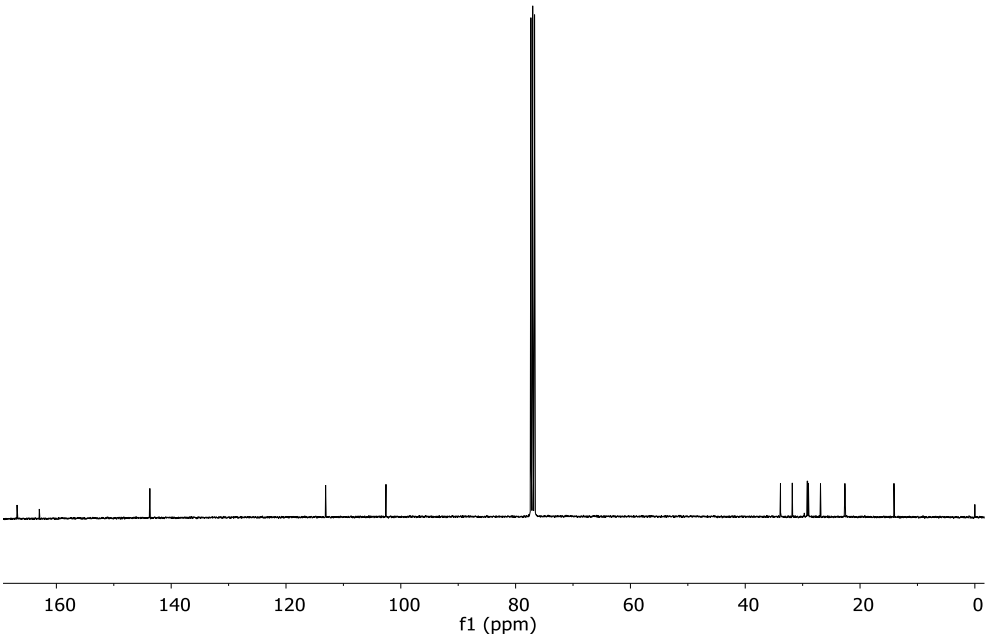

Figure 131. ^{13}C NMR spectra of 6-octyl-2H-pyran-2-one (**107**), *(CDCl₃, 100 MHz).*

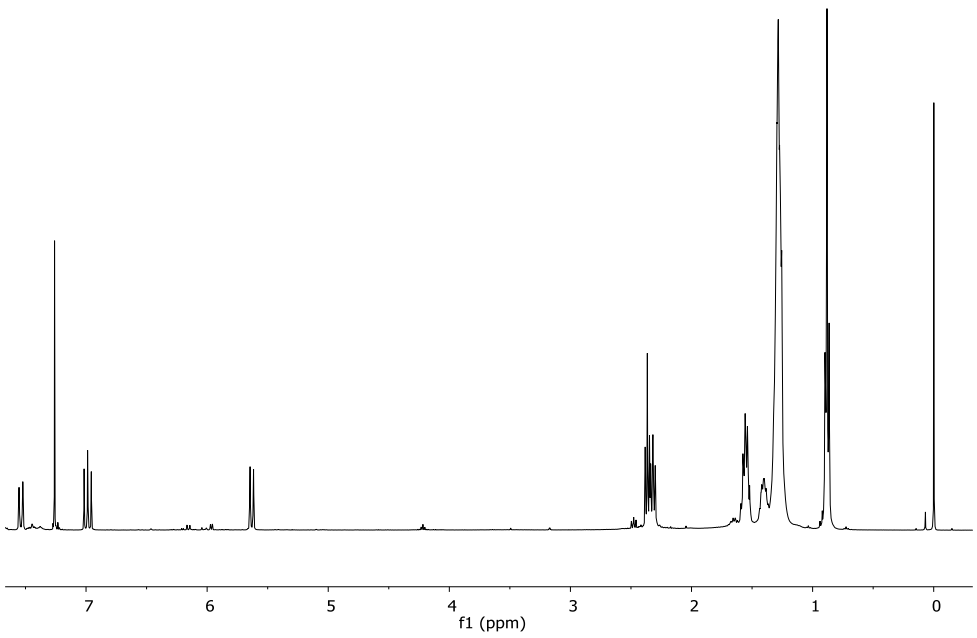

Figure 132. ^{1}H NMR spectra of (*Z*)-5-nonylidenefuran-2(5H)-one, (**105**), *(CDCl₃, 400 MHz).*

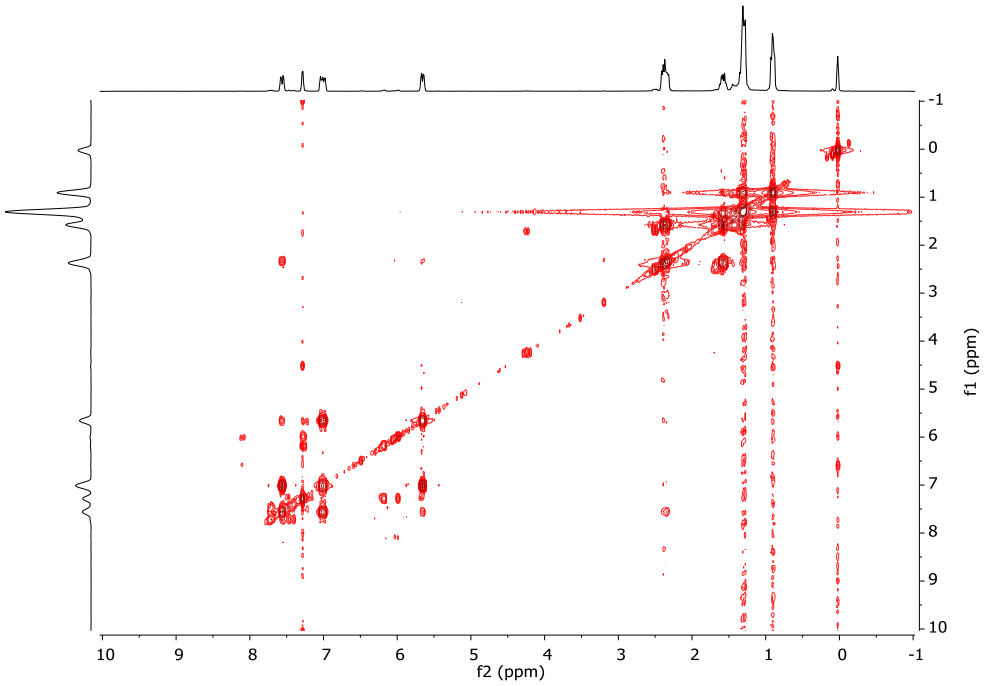

Figure 133. COSY spectra of (*Z*)-5-nonylidenefuran-2(5H)-one, (**105**), *(CDCl₃).*

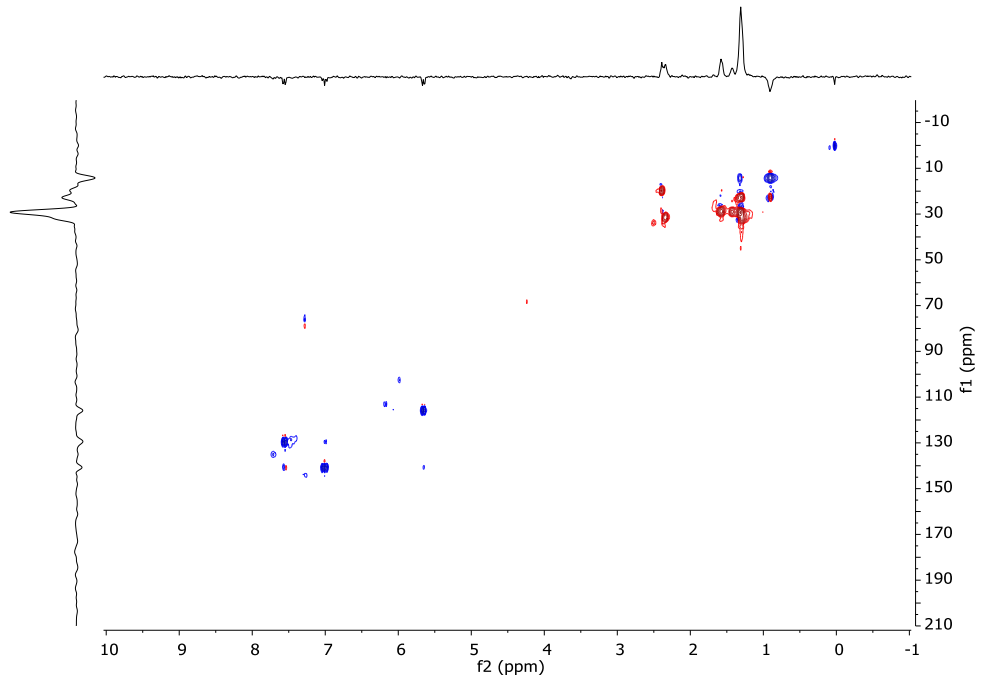

Figure 134. HSQC spectra of (*Z*)-5-nonylidenefuran-2(5H)-one, (**105**), *(CDCl₃).*

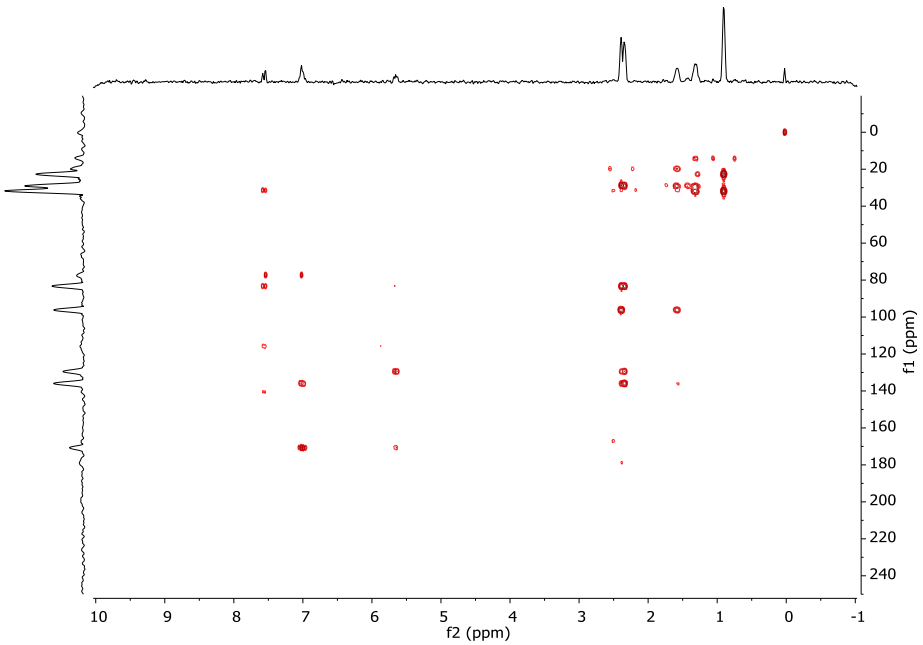

Figure 135. HMBC spectra of (*Z*)-5-nonylidenefuran-2(5H)-one, (**105**), *(CDCl₃).*

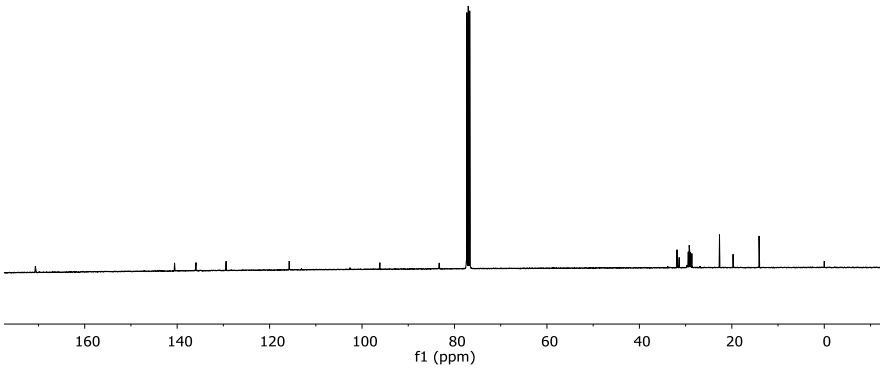

Figure 136. ^{13}C spectra of (*Z*)-5-nonylidenefuran-2(5H)-one, (**105**), *(CDCl₃, 100 MHz).*

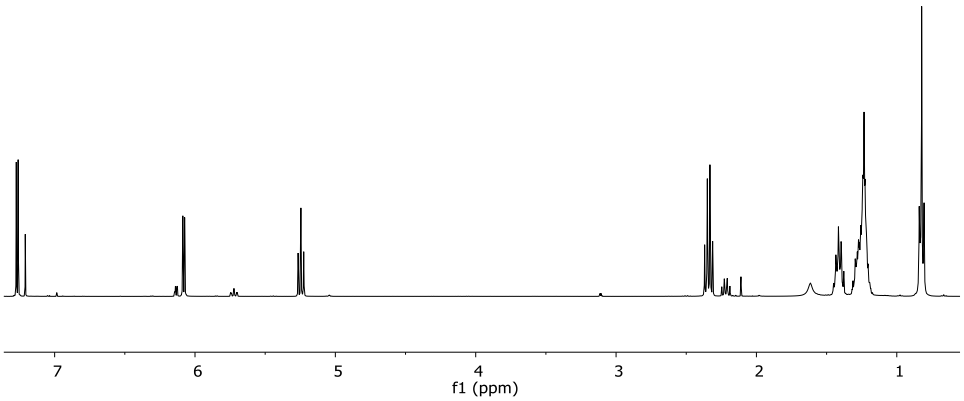

Figure 137. ^{1}H NMR spectra of (*Z*)-5-heptylidenefuran-2(5H)-one, (**108**), *(CDCl₃, 400 MHz).*

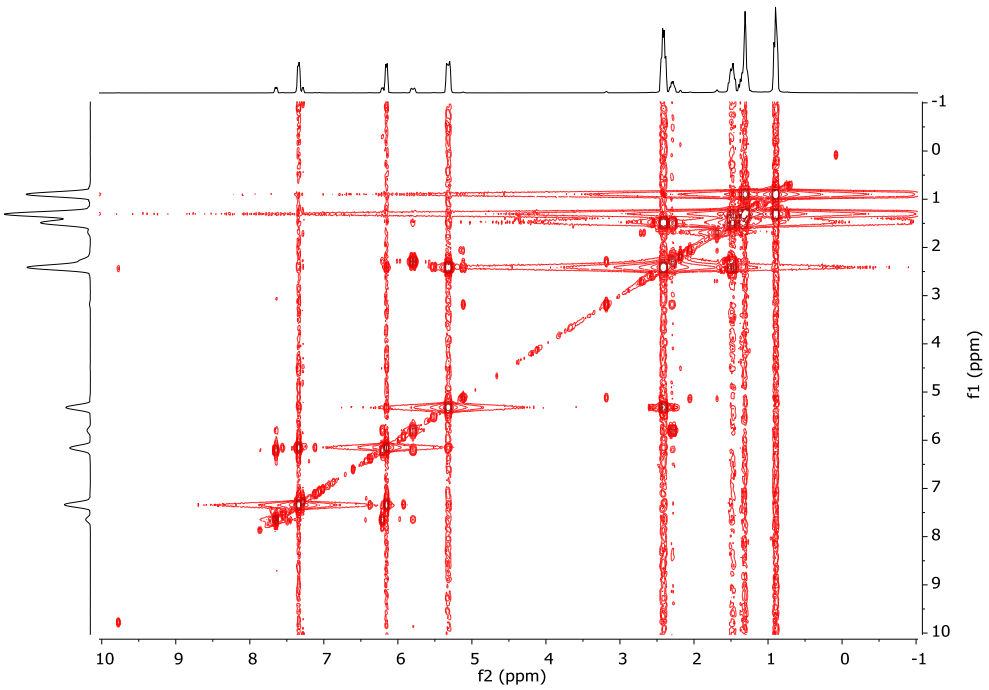

Figure 138. COSY spectra of (*Z*)-5-heptylidenefuran-2(5H)-one, (**108**), *(CDCl₃).*

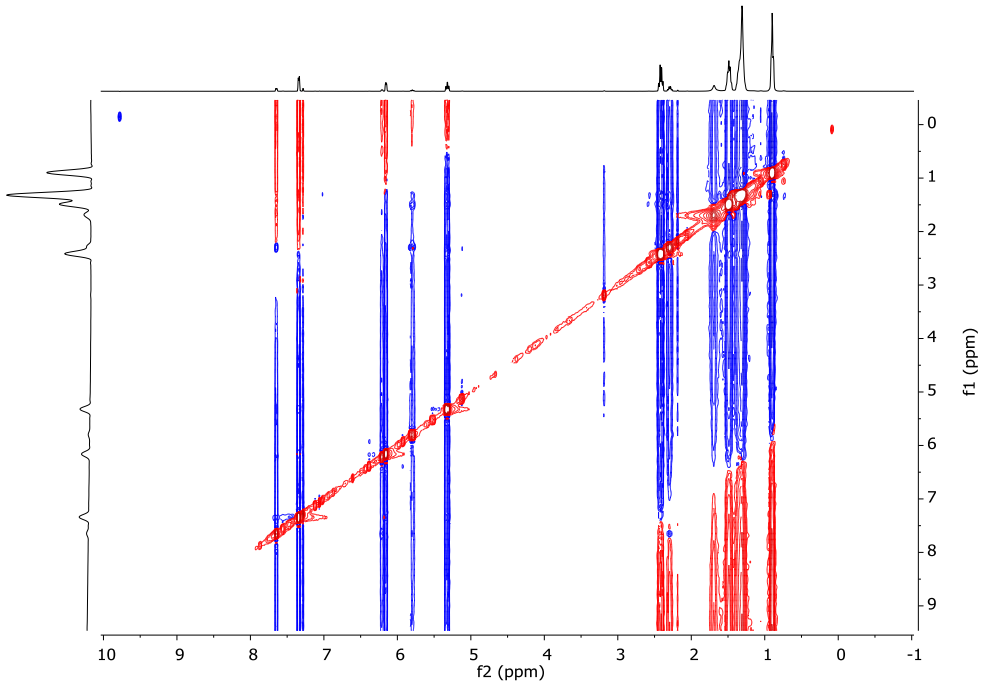

Figure 139. NOESY spectra of (*Z*)-5-heptylidenefuran-2(5H)-one, (**108**), *(CDCl₃).*

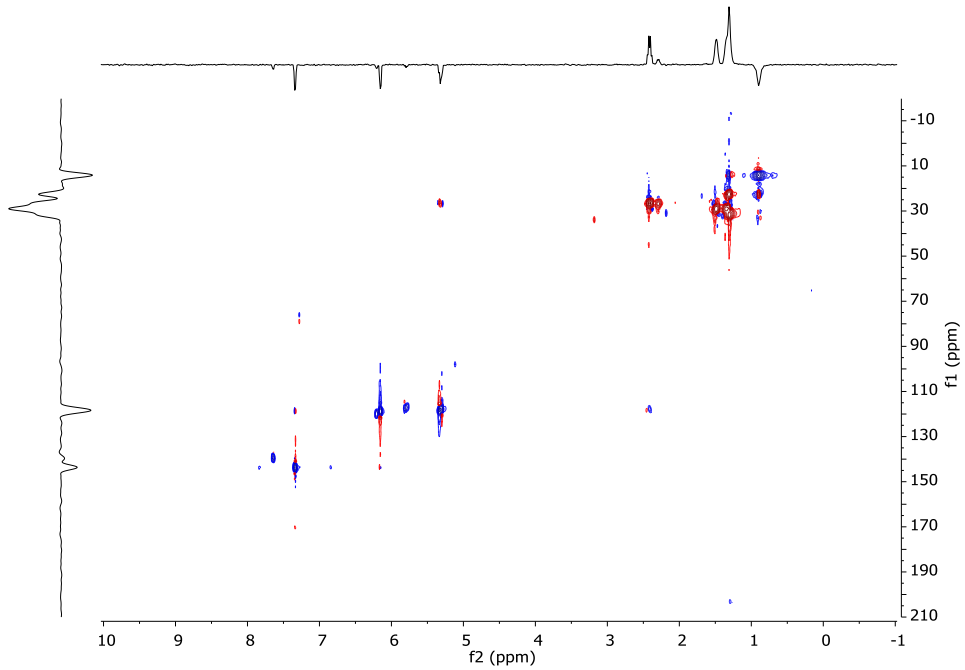

Figure 140. HSQC spectra of (*Z*)-5-heptylidenefuran-2(5H)-one, (**108**), *(CDCl₃).*

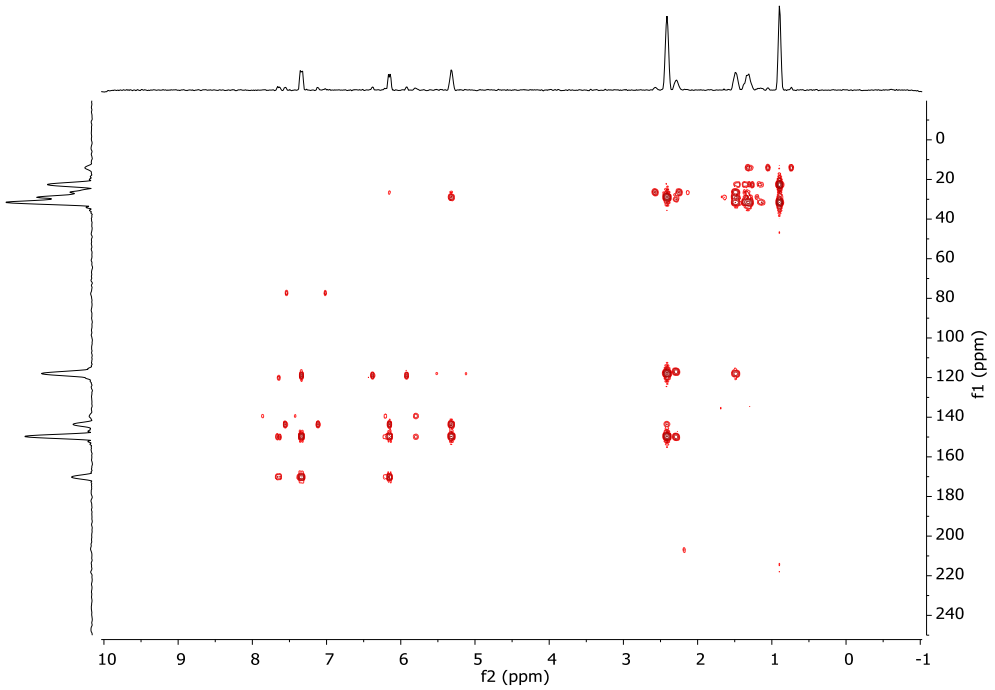

Figure 141. HMBC spectra of (*Z*)-5-heptylidenefuran-2(5H)-one, (**108**), *($CDCl_3$).*

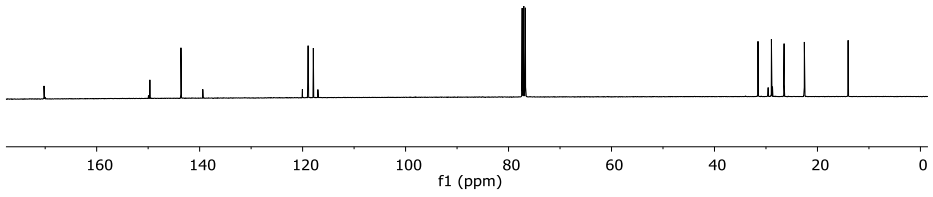

Figure 142. ^{13}C NMR spectra of (*Z*)-5-heptylidenefuran-2(5H)-one, (**108**), *($CDCl_3$, 100 MHz).*

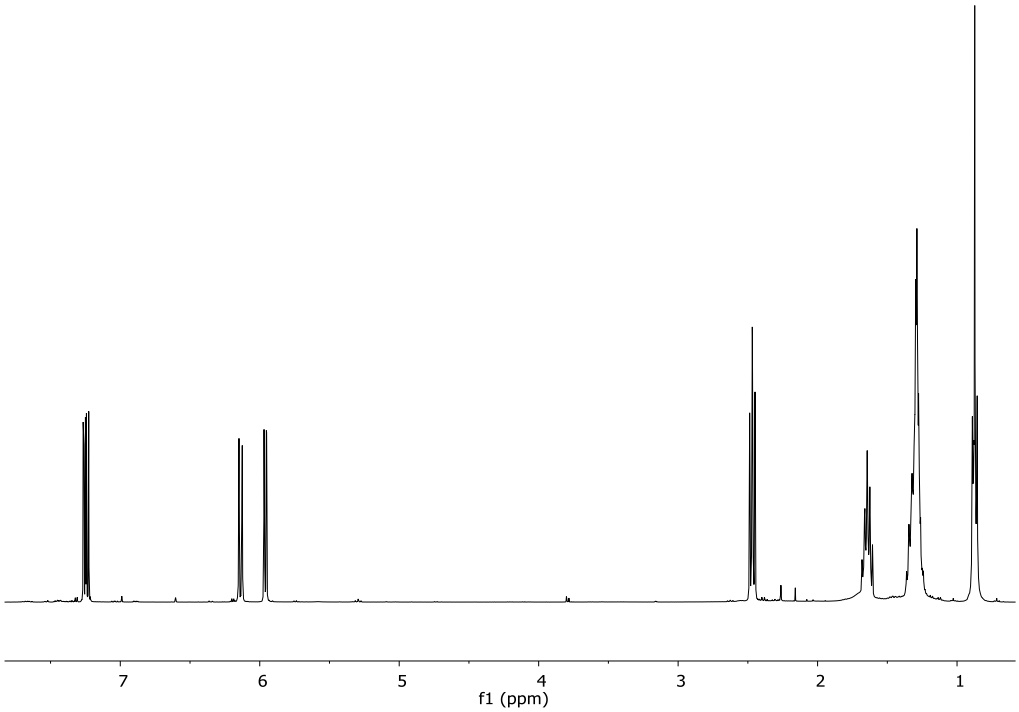

Figure 143. [1]H NMR spectra of 6-hexyl-2H-pyran-2-one, (**110**), *(CDCl₃, 400 MHz).*

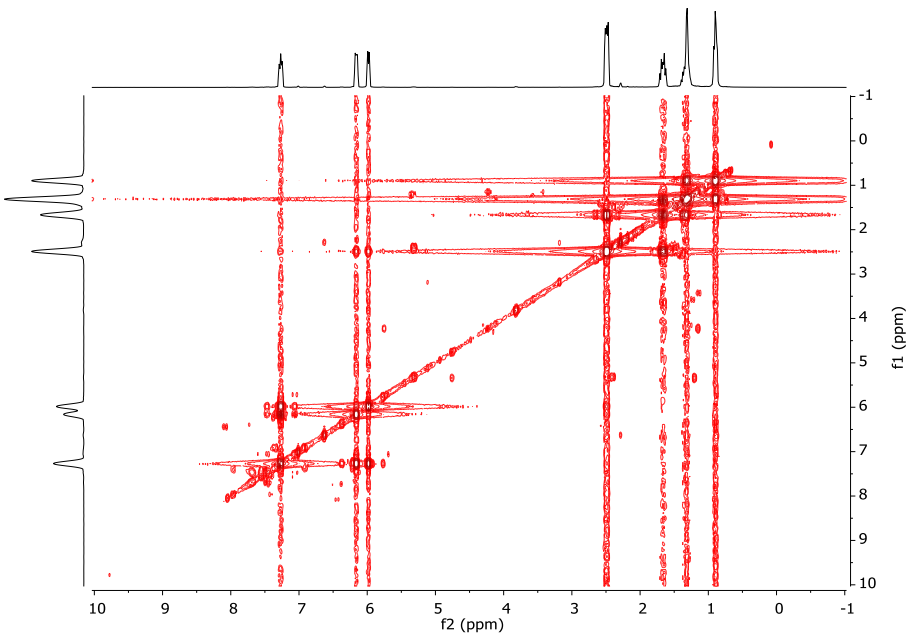

Figure 144. COSY spectra of 6-hexyl-2H-pyran-2-one, (**110**), *(CDCl₃).*

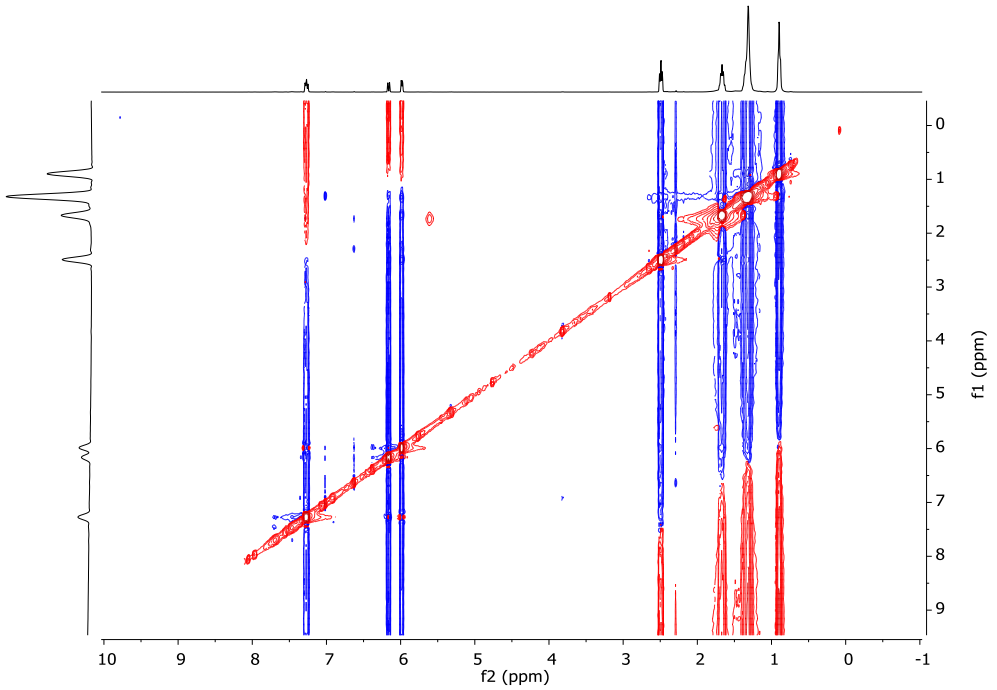

Figure 145. NOESY spectra of 6-hexyl-2H-pyran-2-one, (**110**), *($CDCl_3$).*

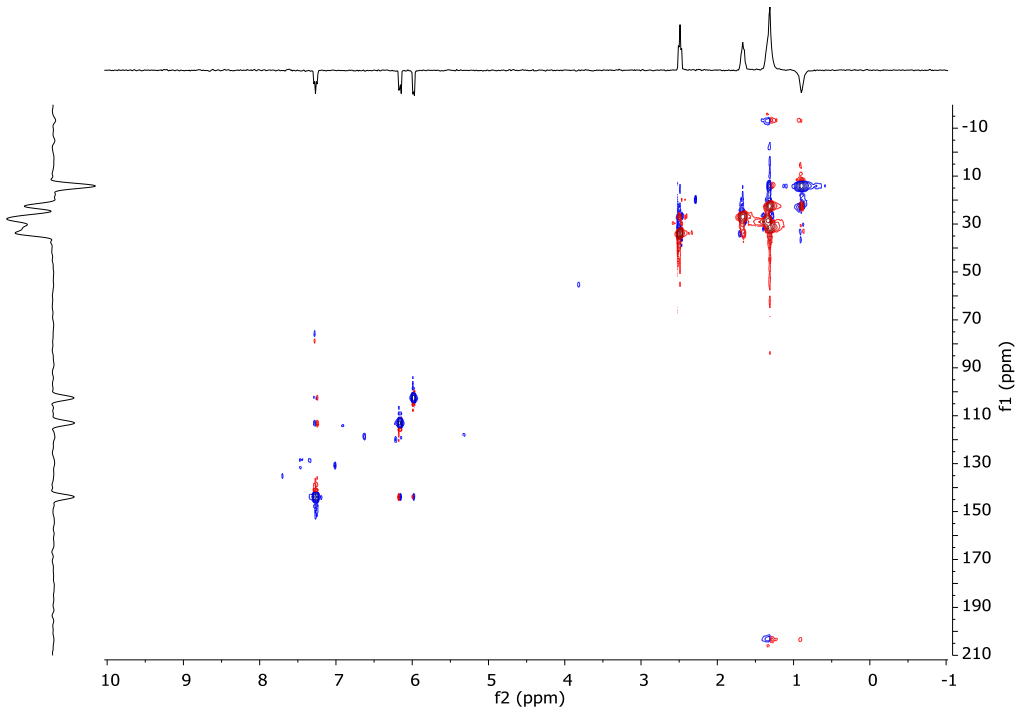

Figure 146. HSQC spectra of 6-hexyl-2H-pyran-2-one, (**110**), *($CDCl_3$).*

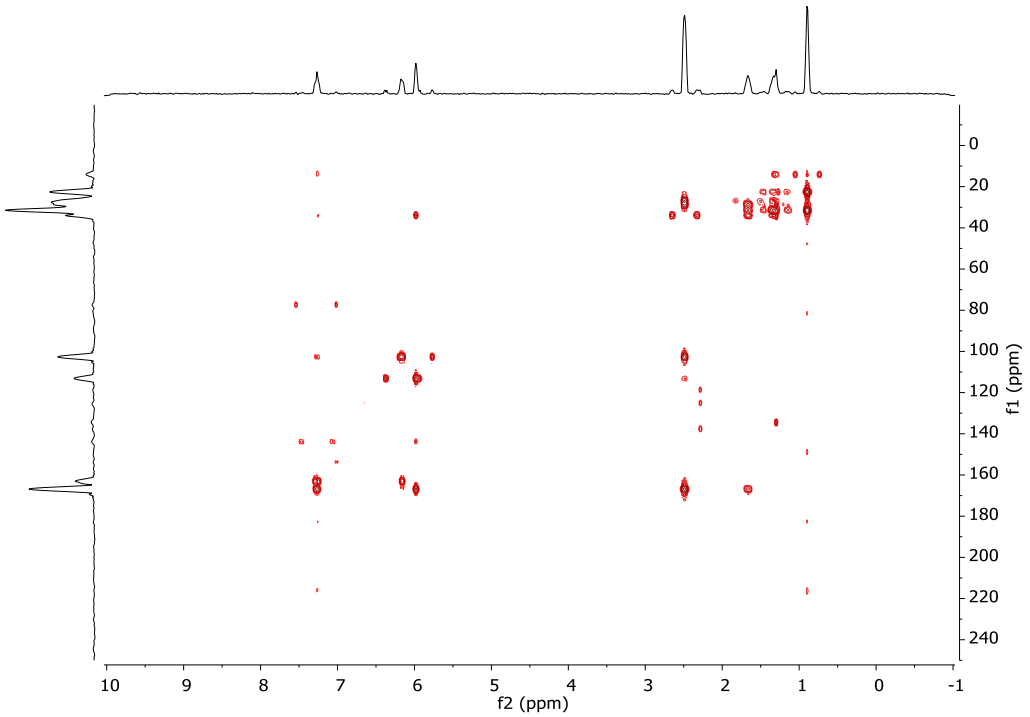

Figure 147. HMBC spectra of 6-hexyl-2H-pyran-2-one, (**110**), *(CDCl₃).*

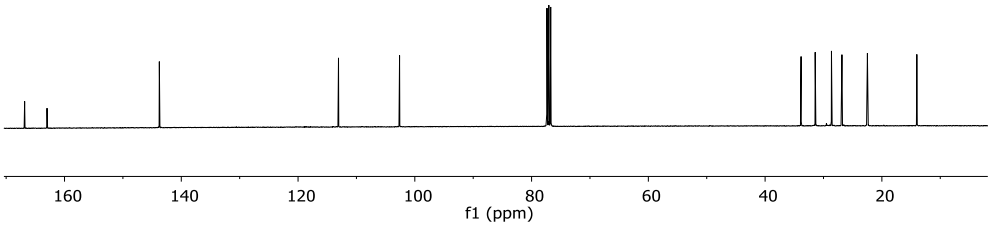

Figure 148. ^{13}C spectra of 6-hexyl-2H-pyran-2-one, (**110**), *(CDCl₃, 100 MHz).*

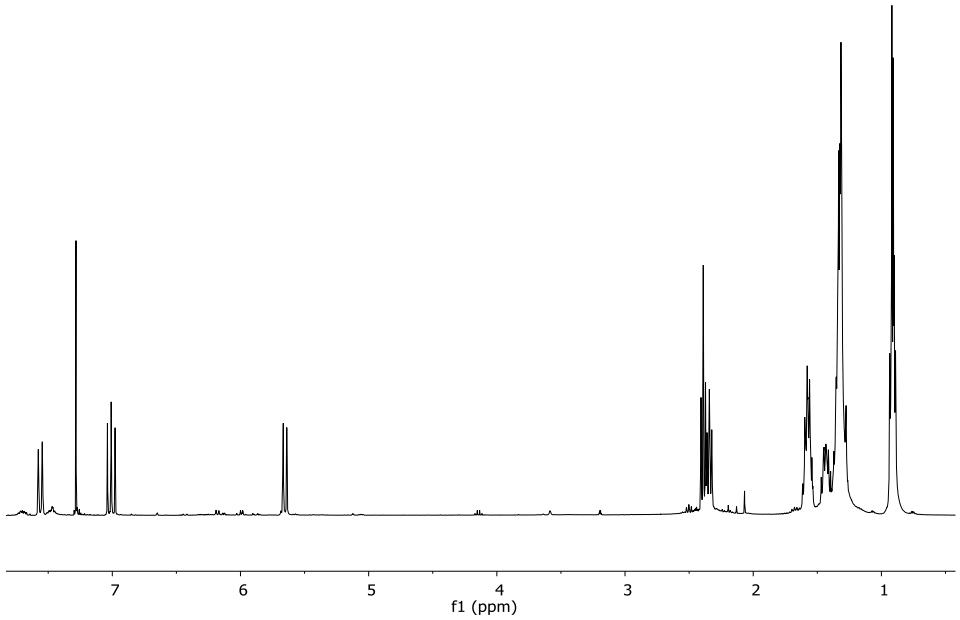

Figure 149. ^{1}H NMR spectra of (*E*)-5-heptylidenefuran-2(5H)-one, (**109**), *(CDCl₃, 400 MHz).*

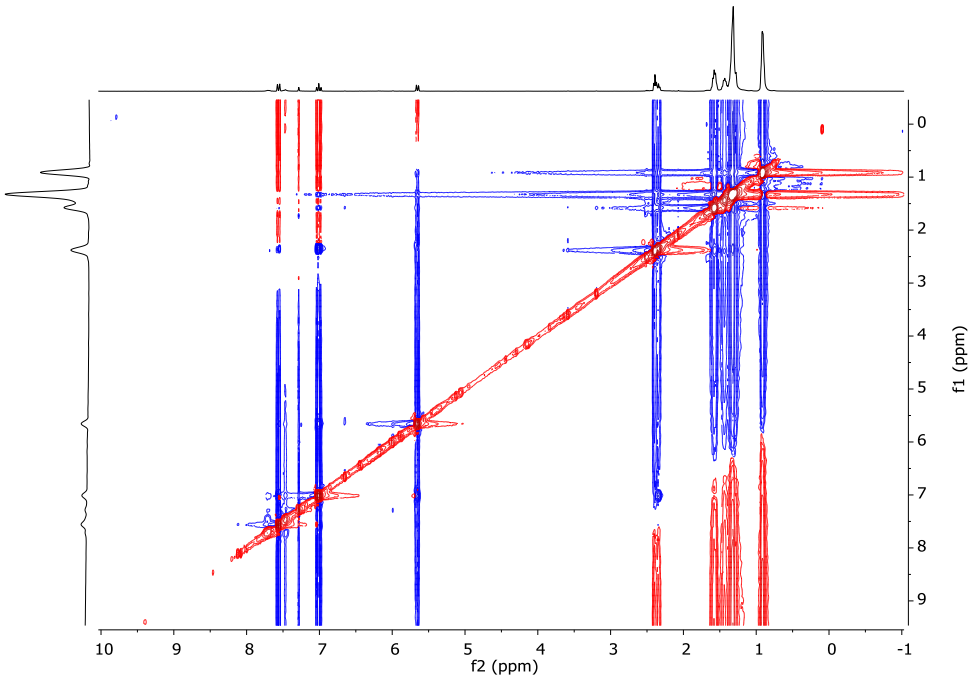

Figure 150. COSY spectra of (*E*)-5-heptylidenefuran-2(5H)-one, (**109**), *(CDCl₃).*

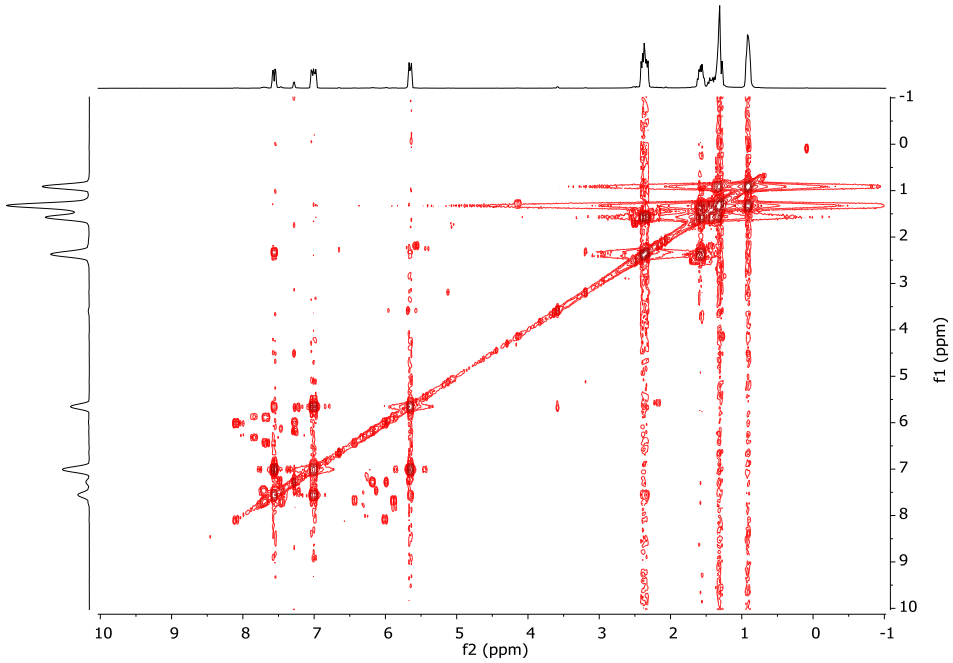

Figure 151. NOESY spectra of (*E*)-5-heptylidenefuran-2(5H)-one, (**109**), *(CDCl₃).*

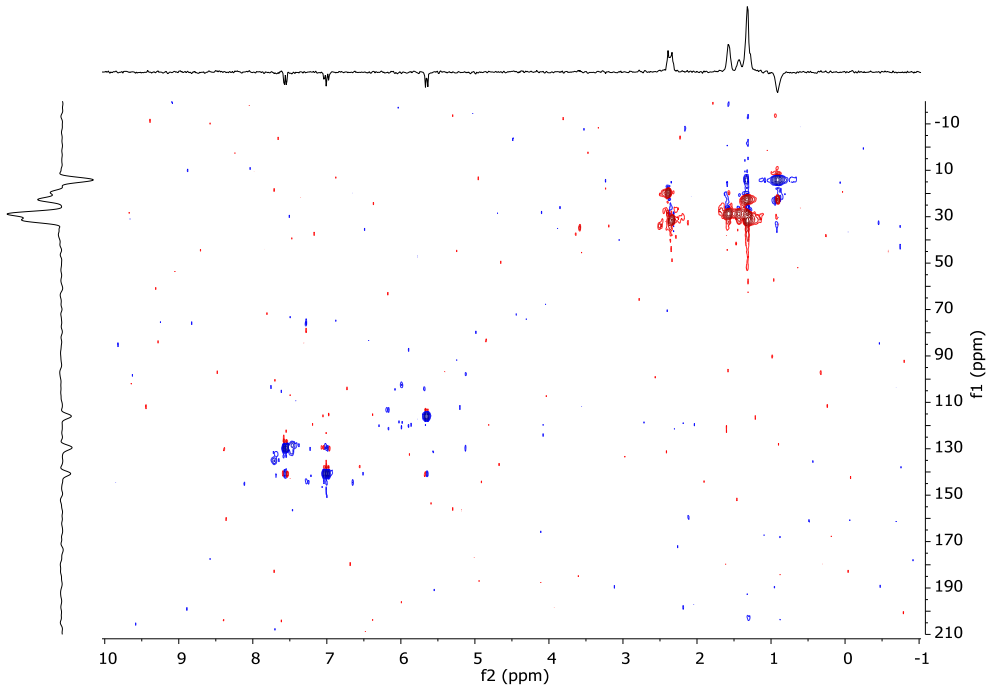

Figure 152. HSQC spectra of (*E*)-5-heptylidenefuran-2(5H)-one, (**109**), *(CDCl₃).*

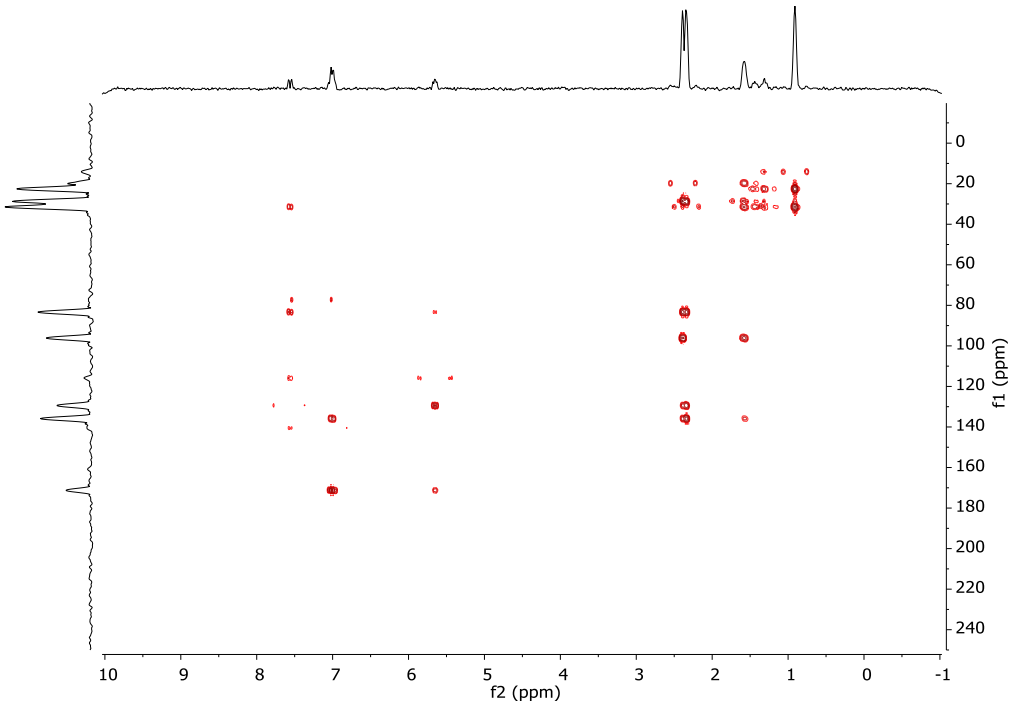

Figure 153. HMBC spectra of (*E*)-5-heptylidenefuran-2(5H)-one, (**109**), *(CDCl₃).*

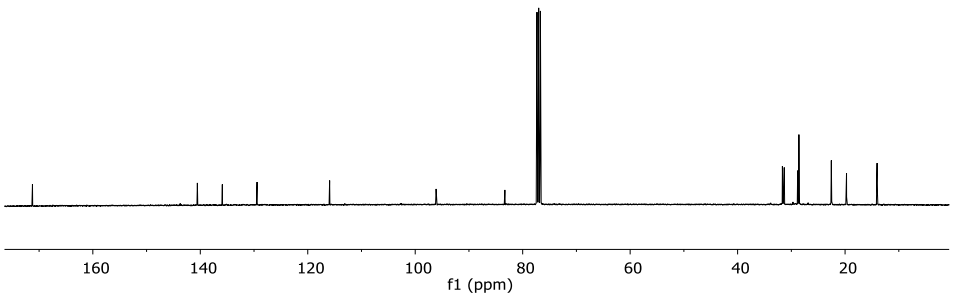

Figure 154. ^{13}C NMR spectra of (*E*)-5-heptylidenefuran-2(5H)-one, (**109**), *(CDCl₃, 100 MHz).*

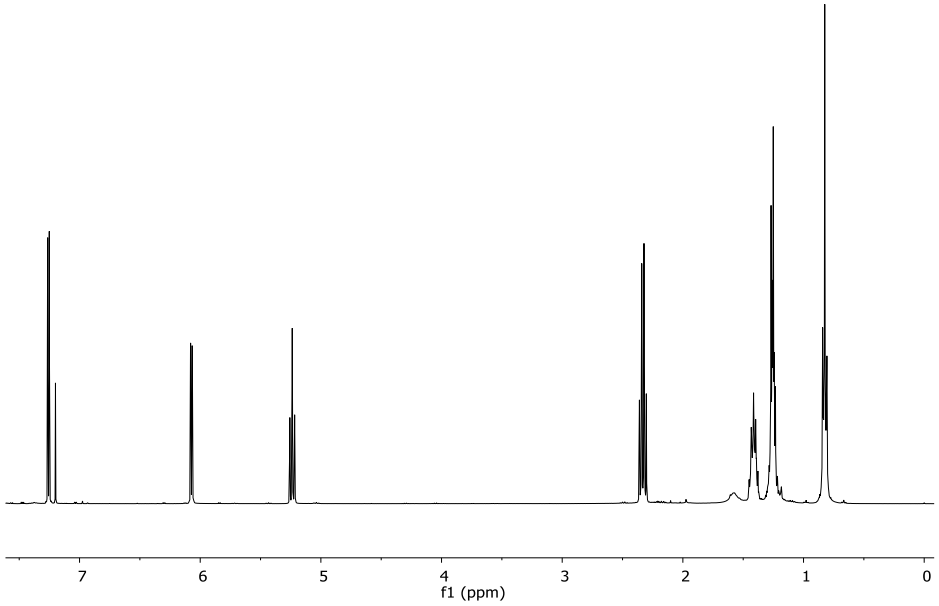

Figure 155. ^{1}H NMR spectra of (Z)-5-hexylidenefuran-2(5H)-one, (**111**), *($CDCl_3$, 400 MHz).*

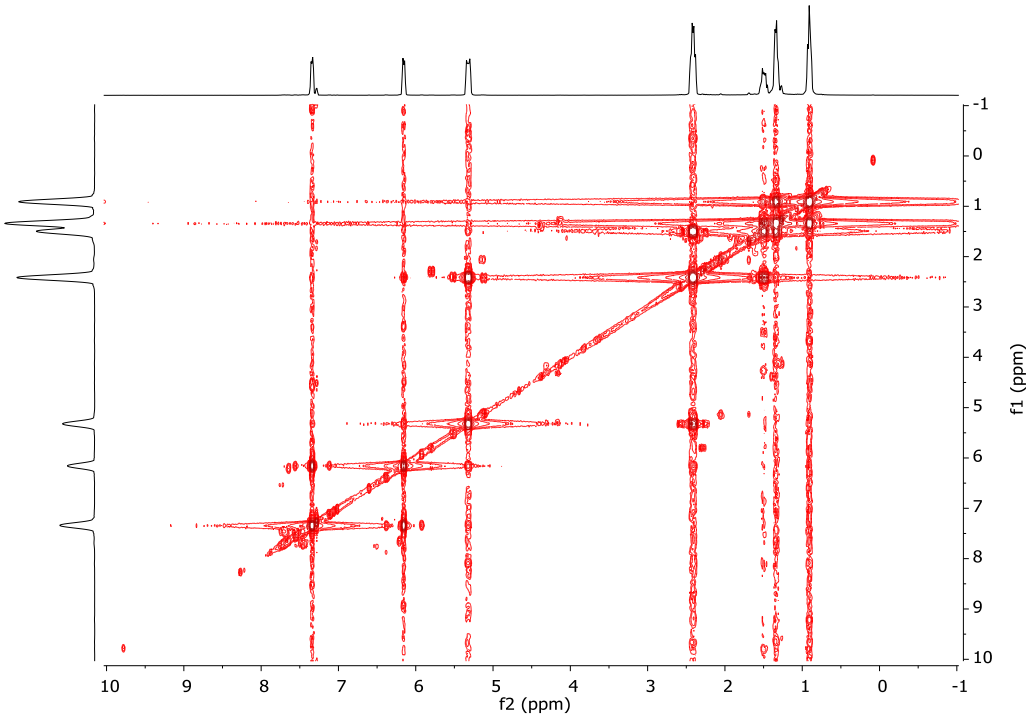

Figure 156. COSY spectra of (Z)-5-hexylidenefuran-2(5H)-one, (**111**), *($CDCl_3$).*

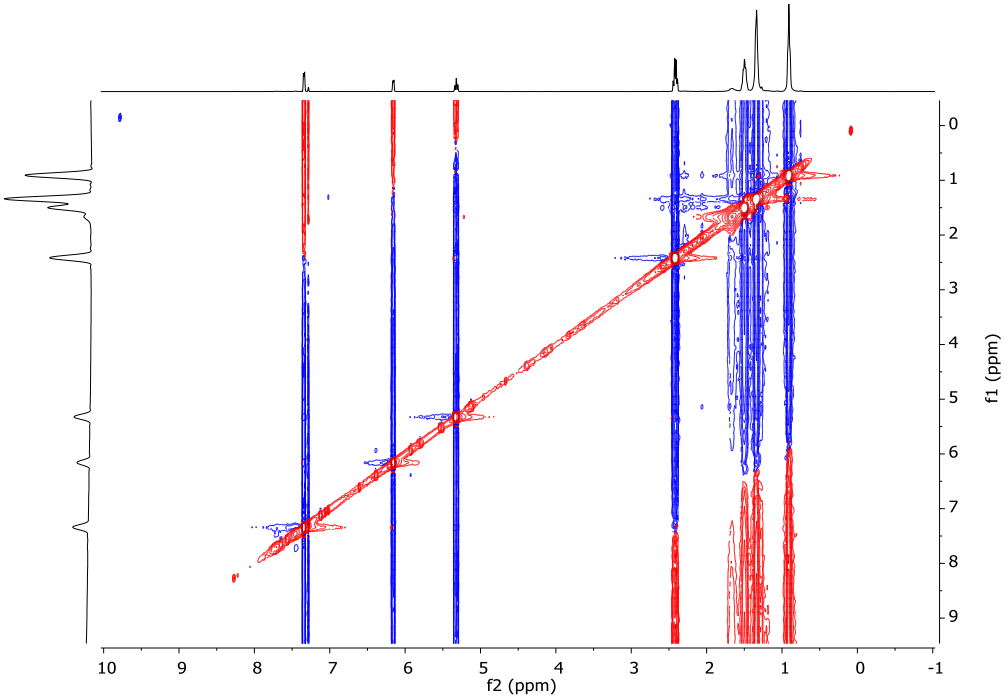

Figure 157. NOESY spectra of (Z)-5-hexylidenefuran-2(5H)-one, (**111**), *($CDCl_3$).*

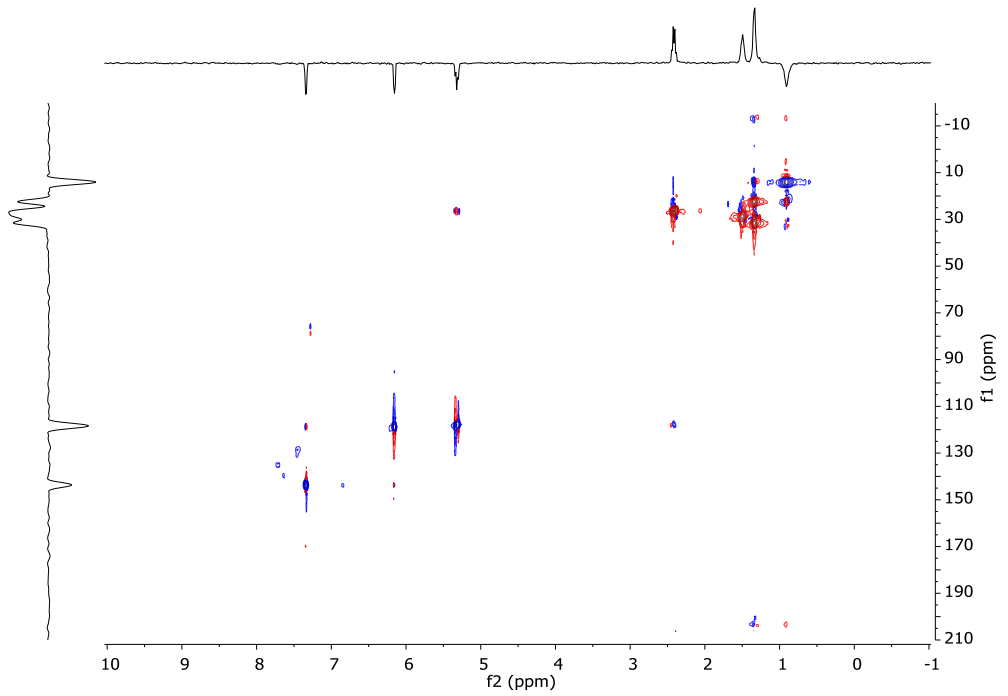

Figure 158. HSQC spectra of (Z)-5-hexylidenefuran-2(5H)-one, (**111**), *($CDCl_3$).*

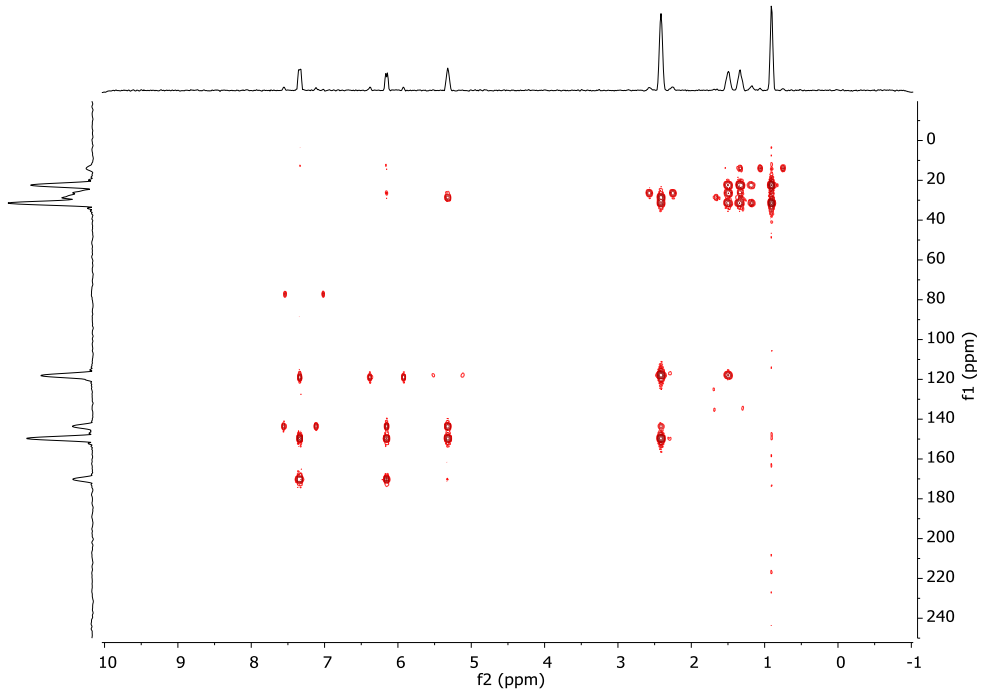

Figure 159. HMBC spectra of (Z)-5-hexylidenefuran-2(5H)-one, (**111**), *(CDCl₃).*

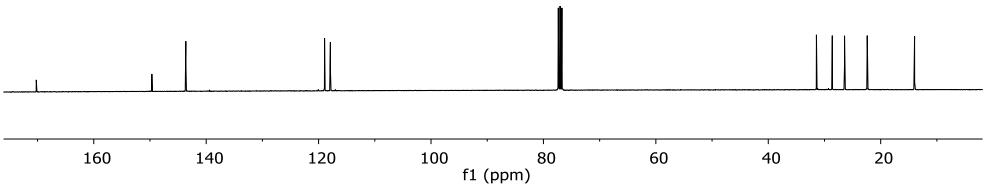

Figure 160. ^{13}C NMR spectra of (Z)-5-hexylidenefuran-2(5H)-one, (**111**), *(CDCl₃, 100 MHz).*

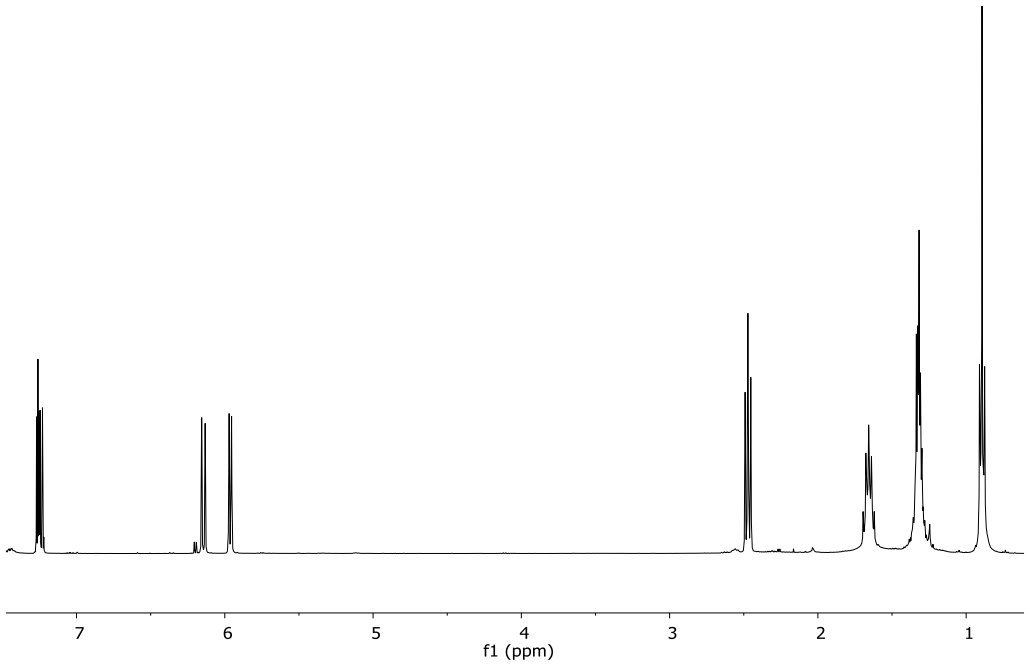

Figure 161. ^{1}H NMR spectra of 6-pentyl-2H-pyran-2-one, (**113**), *($CDCl_3$, 400 MHz)*.

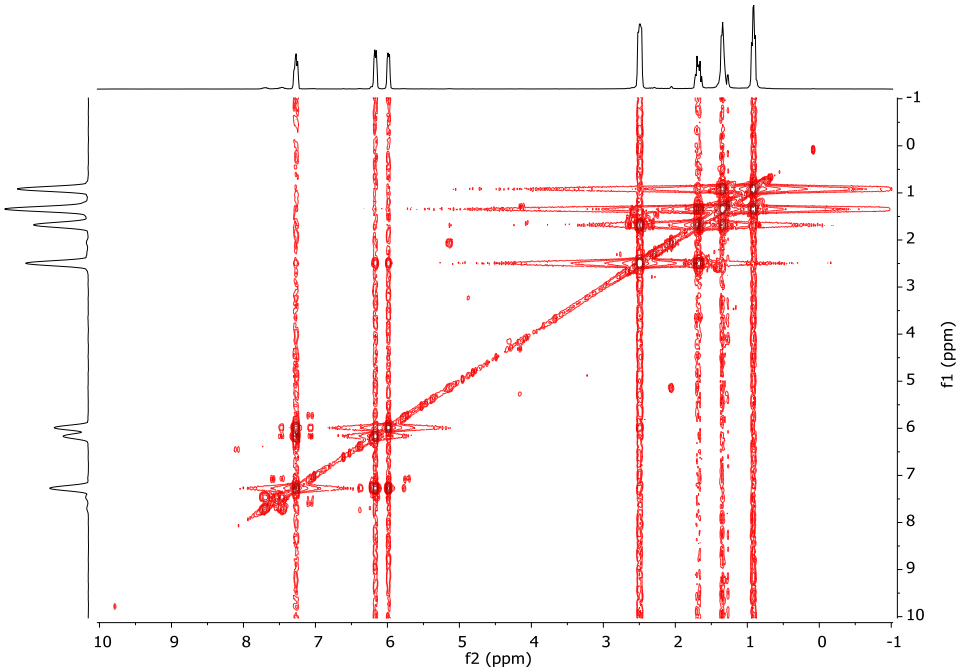

Figure 162. COSY spectra of 6-pentyl-2H-pyran-2-one, (**113**), *($CDCl_3$)*.

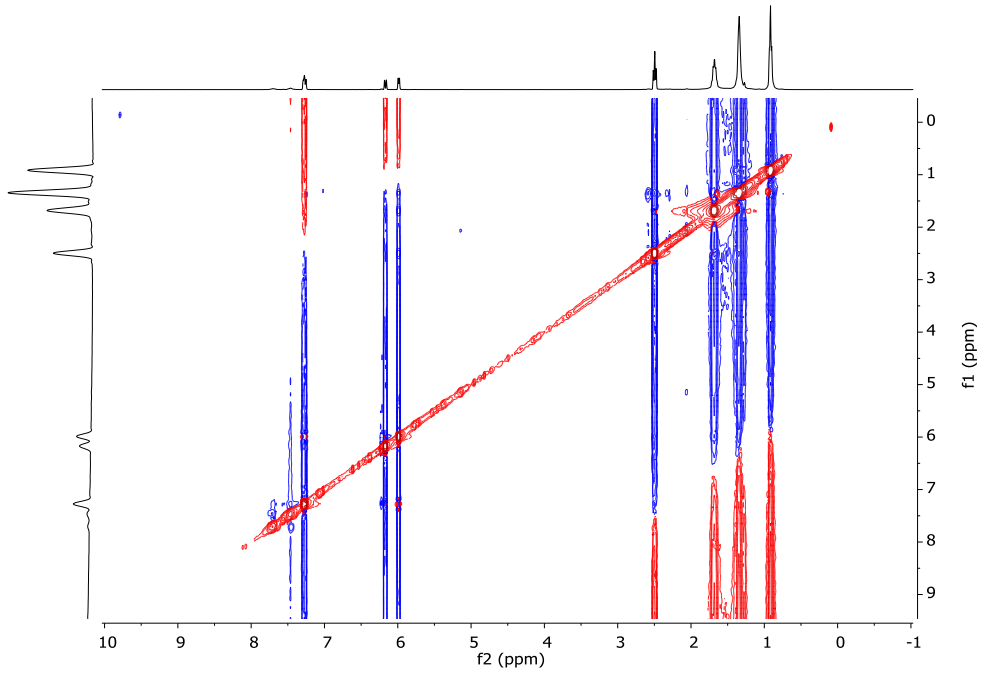

Figure 163. NOESY spectra of 6-pentyl-2H-pyran-2-one, (**113**), *(CDCl₃)*.

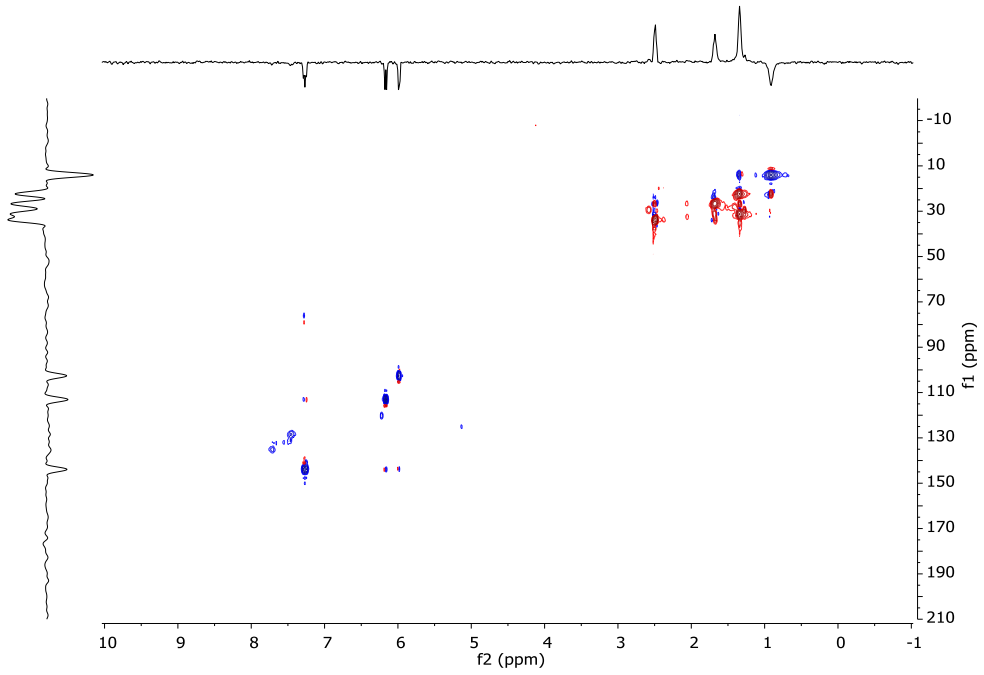

Figure 164. HSQC spectra of 6-pentyl-2H-pyran-2-one, (**113**), *(CDCl₃)*.

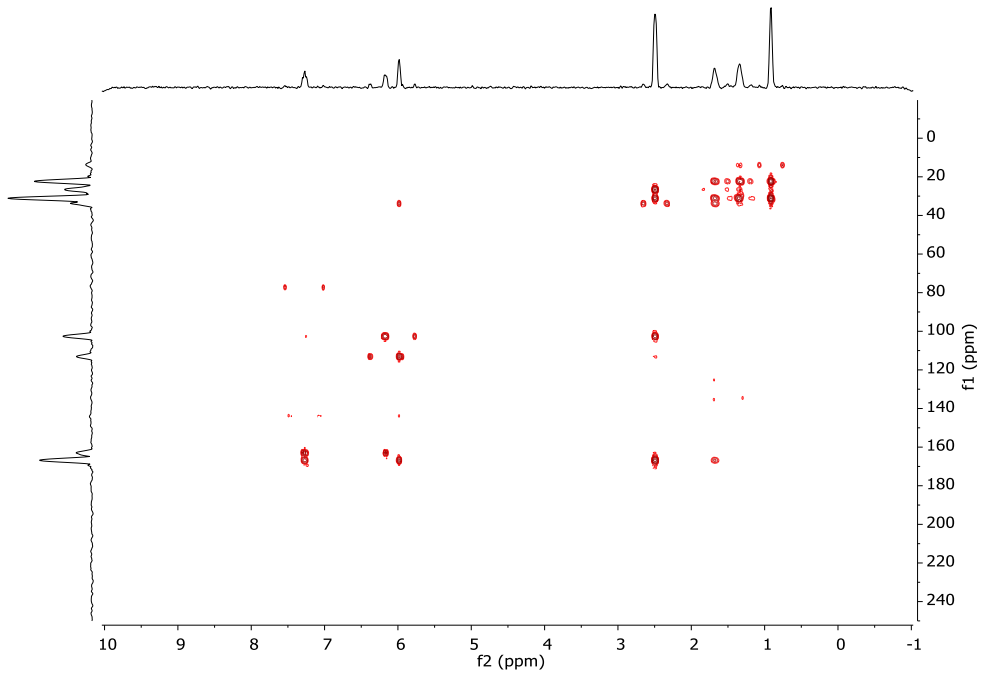

Figure 165. HMBC spectra of 6-pentyl-2H-pyran-2-one, (**113**), *($CDCl_3$).*

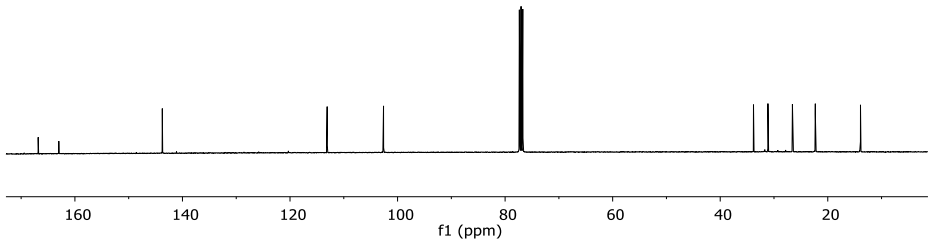

Figure 166. ^{13}C NMR spectra of 6-pentyl-2H-pyran-2-one, (**113**), *($CDCl_3$, 150 MHz).*

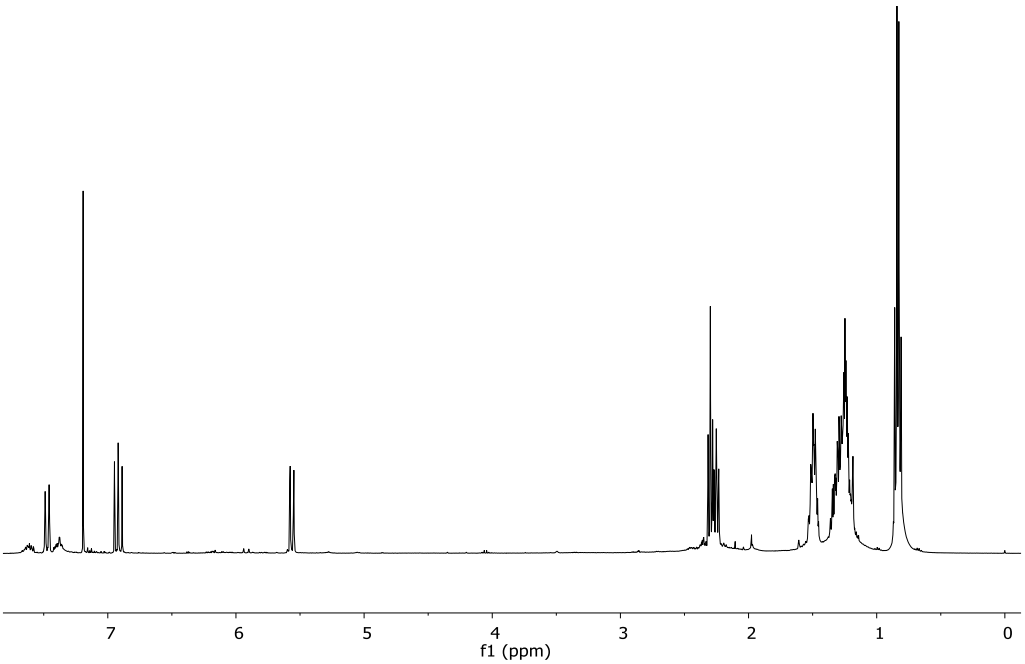

Figure 167. ^{1}H NMR spectra of (*E*)-5-hexylidenefuran-2(5H)-one, (**112**), *(CDCl₃, 400 MHz).*

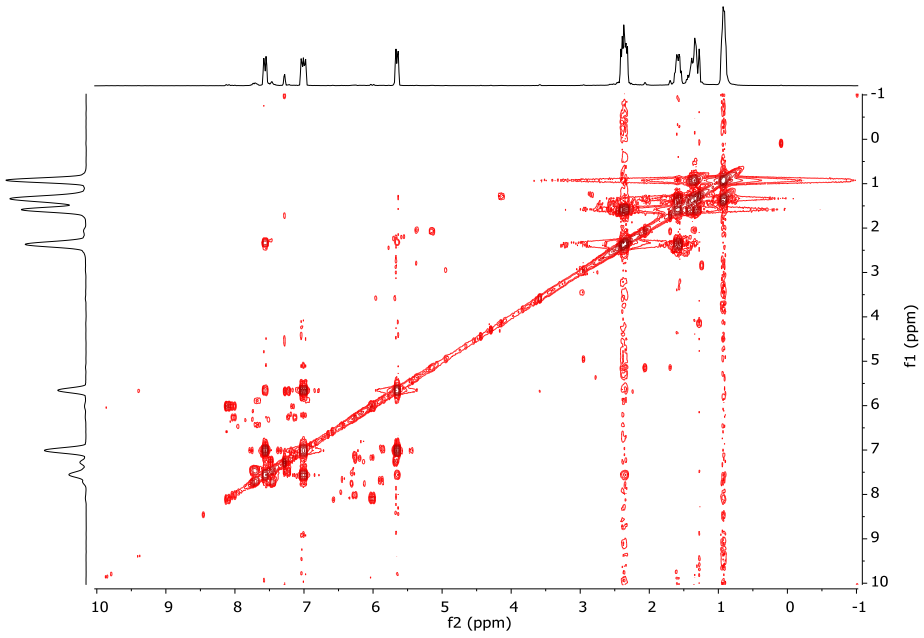

Figure 168. COSY spectra of (*E*)-5-hexylidenefuran-2(5H)-one, (**112**), *(CDCl₃).*

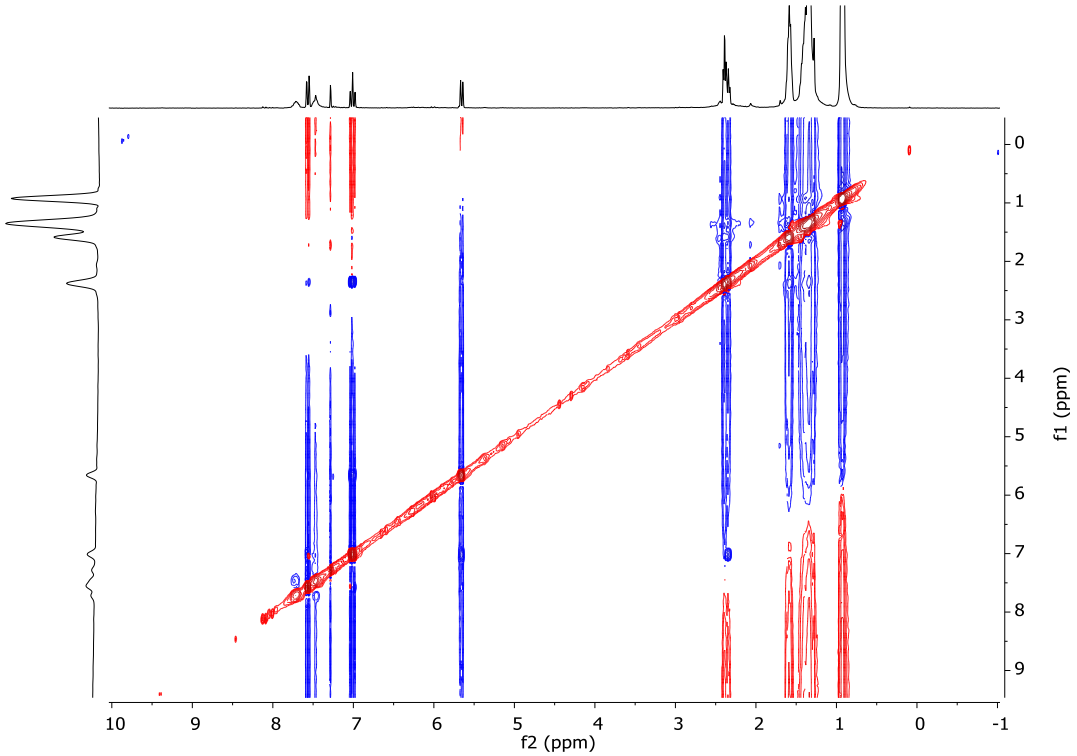

Figure 169. NOESY spectra of (*E*)-5-hexylidenefuran-2(5H)-one, (**112**), *(CDCl₃)*.

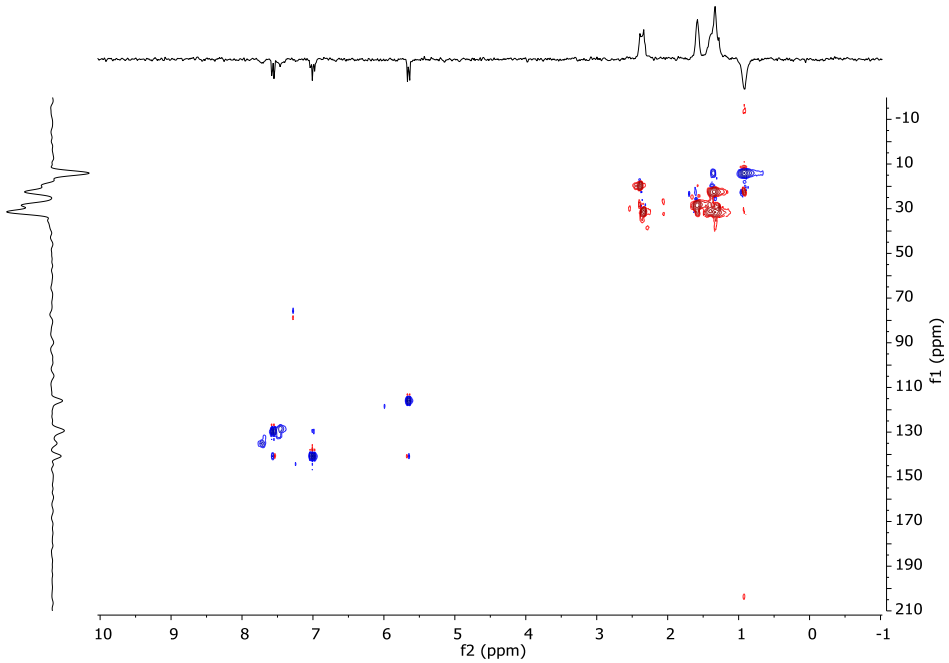

Figure 170. HSQC spectra of (*E*)-5-hexylidenefuran-2(5H)-one, (**112**), *(CDCl₃)*.

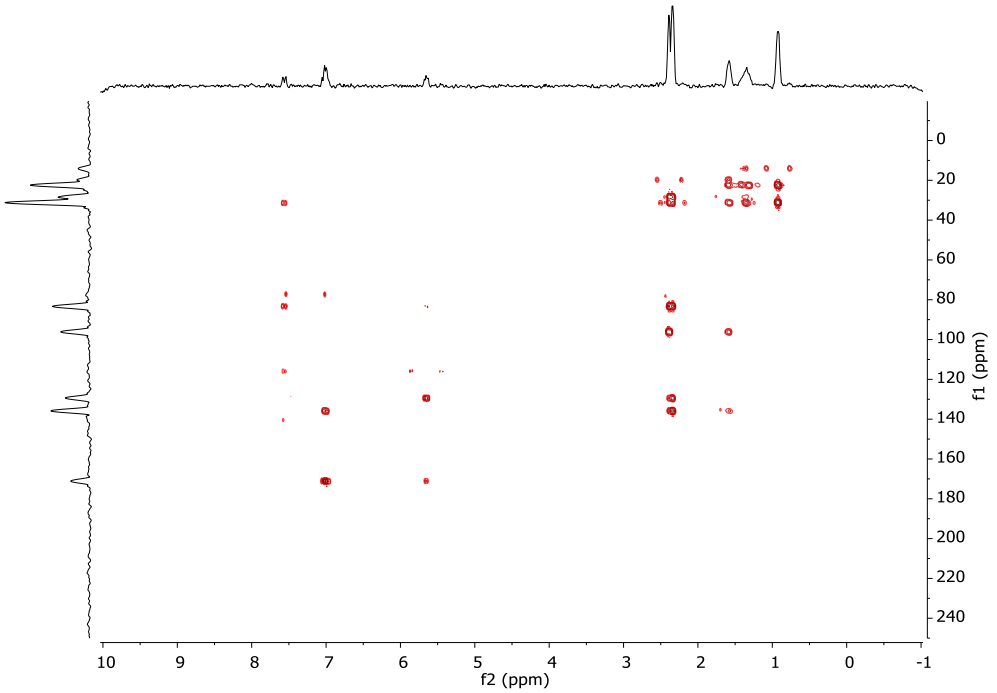

Figure 171. HMBC spectra of (*E*)-5-hexylidenefuran-2(5H)-one, (**112**), *(CDCl₃).*

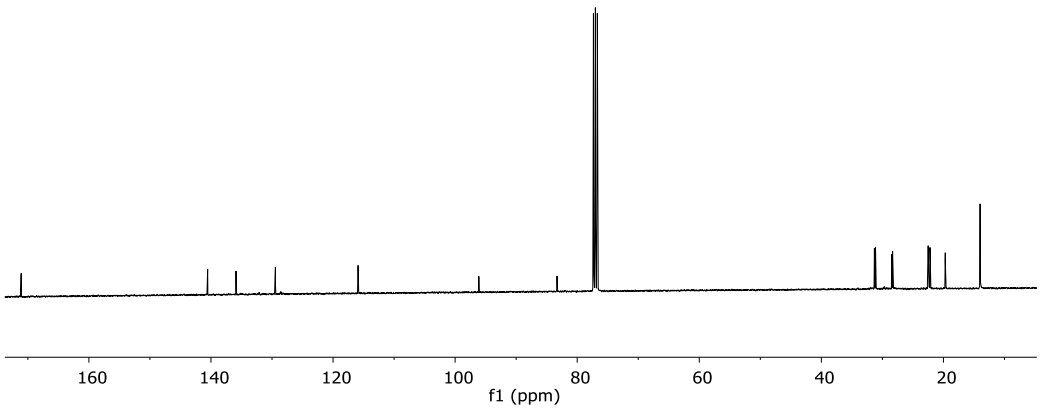

Figure 172. ^{13}C NMR spectra of (*E*)-5-hexylidenefuran-2(5H)-one, (**112**), *(CDCl₃, 100 MHz).*

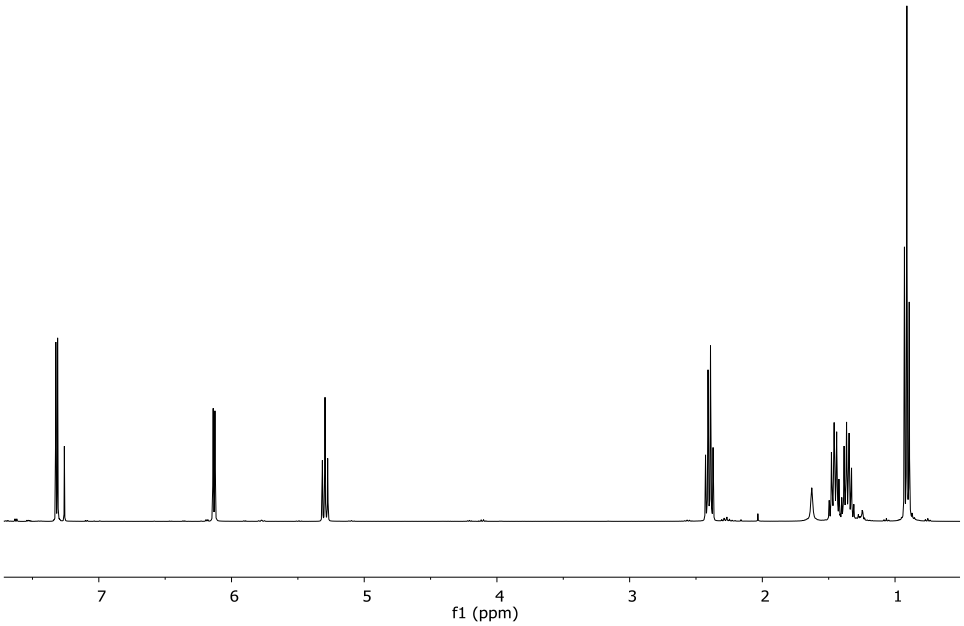

Figure 173. ^{1}H NMR spectra of (*Z*)-5-pentylidenefuran-2(5H)-one, (**114**), *(CDCl₃, 400 MHz).*

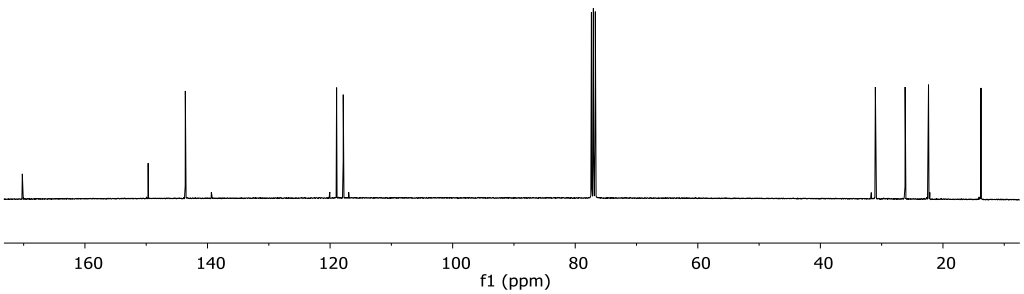

Figure 174. ^{13}C NMR spectra of (*Z*)-5-pentylidenefuran-2(5H)-one, (**114**), *(CDCl₃, 100 MHz).*

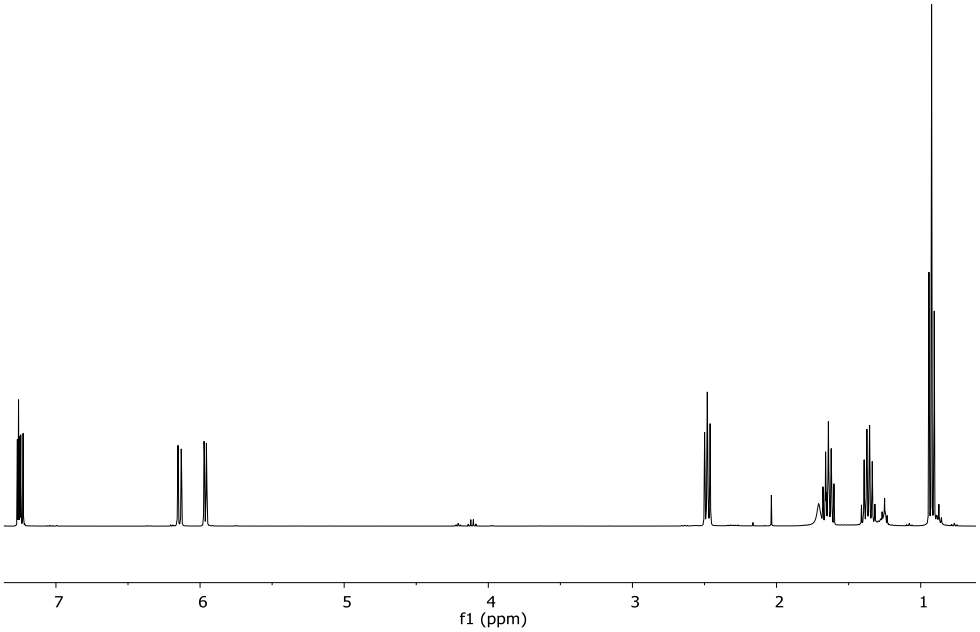

Figure 175. [1]H NMR spectra of 6-butyl-2H-pyran-2-one, (**116**), *(CDCl₃, 400 MHz).*

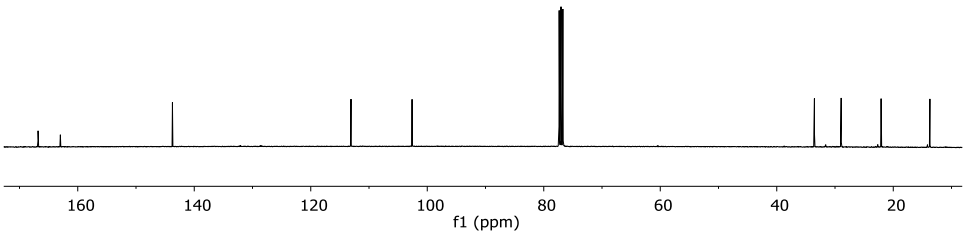

Figure 176. [13]C NMR spectra of 6-butyl-2H-pyran-2-one, (**116**), *(CDCl₃, 100 MHz).*

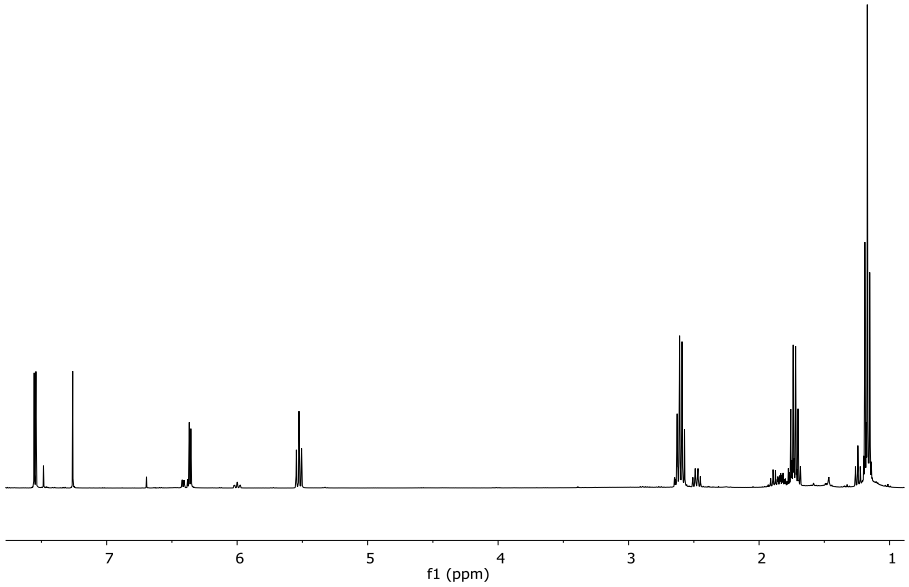

Figure 177. [1]H NMR spectra of (*Z*)-5-butylidenefuran-2(5H)-one, (**117**), *(CDCl₃, 400 MHz).*

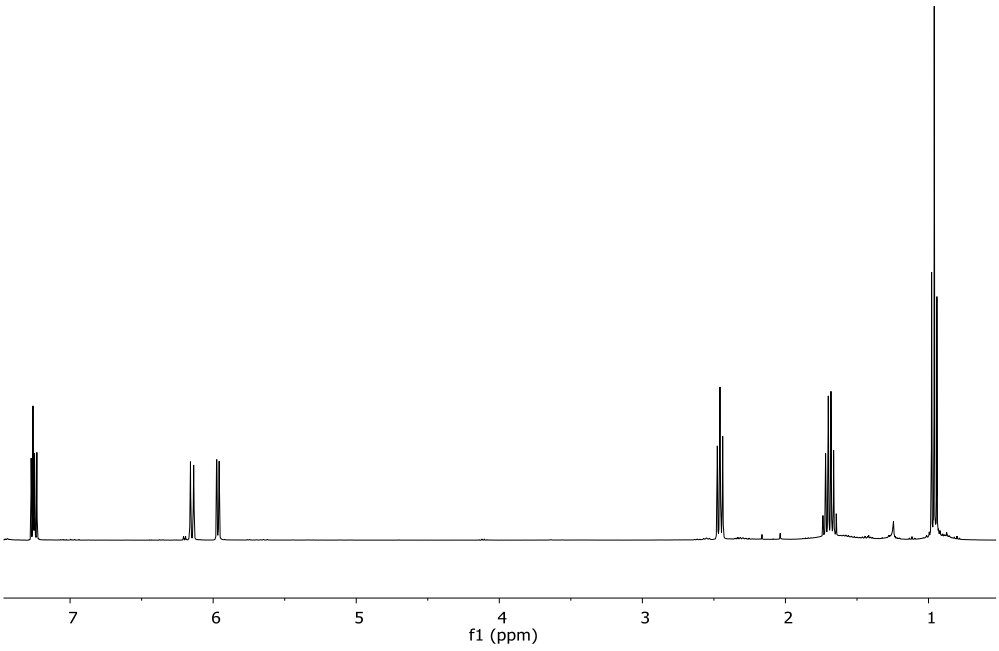

Figure 178. [1]H NMR spectra of 6-propyl-2H-pyran-2-one, (**119**), *(CDCl₃, 400 MHz).*

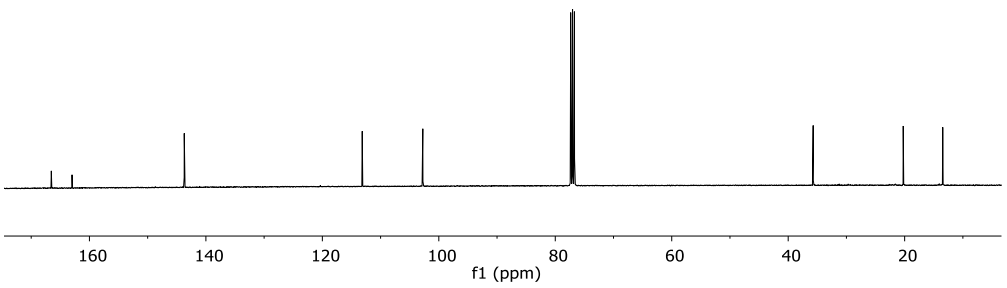

Figure 179. ^{13}C NMR spectra of 6-propyl-2H-pyran-2-one, (**119**), *(CDCl₃, 100 MHz).*

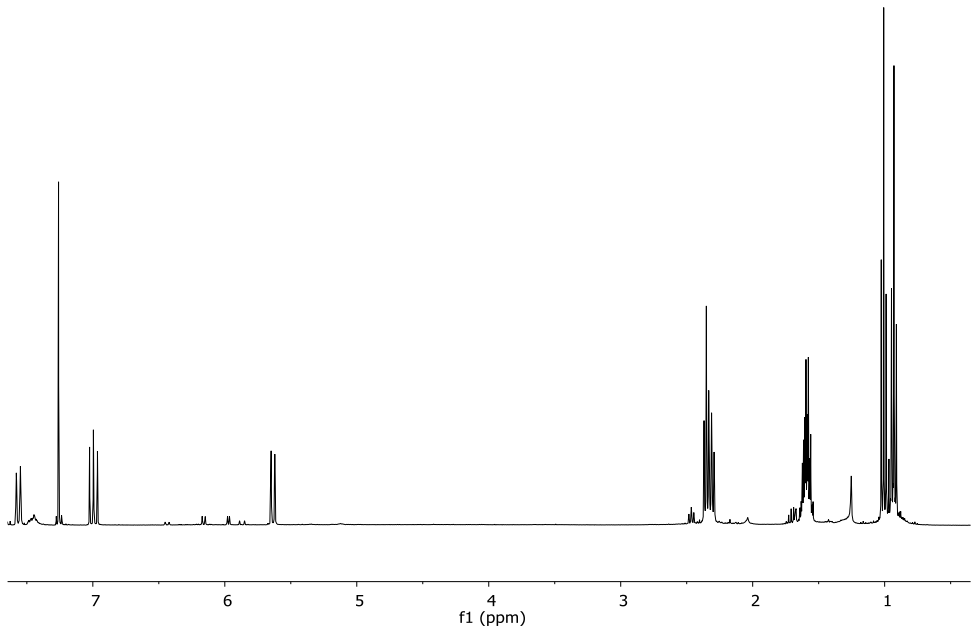

Figure 180. ^{1}H NMR spectra of (*E*)-5-butylidenefuran-2(5H)-one, (**118**) *(CDCl₃, 400 MHz).*

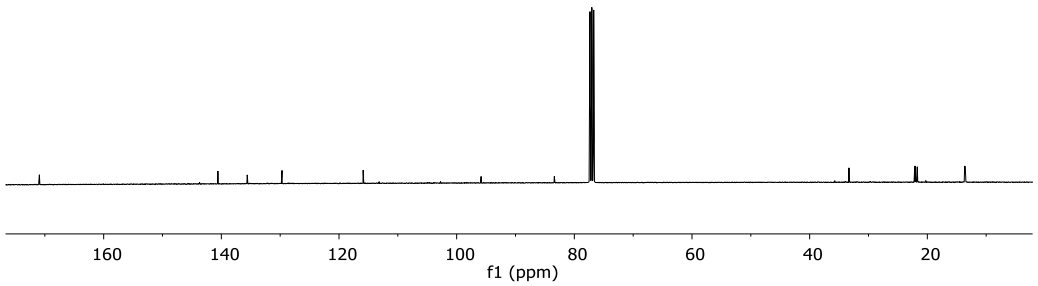

Figure 181. ^{13}C NMR spectra of (*E*)-5-butylidenefuran-2(5H)-one, (**118**) *($CDCl_3$, 100 MHz).*

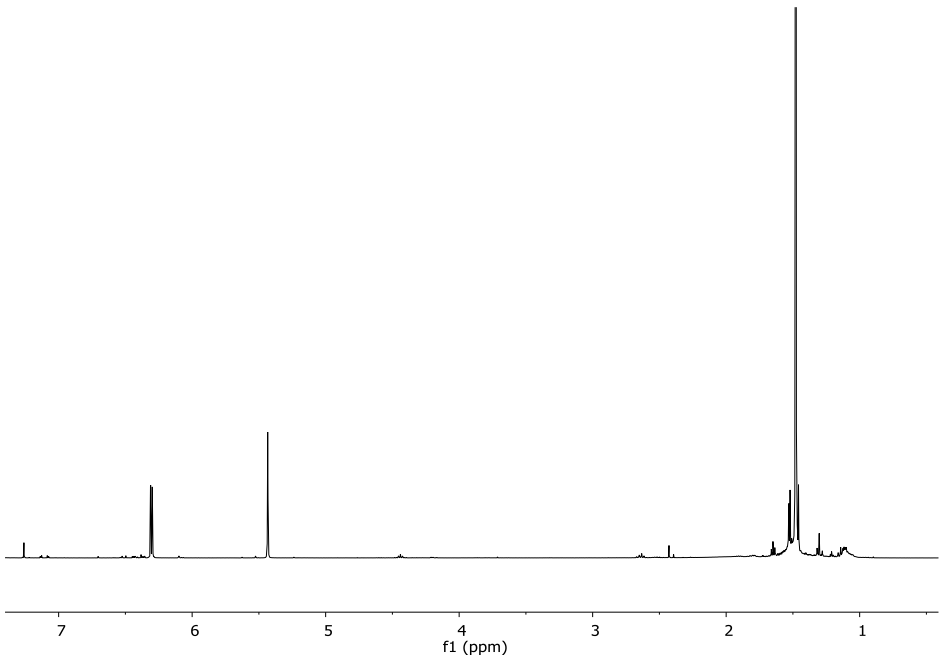

Figure 182. ^{1}H NMR spectra of (*Z*)-5-(2,2-dimethylpropylidene)furan-2(5H)-one, (**120**) *($CDCl_3$, 400 MHz).*

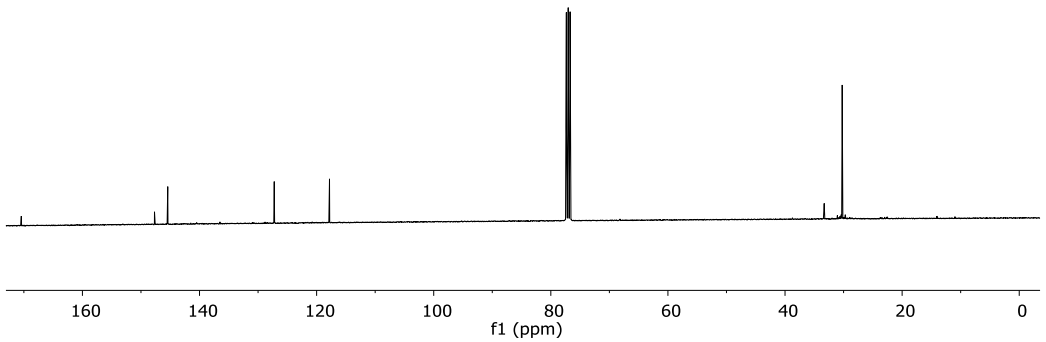

Figure 183. ^{13}C NMR spectra of (*Z*)-5-(2,2-dimethylpropylidene)furan-2(5H)-one, (**120**) *($CDCl_3$, 100 MHz).*

5.11 First attempts of (4*Z*)-Lachnophyllum lactone formulation

Considering the great amount obtained by the total synthesis of (4*Z*)-lachnophyllum lactone, first attempts for its formulation were performed, either through the use of cyclodextrins or the natural surfactants, rhamnolipids.

(4Z)-Lachnoophyllum lactone inclusion into cyclodextrins. Cyclodextrins (CDs, **Figure 184**) are naturally occurring cyclic oligosaccharides composed of six (α-), seven (β-), or eight (γ-) α-d-glucose units connected by α-1,4-glycosidic bonds. These macromolecules possess a hydrophobic cavity that can accommodate molecules of varying sizes, and their polar surface allows solubility in aqueous environments. This unique set of properties enables cyclodextrins to form inclusion complexes, enhancing the water solubility of encapsulated molecules.[224] The versatility of CDs in encapsulation has found extensive applications in pharmacology due to their low toxicity in humans. Interestingly, despite their success in various fields,[225] there is limited literature on the application of CDs in agrochemicals derived from natural products, particularly with saponins (SLs).[224] Conversely, many studies have demonstrated positive outcomes using CDs for diverse applications involving other natural products.[226]

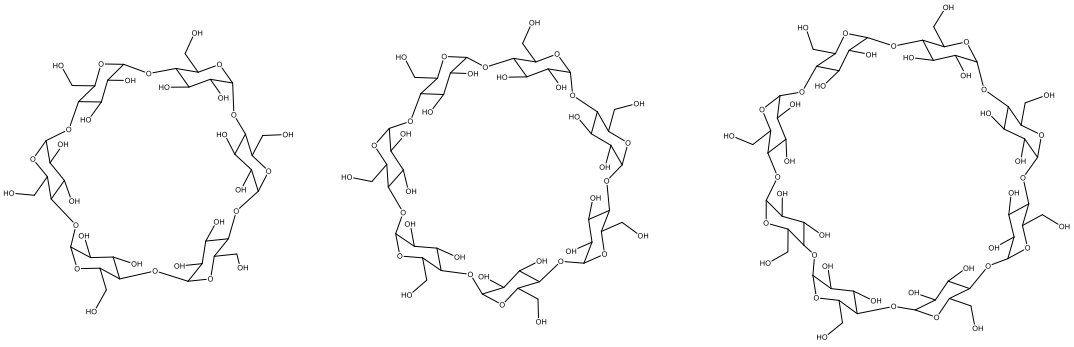

α-CD β-CD γ-CD

Figure 184. *Structure of α-, β- and γ-CD.*

Different preliminary fluorescent and coprecipitation experiments, using three different CDs and the (4Z)-lachnophyllum lactone, aiming to obtain the complexation constants were performed (data not shown). Furthermore, a DFT calculation study concerning the encapsulation of compound **84** into different cyclodextrins was carried out only considering a 1:1 complex ratio. Calculation level was performed by DFT B3LYP/6-31+g(d,p) and applying an empirical dispersion to get a correct representation of the energy of all the molecular orbitals of the guest molecule when is placed in a new nanoenviroment (CDs). Two different possibilities were studied for every CD. Position 1, which represent the initial geometrical input of the lactone ring closer to the narrow part of the toroid; and Position 2, which represent the initial geometrical input of the side chain closer to the narrow part of the toroid. The encapsulation studies were performed in three different environments: vacuum, water and DMSO. Analyzing the contribution of the solvents to the stabilization of the host-guest complex. In general terms, all the CDs are thermodynamically allowing the encapsulation process and despite vacuum simulation are the most generous, the application of water or DMSO generate a strong decrease of the Gibbs Free Energy. α- and β- CDs show negative values for ΔG with solvent contribution, but Gamma CD is on the limit of the spontaneous process. Furthermore, probabilistically, random contacts between host and guest can happen with the two possible allocations. So, average energy values for both positions per CD give a more general idea about the trend of the encapsulation. Considering this, α-CD would be the best candidate for 1:1 complex (**Figure 185**).

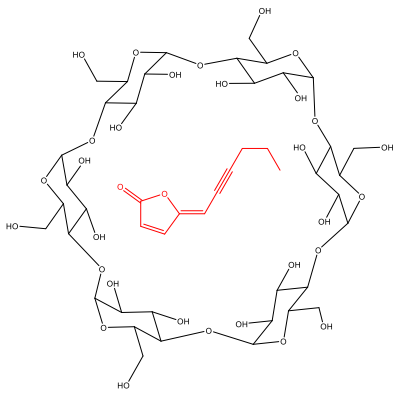

Figure 185. *1:1 complex between α-CD and (4Z)-lachnophyllum lactone.*

Formulation with rhamnolipids. Further attempts of (4*Z*)-lachnophyllum lactone formulation, employing the natural surfactants rhamnolipids (RHLs), were performed. They are glycolipids that exhibit amphiphilic behaviour due to a structure composed by one or two rhamnose units linked to one or more β-hydroxy fatty acids, representing an attractive and promising alternative to the commonly used synthetic surfactants.[227] Due to their ability to exhibit activity at low concentrations and endure harsh conditions such as extreme pH, temperature, and salinity, coupled with their high biodegradability, low toxicity, and enhanced environmental compatibility, rhamnolipids prove to be versatile and resilient compounds.[228] Preliminary experiment results showed that:

- By mixing 10 mg of compound **84** with 1 mL of only water, a cloudy solution was obtained (left, **Figure 186**).
- However, by mixing 10 mg of compound **84** with 1 mL of a water solution of a mixture of RHLs, a transparent clear solution was obtained, thus highlighting the solubilization of (4*Z*)-lachnophyllum lactone (**84**) (right, **Figure 186**).

Further efforts are needed to better characterized the system obtained, but this firsts experiments seems to be encouraging in the view of compound formulation and its application in the field.

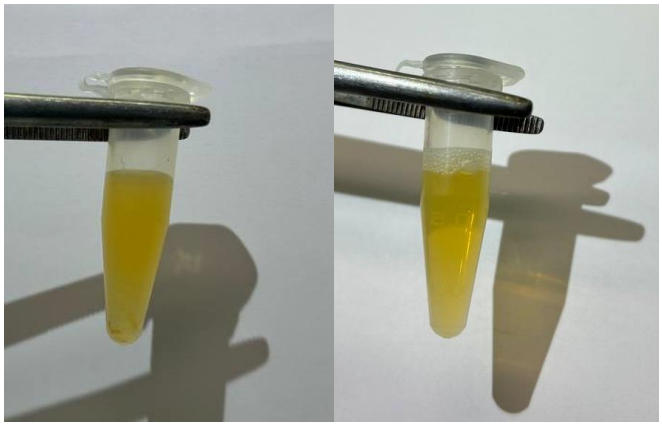

Figure 186. ***Left****: (4Z)-lachnophyllum lactone mixed with 1 ml of only* H_2O*,* ***right****: (4Z)-lachnophyllum lactone mixed with 1 mL of a water solution of a mixture of RHLs.*

6. Conclusions

In conclusion, preliminary assessments of twenty weedy plants organic extracts (**Table 1**), was carried out and many bioactive specialized metabolites were isolated, exhibiting species and concentration dependent activity against the four broomrape species *O. crenata*, *O. minor*, *O. cumana*, *P. ramosa* and the dodder *C. campestris*.

Specifically, using activity guided purification processes:

- from *C. arvenis* plant roots CH_2Cl_2 extract was isolated a mixture of arvensic acids, which are glycosylated fatty acids with inhibitory activity against the plant studied. They differ from each other in the number and nature of monosaccharide units and the nature of fatty acids.
- from *R. raetam* CH_2Cl_2 extract were identified the pure flavonoid ephedroidin, which exhibited a strong inhibition activity, too.
- From *B. trixago* ethyl acetate extract different iridoid glycosides were isolated, in particular: bartsioside, melampyroside and mussaenoside, with growth inhibition activity.

Ecotoxicological bioassays carried out on melampyroside (the most abundant and phytotoxic) showed low or null toxicity. Considering the activity showed and its high natural availability, it was already included into biopolymer of chitosan and alginate for its practical application and the bioassays are in progress.

Moreover, from *C. bonariensis* organic extracts were isolated two compounds with stimulatory activity: methyl 4-hydroxybenzoate, and hispidulin. While, (4*Z*)-lachnophyllum lactone and (4*Z*,8*Z*)-matricaria lactone, resulted to be strong inhibitors of the radicle growth of all parasitic weed species studied. From the structural point of view, the change of geometry from 4Z to 4*E* and the opening of the lactone ring of compounds have been found detrimental for their growth inhibitory activity. Considering the strong inhibitory activity of (4*Z*)-lachnophyllum lactone (**84**) and its low availability from the natural source, a synthetic strategy for its total synthesis was developed and carried out. Specifically, the elaboration led to an efficient synthetic five-step methodology towards (4Z)-lachnophyllum lactone (**84**). The compound, already isolated in low amount from the weed plant *C. bonariensis*, was obtained on gram scale, enabling extensive bioassays across various biological areas,

also in green house, in field as well as ecotoxicological study. Moreover, the butenolide core, peculiar of natural Strigolactones, opens the possibility of exploring (4Z)-lachnophyllum lactone (**84**), as well as the sesquiterpene lactones isolated from *C. cineraria*, for Strigolactone-like bioactivity and their employment as starting materials for synthesizing new strigolactones analogues, by using previously reported strategies,[229] expanding the potential applications. Additionally, the large amount obtained of (4Z)-lachnophyllum lactone (**84**), simplifying the exploration and refinement of bio-formulations. First attempts of compound inclusion into different cyclodextrins and formulation with the natural surfactants rhamnolipids, have led to preliminary encouraging results, highlighting the solubilization of (4Z)-lachnophyllum lactone (**84**) and allowing to obtain an easy-to-use tool for the agrochemical industry.

Hence, all the isolated bioactive specialized metabolites, contribute to enlarge the pool of phytotoxic metabolites that can be used as bio-inspired herbicides against parasitic plant seed germination and growth. Furthermore, ecotoxicological and molecular docking studies, are needed to assess environmental impact and effects on non-target organisms and to enhance the understanding of the mode and site of action, of (4*Z*)-lachnophyllum lactone (**84**), on parasitic plants receptor.

7. References

(1) Pimentel, D.; Zuniga, R.; Morrison, D. Update on the Environmental and Economic Costs Associated with Alien-Invasive Species in the United States. *Ecol. Econ.* **2005**, *52* (3), 273–288.

(2) Phytopathologia Mediterranea : 60, 3, 2021. *Phytopathol. Mediterr. - Quadrimestrale Four-Mon.* **2021**, *60* (3), 389–570.

(3) Rubiales, D. *Broomrape Threat to Agriculture*. https://doi.org/10.1564/v31_jun_12.

(4) Yoneyama, K.; Awad, A. A.; Xie, X.; Yoneyama, K.; Takeuchi, Y. Strigolactones as Germination Stimulants for Root Parasitic Plants. *Plant Cell Physiol.* **2010**, *51* (7),

(5) Cartry, D.; Steinberg, C.; Gibot-Leclerc, S. Main Drivers of Broomrape Regulation. A Review. *Agron. Sustain. Dev.* **2021**, *41* (2), 17.

(6) Hosseini, P.; Osipitan, O. A.; Mesgaran, M. B. Seed Germination Responses of Broomrape Species (Phelipanche Ramosa and Phelipanche Aegyptiaca) to Various Sanitation Chemicals. *Weed Technol.* **2022**, *36* (5), 723–728.

(7) Moreno-Robles, A.; Cala Peralta, A.; Soriano, G.; Zorrilla, J. G.; Masi, M.; Vilariño-Rodríguez, S.; Cimmino, A.; Fernández-Aparicio, M. Identification of Allelochemicals with Differential Modes of Phytotoxicity against Cuscuta Campestris. *Agriculture* **2022**, *12* (10), 1746.

(8) Parker, C. Observations on the Current Status of Orobanche and Striga Problems Worldwide. *Pest Manag. Sci.* **2009**, *65* (5), 453–459. https://doi.org/10.1002/ps.1713.

(9) Parker, C. Parasitic Weeds: A World Challenge. *Weed Sci.* **2012**, *60* (2), 269–276.

(10) *Trabelsi I.; Abbes Z.; Amri M.; Kharrat M. Study of some resistance mechanisms to Orobanche spp. infestation in faba bean (Vicia faba L.) breeding lines in Tunisia*, Plant Prod. Sci. **2016**, 19 (4), 562-573.

(11) Dor, E.; Plakhine, D.; Joel, D. M.; Larose, H.; Westwood, J. H.; Smirnov, E.; ... & Hershenhorn, J. *A new race of sunflower broomrape (Orobanche cumana) with a wider host range due to changes in seed response to strigolactones, Weed Science, **2020**, 60 (2), 134-142.*

(12) kaçan, K.; Tursun, N. Effect of Planting Time and Tomato Varieties on Broomrape (*Phelipanche Aegyptiaca*) Emergence and Tomato Yield in Western Turkey. *Res. Crops* **2012**, *13*, 1070–1077.

(13) Kotoula-Syka, E.; Eleftherohorinos, I. G. *Orobanche ramosa L. (broomrape) control in tomato (Lycopersicon esculentum Mill.) with chlorsulfuron, glyphosate and imazaquin - KOTOULA-SYKA Weed Research - Wiley Online Library*, **1991,** 31, 19-27.

(14) Panetta, F. D.; Lawes, R. Evaluation of the Australian Branched Broomrape (Orobanche Ramosa) Eradication Program. *Weed Sci.* **2007**, *55* (6), 644–651.

(15) Abu-Irmaileh, B. E. *Soil Solarization Controls Broomrapes (Orobanche spp.) in Host Vegetable Crops in the Jordan Valley | Weed Technology | Cambridge Core, **1991**, 5(3), 575-581.*

(16) Sylvestre, H.; Murthy, K.; Hatti, V.; Nduwumuremyi, A. Management of Orobanche in Field Crops-a Review. **2013**, *2*, 144–158.

(17) Dhanapal, G. N.; Struik, P. C.; Udayakumar, M.; & Timmermans; P. C. J. M. *Management of Broomrape (Orobanche spp.) – A review - Dhanapal Journal of Agronomy and Crop Science - Wiley Online Library*, **1996**, 176 (5), 335-359.
(18) Dhanapal, G. N.; Struik, P. C. *Broomrape Control in a Cropping System Containing Bidi Tobacco - Dhanapal - 1996 - Journal of Agronomy and Crop Science - Wiley Online Library*, **1996**, 177 (4), 225-236.
(19) Kusumoto, D.; Goldwasser, Y.; Xie, X.; Yoneyama, K.; Takeuchi, Y.; Yoneyama, K. *Resistance of Red Clover (Trifolium pratense) to the Root Parasitic Plant Orobanche minor is Activated by Salicylate but not by Jasmonate, Annals of Botany, **2007**, 100 (3), 537-544.*
(20) Parker, C. The Parasitic Weeds of the Orobanchaceae. In *Parasitic Orobanchaceae: Parasitic Mechanisms and Control Strategies*; Joel, D. M., Gressel, J., Musselman, L. J., Eds.; Springer: Berlin, Heidelberg, 2013; pp 313–344.
(21) Disciglio, G.; Lops, F.; Carlucci, A.; Gatta, G.; Tarantino, A.; Tarantino, E. Effect of Different Methods to Control the Parasitic Weed *Phelipanche Ramosa* (L.- Pomel) in Tomato Crop. **2015**, *9* (4).
(22) Farah, A. F.; Al-Abdulsalam, M. A. *Effect of field dodder (Cuscuta campestris Yuncker) on some legume crops. **2004**, 5 (1), 103-113.*
(23) Kebede, M., & Ayana, B. Economically Important Parasitic Weeds and Their Management Practices in Crops. *Environ. Earth Sci.* **2018**, *8*(12), 104-115.
(24) Dawson, J. H.; Musselman, L. J.; Wolswinkel, P.; Dörr, I. Biology and Control of *Cuscuta*. *Rev. Weed Sci.* **1994**, *6*, 265–317.
(25) Córdoba, E. M.; Fernández-Aparicio, M.; González-Verdejo, C. I.; López-Grau, C.; del Valle Muñoz-Muñoz, M.; Nadal, S. Search for Resistant Genotypes to Cuscuta Campestris Infection in Two Legume Species, Vicia Sativa and Vicia Ervilia. *Plants* **2021**, *10* (4), 738.
(26) Aly, R. Conventional and Biotechnological Approaches for Control of Parasitic Weeds. *Vitro Cell. Dev. Biol. - Plant* **2007**, *43* (4), 304–317.
(27) Owen, M. D.; Zelaya, I. A. Herbicide-Resistant Crops and Weed Resistance to Herbicides. *Pest Manag. Sci.* **2005**, *61* (3), 301–311. https://doi.org/10.1002/ps.1015.
(28) Panten, U.; Schwanstecher, M.; Schwanstecher, C. Sulfonylurea Receptors and Mechanism of Sulfonylurea Action. *Exp. Clin. Endocrinol. Diabetes* **1996**, *104* (1), 1–9.
(29) Jurado-Expósito, M.; Castejón-Muñoz, M.; García-Torres, L. Broomrape (Orobanche Crenata) Control with Imazethapyr Applied to Pea (Pisum Sativum) Seed. *Weed Technol.* **1996**, *10* (4), 774–780.
(30) Kraehmer, H.; van Almsick, A.; Beffa, R.; Dietrich, H.; Eckes, P.; Hacker, E.; Hain, R.; Strek, H. J.; Stuebler, H.; Willms, L. Herbicides as Weed Control Agents: State of the Art: II. Recent Achievements[C]. *Plant Physiol.* **2014**, *166* (3), 1132–1148.
(31) Nitschke, L.; Schüssler, W. Surface Water Pollution by Herbicides from Effluents of Waste Water Treatment Plants. *Chemosphere* **1998**, *36* (1), 35–41.
(32) Fernández-Aparicio, M.; Reboud, X.; Gibot-Leclerc, S. Broomrape Weeds. Underground Mechanisms of Parasitism and Associated Strategies for Their Control: A Review. *Front. Plant Sci.* **2016**, *7, 135*.

(33) Porter, P. M.; Huggins, D. R.; Perillo, C. A.; Quiring, S. R.; Crookston, R. K. *Organic and Other Management Strategies with Two- and Four-Year Crop Rotations in Minnesota | Agronomy Journal*. **2003**, *95*(2), 233-244.
(34) Hokkanen, H. M. T. Trap Cropping in Pest Management. *Annu. Rev. Entomol.* **1991**, *36* (1), 119–138.
(35) Shelton, A. M.; Badenes-Perez, F. R. Concepts and Applications of Trap Cropping in Pest Management. *Annu. Rev. Entomol.* **2006**, *51* (1), 285–308. https://doi.org/10.1146/annurev.ento.51.110104.150959.
(36) Hess, D. E.; Dodo, H. Potential for Sesame to Contribute to Integrated Control of Striga Hermonthica in the West African Sahel. *Crop Prot.* **2004**, *23* (6), 515–522. https://doi.org/10.1016/j.cropro.2003.10.008.
(37) Kroschel, J. *A Technical Manual for Parasitic Weed Research and Extension*; Springer Science & Business Media, **2002**, 1.1.
(38) Oswald, A.; Ransom, J. K.; Kroschel, J.; Sauerborn, J. Intercropping Controls Striga in Maize Based Farming Systems. *Crop Prot.* **2002**, *21* (5), 367–374.
(39) Joel, D. M.; Hershenhorn, J.; Eizenberg, H.; Aly, R.; Ejeta, G.; Rich, P. J.; Ransom, J. K.; Sauerborn, J.; Rubiales, D. Biology and Management of Weedy Root Parasites. *Hortic. Rev.* **2007**, *33*, 267–349.
(40) McDonald, D. Fumigants and Soil Sterilants: Alternatives to Methyl Bromide. *Int Pest Control* **2002**, *44*, 118–122.
(41) Goldwasser, Y.; Kleifeld, Y. Recent Approaches to Orobanche Management. In *Weed Biology and Management*; Inderjit, Ed.; Springer Netherlands: Dordrecht, **2004**, 439–466.
(42) Katan, J.; DeVay, J. E. *Soil Solarization*; CRC Press, **1991**, 1.
(43) Abu-Irmaileh, B. E. Soil Solarization Controls Broomrapes (Orobanche Spp.) in Host Vegetable Crops in the Jordan Valley. *Weed Technol.* **1991**, *5* (3), 575–581.
(44) Berner, O. K. Striga Research and Control: A Perspective from Africa. *Plant Dis.* **1995**, *79* (7), 652.
(45) Sharma, R.; Punia, S. S. Response of Various Chemicals, Neem Cake and Hand Pulling on Growth and Development of Egyptian Broomrape (*Phelipanche Aegyptiaca*) in Indian Mustard, J. of Crop and Weed, **2019**, 15 (2), 126-131
(46) Lanini, W. T.; Kogan, M. Biology and Management of Cuscuta in Crops. *Int. J. Agric. Nat. Resour.* **2005**, *32* (3), 127–141.
(47) D. Rubiales *Parasitic Plants, Wild Relatives and the Nature of Resistance on JSTOR*. The new Phytologist, **2003**, 160 (3), 459-461.
(48) Yoder, J. I.; Scholes, J. D. Host Plant Resistance to Parasitic Weeds; Recent Progress and Bottlenecks. *Curr. Opin. Plant Biol.* **2010**, *13* (4), 478–484.
(49) Lanini, T. Economical Methods for Controlling Dodder in Tomatoes. *Proc. Annu. Calif. Weed Sci. Soc.* **2004**.
(50) Jacobsohn, R. The Broomrape Problem in Israel and an Integrated Approach to Its Control. In *Biology and Management of Orobanche. Proceedings of the 3rd International Workshop on Orobanche and Related Striga Research. Amsterdam, The Netherlands: Royal Tropical Institute*; 1994; pp 652–658.

(51) Eizenberg, H.; Hershenhorn, J.; Ephrath, J. H.; Kanampiu, F. Chemical Control. In *Parasitic Orobanchaceae: Parasitic Mechanisms and Control Strategies*; Joel, D. M., Gressel, J., Musselman, L. J., Eds.; Springer: Berlin, Heidelberg, 2013; pp 415–432.
(52) Fernández-Aparicio, M.; Sillero, J. C.; Rubiales, D. Resistance to Broomrape in Wild Lentils (Lens Spp.). *Plant Breed.* **2009**, *128* (3), 266–270.
(53) Fernández-Aparicio, M.; Sillero, J. C.; Rubiales, D. Resistance to Broomrape Species (Orobanche Spp.) in Common Vetch (Vicia Sativa L.). *Crop Prot.* **2009**, *28* (1), 7–12.
(54) Lechat, M.-M.; Pouvreau, J.-B.; Péron, T.; Gauthier, M.; Montiel, G.; Véronési, C.; Todoroki, Y.; Le Bizec, B.; Monteau, F.; Macherel, D.; Simier, P.; Thoiron, S.; Delavault, P. PrCYP707A1, an ABA Catabolic Gene, Is a Key Component of Phelipanche Ramosa Seed Germination in Response to the Strigolactone Analogue GR24. *J. Exp. Bot.* **2012**, *63* (14), 5311–5322.
(55) Fernández-Aparicio, M.; Flores, F.; Rubiales, D. *Recognition of root exudates by seeds of broomrape (Orobanche and Phelipanche) species | Annals of Botany | Oxford Academic*. **2009**, 103 (3), 423-431.
(56) Runyon, J. B.; Tooker, J. F.; Mescher, M. C.; De Moraes, C. M. Parasitic plants in agriculture: chemical ecology of germination and host-plant location as targets for sustainable control: a review. *Organic Farming, Pest Control and Remediation of Soil Pollutants: Organic farming, pest control and remediation of soil pollutants*, **2010**, 1, 123-136.
(57) Joel D. M. *Functional Structure of the Mature Haustorium, SpringerLink*, **2013**, 25-60.
(58) Xie, X.; Yoneyama, K.; Yoneyama, K. The Strigolactone Story. *Annu. Rev. Phytopathol.* **2010**, *48* (1), 93–117.
(59) Fernández-Aparicio, M.; Flores, F.; Rubiales, D. The Effect of Orobanche Crenata Infection Severity in Faba Bean, Field Pea, and Grass Pea Productivity. *Front. Plant Sci.* **2016**, *7*.
(60) *Fernández-Aparicio, M.; Delavault, P.; Timko, M. P. Management of infection by parasitic weeds: A review. Plants, **2020**, 9(9), 1184.*
(61) Duke, S. O. Why Have No New Herbicide Modes of Action Appeared in Recent Years? *Pest Manag. Sci.* **2012**, *68* (4), 505–512.
(62) Westwood, J. H.; Charudattan, R.; Duke, S. O.; Fennimore, S. A.; Marrone, P.; Slaughter, D. C.; Swanton, C.; Zollinger, R. Weed Management in 2050: Perspectives on the Future of Weed Science. *Weed Sci.* **2018**, *66* (3), 275–285. https://doi.org/10.1017/wsc.2017.78.
(63) Lins, R. D.; Colquhoun, J. B.; Mallory-Smith, C. A. Investigation of Wheat as a Trap Crop for Control of Orobanche Minor. *Weed Res.* **2006**, *46* (4), 313–318. https://doi.org/10.1111/j.1365-3180.2006.00515.x.
(64) Cimmino, A.; Fernández-Aparicio, M.; Avolio, F.; Yoneyama, K.; Rubiales, D.; Evidente, A. Ryecyanatines A and B and Ryecarbonitrilines A and B, Substituted Cyanatophenol, Cyanatobenzo[1,3]Dioxole, and Benzo[1,3]Dioxolecarbonitriles from Rye (Secale Cereale L.) Root Exudates: Novel Metabolites with Allelopathic Activity on Orobanche Seed Germination and Radicle Growth. *Phytochemistry* **2015**, *109*, 57–65. https://doi.org/10.1016/j.phytochem.2014.10.034.

(65) Rimando, A. M.; Duke, S. O. Natural Products for Pest Management. In *Natural Products for Pest Management*; ACS Symposium Series; American Chemical Society, 2006; Vol. 927, pp 2–21. https://doi.org/10.1021/bk-2006-0927.ch001.
(66) *Zwanenburg, B.; Mwakaboko, A. S.; Kannan, C. Suicidal germination for parasitic weed control. Pest management science, **2016**, 72(11), 2016-2025.*
(67) *Cimmino, A.; Fernandez-Aparicio, M.; Andolfi, A.; Basso, S.; Rubiales, D.; Evidente, A. Effect of fungal and plant metabolites on broomrapes (Orobanche and Phelipanche spp.) seed germination and radicle growth. J. Agric. Food Chem., **2014**, 62(43), 10485-10492.*
(68) Parker, C. Protection of Crops against Parasitic Weeds. *Crop Prot.* **1991**, *10* (1), 6–22.
(69) *Wang, N. Q.; Kong, C. H.; Wang, P.; Meiners, S. J. Root exudate signals in plant–plant interactions. Plant, Cell & Environment, **2021**, 44(4), 1044-1058.*
(70) *Duke* S.O. *Allelopathy: Current status of research and future of the discipline: A Commentary. Allelopathy Journal, **2010**, 25(1).*
(71) *Kostina-Bednarz, M.; Płonka, J.; Barchanska, H. Allelopathy as a source of bioherbicides: Challenges and prospects for sustainable agriculture. Rev. Environ. Sci. BioTechnol., **2023**, 22(2), 471-504.*
(72) *Macias, F. A.; Molinillo, J. M.; Varela, R. M.; Galindo, J. C. Allelopathy—a natural alternative for weed control. Pest Manag. Sci. Formerly Pesticide Science, 2007, 63(4), 327-348.*
(73) Rice, E. L. Allelopathy.,(Academic Press: Orlando, FL). **1984**.
(74) *Duke S.O.; Dayan F.E. Rimando A.M. et al. Chemicals from nature for weed management. Weed Science. **2002**, 50(2), 138-151*
(75) Willis, R. J. The Historical Bases of the Concept of Allelopathy. *J. Hist. Biol.* **1985**, *18* (1), 71–102.
(76) Singh, H. P.; Batish, D. R.; Kohli, R. K. Allelopathy in Agroecosystems. *J. Crop Prod.* **2001**, *4* (2), 1–41.
(77) Weston, L. A. History and Current Trends in the Use of Allelopathy for Weed Manag. *HortTechnology* **2005**, *15* (3), 529–534.
(78) *Allelochemicals as Bioherbicides — Present and Perspectives | IntechOpen*. https://www.intechopen.com/chapters/44466 (accessed 2024-01-23) **2012**, 1.
(79) Hickman, D. T.; Rasmussen, A.; Ritz, K.; Birkett, M. A.; Neve, P. Review: Allelochemicals as Multi-Kingdom Plant Defence Compounds: Towards an Integrated Approach. *Pest Manag. Sci.* **2021**, *77* (3), 1121–1131.
(80) *Soltys, D., Krasuska, U., Bogatek, R., & Gniazdowska, A. Allelochemicals as bioherbicides—Present and perspectives. In Herbicides-Current research and case studies in use. IntechOpen, **2013**, 1.*
(81) Willis, R. J. *The History of Allelopathy*; Springer Science & Business Media, **2007**, 1.
(82) *Allelopathy: Organisms, Processes, and Applications*; Inderjit, Dakshini, K. M. M., Einhellig, F. A., Eds.; ACS Symposium Series; American Chemical Society: Washington, DC, 1994; Vol. 582.
(83) Blum, U. Effects of Microbial Utilization of Phenolic Acids and Their Phenolic Acid Breakdown Products on Allelopathic Interactions. *J. Chem. Ecol.* **1998**, *24* (4), 685–708.

(84) Saxena, S.; Pandey, A. K. Microbial Metabolites as Eco-Friendly Agrochemicals for the next Millennium. *Appl. Microbiol. Biotechnol.* **2001**, *55* (4), 395–403.
(85) *Lorsbach, B. A.; Sparks, T. C.; Cicchillo, R. M.; Garizi, N. V.; Hahn, D. R.; Meyer, K. G. Natural products: a strategic lead generation approach in crop protection discovery. Pest manag. sci.* ***2019****, 75(9), 2301-2309.*
(86) Saxena, R.; Tomar, R. S.; Kumar, M. Allelopathy: A Green Approach for Weed Management and Crop Production. *Int. J. Curr. Res. Biosci. Plant Biol.* **2016**, *3* (4), 43–50.
(87) *Dayan, F. E.; Duke, S. O. Natural compounds as next-generation herbicides. Plant physiology,* ***2014****, 166 (3), 1090-1105.*
(88) Fernández-Aparicio, M.; Cimmino, A.; Evidente, A.; Rubiales, D. Inhibition of Orobanche Crenata Seed Germination and Radicle Growth by Allelochemicals Identified in Cereals. *J. Agric. Food Chem.* **2013**, *61* (41), 9797–9803.
(89) Evidente, A.; Fernández-Aparicio, M.; Cimmino, A.; Rubiales, D.; Andolfi, A.; Motta, A. Peagol and Peagoldione, Two New Strigolactone-like Metabolites Isolated from Pea Root Exudates. *Tetrahedron Lett.* **2009**, *50* (50), 6955–6958.
(90) Scavo, A.; Mauromicale, G. Crop Allelopathy for Sustainable Weed Management in Agroecosystems: Knowing the Present with a View to the Future. *Agronomy* **2021**, *11* (11), 2104.
(91) *Cook, C. E.; Whichard, L. P.; Turner, B.; Wall, M. E.; Egley, G. H. Germination of witchweed (Striga lutea Lour.): isolation and properties of a potent stimulant. Science,* ***1966****, 154(3753), 1189-1190.*
(92) MacAlpine, A.; Raphael, R. A. Synthesis of the Germination Stimulant (*)-Strig0. **1976**.
(93) Butler, L. G. Chemical Communication Between the Parasitic Weed Striga and Its Crop Host. In *Allelopathy*; ACS Symposium Series; American Chemical Society, **1994**, 582, pp 158–168.
(94) Xie, X.; Kusumoto, D.; Takeuchi, Y.; Yoneyama, K.; Yamada, Y.; Yoneyama, K. 2′-Epi-Orobanchol and Solanacol, Two Unique Strigolactones, Germination Stimulants for Root Parasitic Weeds, Produced by Tobacco. *J. Agric. Food Chem.* **2007**, *55* (20), 8067–8072.
(95) Yoneyama, K.; Xie, X.; Yoneyama, K.; Takeuchi, Y. Strigolactones: Structures and Biological Activities. *Pest Manag. Sci.* **2009**, *65* (5), 467–470.
(96) Zwanenburg, B.; Mwakaboko, A. S.; Reizelman, A.; Anilkumar, G.; Sethumadhavan, D. Structure and Function of Natural and Synthetic Signalling Molecules in Parasitic Weed Germination. *Pest Manag. Sci.* **2009**, *65* (5), 478–491.
(97) Mangnus, E. M.; Zwanenburg, Binne. Tentative Molecular Mechanism for Germination Stimulation of Striga and Orobanche Seeds by Strigol and Its Synthetic Analogs. *J. Agric. Food Chem.* **1992**, *40* (6), 1066–1070.
(98) Evidente, A.; Cimmino, A.; Fernández-Aparicio, M.; Andolfi, A.; Rubiales, D.; Motta, A. Polyphenols, Including the New Peapolyphenols A−C, from Pea Root Exudates Stimulate Orobanche Foetida Seed Germination. *J. Agric. Food Chem.* **2010**, *58* (5), 2902–2907.

(99) Bouwmeester, H. J.; Matusova, R.; Zhongkui, S.; Beale, M. H. Secondary Metabolite Signalling in Host–Parasitic Plant Interactions. *Curr. Opin. Plant Biol.* **2003**, *6* (4), 358–364.

(100) Akiyama, K.; Matsuzaki, K.; Hayashi, H. Plant Sesquiterpenes Induce Hyphal Branching in Arbuscular Mycorrhizal Fungi. *Nature* **2005**, *435* (7043), 824–827.

(101) Andolfi, A.; Zermane, N.; Cimmino, A.; Avolio, F.; Boari, A.; Vurro, M.; Evidente, A. Inuloxins A–D, Phytotoxic Bi-and Tri-Cyclic Sesquiterpene Lactones Produced by Inula Viscosa: Potential for Broomrapes and Field Dodder Management. *Phytochemistry* **2013**, *86*, 112–120.

(102) Fernández-Aparicio, M.; Masi, M.; Maddau, L.; Cimmino, A.; Evidente, M.; Rubiales, D.; Evidente, A. Induction of Haustorium Development by Sphaeropsidones in Radicles of the Parasitic Weeds Striga and Orobanche. A Structure–Activity Relationship Study. *J. Agric. Food Chem.* **2016**, *64* (25), 5188–5196.

(103) *Evidente, A.; Maddau, L.; Scanu, B.; Andolfi, A.; Masi, M.; Motta, A.; Tuzi, A. Sphaeropsidones, phytotoxic dimedone methyl ethers produced by Diplodia cupressi: A structure− activity relationship study. Journal of natural products,* ***2011****, 74(4), 757-763.*

(104) Rial, C.; Varela, R. M.; Molinillo, J. M. G.; Peralta, S.; Macías, F. A. Sunflower Metabolites Involved in Resistance Mechanisms against Broomrape. *Agronomy* **2021**, *11* (3), 501.

(105) Burchat, A. F.; Chong, J. M.; Nielsen, N. Titration of Alkyllithiums with a Simple Reagent to a Blue Endpoint. *J. Organomet. Chem.* **1997**, *542* (2), 281–283.

(106) *Gaertner E. E. Studies of seed germination, seed identification, and host relationships in dodders, Cuscuta spp. Memoirs. Cornell Agricultural Experiment Station,* ***1950****, 56.*

(107) *Westwood, J. H.; Foy, C. L. Influence of nitrogen on germination and early development of broomrape (Orobanche spp.). Weed Sci.* ***1999****, 47(1), 2-7.*

(108) Pistelli, L.; Bertoli, A.; Giachi, I.; Manunta, A. Flavonoids from Genista Ephedroides. *J. Nat. Prod.* **1998**, *61* (11), 1404–1406.

(109) *Daina, A.; Michielin, O.; Zoete, V. SwissADME: a free web tool to evaluate pharmacokinetics, drug-likeness and medicinal chemistry friendliness of small molecules. Scientific reports,* ***2017****, 7(1), 42717.*

(110) *Vraka, C.; Nics, L.; Wagner, K. H.; Hacker, M.; Wadsak, W.; Mitterhauser, M. LogP, a yesterday's value?. Nuclear Med. and Biol.* ***2017****, 50, 1-10.*

(111) Bouafiane, M.; Khelil, A.; Cimmino, A.; Kemassi, A. Prediction and Evaluation of Allelopathic Plants Species in Algerian Saharan Ecosystem. *Perspect. Plant Ecol. Evol. Syst.* **2021**, *53*, 125647.

(112) Cimmino, A.; Roscetto, E.; Masi, M.; Tuzi, A.; Radjai, I.; Gahdab, C.; Paolillo, R.; Guarino, A.; Catania, M. R.; Evidente, A. Sesquiterpene Lactones from Cotula Cinerea with Antibiotic Activity against Clinical Isolates of Enterococcus Faecalis. *Antibiotics* **2021**, *10* (7), 819.

(113) *Soriano, G.; Petrillo, C.; Masi, M.; Bouafiane, M.; Khelil, A.; Tuzi, A; ... & Cimmino, A. Specialized metabolites from the allelopathic plant Retama raetam as potential biopesticides. Toxins,* ***2022****, 14(5), 311.*

(114) *Tanaka, T.; Nakashima, T.; Ueda, T.; Tomii, K.; Kouno, I. Facile discrimination of aldose enantiomers by reversed-phase HPLC. Chem. Pharm. Bulletin,* ***2007****, 55(6), 899-901.*

(115) *Fan, B. Y.; He, Y.; Lu, Y.; Yang, M.; Zhu, Q.; Chen, G. T.; Li, J. L. Glycosidic acids with unusual aglycone units from Convolvulus arvensis. J. Nat. prod.* ***2019****, 82(6), 1593-1598.*

(116) Fan, B.-Y.; Lu, Y.; Yin, H.; He, Y.; Li, J.-L.; Chen, G.-T. Arvensic Acids A-D, Novel Heptasaccharide Glycosidic Acids as the Alkaline Hydrolysis Products of Crude Resin Glycosides from Convolvulus Arvensis. *Fitoterapia* **2018**, *131*, 209–214.

(117) Lu, Y.; He, Y.; Yang, M.; Fan, B.-Y. Arvensic Acids K and L, Components of Resin Glycoside Fraction from Convolvulus Arvensis. *Nat. Prod. Res.* **2021**, *35* (14), 2303–2307.

(118) Jackson, B.; Owen, P. J.; Scheinmann, F. Extractives from Poisonous British Plants. Part I. The Structure of Alpinumisoflavone, a New Pyranoisoflavone from Laburnum Alpinum J. Presl. *J. Chem. Soc. C Org.* **1971**, No. 0, 3389–3392.

(119) Olivares, E. M.; Lwande, W.; Monache, F. D.; Marini Bettolo, G. B. A Pyrano-Isoflavone from Seeds of Milletia Thonningii. *Phytochemistry* **1982**, *21* (7), 1763–1765.

(120) Sato, H.; Tahara, S.; Ingham, J. L.; Dziedzic, S. Z. Isoflavones from Pods of Laburnum Anagyroides. *Phytochemistry* **1995**, *39* (3), 673–676.

(121) *Kajiyana, K.; Demizu, S.; Hiraga, Y.; Kinoshita, K.; Koyama, K.; Takahashi, K.; ... & Kinoshita, T. New prenylflavones and dibenzoylmethane from Glycyrrhiza inflata. J. Nat. Prod.* ***1992****, 55(9), 1197-1203.*

(122) *Xu, W. H.M.; Al-Rehaily, A. J.; Yousaf, M.; Ahmad, M. S.; Khan, S. I.; Khan, I. A. Two new flavonoids from Retama raetam. Helvetica Chimica Acta,* ***2015****, 98(4), 561-568.*

(123) Altomare, A.; Burla, M. C.; Camalli, M.; Cascarano, G. L.; Giacovazzo, C.; Guagliardi, A.; Moliterni, A. G. G.; Polidori, G.; Spagna, R. SIR97: A New Tool for Crystal Structure Determination and Refinement. *J. Appl. Crystallogr.* **1999**, *32* (1), 115–119.

(124) Sheldrick, G. M. Crystal Structure Refinement with SHELXL. *Acta Crystallogr. Sect. C Struct. Chem.* **2015**, *71* (Pt 1), 3–8.

(125) Farrugia, L. J. WinGX and ORTEP for Windows: An Update. *J. Appl. Crystallogr.* **2012**, *45* (4), 849–854.

(126) Yusoff, S. F.; Haron, F. F.; Tengku Muda Mohamed, M.; Asib, N.; Sakimin, S. Z.; Abu Kassim, F.; Ismail, S. I. Antifungal Activity and Phytochemical Screening of Vernonia Amygdalina Extract against Botrytis Cinerea Causing Gray Mold Disease on Tomato Fruits. *Biology* **2020**, *9* (9), 286.

(127) Puopolo, G.; Masi, M.; Raio, A.; Andolfi, A.; Zoina, A.; Cimmino, A.; Evidente, A. Insights on the Susceptibility of Plant Pathogenic Fungi to Phenazine-1-Carboxylic Acid and Its Chemical Derivatives. *Nat. Prod. Res.* **2013**, *27* (11), 956–966.

(128) Cui, L.-Q.; Liu, K.; Zhang, C. Effective Oxidation of Benzylic and Alkane C–H Bonds Catalyzed by Sodium o-Iodobenzenesulfonate with Oxone as a Terminal Oxidant under Phase-Transfer Conditions. *Org. Biomol. Chem.* **2011**, *9* (7), 2258–2265.

(129) Delicato, A.; Masi, M.; de Lara, F.; Rubiales, D.; Paolillo, I.; Lucci, V.; Falco, G.; Calabrò, V.; Evidente, A. In Vitro Characterization of Iridoid and Phenylethanoid Glycosides from Cistanche Phelypaea for Nutraceutical and Pharmacological Applications. *Phytother. Res.* **2022**, *36* (11), 4155–4166.

(130) Andrzejewska-Golec, E.; Ofterdinger-Daegel, S.; Calis, I.; Świątek, L. Chemotaxonomic Aspects of Iridoids Occurring inPlantago Subg.Psyllium (Plantaginaceae). *Plant Syst. Evol.* **1993**, *185* (1), 85–89.

(131) *Ersöz, T.; Yalcin, F. N.; TAŞDEMİR, D.; Sticher, O.; ÇALIŞ, İ. Iridoid and Lignan Glucosides from Bellardiatrixago (L.) All. Turkish Journal of Medical Sciences, **1998**, 28(4), 397-400.*

(132) Chaudhuri, R. K.; Afifi-Yazar, F. Ü.; Sticher, O.; Winkler, T. 13C NMR Spectroscopy of Naturally Occurring Iridoid Glucosides and Their Acylated Derivatives. *Tetrahedron* **1980**, *36* (16), 2317–2326.

(133) Chu, H.-B.; Tan, N.-H.; Zhanga, Y.-M. Chemical Constituents from Pedicularis Rex C. B. Clarke. *Z. Für Naturforschung B* **2007**, *62* (11), 1465–1470.

(134) Aly, R.; Goldwasser, Y.; Eizenberg, H.; Hershenhorn, J.; Golan, S.; Kleifeld, Y. Broomrape (Orobanche Cumana) Control in Sunflower (Helianthus Annuus) with Imazapic1. *Weed Technol.* **2001**, *15* (2), 306–309.

(135) Takeda, Y.; Fujita, T. Iridoid Glucosides of Melampyrum Laxum. *Planta Med.* **1981**, *41* (02), 192–194.

(136) Venditti, A.; Ballero, M.; Serafini, M.; Bianco, A. Polar Compounds from Parentucellia Viscosa (L.) Caruel from Sardinia. *Nat. Prod. Res.* **2015**, *29* (7), 602–606.

(137) Otsuka, H.; Watanabe, E.; Yuasa, K.; Ogimi, C.; Takushi, A.; Takeda, Y. A Verbascoside Iridoid Glucoside Conjugate from Premna Corymbosa Var. Abtusifolia. *Phytochemistry* **1993**, *32* (4), 983–986.

(138) ISO, P. 11269: 2; Determination of the Effects of Pollutants on Soil Flora. Part 2: Effects of Contaminated Soil on the Emergence and Early Growth of Higher Plants. *International Organization for Standardization (ISO): Geneva, Switzerland **2012***.

(139) ISO, E. Water Quality—Determination of the Inhibition of the Mobility of Daphnia Magna Straus (Cladocera, Crustacea)—Acute Toxicity Test. *EN ISO*, **1998**, *6341*, 1996.

(140) Bruno, M.; Herz, W. Sesquiterpene Lactones and Flavones from Centaurea Cineraria Subsp. Umbrosa. *Phytochemistry* **1988**, *27* (6), 1873–1875.

(141) Kurita, M.; Tanigawa, M.; Narita, S.; Usuki, T. Synthetic Study of Cnicin: Synthesis of the Side Chain and Its Esterification. *Tetrahedron Lett.* **2016**, *57* (52), 5899–5901.

(142) Sanz, J. F.; Marco, J. A. Ein Neues Butenolid Aus Conyza Bonariensis. *Liebigs Ann. Chem.* **1991**, *1991* (4), 399–400.

(143) *Fernández-Aparicio, M.; Soriano, G.; Masi, M.; Carretero, P.; Vilariño-Rodríguez, S.; Cimmino, A. (4Z)-Lachnophyllum lactone, an acetylenic furanone from Conyza bonariensis, identified for the first time with allelopathic activity against Cuscuta campestris. Agriculture, **2022**, 12(6), 790.*

(144) Sc, Q.; Cl, C.; So, D.; De, W.; Vk, N.; Rm, M.; Al, C. Bioassay-Directed Isolation and Identification of Phytotoxic and Fungitoxic Acetylenes from Conyza Canadensis. *J. Agric. Food Chem.* **2012**, *60* (23).

(145) Csupor-Löffler, B.; Hajdú, Z.; Zupkó, I.; Molnár, J.; Forgo, P.; Vasas, A.; Kele, Z.; Hohmann, J. Antiproliferative Constituents of the Roots of Conyza Canadensis. *Planta Med.* **2011**, *77* (11), 1183–1188.

(146) Yin, X. J.; Xu, G. H.; Sun, X.; Peng, Y.; Ji, X.; Jiang, K.; Li, F. Synthesis of bosutinib from 3-methoxy-4-hydroxybenzoic acid. *Molecules*, **2010**, *15*(6), 4261-4266.

(147) Takahashi, T.; Yamakoshi, Y.; Okayama, K. High-Pressure Mediated Asymmetric Diels-Alder Reaction of Chiral Sulfinylacrylate Derivatives and Its Application to Chiral Synthesis of (-)-COTC and (-)-Gabosine C. *Heterocycles Int. J. Rev. Commun. Heterocycl. Chem.* **2002**, *56*, 209–220.

(148) *Collado, I. G.; Macias, F. A.; Massanet, G. M.; Luis, F. R. Flavonoids from Centaurea clementei. J. Nat. Prod. **1985**, 48(5), 819-822.*

(149) Liu, Y.-L.; Ho, D. K.; Cassady, J. M.; Cook, V. M.; Baird, W. M. Isolation of Potential Cancer Chemopreventive Agents from Eriodictyon Californicum. *J. Nat. Prod.* **1992**, *55* (3), 357–363.

(150) *Rambabu, D.; Bhavani, S.; Nalivela, K. S.; Mukherjee, S.; Rao, M. B.; Pal, M. Pd/C–Cu mediated direct and one-pot synthesis of γ-ylidene butenolides. Tetrahedron Letters, **2013**, 54 (17), 2151-2155.*

(151) Soriano, G.; Arnodo, D.; Masi, M.; Fernández-Aparicio, M.; Landa, B. B., Olivares-García, C.; Cimmino, A.; Prandi, C. *(4Z)-Lachnophyllum Lactone, a Metabolite with Phytotoxic and Antifungal Activity against Pests Affecting Mediterranean Agriculture: A New Versatile and Easy Scalable Parallel Synthesis J. Agric. Food Chem. **2024**, 72 (9), 4737–4746.*

(152) *Kyi, S.; Wongkattiya, N.; Warden, A. C.; O'Shea, M. S.; Deighton, M.; Macreadie, I.; Graichen, F. H. Synthesis and activity of polyacetylene substituted 2-hydroxy acids, esters, and amides against microbes of clinical importance. Bioorganic & medicinal chemistry letters, **2010**, 20(15), 4555-4557.*

(153) Fiandanese, V.; Bottalico, D.; Marchese, G.; Punzi, A. New stereoselective methodology for the synthesis of dihydroxerulin and xerulin, potent inhibitors of the biosynthesis of cholesterol. *Tetrahedron*, **2004**, *60* (50), 11421-11425.

(154) *Siegel, K.; Brückner, R. First total synthesis of dihydroxerulin, a potent inhibitor of the biosynthesis of cholesterol. Chemistry–A European Journal, **1998**, 4(6), 1116-1122.*

(155) *Jung, M. E.; Hagenah, J. A.; Long-Mei, Z. Simple, stereospecific preparation of Z-3-iodoacrylic acid from propiolic acid and methylmagnesium iodide. Tetrahedron Letters, **1983**, 24(37), 3973-3974.*

(156) Chatterjee, S.; Acharyya, R. K.; Pal, P.; Nanda, S. Synthetic Studies towards Naturally Occurring γ-(Z)/(E)-Alkylidenebutenolides through Bimetallic Cascade Cyclization and an Adventitious Photoisomerization Method. *Org. Biomol. Chem.* **2022**, *20* (12), 2473–2499.

(157) Rivera, A. P.; Arancibia, L.; Castillo, M. Clerodane Diterpenoids and Acetylenic Lactones from Baccharris Paniculata. *J. Nat. Prod.* **1989**, *52* (2), 433–435.

(158) Montevecchi, P. C.; Navacchia, M. L. DDQ-Promoted Functionalization of Phenylalkylacetylenes at the Propargylic Carbon. *The Journal Org. Che*m. **1998**, *63*(22), 8035-8037.

(159) Shaner, G. The Effect of Nitrogen Fertilization on the Expression of Slow-Mildewing Resistance in Knox Wheat. *Phytopathology* **1977**, *77* (8), 1051.

(160) Cimmino, A.; Fernández-Aparicio, M.; Andolfi, A.; Basso, S.; Rubiales, D.; Evidente, A. Effect of Fungal and Plant Metabolites on Broomrapes (Orobanche and Phelipanche Spp.) Seed Germination and Radicle Growth. *J. Agric. Food Chem.* **2014**, *62* (43), 10485–10492.

(161) *Adams, R.; Bockstahler, T. E. Preparation and reactions of o-hydroxycinnamic acids and esters. Journal of the American Chemical Society, **1952**, 74(21), 5346-5348.*
(162) Baziramakenga, R.; Leroux, G. D.; Simard, R. R. Effects of Benzoic and Cinnamic Acids on Membrane Permeability of Soybean Roots. *J. Chem. Ecol.* **1995**, *21* (9), 1271–1285.
(163) Abenavoli, M. R.; Lupini, A.; Oliva, S.; Sorgonà, A. Allelochemical Effects on Net Nitrate Uptake and Plasma Membrane H+-ATPase Activity in Maize Seedlings. *Biol. Plant.* **2010**, *54* (1), 149–153.
(164) Moreno-Robles, A.; Cala Peralta, A.; Zorrilla, J. G.; Soriano, G.; Masi, M.; Vilariño-Rodríguez, S.; Cimmino, A.; Fernández-Aparicio, M. Identification of Structural Features of Hydrocinnamic Acid Related to Its Allelopathic Activity against the Parasitic Weed Cuscuta Campestris. *Plants Basel Switz.* **2022**, *11* (21), 2846.
(165) Dewick, P. M. *Medicinal Natural Products: A Biosynthetic Approach*; John Wiley & Sons, **2002**, chapter 1.
(166) *Joel, D. M.; Gressel, J.; Musselman, L. J. Parasitic Orobanchaceae. Parasitic.mechanisms and control strategies. New York, **2013**, 1.*
(167) Cimmino, A.; Masi, M.; Rubiales, D.; Evidente, A.; Fernández-Aparicio, M. Allelopathy for Parasitic Plant Management. *Nat. Prod. Commun.* **2018**, *13* (3), 289-294.
(168) *Fernández-Aparicio, M.; Cimmino, A.; Soriano, G.; Masi, M.; Vilariño, S.; Evidente, A. Assessment of weed root extracts for allelopathic activity against Orobanche and Phelipanche species. Phytopathol. Mediterr. 2021, 60, 455-466.*
(169) Scavo, A.; Mauromicale, G. Integrated Weed Management in Herbaceous Field Crops. *Agronomy* **2020**, *10* (4), 466.
(170) Xie, X. Structural Diversity of Strigolactones and Their Distribution in the Plant Kingdom. *J. Pestic. Sci.* **2016**, *41* (4), 175–180.
(171) Soriano, G.; Fernández-Aparicio, M.; Masi, M.; Vilariño-Rodríguez, S.; Cimmino, A. Complex Mixture of Arvensic Acids Isolated from Convolvulus Arvensis Roots Identified as Inhibitors of Radicle Growth of Broomrape Weeds. *Agriculture* **2022**, *12* (5), 585.
(172) León-Rivera, I.; Mirón-López, G.; Estrada-Soto, S.; Aguirre-Crespo, F.; Gutiérrez, M. del C.; Molina-Salinas, G. M.; Hurtado, G.; Navarrete-Vázquez, G.; Montiel, E. Glycolipid Ester-Type Heterodimers from Ipomoea Tyrianthina and Their Pharmacological Activity. *Bioorg. Med. Chem. Lett.* **2009**, *19* (16), 4652–4656.
(173) *León-Rivera, I., Villeda-Hernández, J., Campos-Peña, V., Aguirre-Moreno, A., Estrada-Soto, S.; Navarrete-Vázquez, G.; ... & Rivera-Leyva, J. C. (2014). Evaluation of the neuroprotective activity of stansin 6, a resin glycoside from Ipomoea stans. Bioorganic & Medicinal Chemistry Letters, **2014**, 24(15), 3541-3545.*
(174) Li, J.-H.; Pan, J.-T.; Yin, Y.-Q. Two Novel Resin Glycosides Isolated from Ipomoea Cairica with α-Glucosidase Inhibitory Activity. *Chin. J. Nat. Med.* **2016**, *14* (3), 227–231.
(175) Harrison, J. J. E. K.; Tabuchi, Y.; Ishida, H.; Kingsford-Adaboh, R. Alpinumisoflavone. *Acta Crystallogr. Sect. E Struct. Rep. Online* **2008**, *64* (4), 713.
(176) Cimmino, A.; Masi, M.; Evidente, M.; Superchi, S.; Evidente, A. Application of Mosher's Method for Absolute Configuration Assignment to Bioactive Plants and Fungi Metabolites. *J. Pharm. Biomed. Anal.* **2017**, *144*, 59–89.
(177) Kuete, V.; Ngameni, B.; Simo, C. C. F.; Tankeu, R. K.; Ngadjui, B. T.; Meyer, J. J. M.; Lall, N.; Kuiate, J. R. Antimicrobial Activity of the Crude Extracts and Compounds from

Ficus Chlamydocarpa and Ficus Cordata (Moraceae). *J. Ethnopharmacol.* **2008**, *120* (1), 17–24.
(178) Barrero, A. F.; Sånchez, J. F.; Cuenca, F. G. Dramatic Variation in Diterpenoids of Different Populations of Bellardia Trixago. *Phytochemistry* **1988**, *27* (11), 3676–3678.
(179) Formisano, C.; Rigano, D.; Senatore, F.; Simmonds, M. S. J.; Bisio, A.; Bruno, M.; Rosselli, S. Essential Oil Composition and Antifeedant Properties of Bellardia Trixago (L.) All. (Sin. Bartsia Trixago L.) (Scrophulariaceae). *Biochem. Syst. Ecol.* **2008**, *36* (5), 454–457.
(180) Soriano, G.; Siciliano, A.; Fernández-Aparicio, M.; Cala Peralta, A.; Masi, M.; Moreno-Robles, A.; Guida, M.; Cimmino, A. Iridoid Glycosides Isolated from Bellardia Trixago Identified as Inhibitors of Orobanche Cumana Radicle Growth. *Toxins* **2022**, *14* (8), 559.
(181) Weinges, K.; Ziegler, H. J. Chemie Und Stereochemie Der Iridoide, XIV. Aucubin Und Scandosid Aus Catalpol. *Liebigs Ann. Chem.* **1990**, *1990* (7), 715–717.
(182) Tietze, L.-F.; Niemeyer, U.; Marx, P.; Glüsenkamp, K.-H.; Schwenen, L. Iridoide—XIII11XII. Mitteil, L.-F. Tietze, U. Niemeyer, P. Marx Und K.-H., Glüsenkamp, Tetrahedron, Im Druck.: Bestimmung Der Absoluten Konfiguration Und Konformation Isomerer Iridoidglycoside Mit Hilfe Chiroptischer Methoden. *Tetrahedron* **1980**, *36* (6), 735–739.
(183) Bianco, A.; Passacantilli, P.; Righi, G.; Nicoletti, M. Iridoid Glucosides from Parentucellia Viscosa. *Phytochemistry* **1985**, *24* (8), 1843–1845.
(184) Petitto, V.; Serafini, M.; Ballero, M.; Foddai, S.; Stanzione, A.; Nicoletti, M. Iridoids from Euphrasia Genargentea, a Rare Sardinian Endemism. *Nat. Prod. Res.* **2009**, *23* (5), 431–435.
(185) Khanh, T. D.; Anh, L. H.; Nghia, L. T.; Huu Trung, K.; Bich Hien, P.; Minh Trung, D.; Dang Xuan, T. Allelopathic Responses of Rice Seedlings under Some Different Stresses. *Plants Basel Switz.* **2018**, *7* (2), 40.
(186) Ahn, B. Z.; Pachaly, P. Melampyrosid, Ein Neus Iridoid Aus Melampyrum Silvaticum L. *Tetrahedron* **1974**, *30* (22), 4049–4054.
(187)Bianco A.; Guiso, M.; Iavarone, C.; Trogolo, C. *IRIDOIDS. XX. BARTSIOSIDE, STRUCTURE AND CONFIGURATION.* **1976**, 106, 725-732.
(188) *Karrer, P.; Schmid, H. Über die Konstitution des Aucubins. Helvetica Chimica Acta, **1946**, 29(3), 525-552.*
(189) Damtoft, S.; Hansen, S. B.; Jacobsen, B.; Jensen, S. R.; Nielsen, B. J. Iridoid Glucosides from Melampyrum. *Phytochemistry* **1984**, *23* (10), 2387–2389.
(190) Takeda, Y.; Nishimura, H.; Inouye, H. Two New Iridoid Glucosides from Mussaenda Parviflora and Mussaenda Shikokiana. *Phytochemistry* **1977**, *16* (9), 1401–1404.
(191) *Pennacchio, M.; Syah, Y. M.; Ghisalberti, E. L.; Alexander, E. Cardioactive iridoid glycosides from Eremophila species. Phytomedicine, **1997**, 4(4), 325-330.*
(192) Kirmizibekmez, H.; Atay, I.; Kaiser, M.; Brun, R.; Cartagena, M. M.; Carballeira, N. M.; Yesilada, E.; Tasdemir, D. Antiprotozoal Activity of Melampyrum Arvense and Its Metabolites. *Phytother. Res. PTR*, **2011**, *25* (1), 142–146.
(193) *Cuendet, M.; Potterat, O.; Hostettmann, K. Note Iridoid Glucosides, Phenylpropanoid Derivatives and Flavanoids from Bartsia alpina. Pharmaceutical biology, **1999**, 37(4), 318-320.*

(194) *Çalis, I.; Kirmizibekmez, H.; TASdemir, D.; Ireland, C. M. Iridoid glycosides from Globularia davisiana. Chemical and pharmaceutical bulletin, **2002**, 50(5), 678-680.*
(195) Liu, X.; Testa, B.; Fahr, A. Lipophilicity and Its Relationship with Passive Drug Permeation. *Pharm. Res.* **2011**, *28* (5), 962–977.
(196) Ohikhena, F. U.; Wintola, O. A.; Afolayan, A. J. Toxicity Assessment of Different Solvent Extracts of the Medicinal Plant, Phragmanthera Capitata (Sprengel) Balle on Brine Shrimp (Artemia Salina). *Int. J. Pharmacol.* **2016**, *12* (7), 701–710.
(197) *Antila, S.; Sundberg, S.; Lehtonen, L. A. Clinical pharmacology of levosimendan. Clinical pharmacokinetics, **2007**, 46, 535-552.*
(198) Commission, E. *Technical Guidance Document in Support of Commission Directive 93/67/EEC on Risk Assessment for New Notified Substances and Commission Regulation (EC) No 1488/94 on Risk Assessment for Existing Substances*; OOPEC, 1996.
(199) *Zorrilla, J. G.; Innangi, M.; Cala Peralta, A.; Soriano, G.; Russo, M. T.; Masi, M.; Fernández-Aparicio M.; Cimmino, A. Sesquiterpene Lactones Isolated from Centaurea cineraria L. subsp. cineraria Inhibit the Radicle Growth of Broomrape Weeds. Plants, **2024**, 13(2), 178.*
(200) Marco, J. A.; Sanz, J. F.; Sancenon, F.; Susanna, A.; Rustaiyan, A.; Saberi, M. Sesquiterpene Lactones and Lignans from Centaurea Species. *Phytochemistry* **1992**, *31* (10), 3527–3530.
(201) Djeddi, S.; Karioti, A.; Sokovic, M.; Koukoulitsa, C.; Skaltsa, H. A Novel Sesquiterpene Lactone from Centaurea Pullata: Structure Elucidation, Antimicrobial Activity, and Prediction of Pharmacokinetic Properties. *Bioorg. Med. Chem.* **2008**, *16* (7), 3725–3731.
(202) Padilla-Gonzalez, G. F.; dos Santos, F. A.; Da Costa, F. B. Sesquiterpene Lactones: More Than Protective Plant Compounds With High Toxicity. *Crit. Rev. Plant Sci.* **2016**, *35* (1), 18–37.
(203) Zorrilla, J. G.; Rial, C.; Varela, R. M.; Molinillo, J. M. G.; Macías, F. A. Facile Synthesis of Anhydrojudaicin and 11,13-Dehydroanhydrojudaicin, Two Eudesmanolide-Skeleton Lactones with Potential Allelopathic Activity. *Phytochem. Lett.* **2019**, *31*, 229–236.
(204) Tice, C. M. Selecting the Right Compounds for Screening: Does Lipinski's Rule of 5 for Pharmaceuticals Apply to Agrochemicals? *Pest Manag. Sci.* **2001**, *57* (1), 3–16.
(205) Nawamaki, T.; Sakakibara, T.; Ohta, K. Isolation and Identification of Lachnophyllum Lactone and Osthol as Repellents against a Sea Snail. *Agric. Biol. Chem.* **1979**, *43* (7), 1603–1604.
(206) Takeda, K.; Sakurawi, K.; Ishii, H. Components of the Lauraceae Family—I: New Lactonic Compounds from Litsea Japoncia. *Tetrahedron* **1972**, *28* (14), 3757–3766.
(207) Fernández-Aparicio, M.; Soriano, G.; Masi, M.; Carretero, P.; Vilariño-Rodríguez, S.; Cimmino, A. (4Z)-Lachnophyllum Lactone, an Acetylenic Furanone from Conyza Bonariensis, Identified for the First Time with Allelopathic Activity against Cuscuta Campestris. *Agriculture* **2022**, *12* (6), 790.
(208) Patel, K.; Patel, D. K. Medicinal Importance, Pharmacological Activities, and Analytical Aspects of Hispidulin: A Concise Report. *J. Tradit. Complement. Med.* **2017**, *7* (3), 360–366.

(209) Liu, K.; Zhao, F.; Yan, J.; Xia, Z.; Jiang, D.; Ma, P. Hispidulin: A Promising Flavonoid with Diverse Anti-Cancer Properties. *Life Sci.* **2020**, *259*, 118395.
(210) Anju, V. T.; Busi, S.; Mohan, M. S.; Ranganathan, S.; Ampasala, D. R.; Kumavath, R.; Dyavaiah, M. In Vivo, in Vitro and Molecular Docking Studies Reveal the Anti-Virulence Property of Hispidulin against Pseudomonas Aeruginosa through the Modulation of Quorum Sensing. *Int. Biodeterior. Biodegrad.* **2022**, *174*, 105487.
(211) Baruah, N. C.; Sarma, J. C.; Barua, N. C.; Sarma, S.; Sharma, R. P. Germination and Growth Inhibitory Sesquiterpene Lactones and a Flavone from Tithonia Diversifolia. *Phytochemistry* **1994**, *36* (1), 29–36.
(212) Scervino, J. M.; Ponce, M. A.; Erra-Bassells, R.; Vierheilig, H.; Ocampo, J. A.; Godeas, A. Flavonoids Exhibit Fungal Species and Genus Specific Effects on the Presymbiotic Growth of Gigaspora and Glomus. *Mycol. Res.* **2005**, *109* (7), 789–794.
(213) Tsanuo, M. K.; Hassanali, A.; Hooper, A. M.; Khan, Z.; Kaberia, F.; Pickett, J. A.; Wadhams, L. J. Isoflavanones from the Allelopathic Aqueous Root Exudate of Desmodium Uncinatum. *Phytochemistry* **2003**, *64* (1), 265–273.
(214) *Peralta, A. C.; Soriano, G.; Zorrilla, J. G.; Masi, M., Cimmino, A.; Fernández-Aparicio, M. Characterization of Conyza bonariensis allelochemicals against broomrape weeds. Molecules,* ***2022****, 27(21), 7421-7433.*
(215) Asaoka, M.; Yanagida, N.; Ishibashi, K.; Takei, H. Synthesis of 4-Ylidenebutenolides from 2-Trimethylsiloxyfuran. *Tetrahedron Lett.* **1981**, *22* (43), 4269–4270.
(216) *Jahnke, E.; Weiss, J.; Neuhaus, S.M; Hoheisel, T. N.; Frauenrath, H. Synthesis of Diacetylene-Containing Peptide Building Blocks and Amphiphiles, Their Self-Assembly and Topochemical Polymerization in Organic Solvents. Chemistry–A European Journal,* ***2009****, 15(2), 388-404.*
(217) *Gutierrez, D. A.; Fettinger, J.; Houk, K. N.; Ando, K.; Shaw, J. T. Diastereoselective addition of prochiral nucleophilic alkenes to α-chiral N-sulfonyl imines. Organic Letters,* ***2022****, 24(5), 1164-1168.*
(218) Ma, S.; Lu, X. A Novel Stereospecific Hydrohalogenation Reaction of Propiolates and Propiolic Acid. *J. Chem. Soc. Chem. Commun.* **1990**, *0* (22), 1643–1644.
(219) *Collins, A.; Mercado-Blanco, J.; Jiménez-Díaz, R. M.; Olivares, C.; Clewes, E.; Barbara, D. J. Correlation of molecular markers and biological properties in Verticillium dahliae and the possible origins of some isolates. Plant Pathology,* ***2005****, 54(4), 549-557.*
(220) *Zorrilla, J. G.; Rial, C.; Varela, R. M.; Molinillo, J. M.; Macías, F. A. Strategies for the synthesis of canonical, non-canonical and analogues of strigolactones, and evaluation of their parasitic weed germination activity. Phytochemistry Reviews,* ***2022****, 21(5), 1627-1659.*
(221) Zwanenburg, B.; Ćavar Zeljković, S.; Pospíšil, T. Synthesis of Strigolactones, a Strategic Account. *Pest Manag. Sci.* **2016**, *72* (1), 15–29.
(222) Amslinger, S. The Tunable Functionality of α,β-Unsaturated Carbonyl Compounds Enables Their Differential Application in Biological Systems. *ChemMedChem* **2010**, *5* (3), 351–356.

(223) *Maydt, D.; De Spirt, S.; Muschelknautz, C.; Stahl, W.; Müller, T. J. Chemical reactivity and biological activity of chalcones and other α, β-unsaturated carbonyl compounds. Xenobiotica,* ***2013****, 43(8), 711-718.*

(224) Cala, A.; Molinillo, J. M.; Fernández-Aparicio, M.; Ayuso, J.; Álvarez, J. A.; Rubiales, D.; Macías, F. A. Complexation of Sesquiterpene Lactones with Cyclodextrins: Synthesis and Effects on Their Activities on Parasitic Weeds. *Org. Biomol. Chem.* **2017**, *15* (31), 6500–6510.

(225) Hedges, A. R. Industrial Applications of Cyclodextrins. *Chem. Rev.* **1998**, *98* (5), 2035–2044.

(226) Ceborska, M.; Zimnicka, M.; Pietrzak, M.; Troć, A.; Koźbia\l, M.; Lipkowski, J. Structural Diversity in Native Cyclodextrins/Folic Acid Complexes–from [2]-Rotaxane to Exclusion Compound. *Org. Biomol. Chem.* **2012**, *10* (27), 5186–5188.

(227) Esposito, R.; Speciale, I.; De Castro, C.; D'Errico, G.; Russo Krauss, I. Rhamnolipid Self-Aggregation in Aqueous Media: A Long Journey toward the Definition of Structure–Property Relationships. *Int. J. Mol. Sci.* **2023**, *24* (6), 5395.

(228) Guzmán, E.; Ortega, F.; Rubio, R. G. Exploring the World of Rhamnolipids: A Critical Review of Their Production, Interfacial Properties, and Potential Application. *Curr. Opin. Colloid Interface Sci.* **2024**, *69*, 101780.

(229) *Zorrilla, J. G.; Cala, A.; Rial, C.; R. Mejías, F. J.; Molinillo, J. M.; Varela, R. M.; Macías, F. A. Synthesis of active strigolactone analogues based on eudesmane-and guaiane-type sesquiterpene lactones. J. Agric. Food Chem.* ***2020****, 68(36), 9636-9645.*

8. Publication and communication list

- M. Fernández-Aparicio, A. Cimmino, **G. Soriano**, M. Masi, S. Vilariño, A. Evidente "Assessment of weed root extracts for allelopathic activity against *Orobanche* and *Phelipanche* species" *Phytopathol. Mediterr.*, 60 (2021), 455-466. https://doi.org/10.36253/phyto-12917

- **G. Soriano**, M. Fernández-Aparicio, M. Masi, S. Vilariño-Rodríguez, A. Cimmino "Complex mixture of arvensic acids isolated from *Convolvulus arvensis* roots identified as inhibitors of radicle growth of *Broomrape* weeds" *Agriculture*, 12 (2022), 585-594. https://doi.org/10.3390/agriculture12050585

- **G. Soriano**, C. Petrillo, M. Masi, M. Bouafiane, A. Khelil, A. Tuzi, R. Isticato, M. Fernández-Aparicio, A. Cimmino "Specialized metabolites from the allelopathic plant *Retama raetam* as potential biopesticides" Toxins, 14 (2022), 311-322. https://doi.org/10.3390/toxins14050311

- **G. Soriano**, A. Siciliano, M. Fernández-Aparicio, A. Cala Peralta, M. Masi, A. Moreno-Robles, M. Guida, A. Cimmino "Iridoid glycosides isolated from *Bellardia trixago* identified as inhibitors of *Orobanche cumana* radicle growth" Toxins, 14 (2022), 559-571. https://doi.org/10.3390/toxins14080559

- M. Fernández-Aparicio, **G. Soriano**, M. Masi, P. Carretero, S. Vilariño-Rodríguez, A. Cimmino "(4*Z*)-Lachnophyllum lactone, an acetylenic furanone from *Conyza bonariensis*, identified for the first time with allelopathic activity against *Cuscuta campestris*" Agriculture, 12 (2022), 790-803. https://doi.org/10.3390/agriculture12060790

- Cala Peralta, **G. Soriano**, J.G. Zorrilla, M. Masi, A. Cimmino, M. Fernández-Aparicio "Characterization of *Conyza bonariensis* allelochemicals against *Broomrape* weeds" Molecules, 27 (2022), 7421-7434. https://doi.org/10.3390/molecules27217421

- Moreno-Robles, A. Cala Peralta, **G. Soriano**, J. G. Zorrilla, M. Masi, S. Vilariño-Rodríguez, A. Cimmino, M. Fernández-Aparicio "Identification of allelochemicals with differential modes of phytotoxicity against *Cuscuta campestris*" Agriculture, 12 (2022), 1746-1760. https://doi.org/10.3390/agriculture12101746

- Moreno-Robles, A. Cala Peralta, J. G. Zorrilla, **G. Soriano**, M. Masi, S. Vilariño-Rodríguez, A. Cimmino, M. Fernández-Aparicio "Identification of structural features of hydrocinnamic acid related to its allelopathic activity against the parasitic weed *Cuscuta campestris*" Plants, 11 (2022), 2846-2856. https://doi.org/10.3390/plants11212846

- Moreno-Robles, A. Cala Peralta, J. G. Zorrilla, **G. Soriano**, M. Masi, S. Vilariño-Rodríguez, A. Cimmino, M. Fernández-Aparicio "Structure− Activity Relationship (SAR) Study of trans-Cinnamic Acid and Derivatives on the Parasitic Weed *Cuscuta campestris*" Plants, 12 (2023), 697-708. https://doi.org/10.3390/plants12040697

- J. G. Zorrilla, M. Innangi, A. Cala Peralta, **G. Soriano**, M. T. Russo, M. Masi, M. Fernández-Aparicio, A. Cimmino "Sesquiterpene Lactones Isolated from *Centaurea cineraria* L. subsp. cineraria Inhibit the Radicle Growth of Broomrape Weeds" Plants, 13 (2024), 178-191. https://doi.org/10.3390/plants13020178

- **G. Soriano**, D. Arnodo, M. Masi, M. Fernández-Aparicio, B. B. Landa, C. Olivares-García, A. Cimmino, and C. Prandi "(4*Z*)-Lachnophyllum Lactone, a Metabolite with Phytotoxic and Antifungal Activity against Pests Affecting Mediterranean Agriculture: a New Versatile and Easy Scalable Parallel Synthesis" *J. Agric. Food Chem*. 72 (2024), 9, 4737–4746. https://doi.org/10.1021/acs.jafc.3c07130

Poster:

1. Poster communication at 13th Green Chemistry Postgraduate Summer School, Venice, **Gabriele Soriano**, A.Cimmino, M. Masi, M. Fernández-Aparicio, C. Prandi and A. Evidente, "**Plant metabolites as stimulants and/or inhibitors of parasitic plant seed germination**"
2. Poster communication during XIII Spanish-Italian Symposium on Organic Chemistry. **G. Soriano**, M. Fernandez-Aparicio, M. Masi, P. Carretero, L.C. Torres-Elizalde and A. Cimmino, "**Specialized metabolites as stimulants and/or inhibitors of parasitic weed germination and seedling growth**"
3. Poster communication at the 31st INTERNATIONAL SYMPOSIUM ON THE CHEMISTRY OF NATURAL PRODUCTS/11th INTERNATIONAL CONGRESS ON BIODIVERSITY, **G. Soriano**, D. Arnodo, M. Masi, M. Fernández-Aparicio, C. Prandi and A. Cimmino, **"TOTAL SYNTHESIS OF (4*Z*)-LACHNOPHYLLUM LACTONE, A SPECIALIZED BIOACTIVE ACETYLENIC FURANONE PRODUCED BY *CONYZA BONARIENSIS*".**

Oral:

- **Oral communication** at 13th Green Chemistry Postgraduate Summer School, Venice, **Gabriele Soriano**, "**Plant metabolites as stimulants and/or inhibitors of parasitic plant seed germination**"

10. Acknowledgement

I would like to thank the INPS (Instituto Nazionale Previdenza Sociale) for funding my Ph.D. project and works.